

**Early Detection System for Water Quality Monitoring of Cyanobacteria and
Hexavalent Chromium using UV-Vis Derivative Spectrophotometry and
Improvement of Detection Limit by Changing Pathlength**

by

Amitesh Malhotra, B. Tech., M. Eng., E.I.T.

A thesis submitted to the Faculty of Graduate and Postdoctoral Affairs

in partial fulfillment of the requirements for the degree of

Doctor of Philosophy

in

Environmental Engineering

Carleton University

Ottawa, Ontario

© 2021 Amitesh Malhotra

Abstract

This work explores the use of readily available spectrophotometry to detect and monitor cyanobacteria and hexavalent chromium (Cr (VI)) under different water matrices. Research has shown that these parameters have been increasing in frequency worldwide with growing anthropological activities and aggravating climate change, resulting in unwanted source water contamination. The aim was to evaluate the potential of derivative spectrophotometry with changing cuvette pathlength (10-, 50-, and 100-mm) to be used as an early warning system for sensitive determination of the aforementioned parameters.

Initially, *Microcystis aeruginosa* (cyanobacteria) and *Chlorella vulgaris* (green algae) were inoculated in deionized (D.I.) water individually and mixed in an equal concentration setting, respectively. The effect of increasing cuvette pathlength was investigated and results indicated a 15-, and 13-fold improvement in sensitivity with absorbance and derivative of absorbance from 10 mm to 100 mm pathlength, respectively. The lowest method detection limit (MDL) was observed using 100 mm and the concentration was found to be 4,916 cells/mL (for cyanobacteria), which is well below the WHO guideline for low probability of adverse health effects (< 20,000 cells/mL). Additionally, the mixed culture test demonstrated the potentiality of spectrophotometry to be able to identify cyanobacteria in mixed setting indicating applicability.

Further microalgal testing was performed using longer pathlengths (50- and 100-mm), to investigate robustness of the developed methodology in surface water and under varying water quality parameters (WQPs) aka salinity, dissolved organic carbon (DOC), and turbidity, for realistic determination. 100 mm pathlength while employing derivative spectrophotometry were found to be most sensitive and concentration as low as 8,546

cells/mL could be detected. As expected, with increasing concentration of WQPs the sensitivity decreased, but overall, spectrophotometry was able to detect cyanobacteria in different water matrices. Lastly, similar methodology as before was exercised but it was applied for early detection of Cr (VI). Derivative spectrophotometry with longest pathlength was primarily utilized to investigate Cr (VI) response in D.I. water, pH water matrices, varying DOC, surface and tap water. Results indicated excellent MDLs as low as 2-, and 5- $\mu\text{g/L}$ for tap and surface water, respectively, implicating practical viability.

Acknowledgements

I would like to express my deepest gratitude to my supervisor Professor Banu Örmeci. Her knowledge, expert guidance and encouragement allowed me to persevere through my entire PhD. Thank you for giving me the most precious thing of all, your time and support, which allowed me to stand where I am today. I would also like to thank Rich Kibbee for all the countless hours that he selflessly put towards helping me. His attention to detail and depth of knowledge never ceases to amaze me. He has been such a positive influence on my life.

I would like to thank NSERC for funding this research and Real Tech Inc. (Whitby, Ontario) for their valuable expertise. To the members of my defence committee, I thank you for your comments and your review of this body of work.

Lastly, I would like to thank and express love for my family and friends, who constantly motivated me and kept me on track throughout my PhD journey. I don't know how to express my gratitude for everything till date, you all helped me to keep strength and never give up!

Table of Contents

Abstract	ii
Acknowledgements	iv
Table of Contents	v
List of Figures	xi
List of Tables	xvii
List of Abbreviations	xx
1. Introduction.....	1
1.1 Thesis outline and objectives	3
1.2 References	7
2. Literature review	9
2.1 UV-Vis Spectrophotometry.....	9
2.2 Derivative Spectrophotometry	11
2.3 Cyanobacteria (Blue-Green algae).....	12
2.3.1 Regulations	20
2.3.2 Occurrences and Impacts	35
2.3.3 Current Detection Methods.....	43
2.4 Chromium (VI).....	66
2.4.1 Regulations	68
2.4.2 Occurrences and Health Impacts	70
2.4.3 Current Detection Methods.....	77
2.5 Summary	91
2.6 References	96
Appendix A.....	120
3. Materials and Methods.....	132

3.1	Culture growth and sustenance	132
3.2	Sample Preparation and Characterization	135
3.2.1	Microalgae experiments.....	135
3.2.2	Chromium (VI)	138
3.2.3	Water parameters	138
3.2.4	Hexavalent chromium verification	145
3.3	Experimental design and operation	146
3.4	First-order derivative of absorbance	148
3.5	Savitzky-Golay first derivative of absorbance	149
3.6	Method detection limit	151
3.7	Statistical analysis	153
3.8	References	154
	Appendix B	157
4.	Monitoring of Cyanobacteria using Derivative Spectrophotometry and Improvement of the Method Detection Limit by Changing Pathlength.....	163
	Abstract	163
4.1	Introduction	164
4.2	Materials and Methods	169
4.2.1	Cultivation of microalgae	169
4.2.2	Preparation of samples	169
4.2.3	UV-Visible spectrophotometry.....	170
4.2.4	First derivative of absorbance.....	171
4.2.5	Savitzky-Golay first derivative of absorbance.....	171
4.2.6	Method detection limit.....	172
4.2.7	Statistical analysis.....	172

4.3	Results	172
4.3.1	Absorbance measurements.....	172
4.3.2	First derivative of absorbance.....	175
4.3.3	Savitzky-Golay first derivative of absorbance.....	178
4.3.4	Spectral comparison of <i>M. aeruginosa</i> and <i>C. vulgaris</i>	182
4.4	Discussion	184
4.5	Conclusion.....	187
4.6	References	189
	Appendix C	201
5.	Detection and Identification of a Mixed Cyanobacteria and Microalgae Culture using Derivative Spectrophotometry	208
	Abstract	208
5.1	Introduction	209
5.2	Materials and Methods.....	213
5.2.1	Cultivation of microalgae	213
5.2.2	Preparation of mixed algal samples	214
5.2.3	Spectrophotometry	215
5.2.4	Derivative of absorbance	215
5.2.5	Method detection limit.....	216
5.3	Results	216
5.3.1	Absorbance measurements.....	216
5.3.2	Savitzky-Golay first derivative of absorbance measurements.....	220
5.3.3	Spectral comparison of mixed-culture with <i>M. aeruginosa</i> and <i>C. vulgaris</i> cultures	225
5.4	Discussion	228
5.5	Conclusion.....	232

5.6	References	234
	Appendix D.....	244
6.	Detection and Monitoring of Cyanobacteria and Green Algae in River Water using Derivative Spectrophotometry	248
	Abstract.....	248
6.1	Introduction	249
6.2	Materials and Methods.....	254
6.2.1	Microalgae growth and cultivation.....	254
6.2.2	Characterization of river water	255
6.2.3	Sample preparation for spectrophotometric analysis.....	255
6.2.4	UV-Vis Spectrophotometry	256
6.2.5	Calculation of Savitzky-Golay first-order derivative of absorbance	257
6.2.6	Establishing detection limit.....	258
6.3	Results	258
6.3.1	Spectrophotometric measurements of <i>M. aeruginosa</i> in river water.....	258
6.3.2	Savitzky-Golay first derivative of absorbance of <i>M. aeruginosa</i> in river water 261	
6.3.3	Comparison of <i>M. aeruginosa</i> and <i>C. vulgaris</i> cultures spectra in river water and D.I. water.....	266
6.4	Discussion	270
6.5	Conclusion.....	273
6.6	References	276
	Appendix E	288
7.	Implications of Water Quality Parameters on Detection and Monitoring of Cyanobacteria using UV-Vis Derivative Spectrophotometry.....	292
	Abstract.....	292

7.1	Introduction	293
7.2	Materials and Methods	298
7.2.1	Cyanobacteria cultivation and growth	298
7.2.2	Sample preparation for spectrophotometric analysis	299
7.2.3	Verification of water quality parameters	301
7.2.4	UV-Vis Spectrophotometry	302
7.2.5	Savitzky-Golay first-order derivative of absorbance	303
7.2.6	Establishing method detection limit.....	304
7.3	Results	305
7.3.1	Spectrophotometric measurements of <i>M. aeruginosa</i> in water matrices..	305
7.3.2	Savitzky-Golay first derivative of absorbance of <i>M. aeruginosa</i> in water matrices	308
7.3.3	Modified application of Savitzky-Golay first derivative of absorbance...	311
7.3.4	Comparison of <i>M. aeruginosa</i> spectra in D.I. water and different water matrices.	318
7.4	Discussion	319
7.5	Conclusion.....	324
7.6	References	326
	Appendix F.....	334
8.	Sensitive Determination of Chromium (VI) using Derivative Spectrophotometry and Monitoring Implications in Different Water Matrices using Longer Pathlengths	342
	Abstract	342
8.1	Introduction	343
8.2	Materials and Methods	348
8.2.1	Sample preparation and characterization for analysis	348
8.2.2	UV-Vis Spectrophotometry	351

8.2.3	Savitzky-Golay first-order derivative of absorbance.....	352
8.2.4	Establishing detection limits.....	353
8.2.5	Statistical analysis.....	353
8.3	Results and Discussions.....	354
8.3.1	Spectrophotometric measurements of Cr (VI) in D.I. water.....	354
8.3.2	pH response.....	357
8.3.3	Surface and tap water response.....	361
8.3.4	DOC response.....	364
8.3.5	Cr (VI) verification results.....	371
8.4	Conclusion.....	374
8.5	References.....	376
9.	Conclusions and Future Work.....	386
9.1	Conclusions.....	386
9.2	Future work.....	389

List of Figures

Figure 2.1: Cyanobacteria in inland water ecosystems. Top left: Photomicrograph of <i>Microcystis aeruginosa</i> (bloom-forming) from a eutrophic lake. The bright areas inside the cells are due to scattering of light by the gas vacuoles Top right: Photomicrograph of <i>Nostoc</i> (filamentous) from a high Arctic lake. The spherical cells are heterocysts, sites of nitrogen fixation. Bottom right: A carotenoid-rich cyanobacteria (mat-forming) in a pond on the McMurdo Ice Shelf, Antarctica. Bottom left: Cyanobacteria (mat-forming) in a geothermal spring, New Zealand (Vincent, 2009).....	15
Figure 2.2: Schematic illustration of scum-forming potential cyanobacteria and changing cyanotoxin risk levels (Bartram & Rees, 2000; Falconer, 1999).....	17
Figure 2.3: Chemical structures of cyanobacterial hepatotoxins, microcystin-LR (left) and nodularin (right) (Oren, 2014).	18
Figure 2.4: An overview of cyanobacterial cell producing potential bioactive metabolites (Saini et al., 2018).....	19
Figure 2.5: Summary of socio-ecological response and impacts associated with freshwater cyanobacterial blooms (Bajpai et al., 2011).....	36
Figure 2.6: Countries reporting one or more cyanoHABs outbreaks (Carmichael, 2006; Hudnell, 2008).	39
Figure 2.7: Categorization of economic costs of CyanoHABs for freshwater ecosystems (Dodds et al., 2009; Oren, 2014).....	41
Figure 2.8: Summary of molecular methods for monitoring and identification of cyanobacteria (Srivastava et al., 2013).	51
Figure 2.9: In vitro absorbance of select chlorophylls distributed among the spectral classes of algae. Individual spectra derived from standards and normalized to their maximum absorbance value (Gray, 2010).	53
Figure 2.10: Absorbance spectra of <i>M. aeruginosa</i> in (a) deionized water and (b) surface water (Agberien & Örmeci, 2019).....	54
Figure 2.11: Savitzky-Golay first derivative of absorbance spectra of <i>M. aeruginosa</i> in (a) deionized water and (b) surface water (Agberien & Örmeci, 2019).....	56
Figure 2.12: Visual representation of an in-situ fluorescence measurement technology (Zamyadi et al., 2016).....	59

Figure 2.13: Chromatogram of purified chlorophyll and carotenoid standards using HPLC followed by analysis using an in-line photodiode array detector (Gray, 2010).....	64
Figure 2.14: Photograph from a groundwater source contaminated with chromium in Kanpur, India (Sharma et al., 2012).....	67
Figure 2.15: Chromate and dichromate structures (PubChem, 2020a, 2020b).....	68
Figure 2.16: Graphical representation of the water utility testing data obtained from state water agencies of US tap-water for Cr (VI) by from the year 2005–2009. Black dots indicate the Environmental Working Group’s test sites and measured Cr (VI) concentrations. The size of the dot reflects the level found. Brown-shaded areas represent population-adjusted average concentrations of total chromium by county (Sutton, 2010).	76
Figure 2.17: Structure of 1,5-diphenyl-carbazide (DPC) (Yarbro, 1976).....	78
Figure 2.18: Absorption spectra of a $K_2Cr_2O_7$ solution (1 mg/L of Cr, pathlength 50 mm) for different pH (Burgess & Thomas, 2017).....	80
Figure 2.19: Absorption spectra (pathlength 50 mm) of synthetic solutions containing 1 mg/L of iron (a-pH 3, b-pH 9, c-pH 9 and addition of Cr (VI)) (Burgess & Thomas, 2017).	81
Figure 2.20: Principle of mass spectrometry (MS) (Guertin et al., 2005).	82
Figure 2.21: Conceptual diagram showing the principle of ion-chromatography (Guertin et al., 2005).	83
Figure 2.22: Simplified representation of a basic ICP system (PerkinElmer, 2018).	85
Figure 2.23: Flame atomic absorption spectroscopy (FAAS) and the general principle of AAS (Guertin et al., 2005).	88
Figure 3.1: Improved Neubauer chamber counting grid details (Bastidas, 2013).	136
Figure 3.2: Zig-zag counting technique (left) and cells to be counted (right) (Bastidas, 2013).	137
Figure 3.3: An example of 30 ppt salinity using a Mettler Toledo conductivity meter..	140
Figure 3.4: HACH 2100AN Turbidimeter.....	142
Figure 3.5: Left: Cary 100 UV-Vis spectrophotometer (Agilent Technologies); Right: Jenway 6850 Double Beam Spectrophotometer (Cole-Parmer).	147

Figure 4.1: Absorbance spectra at higher and lower concentration ranges of <i>M. aeruginosa</i> for 10 mm (a, b), 50 mm (c, d), and 100 mm (e, f) cuvette pathlengths, respectively...	175
Figure 4.2: First derivative of absorbance spectra of <i>M. aeruginosa</i> at higher and lower concentrations for 10 mm (a, b), 50 mm (c, d), and 100 mm (e, f) cuvette pathlength, respectively.	177
Figure 4.3: Savitzky-Golay first derivative of absorbance spectra of <i>M. aeruginosa</i> and <i>C. Vulgaris</i> at lower concentrations for 10 mm (a, b), 50 mm (c, d), and 100 mm (e, f) cuvette pathlength, respectively.	179
Figure 4.4: Absorbance spectra of <i>M. aeruginosa</i> (a) and <i>C. vulgaris</i> (b) using 50 mm pathlength cuvette.	184
Figure C.5: Standard calibration curves for absorbance spectra at higher and lower concentration ranges of <i>M. aeruginosa</i> for 10 mm (a, b), 50 mm (c, d), and 100 mm (e, f) cuvette pathlengths, respectively.	201
Figure C.6: Standard calibration curves for Savitzky-Golay first derivative of absorbance at higher and lower concentration ranges of <i>M. aeruginosa</i> for 10 mm (a, b), 50 mm (c, d), and 100 mm (e, f) cuvette pathlengths, respectively.	202
Figure C.7: Savitzky-Golay first derivative of absorbance spectra of <i>M. aeruginosa</i> and <i>C. Vulgaris</i> at higher concentrations for 10 mm (a, b), 50 mm (c, d), and 100 mm (e, f) cuvette pathlength, respectively.	203
Figure C.8: Absorbance spectra at higher and lower concentration ranges of <i>C. vulgaris</i> for 10 mm (a, b), 50 mm (c, d), and 100 mm (e, f) cuvette pathlengths, respectively.	204
Figure C.9: First derivative of absorbance spectra of <i>C. vulgaris</i> at higher and lower concentrations for 10 mm (a, b), 50 mm (c, d), and 100 mm (e, f) cuvette pathlength, respectively.	205
Figure C.10: Standard calibration curves for absorbance spectra at higher and lower concentration ranges of <i>C. vulgaris</i> for 10 mm (a, b), 50 mm (c, d), and 100 mm (e, f) cuvette pathlengths, respectively.	206
Figure C.11: Standard calibration curves for Savitzky-Golay first derivative of absorbance at higher and lower concentration ranges of <i>C. vulgaris</i> for 10 mm (a, b), 50 mm (c, d), and 100 mm (e, f) cuvette pathlengths, respectively.	207

Figure 5.1: Absorbance spectra at higher and lower concentration ranges of mixed <i>M. aeruginosa</i> and <i>C. vulgaris</i> cultures at 10 mm (a, b), 50 mm (c, d), and 100 mm (e, f) cuvette pathlengths, respectively.	219
Figure 5.2: Savitzky-Golay first derivative of absorbance spectra at higher and lower concentration ranges of mixed <i>M. aeruginosa</i> and <i>C. vulgaris</i> cultures at 10 mm (a, b), 50 mm (c, d), and 100 mm (e, f) cuvette pathlengths, respectively.....	222
Figure 5.3: Absorbance spectra of <i>M. aeruginosa</i> (a), <i>C. vulgaris</i> (b), and mixed-culture (c) using 50 mm pathlength cuvette.....	227
Figure 5.4: Savitzky-Golay first order derivative of absorbance spectra of <i>M. aeruginosa</i> (a), <i>C. vulgaris</i> (b), and mixed-culture (c) using 50 mm pathlength cuvette.....	228
Figure D.5: Standard calibration curves for absorbance spectra at <i>Chl-a</i> peak at higher and lower concentration ranges of mixed-culture for 10 mm (a, b), 50 mm (c, d), and 100 mm (e, f) cuvette pathlengths, respectively.	244
Figure D.6: Standard calibration curves for Savitzky-Golay first derivative of absorbance at <i>Chl-a</i> peak at higher and lower concentration ranges of mixed-culture for 10 mm (a, b), 50 mm (c, d), and 100 mm (e, f) cuvette pathlengths, respectively.....	245
Figure D.7: Standard calibration curves for absorbance spectra at PC peak at higher and lower concentration ranges of mixed-culture for 10 mm (a, b), 50 mm (c, d), and 100 mm (e, f) cuvette pathlengths, respectively.	246
Figure D.8: Standard calibration curves for Savitzky-Golay first derivative of absorbance at PC peak at higher and lower concentration ranges of mixed-culture for 10 mm (a, b), 50 mm (c, d), and 100 mm (e, f) cuvette pathlengths, respectively.....	247
Figure 6.1: Absorbance spectra at higher and lower concentration ranges of <i>M. aeruginosa</i> for 50 mm (a, b), and 100 mm (c, d) cuvette pathlengths, respectively.	261
Figure 6.2: Savitzky-Golay first derivative of absorbance spectra at higher and lower concentration ranges of <i>M. aeruginosa</i> for 50 mm (a, b), and 100 mm (c, d) cuvette pathlengths, respectively.....	263
Figure 6.3: Absorbance spectra of <i>M. aeruginosa</i> and <i>C. vulgaris</i> in river water (a, b), in D.I. water (c, d), and Savitzky-Golay first derivative of absorbance spectra in river water (e, f) using 100 mm cuvette pathlengths, respectively.....	269

Figure E.4: Standard calibration curves for absorbance spectra at <i>Chl-a</i> peak at higher and lower concentration ranges of <i>M. aeruginosa</i> in river water for 50 mm (a, b) and 100 mm (c, d) cuvette pathlengths, respectively.....	288
Figure E.5: Standard calibration curves for Savitzky-Golay first derivative of absorbance at <i>Chl-a</i> peak at higher and lower concentration ranges of <i>M. aeruginosa</i> in river water for 50 mm (a, b) and 100 mm (c, d) cuvette pathlengths, respectively.	289
Figure E.6: Standard calibration curves for absorbance spectra at PC peak at higher and lower concentration ranges of <i>M. aeruginosa</i> in river water for 50 mm (a, b) and 100 mm (c, d) cuvette pathlengths, respectively.....	289
Figure E.7: Standard calibration curves for Savitzky-Golay first derivative of absorbance at PC peak at higher and lower concentration ranges of <i>M. aeruginosa</i> in river water for 50 mm (a, b) and 100 mm (c, d) cuvette pathlengths, respectively.	290
Figure E.8: Standard calibration curves for absorbance spectra at <i>Chl-a</i> peak at higher and lower concentration ranges of <i>C. vulgaris</i> in river water for 50 mm (a, b) and 100 mm (c, d) cuvette pathlengths, respectively.....	291
Figure E.9: Standard calibration curves for Savitzky-Golay first derivative of absorbance at <i>Chl-a</i> peak at higher and lower concentration ranges of <i>C. vulgaris</i> in river water for 50 mm (a, b) and 100 mm (c, d) cuvette pathlengths, respectively.	291
Figure 7.1: Absorbance spectra of <i>M. aeruginosa</i> using 100 mm cuvette pathlength for 20 ppt salinity (a), 5 ppm DOC (b), and 50 NTU turbidity (c).....	308
Figure 7.2: Savitzky-Golay first derivative of absorbance spectra of <i>M. aeruginosa</i> using 100 mm cuvette pathlength for 20 ppt salinity (a), 5 ppm DOC (b), and 50 NTU turbidity (c).....	311
Figure 7.3: Modified Savitzky-Golay first derivative of absorbance spectra using 100 mm cuvette pathlength for 5 ppm DOC matrix water from 800 – 600 nm wavelengths (a), and 750 – 450 nm wavelengths (b).....	312
Figure 7.4: Absorbance (a) and Savitzky-Golay first derivative of absorbance (b) spectra of <i>M. aeruginosa</i> in D.I. water using 100 mm cuvette pathlength, respectively.	319
Figure F.5: Absorbance spectra of <i>M. aeruginosa</i> (180 mins exposure) using 100 mm cuvette pathlength for 10 and 30 ppt salinity (a, b), 1 and 10 ppm DOC (c, d), and 10 and 100 NTU turbidity (e, f).....	334

Figure F.6: Savitzky-Golay first derivative of absorbance spectra of *M. aeruginosa* (180 mins exposure) using 100 mm cuvette pathlength for 10 and 30 ppt salinity (a, b), 1 and 10 ppm DOC (c, d), and 10 and 100 NTU turbidity (e, f). 335

Figure 8.1: Absorbance and Savitzky-Golay first derivative of absorbance spectra of *Cr (VI)* in D.I. water using 10- (a, b), 50- (c, d), and 100 mm (e, f) cuvette pathlengths, respectively. 357

Figure 8.2: Absorbance and Savitzky-Golay first derivative of absorbance spectra of *Cr (VI)* using 100 mm cuvette pathlength at pH 5 (a, b), 6 (c, d), 7 (e, f), 9 (g, h), and 10 (i, j), respectively..... 361

Figure 8.3: Absorbance and Savitzky-Golay first derivative of absorbance spectra of *Cr (VI)* in surface water (a, b) and tap water (c, d) using 100 mm cuvette pathlength. 364

Figure 8.4: Absorbance and Savitzky-Golay first derivative of absorbance spectra of *Cr (VI)* using 100 mm cuvette pathlength at DOC 1- (a, b), 5- (c, d), and 10 mg/L (e, f), respectively. 368

List of Tables

Table 2.1: The 5 orders of cyanobacteria according to the botanical taxonomic scheme (Vincent, 2009).	13
Table 2.2: Examples of guidance values or standards and other national regulations/recommendations for managing cyanotoxins in drinking water (Chorus, 2005, 2012; Health Canada, 2016; Oren, 2014; WHO, 2003a).....	20
Table 2.3: Examples of national regulations or recommendations for managing cyanotoxins in water-bodies used for recreation (Chorus, 2005, 2012; Health Canada, 2016; Oren, 2014; WHO, 2003a).....	26
Table 2.4: A summary of methods used to quantify algae (Bartram & Rees, 2000).....	45
Table 2.5: ELISA commercial assays used for detection and quantification of different cyanotoxins (Moreira et al., 2014).....	47
Table 2.6: Chemical and chromatography-based methods for detecting cyanobacteria and their toxins (Moreira et al., 2014).	62
Table 2.7: A summary of chromium guidelines around the world.	69
Table 2.8: Summary of detection limits of chromium in different water matrices and their respective detection system.....	93
Table A.9: State Guidelines and Regulations for Cyanobacteria and Cyanobacterial Toxins in Drinking and Recreational Waters in the USA (Chorus, 2005, 2012).	120
Table A.10: National and regional drinking and recreational water quality guidelines and standards currently in place across Canada (Chorus, 2012; Health Canada, 2016).	125
Table A.11: Occurrence and characteristics of select algal chlorophylls and their derivatives (Gray, 2010).	127
Table A.12: Commercial characteristics of eleven in vivo fluorescence cyanobacterial probes (*: For measurement unit, see column raw probe reading unit) (PC: phycocyanin; PE: phycoerythrin, Chla: chlorophyll-a) (Zamyadi et al., 2016).	130
Table 3.1: Elemental composition of Upper Mississippi River Natural Organic Matter standard (IHSS, 2020).....	143
Table B.2: Stock concentrate 3N-BBM composition from CPCC at the University of Waterloo (Hellebust et al., 1973).....	157

Table B.3: Stock concentrate BBM composition from CPCC at the University of Waterloo (Hellebust et al., 1973).....	158
Table B.4: Trace Metal Solution composition (BBM Stock 9) (Hellebust et al., 1973).	160
Table B.5: F/2 Vitamin Solution composition (BBM Stock 11) (Hellebust et al., 1973).	160
Table 4.1: Examples of national regulations for managing cyanobacteria/microcystin in water sources.....	166
Table 4.2: Summary of experimental results for <i>Microcystis aeruginosa</i> and <i>Chlorella vulgaris</i> for higher and lower concentration ranges.	180
Table 5.1: Examples of regulations/ guidance values for recreational and drinking water sources.....	210
Table 5.2: Summary of experimental results for mixed equal concentration of <i>Microcystis aeruginosa</i> and <i>Chlorella vulgaris</i> in D.I. water for higher and lower concentration ranges.	222
Table 6.1: Regulations/ guidance value examples for low probability of adverse health effects in drinking and recreational water sources around the world for cyanobacteria.	251
Table 6.2: Results from Rideau River characterization.	259
Table 6.3: Critical data for <i>Microcystis aeruginosa</i> and <i>Chlorella vulgaris</i> in river water for higher (118,750 – 950,000 cells/mL) and lower (1,855 – 59,375 cells/mL) concentration ranges.	264
Table 7.1: Water quality parameters preparation information.....	301
Table 7.2: Elemental composition of Upper Mississippi River Natural Organic Matter standard (IHSS, 2020).....	302
Table 7.3: Critical data for <i>M. aeruginosa</i> in different water matrices for photopigment <i>Chl-a</i> over the concentration range (1,855 – 950,000 cells/mL) after 180 mins exposure.	312
Table 7.4: Critical data for <i>M. aeruginosa</i> in different water matrices for photopigment phycocyanin over the concentration range (1,855 – 950,000 cells/mL) after 180 mins exposure.	315

Table F.5: Critical data for <i>M. aeruginosa</i> in different water quality matrices for photopigments <i>Chl-a</i> and <i>Phycocyanin</i> over the concentration range (1,855 – 950,000 cells/mL) after 90 mins exposure.....	336
Table 8.1: Guidance values (GV) examples for total/hexavalent chromium in drinking water around the world.	345
Table 8.2: Elemental composition of Upper Mississippi River Natural Organic Matter standard (IHSS, 2020).....	350
Table 8.3: Results from surface water and tap water characterization (mean value ± SD).	362
Table 8.4: Summary of critical data for Cr (VI) in different water matrices over the concentration range (1 – 100 µg/L).	368

List of Abbreviations

°C	Degree Celsius
µg	Microgram
µL	Microliter
3N-BBM	BBM with triple Nitrogen stock
A	Absorbance
a.u.	Absorbance Units
AAS	Atomic Absorption Spectroscopy
ACT	Alliance for Coastal Technologies
AES	Atomic Emission Spectroscopy
AUD	Australian Dollars
b	Path Length
BBM	Bold's Basal Medium
BOD	Biological Oxygen Demand
C	Component/concentration
<i>C. vulgaris</i>	<i>Chlorella Vulgaris</i>
C ¹⁸	Carbon 18
CB	Cyanobacteria
CE	Capillary Electrophoresis
Cells	Cell concentration of microalgae
Chl-a	Chlorophyll-a
Chl-b	Chlorophyll-b
CO ₂	Carbon Dioxide
COD	Chemical Oxygen Demand
CPCC	Canadian Phycological Culture Center
Cr (III)	Trivalent Chromium
Cr (VI)	Hexavalent Chromium
Cr-0	Chromium Zero
Cr ₂ O ₇ ⁻²	Dichromate
CrO ₄ ⁻²	Chromate

CyanoHABs	Cyanobacterial Blooms
D.I.	Deionized
DGGE	Denaturing Gradient Gel Electrophoresis
DLLME	Dispersive Liquid-Liquid Microextraction
DOC	Dissolved Organic Carbon
DOM	Dissolved Organic Matter
DPC	1,5-diphenyl-carbazide
EPA	Environmental Protection Agency
ESI	Electrospray Ionization
ETAAS	Electrothermal AAS
FAAS	Flame-AAS
Fe (III)	Trivalent Ferric Ion
FISH	Fluorescence in-situ Hybridization
g	Grams
GFAAS	Graphite Furnace AAS
GV	Guidance Value
HABs	Harmful Algal Blooms
HCrO ₄ ⁻	Hydrogen Chromate
HEPA	High Efficiency Particulate Absorbing filter
HESI	Heated Electrospray Ionization
HPLC	High Pressure Liquid Chromatography
H-V	Hubaux and Vos
I	Transmitted Radiation
IC	Ion Chromatography
ICP	Inductive Coupled Plasma
IHSS	International Humic Substance Society
I ₀	Incident Radiation
J	Concentration Standards
K	Spike Replicates
K ₂ Cr ₂ O ₇	Potassium Dichromate
Kg	Kilogram

km	Kilometer
L	Liter
LC	Liquid Chromatography
LD	Lethal Density
M.aeruginosa	Microcystis Aeruginosa
MALDI-TOF	Matrix-assisted Laser Desorption/ Ionization Time of Flight
MC	Microcystis/Microcystin
MDL	Method Detection Limit
mg	Milligram
MHz	Mega Hertz
mL	Milliliter
mm	Millimeter
mm ³	Cubic Milli-meter
MS	Mass Spectrometry
nm	Nanometers
NOAA	National Oceanic and Atmospheric Administration
NTU	Nephelometric Turbidity Units
OES	Optical Emission Spectroscopy
P	Radiant Power
PC	Phycocyanin
PCR	Polymerase Chain Reaction
PE	Phycoerythrin
ppm	Parts Per Million
ppt	Parts Per Thousand
qPCR	Quantitative PCR
R ²	Coefficient of Determination
RAPD	Random Amplified Polymorphic DNA
R-T	Real-Time
SAR	Synthetic Aperture Radar
S-G	Savitzky-Golay

SiO ₂	Silica
SP	Spectrophotometry
SPE	Solid Phase Extraction
T	Transmittance
T&O	Taste and Odor
TOC	Total Organic Carbon
T-RFLP	Terminal Restriction Fragment Length Polymorphism
TSS	Total Suspended Solids
TVS	Total Volatile Solids
UPLC	Ultrahigh Performance Liquid Chromatography
USA/US	United states of America
UVT	UV Transmittance
UV-Vis	UV-Visible
VBNC	Viable but non-Culturable
WHO	World Health Organization
WQM	Water Quality Monitoring
WQPs	Water Quality Parameters
ϵ	extinction coefficient/ absorptivity
λ	Wavelength

1. Introduction

The need for better, simple, and affordable early detection technologies is imperative with the increasing contamination of water sources worldwide. Ever-increasing and emerging industrial and chemical compounds in water sources are some of the most dominant environmental problems facing humanity. According to the World Health Organization (WHO), 1.8 million deaths each year, of which 88% are children in developing countries, are caused due to water-borne illnesses. Water quality assurance is underemphasized and poses a grave threat to global health, despite models predicting a double increase in water consumption in the next 20 years (Mukhopadhyay & Mason, 2013).

Early detection technologies are typically systems that consist of a monitoring technology which can analyze, interpret and display results in near to real-time as possible (EPA, 2005). The existing laboratory-based methods for water quality monitoring (WQM) are time-consuming, labor-intensive, and often require various reagents and/or pigment extraction to obtain reliable results (Storey et al., 2011). There is a clear necessity to rapidly detect and correct a potential contamination event, which may be either chemical or biological in nature, due to its potentially severe consequences to human health and the environment.

Furthermore, in most cases, many compounds are mixed in our aquatic resources and the question of which compounds are present and how their combined effects affect the quality of the aquatic resource become pertinent (Altenburger et al., 2015). Hence, there is a need to monitor multiple water quality parameters using a minimal number of instruments whilst maintaining high sensitivity in order to implement it as an early warning system (Quansah

et al., 2010). Significant work is yet to be achieved, despite many technological advances in the field of WQM (Mukhopadhyay & Mason, 2013).

The objectives of this research were to investigate detection and monitoring of important water quality affecting parameters such as cyanobacteria (blue-green algae) and hexavalent chromium (Cr (VI)) using UV-Vis spectrophotometry under multifarious conditions. With growing anthropological activities and increasing global warming, fresh water sources have seen a decrease in quality, particularly over the last two decades. Each year reports of toxic cyanobacteria (CB) and hexavalent chromium in water resources have been increasing around the world (McNeill et al., 2012; Mohamed et al., 2015; Pelaez et al., 2010; WHO, 2019).

The aim is to improve (lower) the detection limit of these parameters by using readily available spectrophotometry technology while investigating derivative spectrophotometry as an analytical tool for improving sensitivity. Longer cuvette pathlengths (upto 100 mm) have not been employed in the study of CB or Cr (VI) research before. This study focuses on using existing spectrophotometry technology and modifying cuvette pathlengths to test their effect on detection. Care was taken that the techniques tested could potentially be implemented with ease in a real-time monitoring setting. The constant evolution of water quality standards necessitates the development of faster and cheaper analytical procedures (Burgess & Thomas, 2017). This study aims to lead the way to develop an early warning system that can be used for WQM purposes.

1.1 Thesis outline and objectives

This study is presented in a total of 9 chapters. **Chapter 1** includes a brief introduction and explains the need for the research topic and a description of the research approach and objectives that are to be investigated.

Chapter 2 provides a summary of background literature required to understand relevant information, as well as previous and current studies related to this research. Major regulations, occurrences and health impacts from around the world have also been discussed.

Chapter 3 provides the details of the materials and methods used throughout the experimental phase. Laboratory protocols and validation methods relevant to this study are described in this chapter.

Chapter 4 to 8 are the primary research chapters of the thesis which have been prepared as journal articles.

Chapter 4 and 5 studied the effect of increasing cuvette pathlength on the detection of A non-toxic strain of cyanobacteria i.e., *Microcystis Aeruginosa* and a secondary green microalgae aka *Chlorella Vulgaris* was used for comparative purposes.

- Spectrophotometry (SP) was used to analyze the prepared sample concentration range in deionized (D.I.) water (controlled environment) and monitor peaks of interest at different wavelengths for both algal cultures.
- Characterize and compare the effect of increasing cuvette pathlength (10-, 50-, and 100 mm) on absorbance spectra.

- Determine the effect of changing cuvette pathlength on the method detection limit (MDL) of both algal strains.
- Study the transformation of the peak and absorbance spectra after applying derivative spectrophotometry as a statistical and analytical tool.
- Apply the first derivative of absorbance and Savitzky-Golay (S-G) first derivative of absorbance to examine the possibility to improve the MDL for the algal strains with varying pathlength.
- Validate whether the absorbance and derivative absorbance results follow Beer-Bourguer-Lambert Law (with changing concentration and absorbance at the significant wavelength) for the 3 cuvette pathlengths.
- The above methodology was repeated by mixing equal concentrations of *M. aeruginosa* and *C. vulgaris* and investigating the potential to differentiate cyanobacteria in a mixed-culture setting.

Chapter 6 presents the impact of using longer cuvette pathlengths and derivative spectrophotometry for the detection and monitoring of *M. aeruginosa* and *C. vulgaris* in surface water (to mimic realistic conditions).

- Unfiltered surface water was used for sample preparation and longer pathlengths (50-, and 100-mm) were utilized to characterize the response of individual microalgae in a natural environment.
- S-G first derivative of absorbance was applied in pursuit of improving spectral analysis.
- MDLs for individual pathlengths and microalgal culture were determined while comparing the zero-order absorbance to the derivative of absorbance.

- Beer-Bourguier-Lambert Law validation was performed to ensure conformity of observed experimental data.
- Sensitivity analyses were conducted between both inoculated microalgae in surface water and D.I. water while comparing performance.

Chapter 7 explored the effect of changing different water quality parameters (WQPs) on the detection of cyanobacteria (*M. aeruginosa*), in a controlled environment, using spectrophotometry.

- The effect of changing three concentration levels of salinity, dissolved organic carbon (DOC) and turbidity, on absorbance was analyzed.
- A reliable, reproducible, and consistent methodology for all three parameters was developed for cyanobacterial testing.
- A similar concentration range (as in previous chapters) of cyanobacterial microalgae was used for different water quality control parameters.
- The impact of changing exposure time (90- and 180-min) of cyanobacteria to individual WQP before testing was characterized, and comparative analysis was performed.
- S-G first derivative of absorbance was applied to verify the consistency of the peak of interest.
- Slopes and detection limits were established for both exposure times and each WQP test to better aid during analysis.
- The effect of changing wavelength range on the application of S-G derivative method in order to improve the signal-to-noise ratio and MDL was investigated.

Chapter 8 researched the sensitive determination of hexavalent chromium and its response in different water matrices via spectrophotometry.

- Characterize the effect of changing cuvette pathlength on detection of Cr (VI) in D.I. water.
- Develop a methodology and concentration range of Cr (VI) to be used for all tests which is consistent and repeatable.
- Identify the wavelengths of interest and apply the developed derivative spectrophotometry method from previous chapters to analyze the impact on MDL.
- Characterize the following response of Cr (VI) using the concentration range developed as follows:
 - Evaluate the effect of changing pH (alkaline and acidic) of water and its effect on the shift of absorbance peaks.
 - Inoculate Cr (VI) in tap water and surface water to check for the effect of realistic conditions on Cr (VI) detection.
 - Evaluate the effect of three concentration levels of DOC on the detection of Cr (VI).
- Apply derivative spectrometry and conduct sensitivity analyses to all the aforementioned tests to check the applicability and consistency of the methodology to improve MDL.

Chapter 9 provides the overall conclusions and significant findings of the dissertation, as well as recommendations for future work.

1.2 References

Altenburger, R., Ait-Aissa, S., Antczak, P., Backhaus, T., Barceló, D., Seiler, T.-B., Brion, F., Busch, W., Chipman, K., de Alda, M. L., de Aragão Umbuzeiro, G., Escher, B. I., Falciani, F., Faust, M., Focks, A., Hilscherova, K., Hollender, J., Hollert, H., Jäger, F., ... Brack, W. (2015). Future water quality monitoring—Adapting tools to deal with mixtures of pollutants in water resource management. *Science of The Total Environment*, 512–513, 540–551. <https://doi.org/10.1016/j.scitotenv.2014.12.057>

Burgess, C., & Thomas, O. (2017). UV-Visible Spectrophotometry of Water and Wastewater. In *UV-Visible Spectrophotometry of Water and Wastewater* (pp. 1–524). Elsevier. (ISBN 978-0-444-63897-7) <https://doi.org/10.1016/B978-0-444-63897-7.00001-9>

EPA, U. (2005). *Technologies and Techniques for Early Warning Systems to Monitor and Evaluate Drinking Water Quality* (p. 236). USEPA.

McNeill, L. S., McLean, J. E., Parks, J. L., & Edwards, M. A. (2012). Hexavalent chromium review, part 2: Chemistry, occurrence, and treatment. *Journal - American Water Works Association*, 104(7), E395–E405. <https://doi.org/10.5942/jawwa.2012.104.0092>

Mohamed, Z. A., Deyab, M. A., Abou-Dobara, M. I., El-Sayed, A. K., & El-Raghi, W. M. (2015). Occurrence of cyanobacteria and microcystin toxins in raw and treated waters of the Nile River, Egypt: Implication for water treatment and human health. *Environmental Science and Pollution Research*, 22(15), 11716–11727. <https://doi.org/10.1007/s11356-015-4420-z>

Mukhopadhyay, S. C., & Mason, A. (Eds.). (2013). *Smart Sensors for Real-Time Water Quality Monitoring* (Vol. 4). Springer Berlin Heidelberg. (ISBN 978-3-642-37005-2) <https://doi.org/10.1007/978-3-642-37006-9>

Pelaez, M., Antoniou, M. G., He, X., Dionysiou, D. D., de la Cruz, A. A., Tsimeli, K., Triantis, T., Hiskia, A., Kaloudis, T., Williams, C., Aubel, M., Chapman, A., Foss, A., Khan, U., O’Shea, K. E., & Westrick, J. (2010). Sources and Occurrence of Cyanotoxins Worldwide. In D. Fatta-Kassinos, K. Bester, & K. Kümmerer (Eds.), *Xenobiotics in the*

Urban Water Cycle (Vol. 16, pp. 101–127). Springer Netherlands. (ISBN 978-90-481-3508-0) https://doi.org/10.1007/978-90-481-3509-7_6

Quansah, J. E., Engel, B., & Rochon, G. L. (2010). *Early Warning Systems: A Review*. 2(2), 22.

Storey, M. V., van der Gaag, B., & Burns, B. P. (2011). Advances in on-line drinking water quality monitoring and early warning systems. *Water Research*, 45(2), 741–747. <https://doi.org/10.1016/j.watres.2010.08.049>

WHO. (2019). *Chromium in Drinking-water* (p. 34) [Peer review draft]. World Health Organization. https://www.who.int/water_sanitation_health/water-quality/guidelines/chemicals/draft-chromium-190924.pdf

2. Literature review

2.1 UV-Vis Spectrophotometry

UV-Visible (UV-Vis) spectrophotometry (SP) is a well-established method for identification and determination of components in a variety of water samples. It is a technique that uses electromagnetic radiation to interact with atoms and molecules in specific and distinct ways, which results in characteristic emission or absorption profiles (Burgess & Thomas, 2017). In UV-Vis SP, when the light source impinges on a cuvette that contains the water sample, many optical processes can occur, which when combined with instrumental effects, can result in distortion of the resultant spectrum. The optical processes include transmission, reflection, refraction, scattering, luminescence and/or chiro-optical phenomena (Burgess & Thomas, 2017). These issues should be acknowledged, and care should be taken to minimize their impact while performing tests.

The absorbance (A) of a sample is defined as the difference between the incident radiation (I_0) and the transmitted radiation (I). Contrarily, the transmittance (T) is defined as the fraction of the radiation which passes through the sample (Burgess & Thomas, 2017; Owen, 1998). The absorbance and transmittance are defined by the following equations 2.1 and 2.2, respectively (Owen, 1998).

$$A = -\log \frac{I}{I_0} = -\log T \quad 2.1$$

$$T = \frac{I}{I_0} = 10^{-A} \quad 2.2$$

UV-Vis spectrophotometry is commonly employed for quantitative analysis of water samples containing matter, as most compounds in water samples absorb radiation in the

range of wavelengths between $\lambda = 190$ nm to $\lambda = 800$ nm (Burgess & Thomas, 2017). The UV wavelengths range from $\lambda = 190$ nm to $\lambda = 400$ nm, while the visible wavelengths range between $\lambda = 400$ nm to $\lambda = 800$ nm. In this study, absorption profiles of energy created by molecular and electronic transitions of radiation was used for detection of pollutants.

Beer-Bourguer-Lambert Law

Beer-Bourguer-Lambert Law is the basis for UV-Vis SP as it relates the measured absorbance value to the concentration value of a component. It states that absorbance is linearly proportional to the concentration of the component (C) of interest and the path length (b) of the cuvette containing the sample, through which UV-Vis radiation is transmitted and is given by the equation 2.3 (Burgess & Thomas, 2017; Swinehart, 1962):

$$A = -\log_{10} \frac{P}{P_0} = \epsilon b C \quad 2.3$$

where,

A = absorbance, formerly called the optical density

P = radiant power, formerly called the intensity

ϵ = extinction coefficient/ absorptivity

b = length of the cuvette containing the absorbing medium

C = concentration of the absorbing species

However, the law is based on some assumptions, which are:

- Radiation is perfectly monochromatic.

- Radiation beam strikes the cuvette at normal incidence.
- There are no uncompensated losses due to scattering or reflection processes.
- The temperature remains constant.
- There are no molecular interactions between the absorber and other molecules in the sample.

These assumptions are not always met, and the results might deviate from ideal Beer-Bourguer-Lambert Law behavior (Owen, 1998; Swinehart, 1962).

2.2 Derivative Spectrophotometry

The problem of determining concentration of multiple components can be solved with methods which are based on several wavelength absorbance measurements (assuming the solution is free of interferences). However, there are several physical and/ or chemical interferences when analyzing a real sample. Derivative spectrophotometry is one of the simplest methods which offers the ability to check a sample quality in a robust way (Burgess & Thomas, 2017).

Derivative spectrophotometry is the use of first or higher derivatives of observed absorbance with respect to the recorded wavelength. It is used for qualitative and quantitative analysis (Owen, 1995). Given that the spectral absorbance is expressed as a function of the wavelength (λ), the derivative spectra are:

Zero order/ normal spectrum

$$A = f(\lambda) \tag{2.4}$$

First order

$$\frac{dA}{d\lambda} = f'(\lambda) \quad 2.5$$

nth order

$$\frac{d^n A}{d\lambda^n} = f^n(\lambda) \quad 2.6$$

Derivative spectra do not increase the information content of the traditional spectra, and rather they allow the information to be analyzed in a better manner. Derivative spectra result in information about the slope of the spectrum, as well as the shoulder and inflection points allowing for a better characterisation of a compound. However, one of the main limitations of derivative spectrophotometry is that the random background noise associated with sample analysis increases and results in higher frequency of the signal to be measured. Thus, the peaks obtained are narrower and sharper with increasing derivative order. This can be improved by using filters during analysis, which is described later in the manuscript (Owen, 1995, 1998).

2.3 Cyanobacteria (Blue-Green algae)

Cyanobacteria (CB), more commonly referred to as blue-green algae, are photosynthetic prokaryotes that use various accessory pigments, primarily chlorophyll-a (Chl-a) to capture sunlight for energy production. CB are most commonly found in freshwater lakes, ponds, wetlands, rivers, and streams and can even occur in oceans (Bittencourt-Oliveira et al., 2014; Chorus et al., 2000; Chorus & Bartram, 1999; Codd et al., 1999; Corbel et al., 2014; Falconer, 1993; Figueiredo et al., 2004; Graham et al., 2010; Hudnell, 2008; Mohamed et al., 2015; Sharma et al., 2010; WHO, 2003a; Winter et al., 2011). Cyanobacteria include approximately 2000 species under 150 genera which are classified under 5 broad orders,

which are present in diverse shapes and sizes. Table 2.1 lists the 5 orders of CB; the orders refer to the subsections of Cyanobacteria Phylum.

Table 2.1: The 5 orders of cyanobacteria according to the botanical taxonomic scheme (Vincent, 2009).

Order	Characteristics	Genera
Chroococcales	Cocoid are cells that reproduce by binary fission or budding	<i>Aphanocapsa</i> , <i>Aphanothece</i> , <i>Gloeocapsa</i> , <i>Merismopedia</i> , <i>Microcystis</i> , <i>Synechococcus</i> , <i>Synechocystis</i>
Pleurocapsales	Cocoid cells, aggregates or pseudo-filaments that reproduce by baeocytes	<i>Chroococcidiopsis</i> , <i>Pleurocapsa</i>
Oscillatoriales	Uniseriate filaments, without heterocysts or akinetes	<i>Lyngbya</i> , <i>Leptolyngbya</i> , <i>Microcoleus</i> , <i>Oscillatoria</i> , <i>Phormidium</i> , <i>Planktothrix</i>
Stigonematales	Division in more than one plane; true branching and multiseriate forms; heterocysts	<i>Mastigocladus</i> (<i>Fischerella</i>), <i>Stigonema</i>
Nostocales	Filamentous cyanobacteria that divide in only one plane, with heterocysts; false branching in genera such as Scytonema	<i>Anabaena</i> , <i>Aphanizomenon</i> , <i>Calothrix</i> , <i>Cylindrospermopsis</i> , <i>Nostoc</i> , <i>Scytonema</i> , <i>Tolypothrix</i>

There are three major groups of CB commonly observed in the aquatic environment: bloom-formers, most common in nutrient-rich (eutrophic) conditions and lead to a wide range of water quality issues; mat-forming, which form biofilms over plants, sediments

and rocks; and picocyanobacteria, which as the name suggests, are extremely small cells with diameter $< 3 \mu\text{m}$ that are prolific in clear water lakes (Vincent, 2009). This thesis focused on the detection of a bloom-forming variety of microalgae in water using UV-Vis spectrophotometry.

Cyanobacteria lack membrane-bound organelles but have different cellular structures in the cells that have specialized functions. The cells of bloom-forming CB contain several thousand gas vacuoles, hollow-water impermeable cylinders in nature, that provide buoyancy for the algae to float towards the surface for improved photosynthesis (Vincent, 2009). Figure 2.1 shows some examples of the different algae types observed in nature. Bloom-formers are inclined towards warm, stable, and nutrient-rich lakes and are nonexistent in polar or alpine regions. *Anabaena*, *Aphanizomenon*, and *Microcystis* are the three genera of CB commonly found and often are present concurrently (EPA, 2005; Stefanelli et al., 2014). Studies show that a single factor does not contribute to bloom formation, instead a mixture of nutrients (nitrogen and phosphorous) and environmental conditions (warm temperature, light intensity, growth rate, and stability) present together (Chorus & Bartram, 1999; Health Canada, 2016; Mohamed et al., 2015; Pelaez et al., 2010). In inland water bodies, blooms are often limited by phosphorous availability. Enrichment of lakes by phosphorous leads to eutrophic conditions and dense phytoplankton concentrations (biomass).

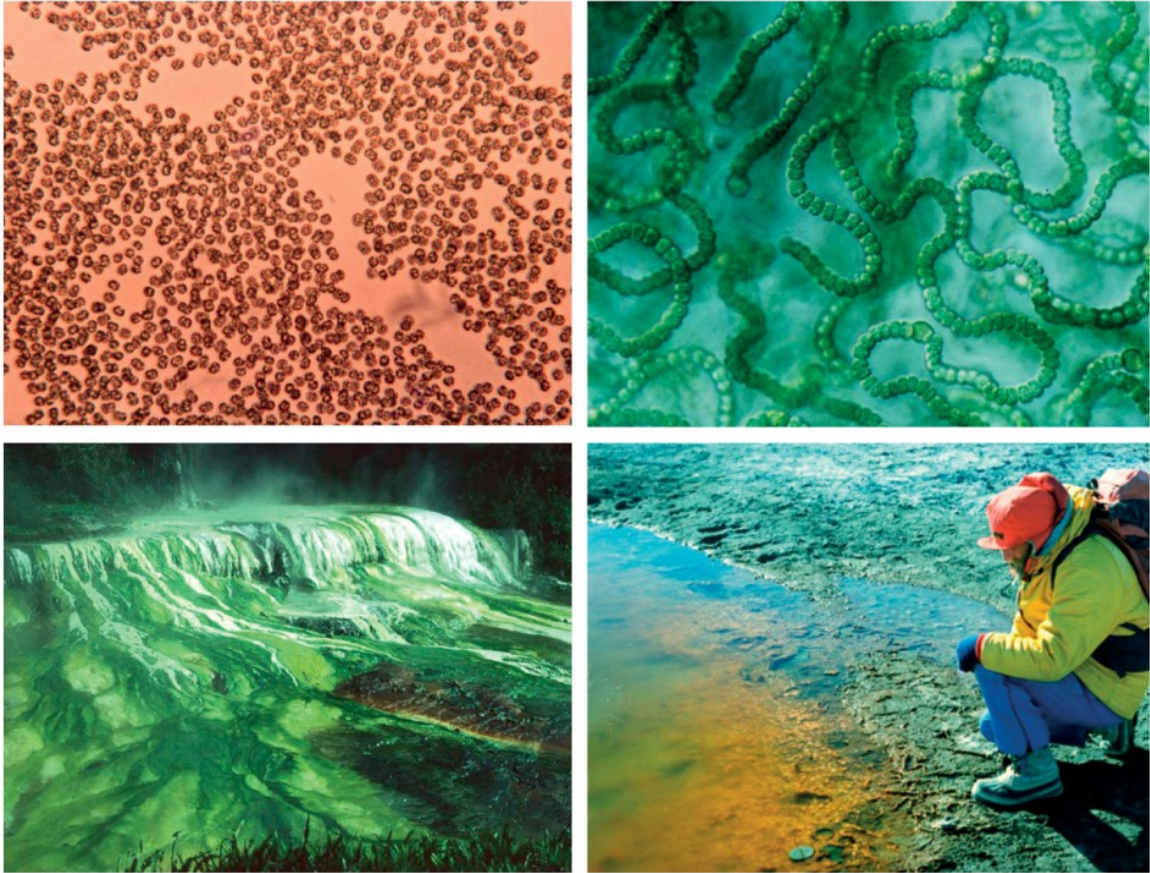


Figure 2.1: Cyanobacteria in inland water ecosystems. Top left: Photomicrograph of *Microcystis aeruginosa* (bloom-forming) from a eutrophic lake. The bright areas inside the cells are due to scattering of light by the gas vacuoles. Top right: Photomicrograph of *Nostoc* (filamentous) from a high Arctic lake. The spherical cells are heterocysts, sites of nitrogen fixation. Bottom right: A carotenoid-rich cyanobacteria (mat-forming) in a pond on the McMurdo Ice Shelf, Antarctica. Bottom left: Cyanobacteria (mat-forming) in a geothermal spring, New Zealand (Vincent, 2009).

Temperature plays a critical role in bloom formation of cyanobacteria. When source water warms above 15 °C, it results in an accelerated growth rate of CB (WHO, 2003a). In addition, CB colonies can adjust their depth in warm water using gas vacuoles to attain optimal conditions, which enhance growth. This buoyancy regulation of bloom-formers, albeit a slow process, can lead to the unforeseen appearance of surface scums, which cause

odors, health, and other water quality issues (Bartram & Rees, 2000). Winds over eutrophic waters might lead to accumulation of scum on shores and bays, which might be significantly more concentrated by a factor of 1,000 or more and result in higher toxicity and exposure risk through recreational waters. Cyanobacteria are able to adapt to extreme environmental conditions and have been found to be able to survive even at 73–74 °C and under extreme pH conditions (4–5) (Oren, 2014). These properties of bloom-formers suggest that with warming global temperatures, the frequency and severity of blooms will become increasingly prevalent. Furthermore, in regions known for CB blooms, with reducing annual rainfall, the nutrient residence time increases and results in an intense proliferation of cyanobacteria (Bartram & Rees, 2000; Figueiredo et al., 2004; Hudnell, 2008; Winter et al., 2011). Thus, there is a need to be able to monitor the source water body for different water quality parameters and detect compounds that can affect the use and safety of water resources.

Cyanobacterial algae can be toxigenic or non-toxigenic in nature; the toxigenic CB release toxins known as cyanotoxins stored inside the cell walls, on cell lysis. The toxins released when the algal cells are still alive and healthy in freshwater are negligible compared to the toxins released on cell lysis (Bartram & Rees, 2000; EPA, 2005). Toxins released in freshwater bodies quickly dissolve in water and rapidly dilute and degrade with time. Cell bound cyanotoxins are, therefore, a bigger concern when it comes to drinking water supply and recreational waters due to increased concentration of localized toxins due to cell lysis in the conformed area (Graham et al., 2010). Figure 2.2 describes the scum-forming potential of cyanobacteria under different concentrations and risk levels to the public from potential exposure.

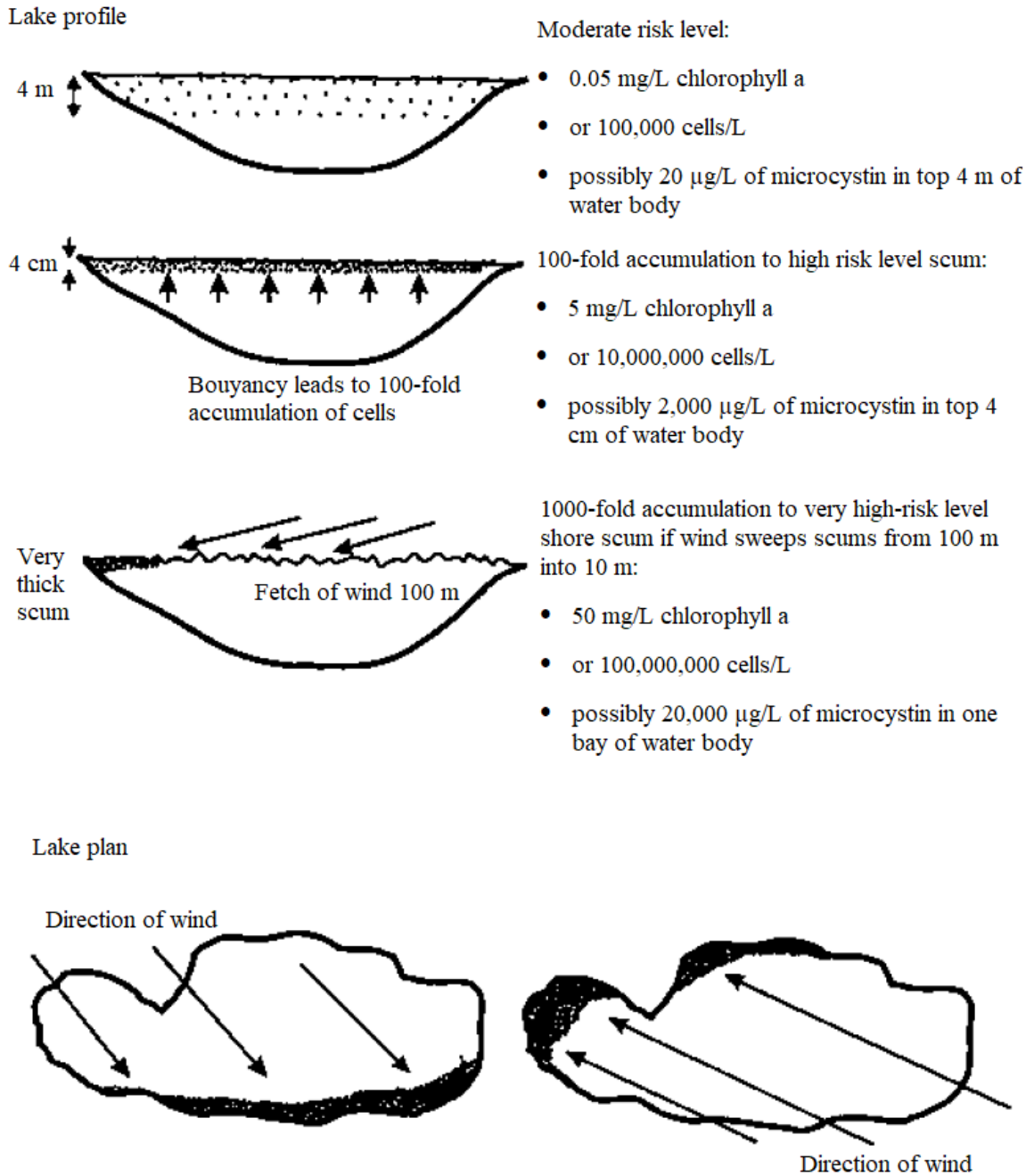


Figure 2.2: Schematic illustration of scum-forming potential cyanobacteria and changing cyanotoxin risk levels (Bartram & Rees, 2000; Falconer, 1999).

This thesis focuses on the detection of planktonic cyanobacteria (also known as microalgae), *Microcystis Aeruginosa*. *Microcystis* can produce toxins called microcystin, which are a group of cyclic peptides that have selective activity against hepatocytes (aka

liver cells) and are known as hepatotoxins. “The cyclic heptapeptides represent two structurally and biologically related classes; microcystin and nodularin, that feature a 3-amino-9-methoxy-2, 6, 8-trimethyl-10-phenyl-4, 6-decadienoic acid (Adda) side group and two variable amino acid positions. These variable amino acids give rise to over 80 different structural isoforms, with each exhibiting a different toxicity profile” (represented in Figure 2.3) (Oren, 2014).

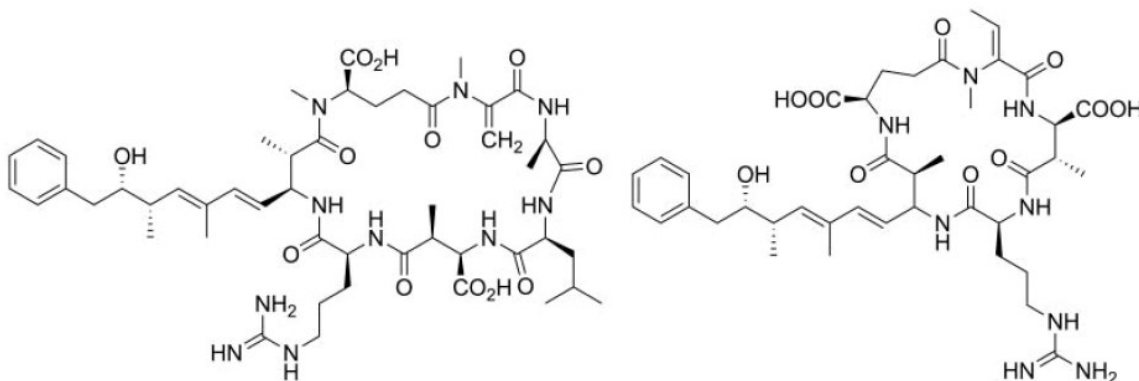


Figure 2.3: Chemical structures of cyanobacterial hepatotoxins, microcystin-LR (left) and nodularin (right) (Oren, 2014).

Cyanobacteria play a vital role in our ecosystem, but excessive proliferation results in environmental and health issues. Many CB species and microalgae are known to produce different kind of bioactive compounds such as mycosporine amino acids (used in cosmetics for its UV absorbing capability), *Spirulina sp.* used in moisturizer (due to moisture retention capability), and *Arthrospira* extract as an anti-aging agent (Saini et al., 2018; Singh et al., 2015). A variety of enzymes produced by CB have industrial potential like hydrolase, cellulase, lipases, proteases, and amylolytic enzymes, among others. Some proteins produced by CB have fungicidal ability. Lipase enzymes have been used to target many cardiovascular diseases and are being tested for the treatment of inflammation, obesity, and pain (Oren, 2014; Saini et al., 2018). Lipase also plays a prime role in biodiesel

production using cyanobacteria (Scaife et al., 2015; Singh et al., 2015). Cyanotoxin is a secondary metabolite produced by CB to help inhibit competing micro-organisms. There has been some research on the use of cyanotoxin for drug development for its anti-bacterial, anti-parasitic, and anti-malarial properties (Mandal & Rath, 2015). Cyanobacteria have also been applied for bioremediation of wastewaters, offering an affordable, sustainable, and alternative method of treatment (AlMomani & Örmeci, 2016; Olsson et al., 2014; Zinicovscaia & Cepoi, 2016).

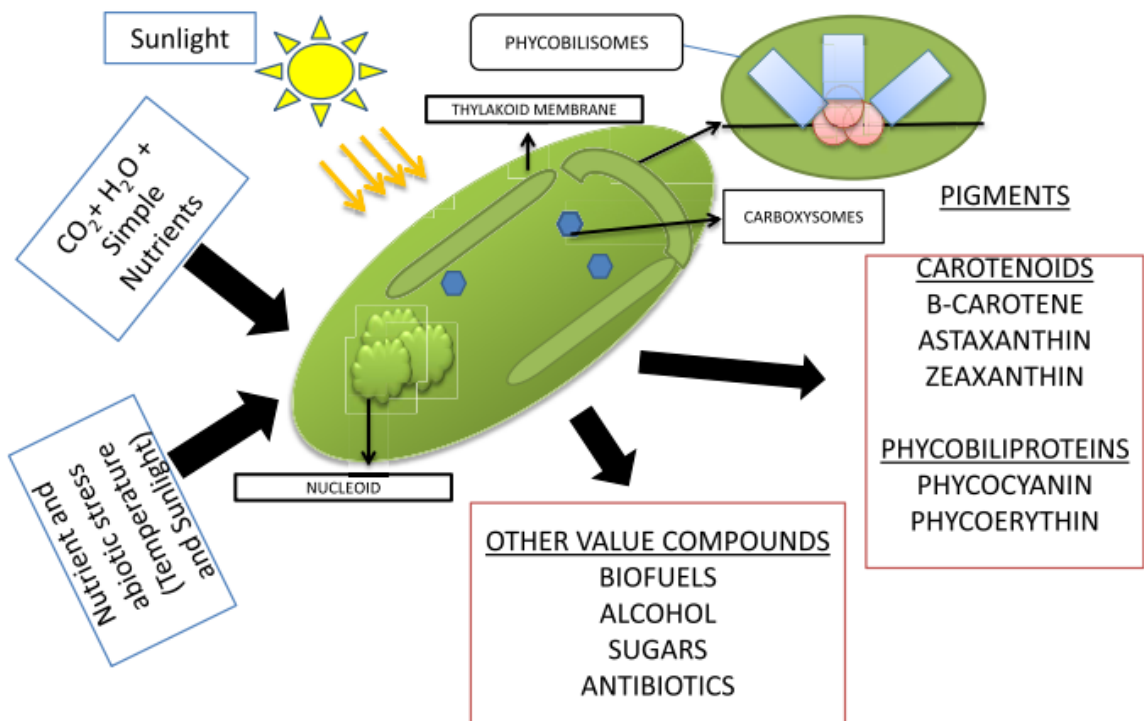


Figure 2.4: An overview of cyanobacterial cell producing potential bioactive metabolites (Saini et al., 2018).

2.3.1 Regulations

Regulations for different cyanobacteria/microalgae and/or their toxins around the world vary based on local occurrences; however, several municipalities/authorities around the world often follow recommendations set by the WHO. Table 2.2 and

Table 2.3 represents guidance values for cyanobacteria and/or their toxin/photopigment around the world, in drinking water and recreational water, respectively. Due to variations in regulations, it is a challenge to rely on a singular monitoring technology for the detection of cyanobacteria/microalgae, and a number of monitoring solutions are used around the world. It should be noted that early detection of potential blooms in water sources assumes that any detected cyanobacteria are to be considered potentially toxic to safeguard public health (EPA, 2015a).

Table 2.2: Examples of guidance values or standards and other national regulations/ recommendations for managing cyanotoxins in drinking water (Chorus, 2005, 2012; Health Canada, 2016; Oren, 2014; WHO, 2003a).

Country/ source	Cyanobacteria and/or Cyanotoxin regulated	Guidance value (GV)	Comments; specific action in case of derogation
WHO	Microcystin-LR	1 µg/L	Depends on setting; strong emphasis on assessing cyanotoxin risks in relation to other risks

Argentina	No requirements for cyanotoxin surveillance, but some water utilities have implemented monitoring; these refer to the provisional guideline by WHO for Microcystin-LR of 1 µg/L		
Australia	Microcystin equivalent to 6500 cells/L or a biovolume of 0.6 mm ³ /L of a highly toxic strain of <i>Microcystis aeruginosa</i>	1.3 µg/L	The Australian Drinking Water Guidelines (2011) are a set of national guidelines which include fact sheets with information on key cyanotoxins. Health Alert can be triggered by the toxin concentrations or the equivalent cell or biovolume concentrations. Trigger levels for each of the 4-key toxin-producing species are also provided for immediate notification to the health authority.
Brazil (2005)	Cyanobacteria	10,000 – 20,000 cells/L	At > 10,000 cells/L, weekly monitoring is required. At > 20,000 cells/L, toxicity testing and/or quantitative cyanotoxin analysis in drinking water are required.
	Microcystins	1 µg/L	
Canada	Microcystin-LR	1.5 µg/L	The limit for Microcystin-LR is considered protective against exposure to other Microcystins; monitoring frequencies driven by bloom occurrence – more frequent where there is a history of bloom formation

Czech Republic	Cyanobacteria in raw water	≥ 1 colony/L or ≥ 5 filaments/L	<u>Vigilance Level</u> : quantification of cyanobacteria in the raw water s at least once per week; visual observations of the abstraction point (water blooms at the surface of water level)
		$\geq 2,000$ cells/L or ≥ 0.2 mm ³ /L biovolume or ≥ 1 µg/L <i>Chl-a</i>	<u>Alert Level 1</u> : attempt reduction by changing abstraction depth. If that is not possible, ascertain that treatment sufficiently reduces cyanobacteria and toxins (data from operational parameters, if necessary, also toxin analyses)
		$\geq 100,000$ cells/mL or ≥ 10 mm ³ /L biovolume or ≥ 10 µg/L <i>Chl-a</i>	<u>Alert Level 2</u> : as Alert Level 1, but with stronger emphasis on treatment efficacy and microcystin monitoring
	Microcystin-LR in treated water	1 µg/L	Monitored once per week in treated water
Cuba	Phytoplankton cells	< 20,000 cells/mL	Monthly visual inspection and sampling at least four months a year
	Cyanobacterial cells	< 1,500 cells/mL	

No regulatory requirement, but framework currently being tested	Phytoplankton and proportion of cyanobacteria	20,000 – 100,000 cells/L; > 50% cyanobacteria	Alert: increased sampling (weekly and more sites); daily inspection; notification to public health unit and local managers; report to local government; warning of the public
	Any report of toxic effect (humans or animals) or bloom scum presence	At least one of the species	Action (in red): as for “Alert”, but with increased actions for public communication and water use restrictions
France	Microcystins	1 µg/L	Analysis required in raw water and at the point of distribution only when cyanobacteria proliferate (visual observation and/or analytical results)
Finland	Potentially toxic Cyanobacteria in raw water (as cell counts or biomass)	> 5000 cells/L or >1 mg/L biomass	Microcystin monitoring; enhanced treatment
		> 100,000 cells/L or > 20 mg/L biomass	Change of abstraction site and/or restrictions of water use; information to the water users, particularly if Microcystins are found in finished drinking water
	Microcystins (raw water)	> 1 µg/L	Restrictions of water use; unlikely on basis of experience

	Microcystins (drinking water)	> 10 µg/L	Ban on water use; highly unlikely
Germany	No specific cyanotoxin regulations as only about 20% of the water supply is from surface water, and that mostly from well protected reservoirs. However, for non-regulated chemicals, the Drinking-water Ordinance requires that they do not occur in hazardous concentrations. On this basis, where cyanobacteria do occur, the WHO GV can be applied for Microcystins . National guidance for substances with incomplete toxicological evidence proposes <0.1 µg/L if carcinogenesis cannot be excluded (until data are generated that allow higher levels), and this can be applied to Cylindrospermopsin .		
Hungary	Drinking-water legislation includes biological parameters to be monitored by microscopy, e.g., Cyanobacteria	Frequency of examination based on the amount of water supplied and source of drinking water (cyanobacteria if source is surface water); at least once a year for every network for all biological parameters	
Italy	The national decree includes algae as an accessory parameter to monitor if local authorities presume a risk, based on the provisional WHO GV for Microcystin-LR .		
New Zealand	Microcystins (as MC-LR equivalents)	1 µg/L	Effective implementation of the protocols required by Public Health Risk Management Plans has prevented concentrations > GV from reaching the consumers

Singapore	Microcystin-LR in free and cell-bound forms	1 µg/L	Every supplier of piped drinking water is legally required to prepare and implement a water safety plan to ensure that the piped drinking water supplied complies with the piped drinking water standards (stated as 1 µg/L for total microcystin-LR, in free and cell-bound forms).
Spain	Microcystins	1 µg/L	To be analysed when eutrophication is evident in the water sources
Turkey	Cyanobacteria	> 5,000 cells/L or > 1 µg/L <i>Chl-a</i>	Monthly analysis if in raw water; if exceeded, weekly sampling (of water column) and toxin analysis
	Sum of all Microcystins	1 µg/L	If exceeding GV, toxin analysis in treated water and advanced treatment (ozonation or activated carbon) or alternative water supply
South Africa	Microcystins-LR	1 µg/L	Supported by guidelines for <i>Chl-a</i> and cyanobacterial cell counts
United States of America	No national requirements, but action taken by many of the States. A general GV for Microcystin of concentration 1 µg/L is widely accepted by most states. Table A.9 (Appendix, shows the approaches pursued by each of 21 states).		

Table 2.3: Examples of national regulations or recommendations for managing cyanotoxins in water-bodies used for recreation (Chorus, 2005, 2012; Health Canada, 2016; Oren, 2014; WHO, 2003a).

Country/ source	Parameter regulated	Values	Action taken/ consequences of derogation
WHO	Cells or <i>Chl-a</i> with dominance of cyanobacteria	20,000 cells/L or 10 µg/L chlorophyll a	Information to site users and relevant authorities. Short-term adverse health outcomes (e.g., skin irritations and gastrointestinal illness, probably at low frequency)
		100,000 cells/L or 50 µg/L chlorophyll a	Information to site users and relevant authorities; watch for scums; restrict bathing and further investigate the hazard. Potential for long-term illness with some species Short-term adverse health outcomes (e.g., skin irritations and gastrointestinal illness).
European Union	Requires ‘bathing water profiles’ indicating – among other parameters – the potential of the site for cyanobacterial proliferation; monitoring based on the bathing water’s history and regional climatic conditions; conformity as a matter of appropriate management measures and quality assurance, not merely of measuring and calculation. Applies to any element of surface water where a large number of people practice bathing and bathing is not prohibited or advised		

	against (termed “bathing water”). When cyanobacterial proliferation occurs and a health risk has been identified or presumed, adequate management measures shall be taken immediately to prevent exposure, including information to the public.		
Australia	Cells or Biovolume	≥500 to <5,000 cells/L <i>M. aeruginosa</i> or biovolume >0.04 to <0.4 mm ³ /L for the combined total of all cyanobacteria	Green level Surveillance mode: Regular monitoring
		≥5,000 to <50 000 cells/L <i>M. aeruginosa</i> or biovolume ≥0.4 to <4 mm ³ /L for the combined total of all cyanobacteria with a known toxin producer dominant or ≥0.4 to <10 mm ³ /L for the combined total of all cyanobacteria where known toxin producers are not present	Amber level Alert mode: Notify agencies as appropriate Increase sampling frequency Regular visual inspections of water surface for scums Decide on the requirement for toxicity assessment or toxin monitoring
		≥ 10 µg/L total Microcystins or ≥ 50,000 cells/L toxic <i>M. aeruginosa</i>	Red level Action mode: Continue monitoring as for alert mode Immediately notify health authorities for advice on health risk

		<p>or biovolume $\geq 4 \text{ mm}^3/\text{L}$ for the combined total of all cyanobacteria with a known toxin producer dominant</p> <p>or $\geq 10 \text{ mm}^3/\text{L}$ for total biovolume of all cyanobacterial material where known toxins are not present</p> <p>or cyanobacterial scums consistently present</p>	<p>Toxicity assessment or toxin analysis (if this has not already been done)</p> <p>Health authorities warn of risk to public health (i.e., the authorities make a health risk assessment considering toxin monitoring data, sample type and variability)</p>
Canada	<p>Microcystin-LR</p> <p>or Cell Counts</p>	<p>$\leq 20 \text{ }\mu\text{g/L}$</p> <p>$\leq 100,000 \text{ cells/L}$</p>	<p>If either of the guideline values is exceeded, a swimming advisory may an advisory has been issued should be avoided until the advisory has been rescinded</p>
Cuba	Phytoplankton	$< 1,500 \text{ cells/L}$	<p>Monthly visual inspection and sampling at least four months a year</p>
	Cyanobacterial	$< 500 \text{ cells/L}$ (or slightly above)	
	<p>Phytoplankton</p> <p>or proportion of cyanobacteria</p>	<p>20,000 – 100,000 cells/L; $>50\%$ cyanobacteria</p>	<p><u>Alert</u>: increased sampling (weekly and more sites); daily inspection; notification to the public health unit and local managers; report to local government; warning of the public</p>

	Any report of toxic effect (humans or animals) or bloom scum presence		Action (in red): as for 'Alert' but with increased actions for public communication
Czech Republic	Cells and/ or Chl-a	>20 000 cells/mL	1 st warning level
		>100 000 cells/mL	2 nd warning level: closure for public recreation
Denmark	Microscopy; Chl-a	High <i>Chl-a</i> > 50 µg/L and cyanobacterial dominance	Relevant authorities are informed and decide when and how the public should be informed
France	Visual inspection	Visible bloom, scums, change in water colour	Microscopy examination. If cyanobacteria are absent: no further action. If present: counting and genus identification
	Cyanobacteria	<20,000 cells/L ± 20 %	Active daily monitoring. Counting at least on a weekly basis. Normal recreational activity at the site
		20,000 – 100,000 cells/L ± 20 %	Active daily monitoring. Counting on a weekly basis. Recreational activities are still allowed; the public is informed by posters on site.
Cyanobacteria and Microcystins	> 100,000 cells/L ± 10 %. 25 µg/L MC-LR equivalent ± 5 %	if MC < 25 µg/L bathing and recreational activities are restricted.	

			<p>if MC > 25 µg/L bathing is banned and recreational activities are restricted.</p> <p>In either case, public is informed.</p>
Germany	<p>Transparency in combination with an indicator for cyanotoxin potential: Chl-a with dominance of cyanobacteria</p> <p>or Biovolume</p> <p>or Microcystins</p>	<p>Secchi Disk reading >1 m and < 40 µg/L <i>Chl-a</i></p> <p>or <1 mm³/L Biovolume</p> <p>or <10 µg/L MC</p>	Monitor further cyanobacterial development
		<p>Secchi Disk reading < 1 m and > 40 µg/L <i>Chl-a</i></p> <p>or > 1 mm³/L Biovolume</p> <p>or > 10 µg/L MC</p>	Publish warnings, discourage bathing, consider temporary closure
	<p>Scums and/ or Microcystins</p>	<p>Observation of heavy scum and/or > 100 µg/L MC</p>	Publish warnings, discourage bathing, temporary closure is recommended
Hungary		< 10 µg/L <i>Chl-a</i>	Excellent

	<p><i>Chl-a</i> with dominance of cyanobacteria</p> <p>or cell counts</p> <p>or Microcystin-LR equivalents</p>	<p>or < 20,000 cells/L</p> <p>or < 4 µg/L MC</p>	
		<p>< 25 µg/L <i>Chl-a</i></p> <p>or < 50,000 cells/L</p> <p>or < 10 µg/L MC</p>	Good
		<p>< 50 µg/L <i>Chl-a</i></p> <p>or < 100,000 cells/L</p> <p>or < 20 µg/L MC</p>	Acceptable
		<p>> 50 µg/L <i>Chl-a</i></p> <p>or > 100,000 cells/L</p> <p>or > 20 µg/L MC</p>	Unacceptable
Italy	<p>Cell counts combined with identification of</p>	< 20,000 cells/L	If possible, daily visual observation; weekly counting
		20,000 – 100,000 cells/L	Daily visual observation; at least weekly counting; information to the public; quantification of microcystins

	genus and, if possible, species	> 100,000 cells/L	Bathing prohibited until quantification of microcystins; information to the public; at least weekly counting
	Microcystins	> 25 µg/L	Bathing prohibited
New Zealand	Cells	< 500 cells/L	<u>Surveillance</u> : Where cyanobacteria are known to proliferate, weekly or fortnightly visual inspection and sampling between spring and autumn
	Biovolume	0.5 to < 1.8 mm ³ /L of potentially toxic cyanobacteria or 0.5 to < 10 mm ³ /L total biovolume of all cyanobacterial material	<u>Alert</u> : increase inspection and sampling to weekly, including multiple sites; notify the public health unit
	Microcystins or Biovolume or Scums	≥ 12 µg/L total microcystins or biovolume ≥ 1.8 mm ³ /L of potentially toxic cyanobacteria or ≥ 10 mm ³ /L total biovolume of all cyanobacterial material or consistent presence of scums	<u>Action</u> : Continue monitoring as for alert; if potentially toxic taxa are present, consider testing samples for cyanotoxins. Notify the public of a potential risk to health.

Singapore	<i>Chl-a</i>	$\leq 50 \mu\text{g/L}$	Status of the sites reviewed annually. If the assessment is that the water body is unsuitable for primary water contact activities, the public is notified.
Spain	Probability for cyanobacterial proliferation	Low probability	Criteria for assessment of health risk and response are set locally; some health authorities use WHO scheme, others include further risk parameters (such as number of users, type of use); temporary closure has occasionally occurred based on the abundance of cyanobacteria
		Medium probability	
		High probability	
Turkey	Cells or Microcystin-LR or <i>Chl-a</i> (if largely from cyanobacteria)	$< 20,000 \text{ cells/L}$ or $< 10 \mu\text{g/L}$ Microcystin-LR or $< 10 \mu\text{g/L}$ <i>Chl-a</i>	<u>Level 1</u> : recreational activities are allowed to continue, and users are informed by posters on site. Monitoring (sampling, counting and species identification) should be done fortnightly.
	Cells or Microcystin-LR	$20,000 - 100,000 \text{ cells/L}$ or $> 25 \mu\text{g/L}$ Microcystin-LR	<u>Level 2</u> : At $> 20,000 \text{ cells/L}$, microcystins are analysed. If MC-LR equivalents $> 25 \mu\text{g/L}$, immediate action to inform relevant authorities and public. Discourage users from swimming and other water-contact activities by advisory signs on site.

	Scums in bathing area	Visual inspection	<u>Level 3</u> : all activities in the water may be prohibited.
United States of America	No national requirements, but action taken by many of the States. Table A.9 (Appendix, shows the approaches pursued by each of 21 states).		

Canada is the second largest country in the world covering 9,984,670 km² area and faces numerous logistical and jurisdictional challenges in ensuring water contaminants are at low levels (minimal impact to human health) to provide safe drinking and recreational waters. Approximately 10% of Canadian land is covered by freshwater and Canada shares some of the largest water bodies like the Great Lakes are shared binationally with the USA, which results in varied water usage, basin development, and nutrient-related impacts. Some of the more densely populated provinces in Canada have developed their own bloom risk management programme, based on the significant differences in population density and associated impact on surface waters, while building on Health Canada, (2016) and WHO, (2003b) frameworks. Table A.10 summarizes national and provincial drinking and recreational water quality guidelines and standards across Canada. (Chorus, 2005, 2012; Health Canada, 2016).

2.3.2 Occurrences and Impacts

Due to eutrophication and climate change, cyanobacterial proliferation is increasing, making it reasonable to predict that the risk of human exposure is rising. Harmful cyanobacterial blooms (CyanoHABs) produce a variety of taste, odor, and toxin compounds which strongly affect water quality. The greatest concern is the production of three major classes of toxins: neurotoxins, which attack the nervous system; hepatoxins, which attack liver cells; and dermatoxins, which result in skin irritation (Health Canada, 2016; Vincent, 2009; Winter et al., 2011). Planktonic toxin-producing cyanobacteria have been found in freshwaters, brackish waters, and marine waters (Codd et al., 1999). The most common and widespread toxin-producing species in eutrophic lakes and reservoirs around the world is *Microcystis aeruginosa*, which is a bloom-forming species that produces a cyclic peptide hepatotoxin known as microcystin, which is known to cause chronic health effects (Pelaez et al., 2010). This specific genera of microalgae are the primary focus of this study for detection in the source water.

Several reports on the death of animals, including farm stock, birds, dogs, fish, invertebrates, and a few humans have been caused by cyanobacterial toxins over the years (Bajpai et al., 2011; Codd et al., 1999; Corbel et al., 2014; Health Canada, 2016; Hudnell, 2008; Mohamed et al., 2015; Pelaez et al., 2010). The presence of toxins in drinking source water bodies and recreational waters are of notable concern, as it directly impacts human and animal health and might cause temporary closure of water supply utilities. The toxins produced by CB are water-soluble and are not destroyed by simple boiling before consumption. It is inherently difficult to manage algae after bloom formation, as there is a large variability in toxin production between different strains of CB of the same species

based on the source water condition (Chorus et al., 2000; Vincent, 2009). This pushes the need for using improved techniques for sensitive detection and regular monitoring of cyanobacteria in source water, prior to a bloom formation, so as to enable local authorities to take corrective action in time (Hudnell, 2008). Figure 2.5 represents the socio-ecological impacts due to cyanoHABs in freshwater (Bajpai et al., 2011).

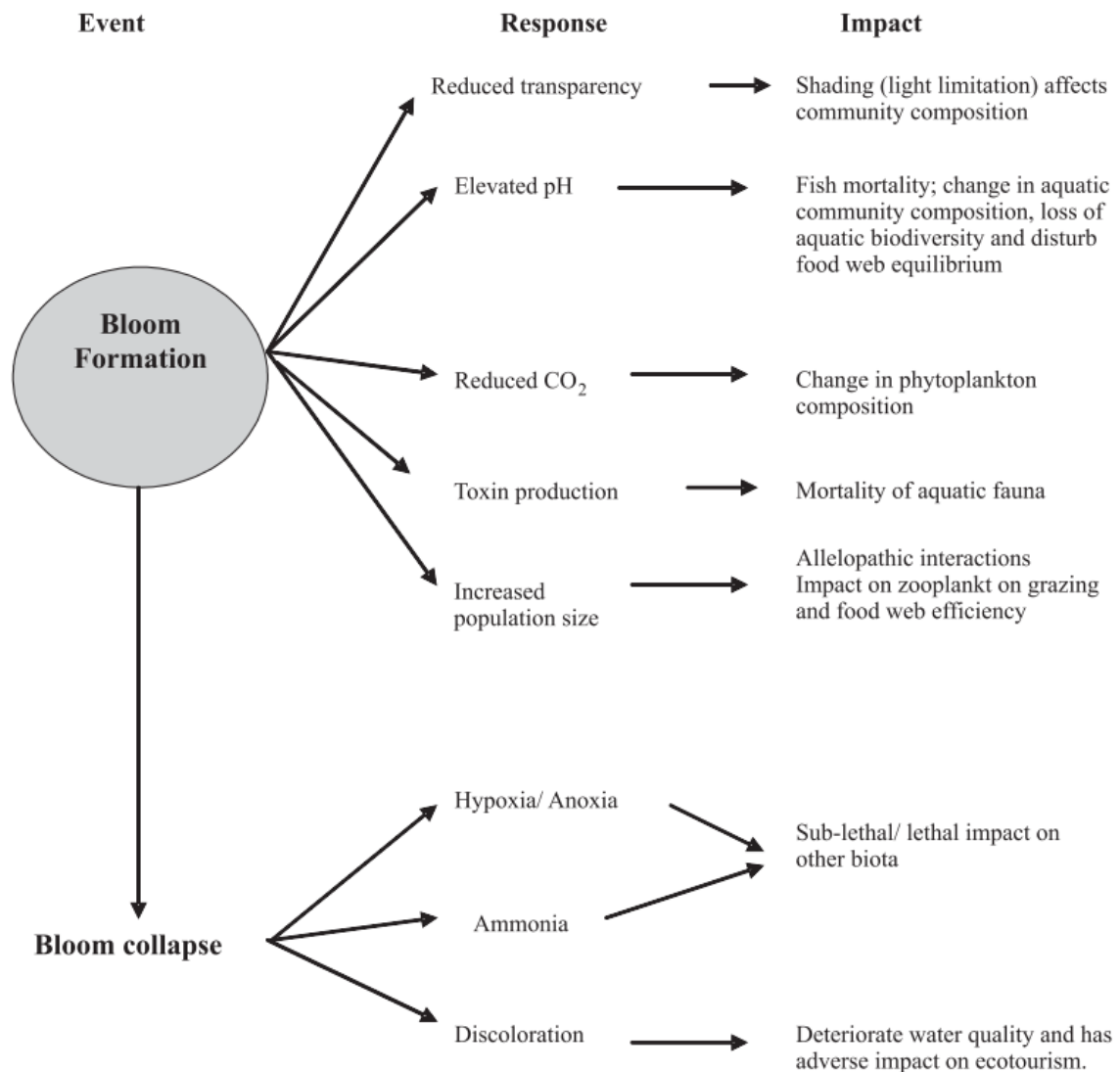


Figure 2.5: Summary of socio-ecological response and impacts associated with freshwater cyanobacterial blooms (Bajpai et al., 2011).

Exposure to cyanotoxins can be caused by three major routes; inhalation (aspiration), dermal contact (skin), and ingestion (oral) (Chorus et al., 2000). Of the three, ingestion is the predominant and lethal route of exposure. It was reported that for microcystin-LR, the lethal density (LD) for inhalation was found to be 10 times greater than oral ingestion (Bajpai et al., 2011; Codd et al., 1999; Pelaez et al., 2010). Daily drinking water and accidental recreational water intake are the most common routes for oral ingestion. Illness associated with ingestion of cyanobacterial toxin via drinking water in Canada, the USA, Australia, and Zimbabwe have been reported before and resulted in several thousand cases for gastroenteritis disorders, liver effects, headache, and muscle weakness (Mohamed et al., 2015). Cases for dermal contact of cyanobacteria leading to skin irritation and allergic reactions have been report for at least the last 50 years in marine coastal waters (Bajpai et al., 2011; Codd et al., 1999; Health Canada, 2016; UNESCO et al., 2004). Usual symptoms of exposure include rashes, asthma, conjunctivitis, blisters, allergic reaction resembling hay fever, ear and eye irritation, some of which have been routinely reported by swimmers in coastal waters containing cyanobacteria around Hawaii, Okinawa, and Florida (Codd et al., 1999).

Freshwater cyanoHABs are pervasive throughout Canada and the US; and throughout the world in various countries as shown in Figure 2.6 (Bláha et al., 2009; Carmichael, 2006; Hudnell, 2008). In Canada, the great lakes are of particular concern with increasing cyanoHABs. Lake Erie has highly variable cyanoHABs, while Lake Ontario has localized HABs. Cyanobacteria is the most prominent bloom former observed in the western basin of Lake Erie, with toxin concentration measured as high as 21 µg/L microcystin-LR (Boyer, 2007, 2008). In 2011-2012, British Columbia reported an unconventional bloom

of *Aphanizomenon* on an inland lake, where the highest toxin concentration measured was 62.40 µg/L for MC-YR and 7 µg/L for MC-LR. Treated drinking water samples from the lake found microcystins greater than the guidance value (GV) of 1.5 µg/L on 10 occasions (Giddings et al., 2012; Health Canada, 2016). In Manitoba, during summer and fall of 2010, a bloom dominated by *Aphanizomenon* (including *Microcystis*) resulted in a cell count of 340,000 cells/L and toxin concentration of 21.8 µg/L. The treated water resulted in counts less than 1,500 cells/L and a toxin concentration below the GV. In Ontario, between 2009 to 2012, cyanobacteria were detected at 24 to 29 different water sources per year from May till the end of November. The highest microcystin concentration detected was 2,800 µg/L, but the majority of samples were below 20 µg/L. The genus *Anabaena* was most prominently recorded, closely followed by *Aphanizomenon* and *Microcystis* (Giddings et al., 2012; Health Canada, 2016). In Quebec, various drinking water treatment plants have documented cyanobacteria and cyanotoxins in raw water since 2001. The average value of cyanobacterial cells was found to be above 20,000 cells/L with a maximum of 2×10^6 cells/L on one occasion (microcystin concentration of 97 µg/L). Treated waters generally had cyanobacterial concentration below 200 cells/L (MC-LR < 0.1 µg/L) (Health Canada, 2016). In places of scum formation, samples had high microcystin concentrations ranging from 8,000 µg/L to 26,000 µg/L. The most common algae found was *Microcystis* (EPA, 2015a, 2015b).

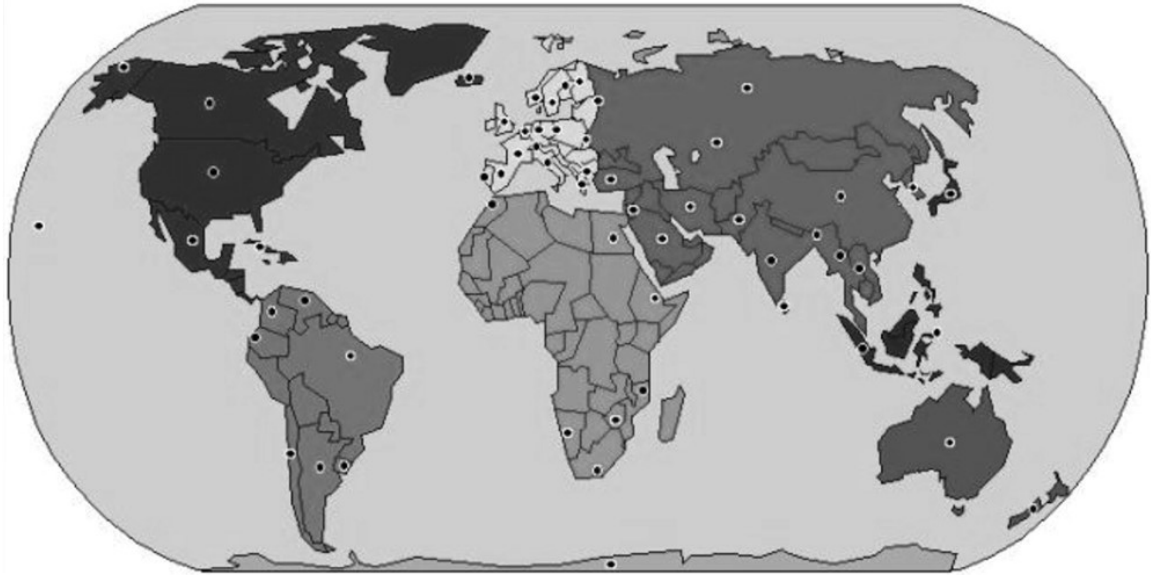


Figure 2.6: Countries reporting one or more cyanoHABs outbreaks (Carmichael, 2006; Hudnell, 2008).

The scarce routes for oral ingestion are via diet (food, especially seafood) and dietary supplements made from cyanobacteria but have been growing recently (due to population growth and global warming). In coastal environments, many toxic species of cyanobacteria occur and have led to several indirect human health impacts after consumption of seafood (such as fish, mussels, shrimp, clams, crabs, among others). It can contain cyanotoxins if farmed from a water source containing CB bloom (due to feeding), and the toxins generated have been shown to bioaccumulate in seafood tissues (Codd et al., 1999; EPA, 2015b; Health Canada, 2016). This is also known as the indirect exposure route. Severely elevated tissue levels of microcystins have been reported in shrimp (55 mg/Kg, hepatopancreas), carp (137 mg/Kg, intestine), tilapia (32 mg/Kg), and prawn (1.2 mg/Kg, hepatopancreas), to name a few (Xie et al., 2005).

Microcystins have been found to accumulate to a lesser extent in the muscle of aquatic organisms; with the highest toxin concentration observed in alewives (20.0 – 37.5 $\mu\text{g/Kg}$)

and northern pike (1.6 – 25.8 µg/Kg) at Lake Erie, and walleye (5.3 – 41.2 µg/Kg), white bass (4.2 – 27.1 µg/Kg), and smallmouth bass (1.5 – 43.6 µg/Kg) at Lake Ontario (Berry et al., 2011; Health Canada, 2016). There have been reports of microcystins in plants and vegetables where contaminated water was used for spray irrigation. Instances of lettuce leaf tissue containing toxins ranging from 8.31 – 177.8 µg/Kg were found (Health Canada, 2016; Wilson et al., 2008). Based on the susceptibility of certain water bodies to form cyanobacterial blooms, exposure through this route is higher in certain regions or populations worldwide (Wilson et al., 2008).

CyanoHABs in source water lead to depletion of dissolved oxygen and loss of water clarity which further deteriorates water quality (Hudnell, 2008; Oren, 2014). Geosmin and 2-methylisoborneol are two of the most prominent molecules that affect the taste and odor of water by imparting an earthy-musty odor to water (Bajpai et al., 2011; Bartram & Rees, 2000; Pelaez et al., 2010; Vincent, 2009). Some CB groups of compounds called cyclocitrals can break down and result in a grassy odor in water.

Stefanelli et al. (2014) conducted an experiments on survival, growth, and toxicity of a strain of *Microcystis aeruginosa* (PCC 7806) while mimicking a few critical features of the gastrointestinal environment. The authors measured growth and toxin production capabilities of *M. aeruginosa* in darkness in the presence of enteric bacteria, at 37 °C and pH 2, following up with recovery in a rich medium in darkness at 37 °C. It was reported that the CB was able to grow in the dark at harsh conditions up to 17 days, and resulted in a survival rate between 30% – 70%, depending on toxicity and age of the cyanobacteria (Stefanelli et al., 2014). The experiments showed that cell lysis in a stimulated gastrointestinal environment resulted in large amounts of toxin released, which were not

affected (degraded) at acidic pH. Following acidic treatment, the authors observed that *M. aeruginosa* restarted growth within 24 hours for 3–4 days independently. This suggests a possible mode of internal exposure to toxins on ingestion of CB, which intricacies risk assessment (Stefanelli et al., 2014).

Economic Impacts

An economic assessment was conducted by Dodds et al. (2009) on the costs associated with harmful algal blooms (HABs) for freshwaters in the United States of America (USA). Figure 2.7 shows several factors that have an impact on the economy due to eutrophication. Due to a wide range of responses induced by different cyanobacterial toxins, it becomes difficult to assess the direct effects of cyanotoxins on human health (Dodds et al., 2009; Oren, 2014). A monetary value cannot be assigned to human death or health from exposure to cyanotoxin, making it difficult to assess the economic impact related to human life. Furthermore, deaths associated with feedstock and wildlife are not well documented and are often not taken into economic assessments (Oren, 2014; Pretty et al., 2003).

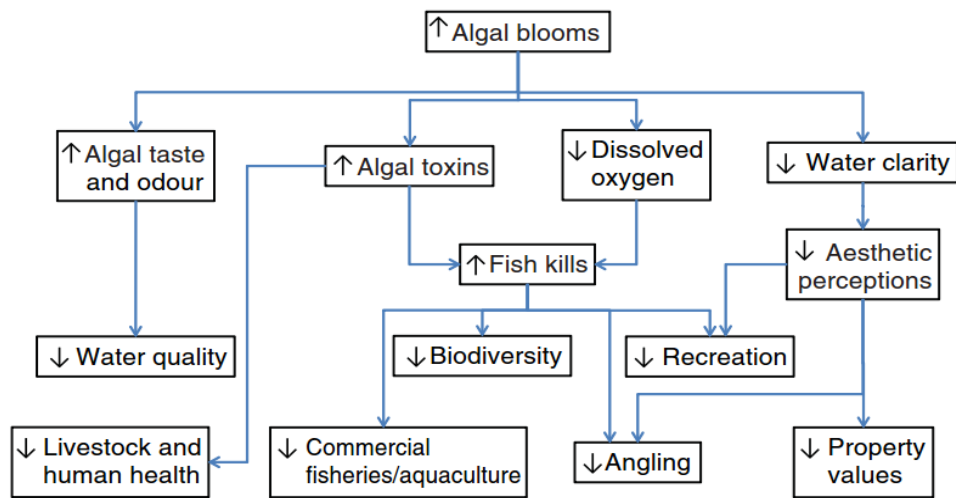


Figure 2.7: Categorization of economic costs of CyanoHABs for freshwater ecosystems (Dodds et al., 2009; Oren, 2014).

The production of foul taste and odor compounds in conjunction with toxin(s) production due to cyanoHABs results in increased costs from added surveillance and monitoring of source waters. Small isolated reservoirs are easier to monitor for cyanobacteria and cost around a few thousand Australian dollars (AUD) per year, typically relying on visual monitoring (Steffensen, 2008). On the other hand, large surface water bodies are significantly more complex to monitor due to variability of CB population, remoteness, multiple water withdrawal points, and a substantial area of bloom (Oren, 2014). China, for example, has persistent and severe HABs on the lakes of Dianchi (298 km²), Taihu (2,537 km²), and Chaohu (775 km²), which results in crucial challenges for monitoring as discussed earlier (Le et al., 2010). The prominent challenge for costs due to cyanoHABs results from the closure of water treatment plants intakes, such as plants in Chaohu (in 1987), and Taihu (in 1990 and 2007), which can result in millions of dollars in closure cost and huge population being impacted (Codd et al., 1999; Le et al., 2010; Oren, 2014; Steffensen, 2008). In 2000, it was estimated that Australia was spending AUD \$8.7 million annually on monitoring and planning for cyanoHABs. In Germany, monitoring of Lake Boehringen (0.735 km²) due to high microcystin concentration (in 2011 and 2012), resulted in estimated cost of €10,000 per year, while requiring additional €80,000 for remediation using an artificial destratification (Oren, 2014). Artificial destratification is the use of external mechanical energy to improve mixing in a reservoir, which in turn is used to reduce the effects of temperature gradient in the water column of source water (Sherman et al., 2010). This further increases the cost of water treatment as additional steps are required to ensure a safe water supply. During a toxic cyanobacterial bloom in Ohio, it

costed an additional US \$300,000 for intensive treatment of water using activated carbon (EPA, 2005).

It should be noted that reducing nutrient input to source water bodies is the most sustainable way for long-term management of HABs. There are substantial costs involved in the management of catchment nutrient loads, including consultation, acquisition of land, and change in land management practices (Oren, 2014). In the United Kingdom (UK), the cost of strategies to reduce nutrient loads due to agricultural sources for eutrophication prevention has been estimated to be US \$4.75 million per year, which is significantly more affordable than the estimated cost to upgrade a wastewater treatment plant of US \$70.4 million per year (Pretty et al., 2003; Steffensen, 2008). In the US, the loss of property was estimated to be in the range US \$14.1 to 141.1 billion per year due to the eutrophication of lakes surrounding private lands (Dodds et al., 2009). Tourism activities related to freshwater are hampered due to cyanoHABs. Dodds et al. (2009) estimated that in the US, the loss incurred to recreational activities and fisheries due to cyanoHABs could near US \$1.16 billion per year. CyanoHABs directly impact fisheries as the toxins in the water kill fish, and cyanotoxins bioaccumulate in fish. Thus, fish farmed from eutrophic water, if consumed, can result in indirect poisoning affecting human health (Falconer, 1999).

2.3.3 Current Detection Methods

The methods used for the determination of cyanobacterial numbers, biomass, and taxa are not universally harmonized and are very variable based on the level of sophistication of the method being used. Simple and rapid methods are often sufficient for preliminary analysis of the algal sample to define the composition at the genus level rather than the species (Bartram & Rees, 2000). It allows determining potential hazard and preliminary

management decisions. More specific methods can be applied to the water sample after confirmation that the sample contains cyanobacteria over a certain threshold and whether it is toxigenic in nature. Currently, there is no single method that can be used for monitoring all cyanotoxins in different water types. The increasing number and variety of cyanotoxins make specific and sensitive evaluation increasingly complex and unachievable (Falconer, 1999; WHO, 2003a). The priority in water monitoring is the analysis of a higher number of samples at a lower level of precision (Bartram & Rees, 2000).

2.3.3.1 Identification

Microscopic inspection of an algal bloom sample is useful and one of the oldest techniques when it comes to the identification of algae (even without quantification). Information obtained on the cyanobacteria detected can be used as an early warning method to alert if harmful cyanotoxins are present. With this information, it makes it easier to determine the appropriate technique for the quantitative determination of toxins (Chorus & Bartram, 1999). It is possible to distinguish most CB from other particles present in water under 200x–400x microscopic magnification based on their morphological features. However, there is some uncertainty to differentiation of cyanobacteria and other algae, as organisms classified under the same species may have significant genetical differences (which decide whether the CB will produce microcystin), despite having similar morphological features (Bartram & Rees, 2000; Srivastava et al., 2013). Thus, the distinction of genera is important for the initial assessment of potential toxicity but lacks certainty for the determination of toxicity.

2.3.3.2 Quantification by direct counting methods

Microscopic enumeration of cyanobacteria is a direct method to detect potentially toxic algae. It requires little equipment other than a microscope, but the method is time-consuming (varying from 10 minutes to 4 hours), depending on the number of species to be identified and the accuracy required (Falconer, 1999; UNESCO, 1996; UNESCO et al., 2004). Table 2.4 shows a summary of the direct counting methods used with their respective preparation time required and sensitivity obtained.

Table 2.4: A summary of methods used to quantify algae (Bartram & Rees, 2000).

Method	Volume (mL)	Sensitivity (cells/L)	Preparation time (mins)
<i>Compound microscope</i>			
Sedgewick-Rafter Cell (counting cell)	1	1,000	15
Palmer-Malloney Cell (counting cell)	0.1	10,000	15
Drops on slide		5,000–10,000	1
<i>Inverted microscope</i>			
Utermöhl (sedimentation chamber)	2–50	20–500 (cells/mL)	2–24 (hours)
<i>Epifluorescence microscopy</i>			
Counting on filters (fluorochrome: Calco Flour)	1–100	10–1,000	15

2.3.3.3 Biochemical methods/ Screening assays

There are two major types of screening assays for cyanotoxins: biochemical and enzyme-linked immunosorbent assays (ELISAs). ELISAs is a more selective method than biochemical assays. Biochemical assays screen compounds based on enzyme inhibition, where the inhibition is inversely proportional to the inhibition of the enzymatic reaction. Inhibition assays often give an overestimation of toxicity as the enzyme can react with other potentially compatible compounds and thus are seldomly used (Altenburger et al., 2015; Gray, 2010; Moreira et al., 2014). On the other hand, immunoassays use antibody interactions to quantify and identify compounds. Antibodies are proteins generated by an immune system in response to the presence of an antigen. Cyanotoxin selective antibodies/ antigens have been developed and are incorporated into assays for cyanobacterial analysis. In a sample, the unknown antigen competes with the known antigen to bind with antibodies. Then the known antigen bound to the antibody is measured, which results in a response inversely proportional to the concentration of the known antigen in the sample. Thus, the greater the response, the fewer toxins are present. ELISAs can use monoclonal or polyclonal antibodies for screening cyanobacterial toxins (Campàs & Marty, 2007). It should be noted that extraction of cyanobacterial toxin is required before performing the screening assay. The detection range, time, cost, and sample size required for ELISAs ranges from 0.02 – 5 µg/L, 60 – 150 mins, US \$360 – 500, and 20 – 100 µL, respectively (Gray, 2010). These assays are very sensitive for detection of cyanotoxin (meeting WHO guidelines for drinking and recreational waters) and do not require a high level of expertise, but have low selectivity because other compounds can cross-react with the binding agents, resulting in interference (possible false positives) and high cost per sample (Srivastava et

al., 2013). Moreover, the elevated cost of enzymes must be considered before using this application. Furthermore, if methods used for the collection of algal samples and toxins are not taken with proper care, errors in qualitative identification increase drastically as the assays have limited shelf life and may underestimate toxin concentration (Campàs & Marty, 2007). Table 2.5 shows examples of commercial assays and their typical detection limit range.

Table 2.5: ELISA commercial assays used for detection and quantification of different cyanotoxins (Moreira et al., 2014).

Toxin	Brand	Concentration range (µg/L)
BMAA	Abraxis	0.05 – 0.50
Microcystin	Beacon	0.10 – 2.00
	Biosense	0.15 – 5.00
	Abraxis	0.15 – 5.00
	Envirologix	0.16 – 2.50
	Enzo	0.15 – 5.00
Nodularin	Beacon	0.04 – 1.00
Saxitoxin	Abraxis	0.02 – 0.40
	Biosense	0.02 – 0.40
	Bioo Scientific	0.02 – 0.32
	Reagen	0.02 – 0.32

2.3.3.4 Molecular methods

Molecular methods have been used to detect, identify, and quantify cyanobacteria and their toxins since the early 1990s. The basis of detection for these methods is by identifying specific genes present in cyanobacteria and their toxins. Molecular methods are more sensitive and specific than other immunological assays. Several methods have been developed and include polymerase chain reaction (PCR) based techniques such as conventional PCR, multiplex PCR, quantitative PCR (qPCR), real-time (R-T) PCR, terminal restriction fragment length polymorphism (T-RFLP), random amplified polymorphic DNA (RAPD), denaturing gradient gel electrophoresis (DGGE); and some non-PCR based methods such as fluorescence in-situ hybridization (FISH) and DNA microarrays (Kurmayer et al., 2017; Lane et al., 2012; Moreira et al., 2011, 2014; Saker et al., 2009). For a detailed description of individual methods and their application, please refer to Herrero & Flores (2008) and Saker et al. (2009). PCR technique is based on in-vitro amplification of a target DNA sequence by utilizing specific primers that target a specific DNA sequence. This is possible due to researched and published PCR protocols that have been developed for detection of cyanobacterial toxins using several biosynthetic primer sequences, based on a previously sequenced cluster of DNA encodes (Loza et al., 2013; Moreira et al., 2014; Saker et al., 2009). PCR-based techniques require reagents and extensive DNA extraction/ isolation before implementing a molecular method. Thus, if the time between sample collection and analysis is high, the resultant quantification might not be accurate (Loza et al., 2013; Mankiewicz-Boczek et al., 2006). qPCR is a versatile method that allows assessment of toxic and non-toxic CB (based on proportion) in a cyanobacterial bloom while quantifying individual algal species present by amplifying the

target DNA present in the sample. Figure 2.8 shows a summary of the approach for molecular-based methods.

R-T PCR is highly useful for quantitative analysis of cyanobacteria and algal-community structure can be evaluated using DGGE analysis or using a fluorescent dye (Srivastava et al., 2013). R-T qPCR for cyanobacterial monitoring is based on the detection of the microcystin synthetase A (*mcyA*) gene from the microcystin gene cluster. RT-qPCR is highly sensitive with detection limits as low as 8.8 – 140 cells/L for *Microcystis spp.* and 258 cells/L for *Cylindrospermopsis* from field samples (Furukawa et al., 2006; Moreira et al., 2011; Zhang et al., 2014). PCR-based methods are highly specific and sensitive while being less time-consuming and labor-intensive than conventional techniques. But PCR methods lack validation in comparison to other well-established chemical methods (such as chromatography). A major drawback of PCR-based techniques is that presence of a toxic marker in cyanobacteria does not necessarily mean the presence of toxicity in source water (as some non-toxic cyanobacteria might possess the same DNA marker as the toxic species). Also, for an unknown algal sample, if an incompatible primer is selected, it might result in incorrect analysis. Analysis time for molecular techniques can range from 16 mins to 18 hrs based on the method being used (Kurmayer et al., 2017; Loza et al., 2013; Moreira et al., 2011, 2014; Ölcer et al., 2015). R-T qPCR can sometimes over-/ under-estimate the concentration of the *mcyA* gene because of uncoupling of DNA during replication, and subsequent cell division, which is attributed to the increase in the quantity of *mcyA* gene during PCR (Furukawa et al., 2006).

Non-PCR based molecular methods such as FISH and DNA microarrays (DNA probes) are relatively recent techniques developed to detect cyanobacteria but are not used and

researched extensively. They can identify cyanotoxins but are not as sensitive as PCR-based methods and are equally time-intensive (Kurmayer et al., 2017; Moreira et al., 2014). Ölcer et al. (2015) developed an on-line DNA hybridization method for cyanobacteria genome detection using a sensitive nucleic acid-based biosensor assay for freshwater detection. The biochip developed used two sets of gold electrodes for the assay and required a set of primers for the experiment. The required analysis time was 25 mins with the application of a high temperature (55 °C) assay for 5 mins and resulted in a detection limit of 6×10^{-12} M of target DNA (Ölcer et al., 2015). Van de Waal et al. (2018) tested multi-probe RNA chips to detect cyanobacteria in six Dutch lakes and found the MDL for anatoxin, cylindrospermopsis, microcystins, and nodularin, to be 5–, 3–, 3.9–, and 3.9– $\mu\text{g/L}$, respectively. Sandwich hybridization assay and FISH assays have improved over the last decade with growing research, and can now be implemented in under 30 mins, and have a detection limit of 2.5×10^4 cells/L and 7×10^4 cells/L, respectively (Greenfield et al., 2008). These techniques are rapid but requires expensive equipment and sample processing.

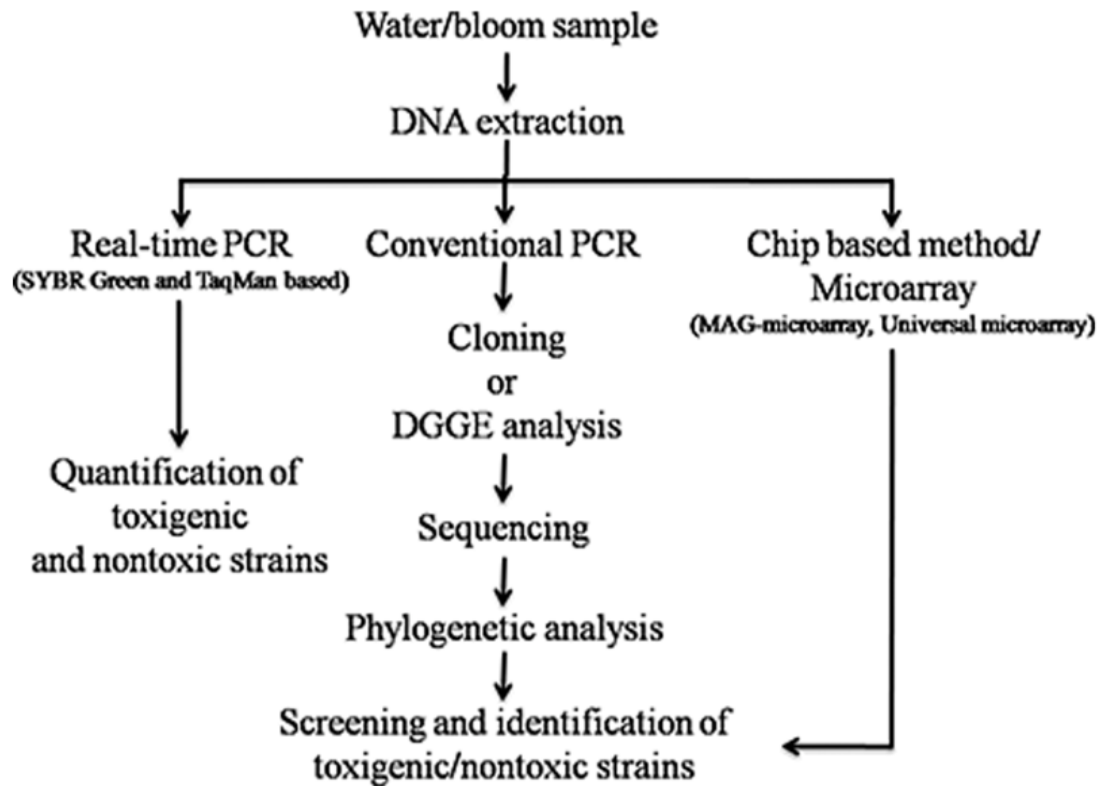


Figure 2.8: Summary of molecular methods for monitoring and identification of cyanobacteria (Srivastava et al., 2013).

2.3.3.5 Spectrophotometric techniques

Pigments are compounds that absorb light at different wavelength ranges in the visible spectrum. The backbone of pigments consists of isoprene and tetrapyrrole rings. The complex structure of these pigments enables them to absorb light and excite electrons at different energy levels. Upon excitation by light, electrons inside the chlorophyll molecule are raised to a higher level and return to the unexcited state after releasing potential energy through light emission, heat, and/ or through a photochemical reaction. Chlorophyll has tetrapyrrole ring structure and is the main light-harvesting pigment in cyanobacteria (Carmichael, 2006; Saini et al., 2018). Six different types of chlorophyll (*Chl-a*, b, d, f, and

divinyl-chl a and b) occur naturally in cyanobacteria, but chlorophyll-a predominates in cyanobacteria (Refer Table A.11 in the appendix for additional detail). Chlorophyll is an excellent photoreceptor and thus is the primary pigment for the detection of cyanobacteria in water sources (Mohamed et al., 2015; Saini et al., 2018). Chlorophylls absorb most in the red region (600–700 nm) of the visible spectrum, while all plants absorb maximum light in the blue region (400–500 nm). Figure 2.9 illustrates the main chlorophylls and their individual absorbance spectra via spectrophotometry (Gray, 2010).

Spectrophotometric analysis is the most common method used to estimate chlorophyll concentrations in samples. It is based on absorbance measurements of the pigment in a sample solution (at single or multiple wavelengths), with a subsequent estimation of chlorophyll concentration (taking cuvette path length into consideration). It should be noted that greater values of absorbance can be achieved by keeping the sample volume to a minimum and increasing the path length of the cuvette (thereby improving the signal-to-noise ratio) (Gray, 2010). The dominant advantage of the spectrophotometric method lies in its simplicity, rapidness, flexibility to measure a variety of pigments with no reagent/pigment extraction, and its ability to analyze and transmit data in real-time.

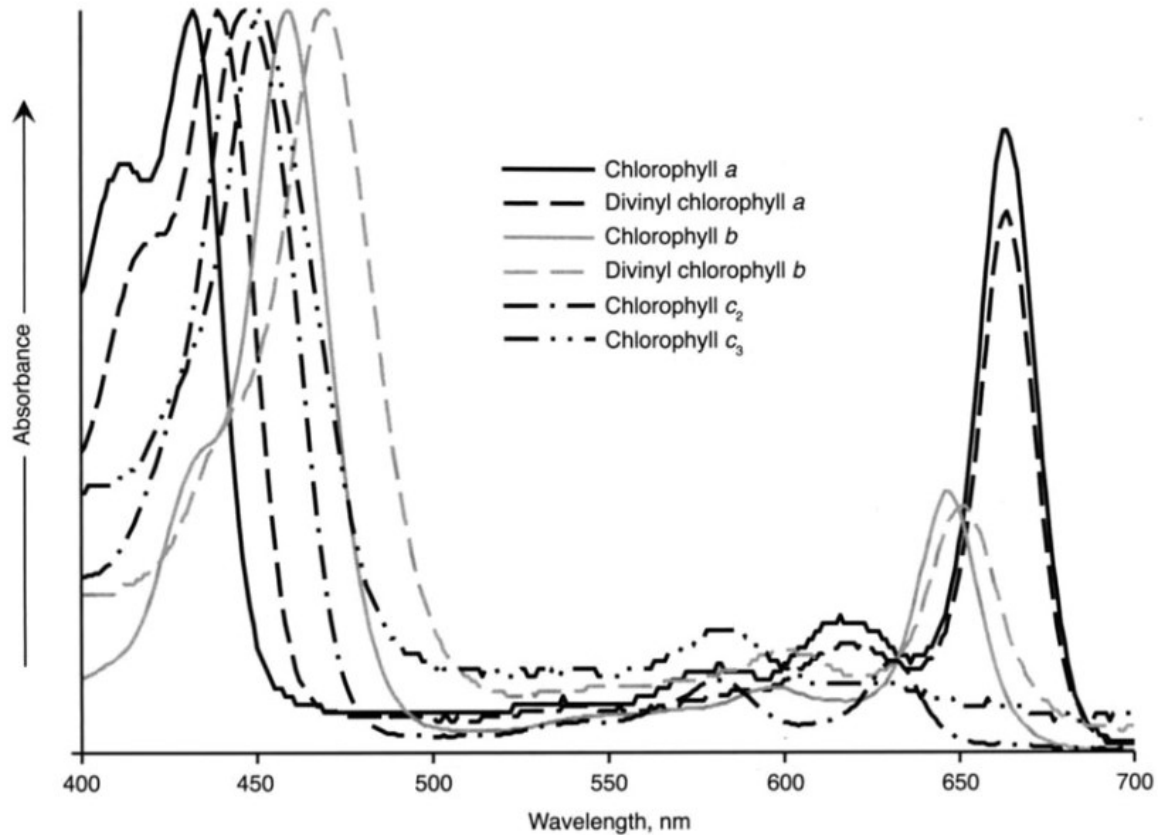


Figure 2.9: In vitro absorbance of select chlorophylls distributed among the spectral classes of algae. Individual spectra derived from standards and normalized to their maximum absorbance value (Gray, 2010).

Additionally, the capital cost required for a spectrophotometer is lower than other technologies and is readily available in most laboratories. However, it comes with its set of disadvantages. It can overestimate chlorophyll concentration in the presence of other interfering pigments (notably phaeopigments aka degradation products as a result of algal chlorophyll pigments). Furthermore, green-sulfur bacteria present in both freshwater and marine systems can cause interference in the estimation and/ or misinterpretation of algae chlorophyll concentration. The main constraints of this method are that it is susceptible to background noise in presence of other constituents (like turbidity), and baseline shift due to changing water characteristics over the year (such as organic carbon content, total solids,

temperature, to name a few) (AlMomani & Örmeci, 2018). Agberien & Örmeci (2019) studied the detection of a toxigenic strain of cyanobacteria (*Microcystis aeruginosa*) in D.I. water and surface water using a 10 mm optical cuvette pathlength. Figure 2.10 represents the absorbance spectra of *M. aeruginosa* in D.I. water and surface water. The study reported detection limits for the cyanobacteria as 338,950 cells/L and 392,982 cells/L for D.I. water and surface water, respectively (Agberien & Örmeci, 2019). Direct UV-Vis spectrophotometric measurement of cyanobacteria shown may not be sensitive enough for early detection of cyanobacteria.

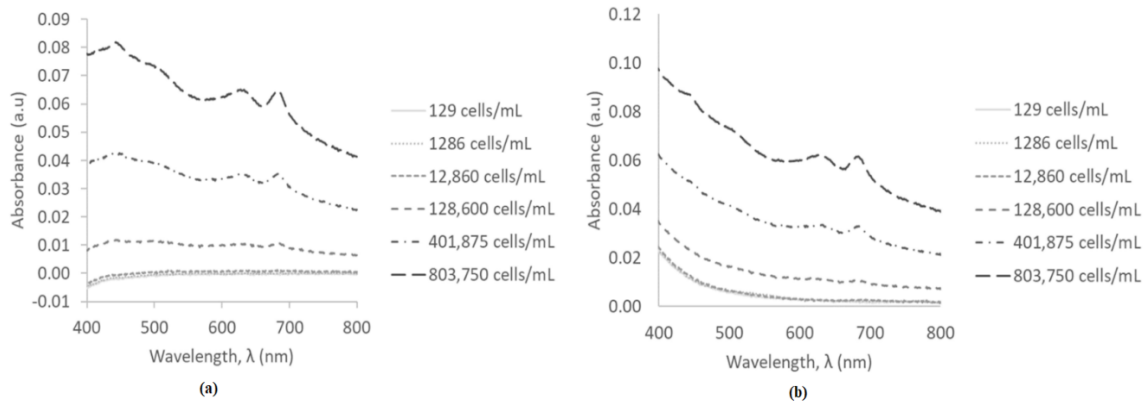


Figure 2.10: Absorbance spectra of *M. aeruginosa* in (a) deionized water and (b) surface water (Agberien & Örmeci, 2019).

First-order derivative of absorbance was implemented in a study to identify key wavelengths to improve the signal-to-noise ratio and reduce background noise while reducing issues that arise from shifting water baseline and overlapping spectral peaks (AlMomani & Örmeci, 2018). Derivative spectrophotometry has gained traction in recent years and has been investigated for detecting cyanobacteria. AlMomani & Örmeci, (2018) investigated the detection of *C. vulgaris* in distilled water, surface water, and wastewater using 10 mm optical pathlength cuvette and found detection limits for the three waters to

be 0.47 mg TVS/L, 0.56 mg TVS/L, and 1.96 mg TVS/L, respectively. The method was compared to the chlorophyll extraction method, which showed detection limits of 19.6 mg TVS/L for distilled water, 38.6 mg TVS/L in surface water, and 48.3 mg TVS/L in wastewater (AlMomani & Örmeci, 2018), proving UV-Vis spectrophotometry to be significantly more sensitive than chlorophyll extraction method. Agberien & Örmeci (2019) researched the effect of Savitzky-Golay first derivative of absorbance to smoothen the derivative spectra and were able to increase the sensitivity of UV-Vis spectrophotometric method using a 10 mm optical pathlength. Figure 2.11 represents the Savitzky-Golay first derivative of absorbance spectra of *M. aeruginosa* in D.I. water and surface water. The peaks observed in the figure are sharper than the traditional spectrophotometric method. For the cyanobacteria under study, the detection limits found were 41,802 cells/mL and 90,231 cells/mL in D.I. water and surface water, respectively (Agberien & Örmeci, 2019). Derivative spectrophotometry shows promise for early detection but at its current stage, may not be sensitive enough to be used as an early warning system. The use of online and real-time spectrophotometers has dramatically increased in recent years as it enables measurement of multiple water quality parameters in tandem such as TOC, COD, BOD, DOM, UV absorbance/ transmittance, nitrogen compounds (like nitrates), and TSS (Burgess & Thomas, 2017). This can minimize cost, multiple equipment requirements, and complexity, making it easier for water utility managers to monitor multiple parameters. However, they have not been extensively studied/employed for real-time monitoring of cyanobacteria and/or microalgae (AlMomani & Örmeci, 2018).

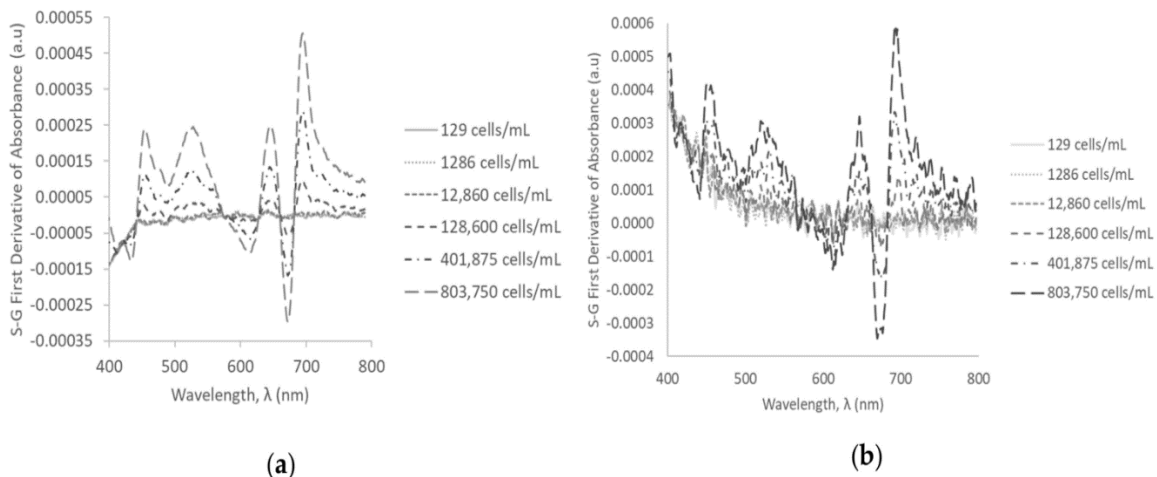


Figure 2.11: Savitzky-Golay first derivative of absorbance spectra of *M. aeruginosa* in (a) deionized water and (b) surface water (Agberien & Örmeci, 2019).

2.3.3.6 Fluorometric techniques

Fluorescence-based sensors are sensitive tools that can provide discrete and continuous monitoring of relative algal biomass but require high caution for interpreting fluorescence measurements for concentration data. The data obtained is relative in comparison to standard laboratory methods, and hence are reported as relative fluorescence units (Gray, 2010; McCullough, 2007). There are two techniques for fluorometric assessment: in-vitro and in-vivo. In-vitro assessment is based on the reaction of chlorophyll molecules solubilized in organic solvents (pigment extraction), followed by excitation with high-energy light. *Chl-a* molecules become excited upon exposure (650 – 850 nm wavelength range) and subsequently emit light (of lesser energy and longer wavelength as energy is inversely proportional to wavelength), which fluoresces red light that can be measured for quantitative estimation (Arar & Collins, 1997; Liu et al., 2020; Millie et al., 2002). However, part of the emitted light may be reabsorbed by *Chl-a* and result in diminished

fluorescence measurement. For in-vivo assessment, live chlorophyll cells are suspended in water and estimated via excitation/ emission characteristics (similar to in-vitro), without the use of chemical/ pigment extraction (reducing analysis time) (Demadrille et al., 2004; Garrido et al., 2019; Gray, 2010; Liu et al., 2020). It is possible to estimate the biomass of a specific class of phytoplankton through the analysis of their spectral signature generated in response to pigment excitation. Eukaryotic algae fluoresce at a peak of around 685 nm (*Chl-a*) and are excited by blue light (410 – 430 nm); cyanobacteria containing phycocyanin (PC) pigment is excited by orange and red light (590 – 630 nm) and emits at a wavelength of 650 nm; and marine cyanobacteria have phycoerythrin (PE) as the primary pigment which is excited by light between 550 – 570 nm wavelength and has a peak emission at 578 nm (Millie et al., 2002; Zamyadi et al., 2016).

Phytoplankton often has a distinct diurnal signal in fluorescence, and the fluorescence measured by the sensor provides data on the photo adaptive state of the cyanobacterial cells and the specific light regime at the measurement time (Gray, 2010). So, the fluorescence yield of the cyanobacterial cell adapted to high irradiance is lower than the yield of the cell adapted to lower irradiance, making it difficult to accurately measure concentration. Additionally, fluorescence yield is temperature-dependent and sensors must be calibrated to a known biological entity to be able to measure a specific bloom of interest (i.e., a unialgal culture for a monospecific bloom or *Chl-a* for mixed blooms) (Zamyadi et al., 2016). A single calibration factor cannot be relied on for every bloom, as different water sources have varied composition and thus needs multiple fluorescence measurements of the source water before implementation of the sensor. Therefore, fluorescence sensors do not quantify data on cyanobacterial biomass or concentration but rather provide relative

phytoplankton concentration. It should be noted that for in-vivo, the fluorescence measured can be from excited chlorophyll-a molecules and/or from other excited photopigments (Demadrille et al., 2004; Gray, 2010). Compared to the spectrophotometric method, fluorometry is more sensitive and does not depend on cuvette handling. Thus, fluorometry is more commonly used for chlorophyll measurement. However, it is not as accurate as spectrophotometric method as it can over- and underestimate the amount of chlorophyll due to degradation products.

The emergence of real-time fluorescent monitoring equipment in the last decade has been widely used for early warning of potentially toxic cyanobacterial blooms. Most R-T technologies have been based on in-situ fluorescence, as each cyanobacterial cell has a fluorescent pigment (Zamyadi et al., 2012a, 2016). A visual example of an in-situ fluorescent probe for the measurement of *D. circinale* (CB) is shown in Figure 2.12. Submersible fluoroprobes are most widely employed, considering their ability for automatic monitoring (at least once every 60 mins), affordable cost, rapidness, and ease of deployment (handling and function). But as there are limited publications validating probes employed in field conditions to consider it the most appropriate technology. The detection limit of the probes has been reported to be between 0.3 – 4 µg/L and 150 – 200 cells/mL (Zamyadi et al., 2016). Refer to Table A.12 for more information on some of the commercially available probes, along with their individual excitation and emission wavelengths. However, probes come with several disadvantages such as a wide wavelength bandpass, complex calibration process (varying with each manufacturer), and the necessity for calibration and biweekly maintenance depending on the source water quality. It should

be noted that all in-vivo probes measure relative fluorescence of specific pigments to estimate concentration (Garrido et al., 2019; Zamyadi et al., 2012b, 2012a).

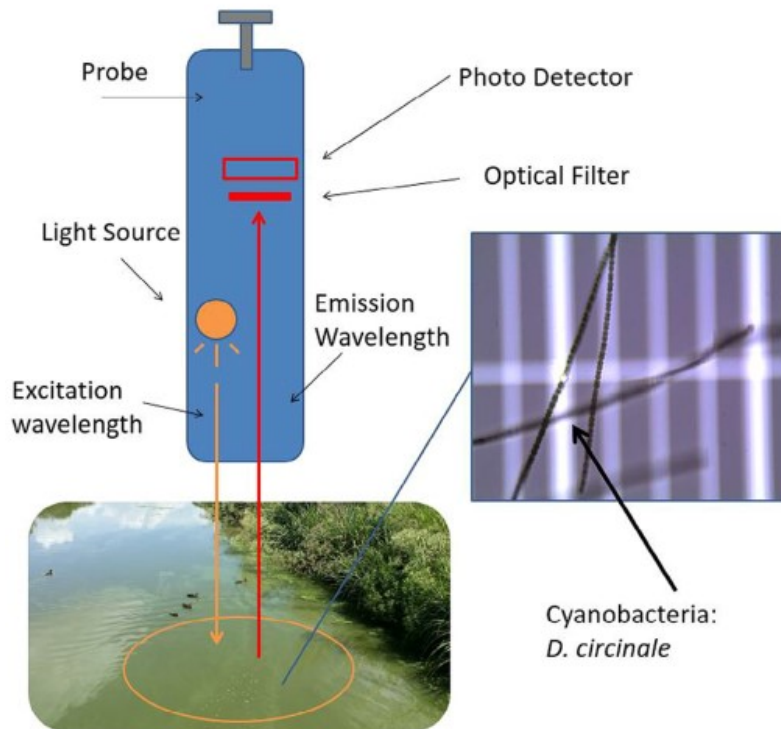


Figure 2.12: Visual representation of an in-situ fluorescence measurement technology (Zamyadi et al., 2016).

Apart from the aforementioned drawbacks, there are various sources of interferences due to cyanobacterial cell characteristics and interferences due to water column optics and water quality to be aware of when implementing in-situ fluorescence techniques (Bertone et al., 2018; McQuaid et al., 2011). Interferences due to cyanobacterial cell character are due to the following sources: (1) varying pigment cell content, (2) varying cell size, biovolume and cellular agglomeration, (3) prior light exposure of cyanobacterial cells to light, (4) presence of *Chl-a* from other phytoplankton and mixed phytoplanktonic populations, (5) presence of other phycobilin protein-containing species, and (6) cell-

bound and dissolved pigment ratio in a natural environment. Additionally, water column optics and water quality interferences are caused by: (1) water turbidity and influence of light scattering particles, and (2) source water temperature, which can result in measurement bias. Studies reported that these interference factors could cause an error in measurement ranging from 20 – 600 % for in-situ measurements. For more detailed information on the sources of interferences, please refer to (Bertone et al., 2018; Bowling et al., 2016; McQuaid et al., 2011; Zamyadi et al., 2016). It was reported that if the calibration range were too wide, a high relative error would occur when measuring low cell concentration. Conversely, having a wide measurement (calibration) range would result in lower accuracy. In addition, for calibration, pure pigments are required, increasing operational costs (Zamyadi et al., 2016).

2.3.3.7 Chromatographic techniques

Chromatography is a reliable and precise method for the separation and quantification of chlorophylls, chlorophylls derivative, and carotenoids (photopigments) at an extremely low detection level (in single or mixed algal samples). It can identify molecules based on their phylogenetic group while identifying their distinct taxa within mixed samples. Pigment chromatography is based on the partitioning of chlorophylls between a polar organic solvent (also known as the mobile phase) and a non-polar substrate (known as stationary phase) (Gray, 2010; Schlüter et al., 2018). An advanced method for definitive separation and quantification of chlorophylls in a multi-pigment mixture was developed based on traditional chromatography and coined high-performance liquid chromatography (HPLC). In HPLC, pigments with the highest polarity elute first, followed by pigments of lower polarities. For analysis, a clarified extract is injected and passed through a

temperature-controlled (usually 40 °C) column packed with spherically shaped ¹⁸C-bonded silica particles via organic solvents at high pressure (Gray, 2010). Pigments attract to the packing particles and layer onto them throughout the column, followed by subsequent elution (based on polarities) and exit the column. Upon leaving the column, they are analyzed using in-line spectrophotometers, photodiode array detectors, and/ or fluorometers. Chromatography techniques are mostly used in conjunction with another analytical method for combined quantitative and qualitative analysis of cyanobacteria (Boiteau et al., 2013; Ortelli et al., 2008). Often a buffering agent (in the mobile phase) is injected into the extract to improve and amplify peaks for detection (Moreira et al., 2014). Table 2.6 shows a review of typical chromatography-based analytical methods used for cyanobacteria and cyanotoxin detection with their respective MDLs and preparation. Currently, LC with a UV, MS, and/ or an ESI detector is the most commonly employed method for cyanotoxin detection. Liquid chromatography-mass spectrometry (LC-MS) is used for the identification and verification of the cyanotoxin variant present in the sample. Matrix-assisted laser desorption/ ionization time of flight (MALDI-TOF) is used for qualitative assessment of cyanobacteria but cannot be implemented for quantification like the other chromatography methods (Moreira et al., 2014; Ortelli et al., 2008). Quantitative analysis is only possible if known toxin standards are available; however, using LC-MS it is possible to identify the cyanotoxin variant present without an available standard (Klejdus et al., 2009). It should be noted that these methods are mandatory by legislation when establishing a toxic bloom response. The main disadvantage of these methods is that they rely on specialized and expensive equipment, which requires an expert to conduct the analysis and interpret the data. Furthermore, sample preparation and pre-treatment are

required, which adds to the analysis time required and increases reagent waste (Moreira et al., 2014; Schlüter et al., 2018; Yen et al., 2011). Figure 2.13 represents the chromatogram obtained via HPLC of some standard chlorophylls and carotenoid (Gray, 2010).

Table 2.6: Chemical and chromatography-based methods for detecting cyanobacteria and their toxins (Moreira et al., 2014).

Analytical Method	Cyanotoxin	MDL	Sample preparation	Reference
HPLC-UV	Microcystins	5 ng (standards) 34 – 170 ng/L (treated and raw water)	C ¹⁸ SPE	(Lawton et al., 1994)
	Microcystin-LR and -RR	1 ng/L	Magnetic SPE	(Li et al., 2017)
MALDI-TOF	Microcystins	0.1 µg/L (water) 0.1 – 0.2 µg/g (microalgae)	Micro SPE-capillary	(Ortelli et al., 2008)
SELDI-TOF	Microcystins	2.5 pg/ 2 µL (water)	Hydrophobic (H ⁴) chips	(Yuan & Carmichael, 2004)
UPLC-ESI-MS/MS	Microcystins	0.04 – 0.1 µg/L (water)	SPE	(Li et al., 2011)
UPLC-MS/MS	Microcystin conjugates and Nodularins	0.001 – 0.04 µg/L	On-line SPE	(Beltrán et al., 2012)
LC-MS/MS	Microcystins and conjugates	0.35 µg/g (fish tissues)	C ¹⁸ HLB	Oasis (Dai et al., 2008)

		Microcystin conjugates and Nodularins	2 – 10 ng/L	C ¹⁸ SPE	(Yen et al., 2011)
On-line MS/MS	LC-	Microcystin conjugates and Nodularins	0.1 – 0.2 µg/L	On-line SPE	(Balest et al., 2016)
On-line HESI-MS/MS	LC-	Microcystin conjugates, Cylindrospermopsin, Anatoxins and Nodularins	0.01 – 0.02 µg/L	On-line SPE	(Fayad et al., 2015)
On-line TOF/MS	LC-	Microcystin conjugates and Anatoxin	0.05 µg/L	On-line SPE	(Ortiz et al., 2017)

HESI heated electrospray ionization, LC-ESI-MS liquid chromatography-electrospray ionization-mass spectrometry, SELDI-TOF surface-enhanced laser desorption/ionization time of flight, SPE solid phase extraction, UPLC-ESI-MS ultrahigh performance liquid chromatography–electrospray ionization in tandem with mass spectrometry

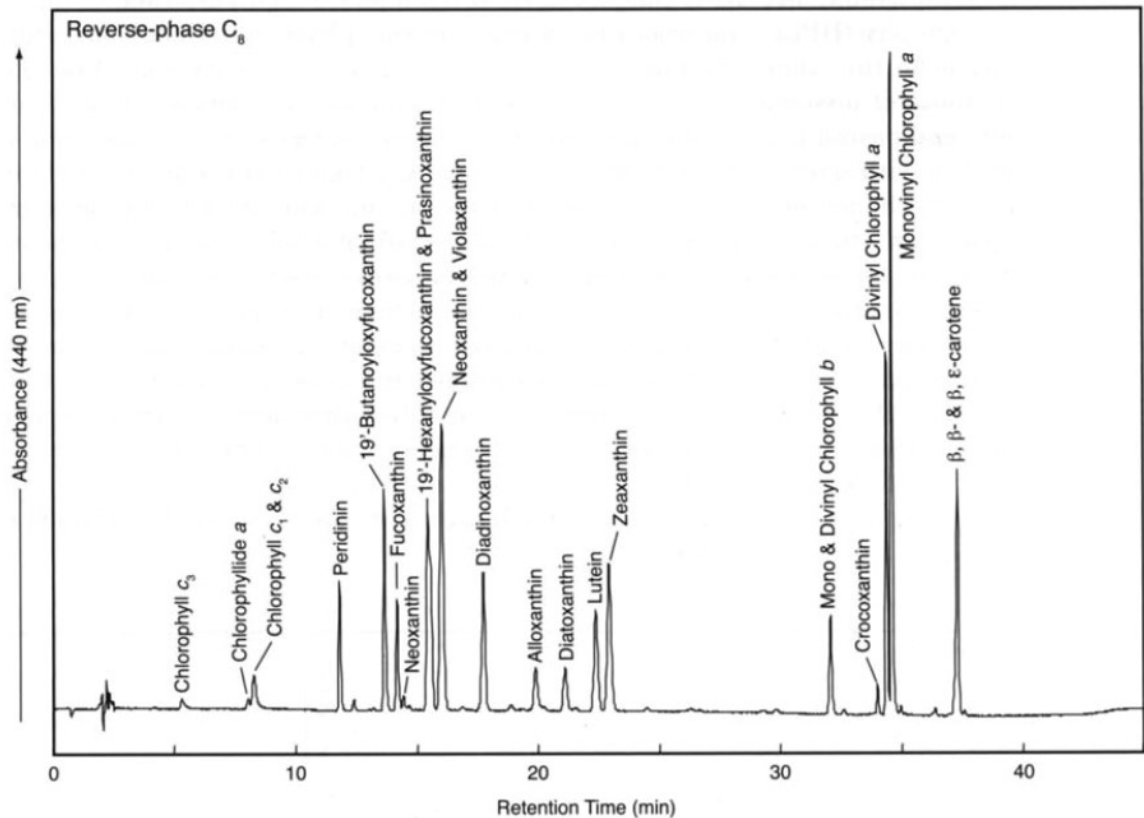


Figure 2.13: Chromatogram of purified chlorophyll and carotenoid standards using HPLC followed by analysis using an in-line photodiode array detector (Gray, 2010).

2.3.3.8 Remote sensing

Remote sensing enables rapid observation and changes in algal blooms in a source water body. Remote sensing uses satellite optical sensors to capture spectral data of source water to monitor the position and area of a HAB. Optical sensors capture electromagnetic energy due to light reflected from the source water body to produce spectral images (Furevik et al., 2004). As optical sensors work in visible and infrared wavelengths, they cannot function under cloudy conditions as it results in masking the sensor signal and reducing monitoring capability (Wang et al., 2015). To overcome the optical sensor issue, synthetic aperture radar (SAR) systems are used to supplement optical remote sensing. SAR systems can provide images irrespective of the weather conditions and can function at all times of

the day. It is challenging to monitor algae blooms using radar systems alone as SAR images create dark regions which correspond to algal blooms, but the same dark regions can be influenced by other environmental factors (such as weather) as well. Several studies have shown SAR and optical sensors used in combination to detect algal blooms (Furevik et al., 2004; Gade et al., 1998; Greenfield et al., 2008). Wang et al. (2015) studied the use of SAR images for bloom monitoring under cloudy conditions and found the overall accuracy of the method to be 67.74%. The authors found that classification accuracy was higher with larger SAR dark regions. SAR images, if not interpreted with care, can result in identifying non-bloom zones as bloom-alike zones. This can be caused by low-wind conditions, which result in low-backscatter regions in SAR images, resulting in the bloom-alike zones. It is virtually impossible to distinguish a bloom zone and bloom-alike zone under low-wind conditions if the two water zones are connected (Wang et al., 2015). Another remote sensing technique involves using a visible infrared imaging radiometer to monitor source waters turbidity for lakes to complement bloom monitoring (Son & Wang, 2019). Remote sensing can be implemented for water bodies known for cyanobacterial blooms and where wide area of sensing is required. However, it cannot classify algal type precisely as the interpretation of images are operator dependent and can result in false positives.

There are specific limitations to all monitoring technologies given their basic design features. Data acquired by sondes deployed at a fixed depth and located at a single site are limited to characterization of that particular site and are not be able to monitor changes at distant sites. This also restricts the information obtained on the water column conditions above or below the sampling point (Gray, 2010; Storey et al., 2011). As chlorophyll-a is used for estimating algal biomass, extreme care and adherence to protocols should be taken

to minimize the impact of sample handling and processing upon chlorophyll transformation and/or degradation (Gray, 2010; Storey et al., 2011).

2.4 Chromium (VI)

Chromium is an odorless and tasteless metallic compound that can be found naturally in humans and animals, as well as in soil, plants, rocks, and volcanic dust. It is a widely distributed metal in the Earth's crust (WHO, 2017). When dissolved in water, chromium changes the water to yield a yellowish color liquid (Figure 2.14). Chromium can exist in the valences of +2 to +6. Trivalent chromium (Cr (III)), hexavalent chromium (Cr (VI)), and the metal form chromium zero (Cr-0) are the three forms of chromium commonly found in the environment. Among the three forms, Cr (VI) is the oxidized and most toxic form of chromium, while Cr (III) is the most stable and less oxidized form (Saha et al., 2011). While Cr (VI) and Cr-0 are mostly produced by industrial processes and found in industrial wastewater due to various metal processing activities (such as electroplating), Cr (VI) can be present naturally in groundwater due to weathering of rocks. Cr (III), on the other hand, occurs naturally in vegetables, fruits, grains, yeast, and meat (Canter, 1985; EPA, 2010). More often than not, chromium is released to the environment due to poor storage, leakage, and/ or improper disposal practices. Chromium compounds are environmentally persistent in water as sediments (EPA, 2010).



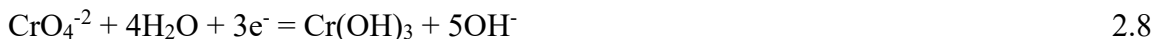
Figure 2.14: Photograph from a groundwater source contaminated with chromium in Kanpur, India (Sharma et al., 2012).

The natural distribution of Cr (III) and Cr (VI) in the environment depends on the redox potential, kinetics, presence of oxidizing or reducing compounds, pH of the solution, formation of Cr (III) salt, and the total chromium concentration (WHO, 2019). Cr (III) predominates in the soil as Cr (VI) is readily reduced to Cr (III) by organic matter. Cr (VI) is 100-fold more toxic than Cr (III) and is highly soluble in water, making it mobile (Saha et al., 2011). Cr (VI) is a strong oxidizing agent and is consistently linked with oxygen. Chromate (CrO_4^{2-}) and dichromate ($\text{Cr}_2\text{O}_7^{2-}$) (illustrated in Figure 2.15) are the most prevalent dissolved hexavalent chromium ions found in the environment, with hydrogen chromate (HCrO_4^-) being the least common form. The three forms of hexavalent chromium exist commonly under different pH regions and can be distinguished by HCrO_4^- and $\text{Cr}_2\text{O}_7^{2-}$ being present between the pH of 2–6, and CrO_4^{2-} at a pH greater than 6. Dichromate,

when present under acidic conditions, is reduced to Cr (III) (Yarbro, 1976). The reduction process of Cr (VI) in acidic conditions can be expressed by:



and under alkaline conditions:



Hexavalent chromium is not effectively removed by traditional alum and ferric coagulants and hence, can pass through the drinking water treatment system with ease (Saha et al., 2011). Cr (VI) must be reduced to Cr (III) during the treatment process to meet safety standards for drinking water consumption. Thus, Cr (VI) monitoring is usually limited to water treatment facilities and effluent discharge from industries (WHO, 2019).

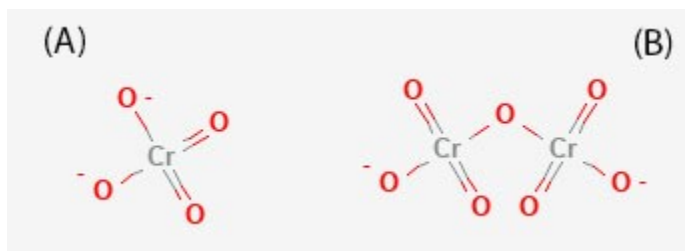


Figure 2.15: Chromate and dichromate structures (PubChem, 2020a, 2020b).

2.4.1 Regulations

Regulations around the world vary based on local government directives and action plans. The European commission currently follows the WHO guideline for 50 µg/L as the maximum contaminant level for total chromium but plans to reduce the value by 50% by forcing the directive to 25 µg/L across Europe starting 2027 (European Commission, 2017). With increasing industrial applications and growing wastewater generation, the

need for monitoring will increase every year. Regulatory bodies often measure total chromium as Cr (III) and Cr (VI) can convert back and forth in the human body and in water depending on their environmental conditions. To ensure that the highest potential risk is addressed, the sample measured for total chromium is assumed to be 100% Cr (VI) (EPA, 2010; WHO, 2017). According to studies conducted by NTP (2008), a concentration of Cr (VI) up to 4.1 µg/L and 2.4 µg/L in drinking water will have no adverse health effects on adults and children, respectively. The state of California has been pushing for stringent Cr (VI) requirements time and time again due to unknown lifelong effects of orally ingesting Cr (VI). They proposed a limit of 10 µg/L as the maximum contaminant level in drinking water to be enforced by law and to further reduce it to a value of 0.02 µg/L in the future (OEHHA, 2011). With the world trend moving towards more conservative guideline value for Cr (VI), it gives a rise to necessity for easier and early monitoring methods.

Table 2.7: A summary of chromium guidelines around the world.

Country/ Source	Contaminant	GV	Reference
EPA	Total chromium	100 µg/L	(EPA, 2010)
WHO	Total chromium	50 µg/L	(WHO, 2017)
FDA	Total chromium	100 µg/L	(ATSDR, 2012)
Canada	Total Chromium	50 µg/L	(Health Canada, 2018)
European Union	Total Chromium	50 µg/L	(European Commission, 2017)
UK	Cr (VI)	50 µg/L	(Rockett et al., 2015)
Australia	Cr (VI)	50 µg/L	(NRMMC, 2017)

2.4.2 Occurrences and Health Impacts

Studies have shown that over 70% of chromium in the environment is from anthropogenic sources, such as metal smelters, refineries, stormwater runoff, leather tanning industries, and discharge from thermal generating stations, among others (Health Canada, 2015; WHO, 2019). Erosion of natural deposits and wastewater discharge from steel and pulp mills are the major sources of Cr (VI). Chromium in different forms is used for chrome plating, making steel and other alloys, for dyes and pigments, catalyst manufacturing, fungicides, ceramic and glass industry, corrosion control, and for leather and wood preservation (Moffat et al., 2018; WHO, 2019). The natural sources for Cr (VI) are rocks (volcanic or metamorphic) and soils, which due to weathering and erosion processes, can release high amounts of toxic Cr (VI) in groundwater and surface water. In summary, the concentrations of Cr in groundwater aquifers and surface water are dependent on the regional geology, weathering processes, precipitation, local industry, and sediment loading rates (Health Canada, 2015, 2018).

Toxicity of a substance is studied with respect to the amount of dose and time scales. A large dose received within a short period is known as acute toxicity, while the same amount of dose received over a longer period in small increments is known as chronic toxicity. Cr (VI) strong oxidizing capacity and ability to penetrate cell membranes readily cause it to be a major concern as an irritant and toxic carcinogen. Hexavalent chromium strongly reacts with DNA and can reduce Cr (VI) to Cr (III) while producing free radicals that can bind themselves to DNA. The intermediates produced during the reduction have been

reported to induce DNA strand breaks in-vitro and mutations in biological systems (McNeill et al., 2012a; Moffat et al., 2018; Saha et al., 2011). Jarczewska et al. (2015) conducted a study on absorption of Cr (VI) in the form of $K_2Cr_2O_7$ which resulted in a direct correlation between increasing dose and induced DNA damage in an immobilized system. For detailed information on the molecular mechanism and metabolism of Cr (VI) in living organisms and thereby induced carcinogenesis, please refer to Saha et al. (2011) and Rockett et al. (2015). Until the early 1980s, incidences among chromate workers for acute and chronic respiratory diseases were well known. Major symptoms due to Cr (VI) inhalation include (but not limited to) ulcers, perforation of the nasal septum, sinusitis, asthma, rhinitis, laryngitis, acute chemical pneumonitis, and bronchogenic carcinoma (EPA, 1998; Yarbrow, 1976). Although inhalation is a serious route, this study focused on the solubilized ingestion route via oral ingestion.

Cr (III) is very mildly toxic to human health, and a minimal lethal dose for humans has been set at 2.29 g/Kg of body weight (Yarbrow, 1976). However, Cr (III) plays an important role in normal biological metabolism and is a required nutrient for our human body (McNeill et al., 2012a; WHO, 2011). According to WHO (2011), 20 – 45 μ g Cr (III) per day is essential for normal energy metabolism. In the stomach and gastrointestinal tract, low doses of Cr (VI) are reduced to Cr (III) (which is considered non-toxic at low doses) due to intragastric reduction, effectively reducing its biological activity. Kirman et al. (2017) reported that there was a higher reduction of Cr (VI) in the gastrointestinal tract of a post-meal sample (at pH 2.0, higher stomach pH) as compared to a fasted sample (lower stomach pH). Thus, increasing the risk for individuals with elevated gastric pH levels (particularly infants), pre-existing conditions of hypochlorhydria, and users of proton pump

inhibitors (De Flora et al., 2016; Kirman et al., 2017). Studies have reported that tissue Cr (VI) levels in rats that have been exposed to Cr (VI) in drinking water were 4 – 15 times higher than those exposed to Cr (III), thus concluding the increased risk of Cr (VI) absorption into human tissues via the gastrointestinal tract (EPA, 1998).

Chronic exposure to Cr (VI) results in a higher concentration of the toxic contaminant in red blood cells, plasma, liver, and kidney. Dermal contact of Cr (VI) can cause potential dermatological effects by chronic exposure at higher doses such as allergic dermatitis, skin allergies, dermal necrosis, and dermal corrosion (Moffat et al., 2018; Saha et al., 2011). Cr (VI) is a known high-risk carcinogen when ingested at higher concentrations over a lifetime (WHO, 2011, 2017). Upon acute Cr (VI) ingestion, humans exhibit severe liver and kidney damage, cardiovascular collapse, and several gastrointestinal disorders. Several deaths have been reported due to acute exposure to chromium in children and adults. A dose of 1 g of potassium dichromate ($K_2Cr_2O_7$) is considered lethal (ATSDR, 2012). Short-term exposure to mild doses of Cr (VI) (between 0.03 – 4 mg/ d) has been reported to have no apparent health effects. However, due to chronic exposure of Cr (VI) from well water containing concentration of 20 mg Cr (VI)/L in China, individuals reported having severe gastrointestinal effects such as diarrhea, indigestion, abdominal pain, and vomiting (ATSDR, 2012). Another example of Cr (VI) effect in drinking water is of the town of Hinkley, California from 1966, where groundwater contaminated with Cr (VI) (reported concentration as high as 580 $\mu\text{g/L}$), which was the primary source of freshwater, induced carcinogenicity in a large number of people living in the town (Sutton, 2010). In Glasgow, UK, a report showed leakage of leachate from a landfill into groundwater which had a total chromium concentration of 3,920 $\mu\text{g/L}$, which resulted in widespread contamination of

groundwater resource. Furthermore, a survey conducted by the University of Athens in Greece between September and December 2008 found Cr (VI) concentrations in drinking water samples ranging from 41 – 53 µg/L (Rockett et al., 2015). A study conducted by Ball & Izbicki (2004) reported Cr (VI) concentration in groundwater wells in western Mojave Desert, California to be ranging from 0.1 µg/L to a high of 60 µg/L. In Kanpur, India, due to poor disposal practices, Cr (VI) concentrations in groundwater reached a level of 16.3 mg/L, which was being used as a primary source for drinking water (Sharma et al., 2012). Lastly, industrial runoff from a tannery industry resulted in Cr (VI) concentrations of 50 mg/L in Leon Valley, Mexico (Armienta et al., 2001). Instances of chromium contamination have been reported all over the world including UK, Europe, the Americas (North & South), and Asia, increasing the need for early and sensitive detection of Cr (VI) in water sources (EPA, 2010; Guertin et al., 2005; Health Canada, 2018; McNeill et al., 2012b, p. 2; Rockett et al., 2015; WHO, 2019).

Often, in cases of accidental ingestion of chromium, the amount is unknown. For example, a 22-month old infant died within 18.5 hours after accidentally ingesting an unknown amount of $\text{Na}_2\text{Cr}_2\text{O}_7$, which resulted in liver congestion, pulmonary edema, severe bronchitis, and necrosis of the liver, renal tubes, and gastrointestinal tract. (Ellis et al., 1982). Another case involved the death of a 2-year child due to accidental ingestion of ammonium dichromate, which resulted in severe dehydration, caustic burns in the mouth, blood discharge in diarrhea, irregular and labored respiration (Sunilkumar et al., 2014). There have been several other reports of accidental and intentional ingestion of chromium which have resulted in cases of death and severe illness around the world (ATSDR, 2012; McLean et al., 2012, p. 1). Unfortunately, there is a lack of reported data and ecological

studies on human carcinogenicity via oral ingestion. Nevertheless, animal studies have been conducted on the effects of Cr (VI) exposure which are used to identify potential dangers to human health.

On short-term exposure of Cr (VI) concentration from 0 – 350 mg/L, rats and mice exhibited a significant decrease in body weight, significant decrease in mean corpuscular hemoglobin, and developed lesions in the small intestine, which showed an increase in incidence and severity with increasing dose (Cullen et al., 2016). Long-term exposure study (2-years) of Cr (VI) in drinking water on rats and mice in the concentration range from 0 – 257.4 mg/L resulted in accumulation of Cr (VI) in a number of tissues, hematological effects (such as hypochromic anemia), histiocytic (white-blood) cellular infiltration in the liver, mesenteric lymphadenitis (inflammation of lymph nodes), and hyperplasia of small intestine and liver (NTP, 2008). Adverse reproductive effects have been observed due to chronic exposure of Cr (VI) in drinking water on animals (monkeys, rats, and mice), where functional and morphological effects of reproductive organs (both males and females) were reported (ATSDR, 2012). According to NTP (2008), the maximum benchmark dose limit for intermediate (hypochromic anemia in rats) and chronic exposure (hyperplasia of the small intestine in mice) via the oral route for Cr (VI) is 0.52 mg/Kg-day and 0.09 mg/Kg-day, respectively. Among the effects, decreased motility and sperm count (by 25%), changes to the epididymis, altered reproductive organ weights, reduction of ovarian follicles, changes to hormone levels, accumulation in foetal tissues (bypassing placental barrier), inhibition of sexual behavior, and aggression has been reported (Health Canada, 2015; NTP, 2010). Furthermore, studies indicate a significant increase in the incidence of

carcinoma cells and/ or papilloma cells in oral mucosa and tongue in male and female rats with increasing Cr (VI) dosage in drinking water (NTP, 2010; WHO, 2019).

Uncontaminated waters have a natural total chromium concentration of between 0.05 – 2 µg/L, but wastewater leached from a landfill or due to industrial processes can cause contamination of source water. Rainwater has an average total Cr between 0.02 – 1 µg/L, while seawater ranges between 0.05 – 0.5 µg/L. However, in Antarctic lakes, concentrations between 0.6 – 30 µg/L have been reported (Rockett et al., 2015). In 2016, of all the drinking water samples analyzed in England and Wales, the maximum concentration of Cr (VI) reported was 15 µg/L, while most samples had a concentration below 1 µg/L (WHO, 2019). A survey conducted by Health Canada (2015) reported an average amount of 2 µg/L of total chromium in Canadian drinking water, with the highest concentration of 18.9 µg/L from a groundwater source (generally lower than 1 µg/L). On the other hand, Canadian surface water concentrations for total chromium have been found to be in the range of 0.2 – 44 µg/L (Health Canada, 2018). In the US, from 2013 – 2015, the amount of Cr (VI) in drinking water across all states was reported to be between 0.057 and 12.9 µg/L, but instances of surface water concentrations up to 84 µg/L have been found (Sutton, 2010; WHO, 2019). Figure 2.16 represents total chromium detected in US tap-water from 2005 – 2009 by state agencies and environmental working group testing. In India, most water sources (surface and groundwater) were reported to have a concentration of total chromium below 2 µg/L, while in Rhine, the concentrations for water sources reported are mostly below 10 µg/L (AWWA, 2013). Generally, little to no data is available on the speciation of chromium salts in drinking waters (AWWA, 2013; Moffat et al., 2018; WHO, 2019).

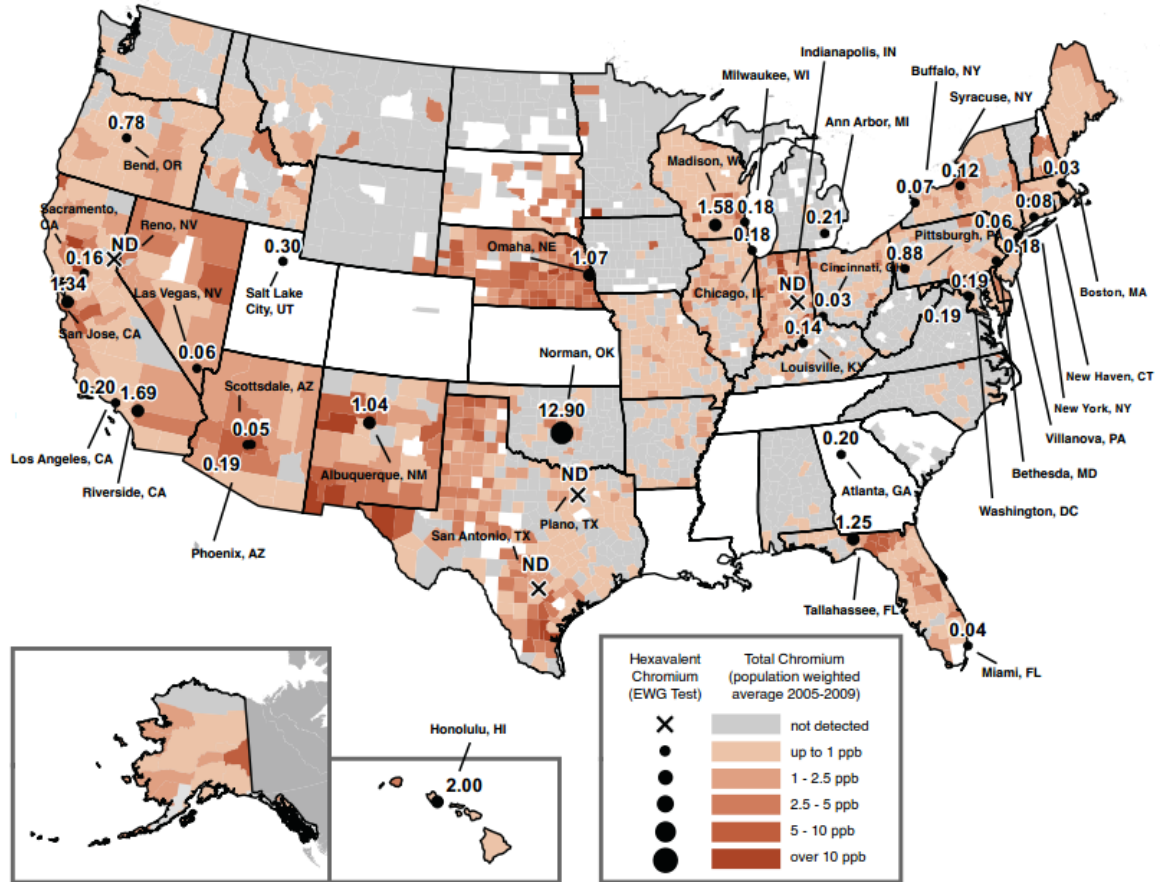


Figure 2.16: Graphical representation of the water utility testing data obtained from state water agencies of US tap-water for Cr (VI) by from the year 2005–2009. Black dots indicate the Environmental Working Group’s test sites and measured Cr (VI) concentrations. The size of the dot reflects the level found. Brown-shaded areas represent population-adjusted average concentrations of total chromium by county (Sutton, 2010).

Lastly, there is also a considerable need for monitoring of Cr (VI) from industrial waste processing streams as industries have to do on-site treatment before discharging water into a municipal sewer or into a receiving water body. For example, a typical waste stream from boilers from a co-generation power plant can contain Cr (VI) of over 16 mg/L, while electroplating and tanneries can have Cr (VI) concentrations between 20 – 60 mg/L in their effluent streams (Guertin et al., 2005). Chromium and its salts are considered non-bioaccumulating in the aquatic food chain. Cr (VI) taken up by fish is transformed to Cr

(III), indicating negligible mobility through this route (EPA, 1998; McLean et al., 2012, p. 1). However, the transfer of Cr salts from soil to food crops and subsequent biomagnification in the food chain is unknown (Health Canada, 2015). According to Health Canada (2018), approximately 50% of the total daily intake of Cr (VI) for Canadian adults is via drinking water.

2.4.3 Current Detection Methods

2.4.3.1 Photometric methods

Several analytical methods exist for the quantification of Cr (VI), but most techniques are very complex. 1,5-diphenyl-carbazide (DPC) colorimetric method is one of the most common and widespread (but time-consuming) methods for the determination of Cr (VI) and has a detection limit of 1 µg/L (Burgess & Thomas, 2017). The first step in a colorimetric method is the destruction of the organic matrix (aka DPC) by digestion using concentrated acid. Under proper conditions, Cr (VI) reacts (oxidizes) with the reagent to produce a complex of DPC-Cr (VI), which is an intensely red-violet compound and only forms in the presence of Cr (VI). The structure of DPC is shown in Figure 2.17 below. The molar absorptivity of the DPC-Cr (VI) complex is known to be 31,400 L/ mole-cm (based on molarity of dichromate), and has an absorption maximum at 540 nm, which is used to estimate the concentration (Osaki et al., 1983; Yarbrow, 1976). Although this method is very sensitive, the range of linearity for Cr (VI) concentration is narrow, ranging from 0 to 0.5 mg/L. Studies have reported that for solutions containing Cr (VI) concentration from 30 to 500 mg/L, the DPC-Cr (VI) method cannot accurately estimate concentration and results in a standard deviation of 20 to 50 % (EPA, 1992). Additionally, the complex formed with this method has limited stability, and thus makes the measurements time

sensitive, which increases the chance of error in data reporting (Osaki et al., 1983; Sanchez-Hachair & Hofmann, 2018). A method to overcome the limited stability of the DPC method was suggested by using o-tolidine to form a stable intermediate complex. However, the reagent used tends to form complexes with all heavy metals found in a given sample, which would result in reduced sensitivity. Therefore, a preliminary separation of chromium would be a necessary step for analysis, thus adding to the analysis time and making this process labor-intensive. The o-tolidine method is less desirable for routine analysis as compared to DPC colorimetric method (Yarbro, 1976). Lace et al. (2019) modified the DPC method by using microfluidic detection-based analysis, which eliminates steps needed for conventional DPC analysis. The study showed a method that could analyze Cr (VI) within 10 mins but increased the detection limit of the method to 23 $\mu\text{g/L}$, making the method a tradeoff between sensitivity and analysis time (Lace et al., 2019).

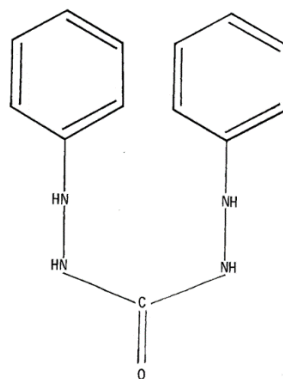


Figure 2.17: Structure of 1,5-diphenyl-carbazide (DPC) (Yarbro, 1976).

2.4.3.2 Spectrophotometric method

UV-visible spectrophotometric determination of Cr (VI) is a well-established method for field examination of groundwater and industrial wastewater. Quantification of Cr (VI) is

based on the absorption spectra of the yellow color of chromate ions. This method is rapid, simple, non-destructive (for the sample), and sensitive with a reported detection limit of approximately 5 µg/L with a 50 mm optical pathlength, and applicable for a concentration range of 5 – 1000 µg/L (Burgess & Thomas, 2017). A higher optical pathlength is necessary for the detection of Cr (VI) because of stringent effluent regulations and drinking water regulation constraints. Chromium VI spectra vary depending on the pH value of the solution and result in two absorption peaks in the UV region. Figure 2.18 shows the absorption spectra of potassium dichromate with varying pH values. As seen from the figure, at a higher pH value (alkaline condition), the absorbance is higher, and the Cr (VI) peak is prominent. On the other hand, at lower pH (acidic condition), the peak loses its prominence. There is a slight residual absorbance in the visible range but is not taken into consideration due to low resultant absorbance (Burgess & Thomas, 2017). At a pH below 6.4 (towards acidity), the maximum absorption lies at 350 nm wavelength, and the concentration linearity ranges from 0.5 to 100 mg/L; similarly, for a pH above 6.4 (towards alkalinity), the maximum absorption lies at 372 nm, and the concentration linearity ranges from 0.5 to 25 mg/L. The relative standard deviation for Cr (VI) using this method is less than 1% at higher concentrations (Sanchez-Hachair & Hofmann, 2018).

As the method is designed to be applied for industrial wastewaters as well, some metallic compounds like copper (II), iron (III), lead (II), and mercury (II), can potentially result in interference for Cr (VI) measurement. However, Fe³⁺ is an exception as the error is lower than 5% if the iron concentration is between 0.5 – 1 mg/L, while the error in measurement due to other ions is lower than 15%. Under acidic conditions, Fe³⁺ absorbs at around 300 nm, which can result in interference when Fe³⁺ is dissolved in water. But, with increasing

pH (up to a value of 9), the hydroxide form of iron precipitates and reduces interference for measurement as compared to the diphenyl-carbazide colorimetric method (Burgess & Thomas, 2017). Figure 2.19 shows the absorption spectra of iron under different conditions. This method is attractive for various field applications (such as environmental chemistry) given its accuracy and reliability over a wide concentration range. Based on the pathlength selected, dilution of the sample can be avoided increasing efficiency. At low and medium ionic strengths, inorganic background ions have minimal interference on the absorption of the sample, but in the presence of organometallic complexes, interference factors should be taken into consideration (Sanchez-Hachair & Hofmann, 2018).

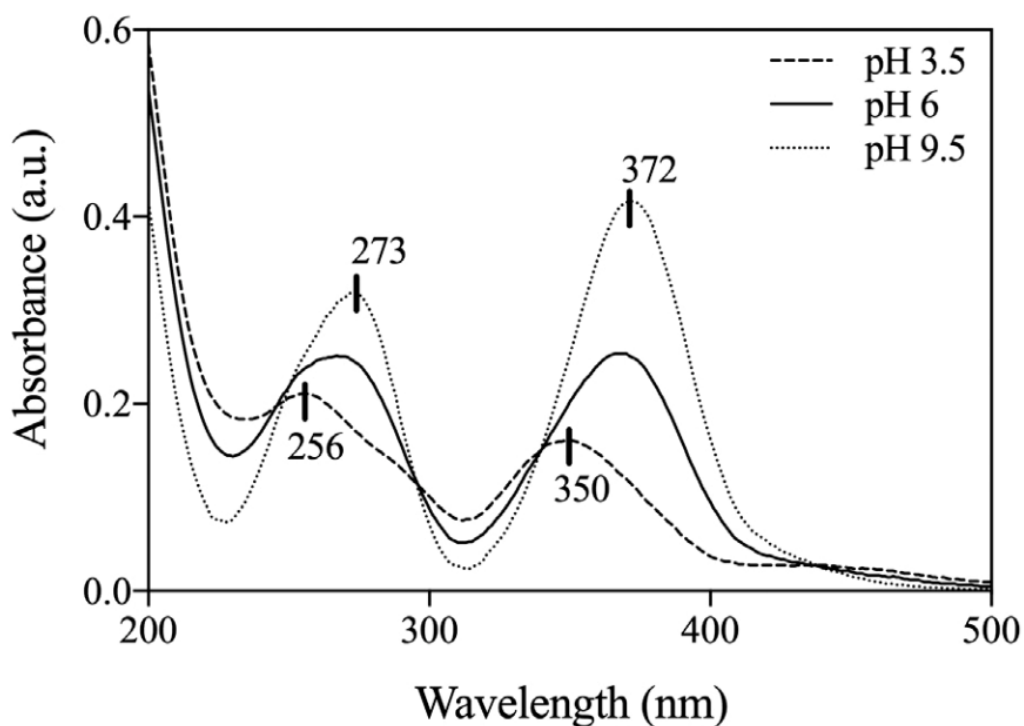


Figure 2.18: Absorption spectra of a $K_2Cr_2O_7$ solution (1 mg/L of Cr, pathlength 50 mm) for different pH (Burgess & Thomas, 2017).

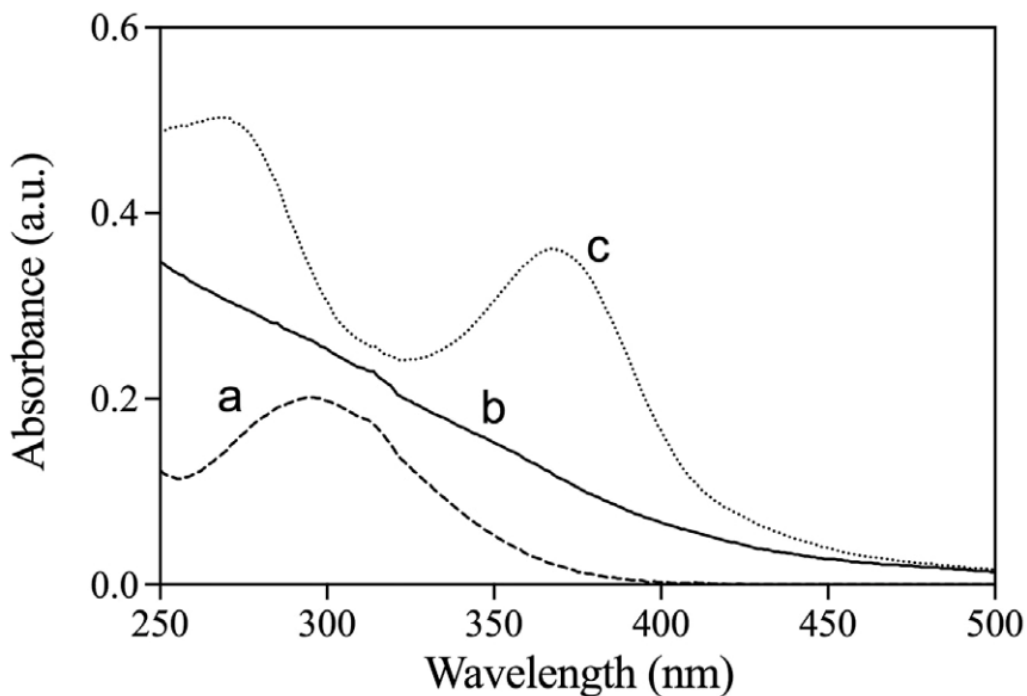


Figure 2.19: Absorption spectra (pathlength 50 mm) of synthetic solutions containing 1 mg/L of iron (a-pH 3, b-pH 9, c-pH 9 and addition of Cr (VI)) (Burgess & Thomas, 2017).

A novel method of using dispersive liquid-liquid microextraction (DLLME) was developed by Alexovič et al. (2012) for extraction of Cr (VI) from water samples. UV-Vis spectrophotometric method has been the most common method for Cr (VI) detection when coupled with DLLME (Ahmad et al., 2016a, 2016b; Alexovič et al., 2012, 2013). The principle for DLLME is based on the acidic reaction of a dye reagent (such as dimethylindocarbocyanine) with Cr (VI) to form an associate ion, followed by microextraction of the associated ion into an organic phase in the presence of an extraction, auxiliary and dispersive solvent. DLLME has been reported to have higher extractive efficiency while being simpler than other extraction methods such as SPE (Alexovič et al., 2012). Although this technique is efficient, it is critical to note that DLLME requires a greater number of reagents, leading to increased waste.

2.4.3.3 Mass Spectrometry

Mass spectrometry (MS) is the technique where the atoms or molecules of a substance are ionized, accelerated via an electric field, and subsequently separated according to their mass. Charged plates accelerate the ions inside the tube in a specific direction, and lighter ions move more rapidly towards the detector compared to the heavier ions separating the components of the sample by mass (Guertin et al., 2005). The ion current, on the other hand, is a measure of the quantity of ions and relates to the concentration of the individual components in the sample. MS separates ions according to their mass to charge ratio rather than according to their wavelengths. It requires samples to be in the gas phase, and all operations are carried out in a vacuum. Before ionization, solid and liquid samples have to be converted to gas for analysis. MS can be used for measuring elemental concentration and species identification (Guertin et al., 2005). MS is used as a detector to improve the MDL with other techniques such as ICP and GFAAS.

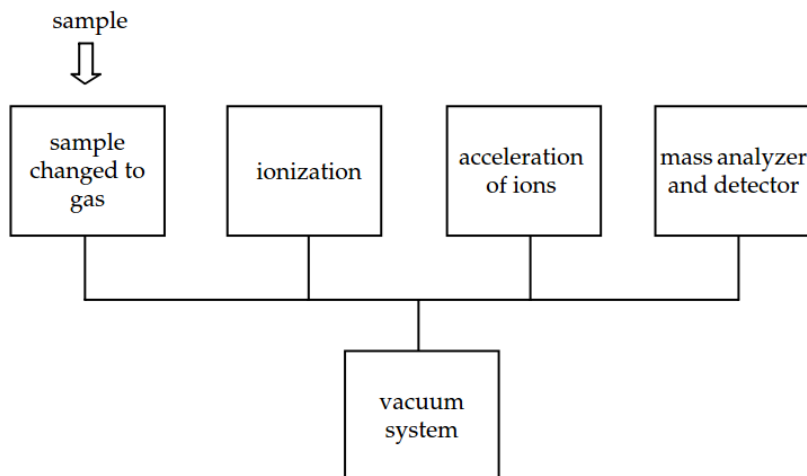


Figure 2.20: Principle of mass spectrometry (MS) (Guertin et al., 2005).

Electrospray ionization (ESI) is a technique used with MS for the detection of chromium. In ESI, a high voltage electrospray is applied to a liquid sample to create aerosol, which

separates the sample into individual ions. These ions are passed through as MS for detection and quantification (Harris & Lucy, 2015; Weldy et al., 2013).

2.4.3.4 Chromatography

In ion chromatography (IC), a mixture of ions from the mobile phase (in solvent) flow into a column, also known as the stationary phase, which is filled with packaging (such as resin). IC requires a separation of ions from an unknown sample before analysis. Based on the affinity of different ions towards the two phases, a different rate of movement occurs for different ions through the column and this results in the separation of the eluted ions. The resulting electrical conductivity of the eluting mobile phase is measured using a conductivity detector. Resin is used for ion exchange where ionic species are retained on the resin. Based on the sample, the exchange of the ions can be anions or cations, or both. IC has the ability to determine different oxidation states of a species (Guertin et al., 2005).

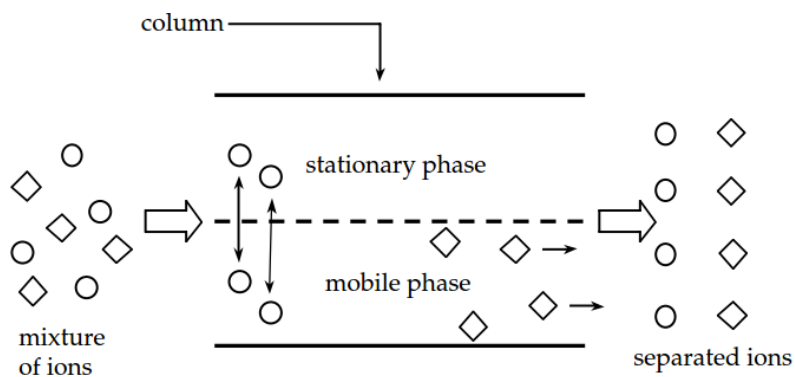


Figure 2.21: Conceptual diagram showing the principle of ion-chromatography (Guertin et al., 2005).

In liquid chromatography (LC), the solute (sample) equilibrates between a polar organic solvent (also known as the mobile phase) and a non-polar substrate (known as stationary phase) which results in the separation of ions (Gray, 2010). The efficiency of a

chromatographic process can be improved by increasing the rate at which solute travels within the column, thus leading to the use of high-pressure liquid chromatography (HPLC). As the name suggests, HPLC uses high pressure and forces the solute to separate into individual ions at a significantly higher rate as compared to traditional LC (Harris & Lucy, 2015). Chromatographic techniques are mostly used in conjunction with other techniques for sensitive determination of Chromium in different water matrices.

2.4.3.5 Inductive Coupled Plasma

Inductive Coupled Plasma (ICP) uses an argon plasma formed by passing argon gas between two quartz tubes and is maintained by the interaction of a radiofrequency field (at 27 MHz) on a copper coil and an oscillating magnetic field. The argon plasma emits elemental-specific energies or wavelengths which are used for atomization and excitation of the atoms within a sample. The plasma can reach temperatures as high 9,727 °C but generally is between the range of 5,227 – 7,227 °C (Boss & Fredeen, 2004). These high temperatures allow complete atomization of the elements in the sample and reduce potential chemical interferences generally associated with the Atomic Absorption Spectroscopy (AAS) technique. ICP is used in conjunction with different detectors to quantify analytes (Boss & Fredeen, 2004).

Inductive Coupled Plasma-Optical Emission Spectroscopy (ICP-OES) is the technique that measures the light emitted by the elements from a sample introduced into an ICP source. The intensity of the emitted light from the unknown sample is measured and compared to that of standards of known elemental concentrations (Harris & Lucy, 2015). The optical system uses a spectrometer to separate emitted light into individual wavelengths, which are then measured using a detector (Figure 2.22). Typically, ICP-OES has a working range

between 0.1 – 10 µg/L and costs between \$60K – \$100K. ICP-OES require a higher initial investment but have a wide analytical range for multi-elemental quantification (PerkinElmer, 2018; Sanz-Medel et al., 2009).



Figure 2.22: Simplified representation of a basic ICP system (PerkinElmer, 2018).

The other common method used for Chromium detection with ICP is using mass spectrometry (MS), where the argon ICP excites ions within a sample, which in turn get directed towards an MS where they are separated according to their mass to charge ratio. A detector is used to determine the number of ions present in the sample. ICP-MS allows the quantification of multiple elemental isotopes and ratios, enabling the determination of exact species present, in addition to the total concentration (Krishna et al., 2005; PerkinElmer, 2018). However, there are limits to the amount of sample matrix that can be introduced into the equipment. For example, ICP-MS requires TDS of the sample to be generally below 0.2% for maximum stability and smooth operation. Furthermore, interface cones and ion lenses located between the ICP source and the MS have to be cleaned regularly to maintain optimal performance levels. Moreover, method development for ICP-MS is more complex as compared to other techniques. Typically, ICP-MS has a working range between 1×10^{-5} – 1 µg/L and costs between \$130K – \$200K, making this a very sensitive method but with a very high initial investment (Harris & Lucy, 2015; PerkinElmer, 2018).

An improved and sensitive technique for analysis of Cr that has been developed uses a combination of HPLC-ICP-MS (Neubauer et al., 2003; Rakhunde et al., 2012). As the Cr (VI) species are anionic as opposed to Cr (III), which are cationic in nature, the HPLC column installed can be made selective for Cr (VI). This results in fastening the separation process (Health Canada, 2015). Neubauer et al. (2003) reported that Cr (III) and Cr (VI) could be separated using HPLC and detected with ICP-MS within 3 mins. The reported MDLs for Cr (VI) using this method were reported to be between 0.009 – 1 µg/L (McNeill et al., 2012b). However, it should be noted that factors such as column cleaning and pretreatment, reagent concentration, and detection mode, among others, have to be optimized beforehand to achieve optimal separation and reproducibility. In addition, significant issues due to water matrix interferences have been reported when trying to measure low levels of chromium (Rakhunde et al., 2012). Before the operation, the column has to be washed and achieve equilibrium which is done by running the eluent for at least 60 min through the equipment. It has been reported that there is a drastic drop in performance and sensitivity by using unwashed columns (Basumallick & Rohrer, 2016; Neubauer et al., 2003).

2.4.3.6 Atomic Absorption

AAS is a spectroanalytical procedure to determine elemental/chemical composition by measuring the absorption of light from free ions using electromagnetic or mass spectrum (PerkinElmer, 1996). Atomic absorption occurs when an atom in the ground state absorbs energy via the excitation of light of a specific wavelength. With an increasing number of atoms, the amount of light energy absorbed also increases. This relationship is used to determine the quantity of an unknown substance by comparing it to the light absorbed by

a standard of a known elemental quantity (PerkinElmer, 2018). In Flame-AAS (FAAS), the sample is introduced into the equipment in an aerosol form where it is vaporized by an air/ acetylene or a nitrous oxide/ acetylene flame to form free analyte atoms. The flame burner is aligned in a way that a light beam (from the source lamp) passes through the flame, where energy (as light) is absorbed by the atoms. A detector, on the other end, measures the resultant wavelength intensity, which is in turn used for elemental quantification (as the measured intensity is inversely proportional to the concentration of the element) of the unknown sample (Harris & Lucy, 2015). In principle, the light of a specific wavelength from an element-specific lamp passes through the flame of the atomized sample, where the atoms absorb light (excitation) and emit light (decay), which is separated into its wavelengths by a prism which can then be measured (Figure 2.23) (Guertin et al., 2005). Typically, FAAS has a working range between 1 – 100 $\mu\text{g/L}$ and costs between \$15K – \$25K (PerkinElmer, 2018). The major limitation of FAAS is that the burner system is an inefficient sampling device, which allows only a small fraction of the sample to reach the flame and the atomized sample quickly passes through the light path lowering the sensitivity of the method (PerkinElmer, 2018). It is a low-cost, simple, and reliable technique but is only capable of single-elemental analysis for metal and metalloids and is temperature-dependent. At low temperatures, interferences by refractory compounds are considerable (Sanz-Medel et al., 2009).

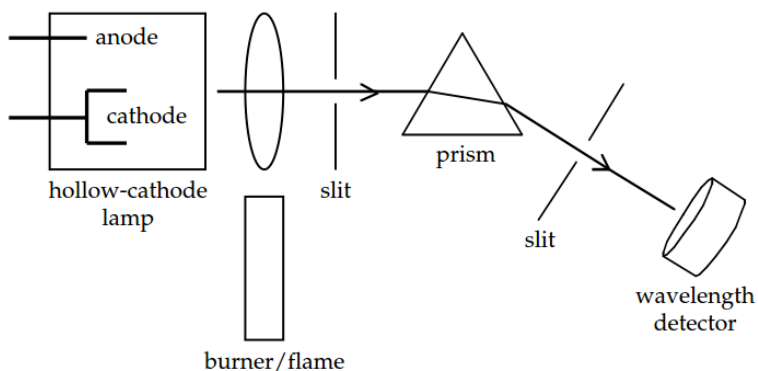


Figure 2.23: Flame atomic absorption spectroscopy (FAAS) and the general principle of AAS (Guertin et al., 2005).

Graphite furnace atomic absorption spectroscopy (GFAAS) or also known as electrothermal atomic absorption spectroscopy (ETAAS), a graphite furnace is used for electrothermal vaporization of the sample, which contains electrically heated graphite tubes where the entire sample can be directly inoculated. The heat inside the tube removes solvents and other matrix components, allowing the sample to be atomized (PerkinElmer, 1996). Typically, GFAAS has a working range between 0.001 – 5 $\mu\text{g/L}$ and costs between \$30K – \$60K (PerkinElmer, 2018). GFAAS is an improvement on the AAS as it enables atomization of the entire sample, and the sample is then retained within the tube, which allows for longer exposure time, thus greatly improving the sensitivity. GFAA also requires small sample sizes (< 1 mL) and has sub-ppm detection limits (typically 10 times more sensitive than FAAS) for measuring a few elements simultaneously. However, it is difficult to optimize, has a higher cost than traditional AAS, a longer analysis time is required using GFAA, and is mostly reliable for single elemental analysis (Sanz-Medel et al., 2009).

Atomic emission spectroscopy (AES) is another modification of the traditional AAS, which uses quantitative measurements of optical emission to determine the sample analyte concentration. Atoms in the unknown sample are excited by simultaneous vaporization and

atomization using a flame, a plasma, or a discharge (PerkinElmer, 1996). The excited atoms emit light (decay) which is characteristic of an individual type of element, that can be measured by a detector to quantify the unknown sample. Unlike AAS, no primary light source is required for AES (PerkinElmer, 1996). Table 2.8 summarizes the MDLs for Chromium using different techniques discussed above.

2.4.3.7 Electrochemical methods

Methods that determine the change of chemical parameters with respect to electrical quantities of current, potential, or charge are known as electrochemical methods (Jin & Yan, 2015). Amperometry, is the measure of electric currents between a pair of electrodes in an electrochemical reaction. Voltammetry are techniques which relate current and voltage from the electrodes to the concentration of the analyte being measured in an electrolytic solution (Harris & Lucy, 2015). Electrophoresis is another widely used electrochemical method that is based on the migration of ions in a sample solution under the influence of an electric current. Capillary electrophoresis (CE) is an advanced form of electrophoresis where silica (SiO_2) fused capillary tube is used for ionic separation. An electric voltage is applied to the tube from end to end where different ions having different mobilities migrate through the tube at different speeds enabling the measurement and quantification of ions (Harris & Lucy, 2015). CE is a low-cost and rapid method for the determination of Cr (VI) but has poor sensitivity ranging from 8,000 – 30,000 $\mu\text{g/L}$ and requires chelation as sample pretreatment (Rakhunde et al., 2012). To improve the detection limit, CE is often paired with ICP and/ or MS to improve sensitivity.

Another electrocatalyst for Cr (VI) reduction and subsequent detection are gold-based electrodes and nanoparticles. Studies have found that the reduction of Cr (VI) happens

more rapidly and at a lower potential when using gold as compared to other rare elements (such as platinum) (Jin & Yan, 2015). Ouyang et al. (2012) developed a method for very sensitive determination of Cr (VI) by using gold nanoparticles on carbon electrode and reported a detection limit of 0.0029 $\mu\text{g/L}$ and a working range between 0.01 – 1.2 $\mu\text{g/L}$. The preparation time reported for this method was over 30 mins with an analysis time of 5 mins (Ouyang et al., 2012). Another study used gold nanoparticles on an electrode for detecting Cr (VI) and reported an MDL of 0.1 $\mu\text{g/L}$ with a preparation time of 20 min and analysis time of 5 min and a working range between 0.2 – 3 $\mu\text{g/L}$ (Jena & Raj, 2008). It should be noted that using gold raises the cost of the entire process, and the working range for this method is very specific, limiting its application to certain fields. Additionally, electrochemical methods can have potential interferences from coexisting ions in a mixed water matrix which can impact the overall efficiency of the technique.

2.4.3.8 Fluorometry

This method involves the fluorescence response generated by the excitation of the Cr (VI) molecule. Different compounds are known to associate with different fluorescence excitation wavelengths, and they in turn can be used to measure based on their specific emission wavelengths. Cr (VI) quantification via fluorescence relies predominantly on using luminescent carbon dots to form sensors (Mutuyimana et al., 2019; Vaz et al., 2017; Wang et al., 2019b). Carbon dots are nano-sized particles that essentially constitute carbon, hydrogen and oxygen in varying quantities based on the synthesis method used. The surface contains organic functional groups containing nitrogen and sulfur atoms in addition to carbon, hydrogen and oxygen (such as $-\text{COOH}$, $-\text{NH}_2$, and $-\text{SO}_3\text{H}$) to improve solubility and increase stability for sample measurements (Vaz et al., 2017). They are non-toxic in

nature and can be used to detect multiple heavy metals such as Fe (II), Pb (II), Hg (II), among others (Wang et al., 2019a). The detection limits using carbon dots and fluorescence for quantification of Cr (VI) were reported to be around 20-110 $\mu\text{g/L}$ (Mutuyimana et al., 2019; Vaz et al., 2017; Wang et al., 2019a, 2019b). A study by Vaz et al. (2017) reported that after optimization, the method had a linear range from 100 – 1200 $\mu\text{g/L}$ and would result in accuracy loss outside that range. The method is relatively sensitive and fast but relies on nanotechnology, which requires skilled personnel for preparation (further increasing costs) and often requires filtration before sample analysis (Wang et al., 2019a, 2019b). Lastly, it has not been commonly applied for Cr (VI) realistic monitoring purposes yet (Mutuyimana et al., 2019).

2.5 Summary

The literature review outlines the current state of knowledge regarding cyanobacteria and hexavalent chromium around the world. Source water quality has been declining with every passing year. Presence of CB in source waters is a critical concern as CB can potentially be toxic in nature, produce taste and odor compounds, negatively impact aquatic habitat, and increase water treatment operational cost. Upon ingestion, CB also pose a grave hazard to human and animal health alike. Correspondingly, Cr (VI) in source water is of consequence due to its inherent carcinogenic nature. Many techniques that are presently being employed rely on sample pretreatment such as pigment extraction, filtration, SPE, nanomaterials, and acidification among others, before analysis. This increases overall analytical cost and time required to obtain quantitative results. Additionally, existing methods often requires skilled personell for operation and maintenance purposes. There is a clear need for simple, sensitive, affordable and readily available detection methods which

do not require sample preparation, can generate quantifiable data rapidly and be implementable as an early detection system.

As discussed in this chapter, the regulations for monitoring of cyanobacteria and Cr (VI) vary, depending on local water authorities around the globe. This makes it difficult to select a single technology for universal monitoring needs. However, using spectrophotometry, it is possible to measure multiple parameters and photopigments simultaneously and SP can be applied for in-line, real-time monitoring purposes. In addition, current studies lack data on the effect of using longer pathlength cuvettes for monitoring purposes, via UV-Vis SP. Furthermore, derivative spectrophotometry has not been explored enough for cyanobacterial or Cr (VI) detection. Lastly, the impact of different WQPs such as turbidity, DOC, salinity and pH among others, on monitoring has not been widely researched before and is a research gap that is need of being filled in the field of water quality monitoring.

Table 2.8: Summary of detection limits of chromium in different water matrices and their respective detection system.

Detection system	Compound	Sample preparation	Water matrix	Time (min)	MDL ($\mu\text{g/L}$)	Source
FAAS	Cr (VI)	SPE	Tap	> 72	45	(Tunçeli & Türker, 2002)
FAAS	Cr (VI)	C ¹⁸ silica SPE	River	> 20	15	(Tehrani et al., 2004)
GFAAS	Cr (VI)	SPE	Mineral	> 40	0.3	(Tuzen & Soylak, 2006)
FAAS	Cr (VI)	SPE	Ground	> 100	145	(Krishna et al., 2005)
FAAS	Cr (VI)	SPE	Tap & mineral	> 40	7.7	(Narin et al., 2008)
AAS	Total Cr	Acidification	Drinking	> 40	2	(Rice et al., 2017)
GFAAS	Total Cr	Acidification	Drinking	–	0.1	(EPA, 1996a, p. 9)
Portable UV-Vis SP	Cr (VI)	C ¹⁸ SPE	Drinking	10	3	(Ma et al., 2012)
UV-Vis SP	Cr (VI)	SPE	Tap & mineral	15	50	(Hoshi et al., 1998)
UV-Vis SP	Cr (VI)	Mixed-bed SPE	Well & tap	> 62	6	(Rajesh et al., 2008)
UV-Vis SP	Cr (VI)	SiO ₂ SPE	Tap, sewage & ground	17	0.4	(Sereshti et al., 2016)

UV-Vis SP	Cr (VI)	No pretreatment	Natural	> 5	5	(Burgess & Thomas, 2017)
UV-Vis SP	Cr (VI)	DPC	Natural	> 10	20	(Pressman & Aldstadt, 2003)
UV-Vis SP	Cr (VI)	No pretreatment	Pharmaceuticals	–	23	(Mulaudzi et al., 2002)
DLLME-UV SP	Cr (VI)	Acidification	Lake, spring & river	–	30	(Alexovič et al., 2012)
DLLME-UV SP	Cr (VI)	Acidification	Tap & sea	> 10	7.48	(Ahmad et al., 2016b)
ICP-AES	Total Cr	Solubilization	Drinking & tap	–	4.7	(EPA, 1996b)
ICP-AES	Total Cr	Solubilization	Drinking & tap	> 150	0.2	(EPA, 2003, p. 5)
ICP-AES	Total Cr	Solubilization	Drinking	> 20	7	(Rice et al., 2017)
ICP-MS	Cr (VI)	SPE	Tap & mineral	> 20	0.05	(Krishna et al., 2005)
On-Line OES	ICP- Cr (VI)	Acidification	Tap & mineral	> 10	0.9	(Hwang et al., 2006)
IC-MS	Cr (VI)	Solubilization	Drinking	> 15	0.001	(Basumallick & Rohrer, 2016)
IC-UV SP	Cr (VI)	SPE+DPC	Drinking & tap	–	0.015	(EPA, 2011, p. 7)
IC-UV SP	Cr (VI)	SPE+DPC	Wastewater	> 15	6	(Onchoke & Sasu, 2016)
IC-GFAAS	Cr (VI)	SPE	Municipal wastewater	> 30	0.45	(Stasinakis et al., 2003)

IC-ICP-MS	Cr (VI)	SPE+EDTA	Synthetic & brackish	> 20	0.012	(Gürleyük & Wallschläger, 2001)
CE	Cr (VI)	Ultrasonic	Wastewater	> 12	39	(Kubáň et al., 2003)
ESI-MS	Cr (VI)	EDTA complex	Wastewater	> 20	0.1	(Chen et al., 2007)
HPLC	Cr (VI)	SPE	Tap & ground	> 5	210	(Sadeghi & Moghaddam, 2015)
HPLC	Cr (VI)	Ultrasonic+SPE	Tap & mineral	> 30	5.2	(Tang et al., 2004)
LC-ICP-MS	Cr (VI)	SPE+EDTA	Drinking	> 10	0.01	(Ernstberger & Neubauer, 2015)
HPLC-ICP-MS	Cr (VI)	SPE	Tap	> 6	0.05	(Neubauer et al., 2003)
HPLC-ICP-MS	Cr (VI)	SPE	Mineral & spring	> 8	0.056	(McSheehy et al., 2010)
Photo electrochemical	Cr (VI)	No pretreatment	D.I. water	>10	0.006	(Fang et al., 2016)
Colorimetry	Cr (VI)	Digestion	Groundwater	> 60	50	(EPA, 1992)
Carbon dots- fluorescence	Cr (VI)	Carbon dots using L-glutathione heat	Drinking, tap, fresh & brackish water	> 5	30	(Vaz et al., 2017)

2.6 References

Agberien, A. V., & Örmeci, B. (2019). Monitoring of Cyanobacteria in Water Using Spectrophotometry and First Derivative of Absorbance. *Water*, 12(1), 124. <https://doi.org/10.3390/w12010124>

Agency for Toxic Substances and Disease Registry. (2012). *Toxicological Profile for Chromium* (p. 592). Agency for Toxic Substances and Disease Registry. <https://www.atsdr.cdc.gov/toxprofiles/tp7.pdf>

Ahmad, W., Al-Sibaai, A., Bashammakh, A., Alwael, H., & El-Shahawi, M. (2016a). An ultrasound-assisted ion association dispersive liquid–liquid microextraction coupled with micro-volume spectrofluorimetry for chromium speciation. *RSC Advances*, 6(73), 69492–69500. <https://doi.org/10.1039/C6RA13072K>

Ahmad, W., Bashammakh, A., Al-Sibaai, A., Alwael, H., & El-Shahawi, M. (2016b). Trace determination of Cr(III) and Cr(VI) species in water samples via dispersive liquid-liquid microextraction and microvolume UV–Vis spectrometry. Thermodynamics, speciation study. *Journal of Molecular Liquids*, 224, 1242–1248. <https://doi.org/10.1016/j.molliq.2016.10.106>

Alexovič, M., Andruch, V., Balogh, I. S., & Šandrejová, J. (2013). A single-valve sequential injection manifold (SV-SIA) for automation of air-assisted liquid-phase microextraction: Stopped flow spectrophotometric determination of chromium(VI). *Analytical Methods*, 5(10), 2497–2502. <https://doi.org/10.1039/C3AY40284C>

Alexovič, M., Balogh, I. S., Škrliková, J., & Andruch, V. (2012). A dispersive liquid–liquid microextraction procedure for UV-Vis spectrophotometric determination of chromium(vi) in water samples. *Analytical Methods*, 4(5), 1410. <https://doi.org/10.1039/c2ay25133g>

AlMomani, F. A., & Örmeci, B. (2016). Performance Of *Chlorella Vulgaris*, *Neochloris Oleoabundans*, and mixed indigenous microalgae for treatment of primary effluent, secondary effluent and centrate. *Ecological Engineering*, 95, 280–289. <https://doi.org/10.1016/j.ecoleng.2016.06.038>

AlMomani, F. A., & Örmeci, B. (2018). Monitoring and measurement of microalgae using the first derivative of absorbance and comparison with chlorophyll extraction method. *Environmental Monitoring and Assessment*, 190(2), 90. <https://doi.org/10.1007/s10661-018-6468-y>

Altenburger, R., Ait-Aissa, S., Antczak, P., Backhaus, T., Barceló, D., Seiler, T.-B., Brion, F., Busch, W., Chipman, K., de Alda, M. L., de Aragão Umbuzeiro, G., Escher, B. I., Falciani, F., Faust, M., Focks, A., Hilscherova, K., Hollender, J., Hollert, H., Jäger, F., ... Brack, W. (2015). Future water quality monitoring—Adapting tools to deal with mixtures of pollutants in water resource management. *Science of The Total Environment*, 512–513, 540–551. <https://doi.org/10.1016/j.scitotenv.2014.12.057>

American Water Works Association (Ed.). (2011). *Algae: Source to Treatment* (1st ed.). American Water Works Association. (ISBN 1-58321-787-8)

American Water Works Association. (2013). Chromium in Drinking Water: A Technical Information Primer. *American Water Works Association*, 11.

Arar, E. J., & Collins, G. B. (1997). *In Vitro Determination of Chlorophyll a and Pheophytin a in Marine and Freshwater Algae by Fluorescence*. 22.

Armienta, M. A., Morton, O., Rodríguez, R., Cruz, O., Aguayo, A., & Ceniceros, N. (2001). Chromium in a Tannery Wastewater Irrigated Area, León Valley, Mexico. *Bulletin of Environmental Contamination and Toxicology*, 66(2), 189–195. <https://doi.org/10.1007/s0012800224>

Bajpai, R., Sharma, N. K., & Rai, A. K. (2011). Cyanotoxins: An Emerging Environmental Concern. *Advances in Life Science*, 187–211.

Balest, L., Murgolo, S., Sciancalepore, L., Montemurro, P., Abis, P. P., Pastore, C., & Mascolo, G. (2016). Ultra-trace levels analysis of microcystins and nodularin in surface water by on-line solid-phase extraction with high-performance liquid chromatography tandem mass spectrometry. *Analytical and Bioanalytical Chemistry*, 408(15), 4063–4071. <https://doi.org/10.1007/s00216-016-9495-y>

- Ball, J. W., & Izbicki, J. A. (2004). Occurrence of hexavalent chromium in ground water in the western Mojave Desert, California. *Applied Geochemistry*, *19*(7), 1123–1135. <https://doi.org/10.1016/j.apgeochem.2004.01.011>
- Bartram, J., & Rees, G. (Eds.). (2000). *Monitoring Bathing Waters: A Practical Guide to the Design and Implementation of Assessments and Monitoring Programmes* (0 ed.). CRC Press - WHO. (ISBN 978-0-429-20430-2) <https://doi.org/10.4324/9780203478264>
- Basumallick, L., & Rohrer, J. (2016). Sensitive Determination of Hexavalent Chromium in Drinking Water. *Thermo Scientific, Application Update 179*, 6.
- Beltrán, E., Ibáñez, M., Sancho, J. V., & Hernández, F. (2012). Determination of six microcystins and nodularin in surface and drinking waters by on-line solid phase extraction–ultra high pressure liquid chromatography tandem mass spectrometry. *Journal of Chromatography A*, *1266*, 61–68. <https://doi.org/10.1016/j.chroma.2012.10.017>
- Berry, J. P., Lee, E., Walton, K., Wilson, A. E., & Bernal-Brooks, F. (2011). Bioaccumulation of microcystins by fish associated with a persistent cyanobacterial bloom in Lago de Patzcuaro (Michoacan, Mexico). *Environmental Toxicology and Chemistry*, *30*(7), 1621–1628. <https://doi.org/10.1002/etc.548>
- Bertone, E., Burford, M. A., & Hamilton, D. P. (2018). Fluorescence probes for real-time remote cyanobacteria monitoring: A review of challenges and opportunities. *Water Research*, *141*, 152–162. <https://doi.org/10.1016/j.watres.2018.05.001>
- Bittencourt-Oliveira, M. D. C., Piccin-Santos, V., Moura, A. N., Aragão-Tavares, N. K. C., & Cordeiro-Araújo, M. K. (2014). Cyanobacteria, microcystins and cylindrospermopsin in public drinking supply reservoirs of Brazil. *Anais Da Academia Brasileira de Ciências*, *86*(1), 297–310. <https://doi.org/10.1590/0001-3765201302512>
- Bláha, L., Babica, P., & Maršálek, B. (2009). Toxins produced in cyanobacterial water blooms—Toxicity and risks. *Interdisciplinary Toxicology*, *2*(2). <https://doi.org/10.2478/v10102-009-0006-2>
- Boiteau, R. M., Fitzsimmons, J. N., Repeta, D. J., & Boyle, E. A. (2013). Detection of Iron Ligands in Seawater and Marine Cyanobacteria Cultures by High-Performance Liquid

Chromatography–Inductively Coupled Plasma–Mass Spectrometry. *Analytical Chemistry*, 85(9), 4357–4362. <https://doi.org/10.1021/ac3034568>

Boss, C. B., & Fredeen, K. J. (2004). Concepts, Instrumentation and Techniques in Inductively Coupled Plasma Optical Emission Spectrometry. *PerkinElmer, 3rd Edition*, 120.

Bowling, L. C., Zamyadi, A., & Henderson, R. K. (2016). Assessment of in situ fluorometry to measure cyanobacterial presence in water bodies with diverse cyanobacterial populations. *Water Research*, 105, 22–33. <https://doi.org/10.1016/j.watres.2016.08.051>

Boyer, G. L. (2007). The occurrence of cyanobacterial toxins in New York lakes: Lessons from the MERHAB-Lower Great Lakes program. *Lake and Reservoir Management*, 23(2), 153–160. <https://doi.org/10.1080/07438140709353918>

Boyer, G. L. (2008). *Chapter 7: Cyanobacterial Toxins in New York and the Lower Great Lakes Ecosystems*.

Burgess, C., & Thomas, O. (2017). UV-Visible Spectrophotometry of Water and Wastewater. In *UV-Visible Spectrophotometry of Water and Wastewater* (pp. 1–524). Elsevier. (ISBN 978-0-444-63897-7) <https://doi.org/10.1016/B978-0-444-63897-7.00001-9>

Campàs, M., & Marty, J.-L. (2007). Highly sensitive amperometric immunosensors for microcystin detection in algae. *Biosensors and Bioelectronics*, 22(6), 1034–1040. <https://doi.org/10.1016/j.bios.2006.04.025>

Canter, L. W. (1985). *River water quality monitoring*. Lewis Publishers. (ISBN 978-0-87371-011-4)

Carmichael, W. (2006). *Chapter 4: A world overview—One-hundred- twenty-seven years of research on toxic cyanobacteria—Where do we go from here?* 21.

Chen, Z., Megharaj, M., & Naidu, R. (2007). Speciation of chromium in waste water using ion chromatography inductively coupled plasma mass spectrometry. *Talanta*, 72(2), 394–400. <https://doi.org/10.1016/j.talanta.2006.10.041>

- Chorus, I. (2005). Current approaches to cyanotoxin risk assessment, risk management and regulations in different countries. *Federal Environmental Agency, 1*, 122.
- Chorus, I. (2012). Current approaches to Cyanotoxin risk assessment, risk management and regulations in different countries. *Federal Environment Agency, 2*, 151.
- Chorus, I., & Bartram, J. (Eds.). (1999). *Toxic cyanobacteria in water: A guide to their public health consequences, monitoring, and management*. E & FN Spon. (ISBN 978-0-419-23930-7)
- Chorus, I., Falconer, I. R., Salas, H. J., & Bartram, J. (2000). Health risks caused by freshwater cyanobacteria in recreational waters. *Journal of Toxicology and Environmental Health, Part B, 3*(4), 323–347. <https://doi.org/10.1080/109374000436364>
- Codd, G., Bell, S., Kaya, K., Ward, C., Beattie, K., & Metcalf, J. (1999). Cyanobacterial toxins, exposure routes and human health. *European Journal of Phycology, 34*(4), 405–415. <https://doi.org/10.1080/09670269910001736462>
- Corbel, S., Mougin, C., & Bouaïcha, N. (2014). Cyanobacterial toxins: Modes of actions, fate in aquatic and soil ecosystems, phytotoxicity and bioaccumulation in agricultural crops. *Chemosphere, 96*, 1–15. <https://doi.org/10.1016/j.chemosphere.2013.07.056>
- Cullen, J. M., Ward, J. M., & Thompson, C. M. (2016). Reevaluation and Classification of Duodenal Lesions in B6C3F1 Mice and F344 Rats from 4 Studies of Hexavalent Chromium in Drinking Water. *Toxicologic Pathology, 44*(2), 279–289. <https://doi.org/10.1177/0192623315611501>
- Dai, M., Xie, P., Liang, G., Chen, J., & Lei, H. (2008). Simultaneous determination of microcystin-LR and its glutathione conjugate in fish tissues by liquid chromatography–tandem mass spectrometry. *Journal of Chromatography B, 862*(1–2), 43–50. <https://doi.org/10.1016/j.jchromb.2007.10.030>
- De Flora, S., Camoirano, A., Micale, R. T., La Maestra, S., Savarino, V., Zentilin, P., Marabotto, E., Suh, M., & Proctor, D. M. (2016). Reduction of hexavalent chromium by fasted and fed human gastric fluid. I. Chemical reduction and mitigation of mutagenicity.

Toxicology and Applied Pharmacology, 306, 113–119.
<https://doi.org/10.1016/j.taap.2016.07.004>

Demadrille, R., Rabourdin, A., Campredon, M., & Giusti, G. (2004). Spectroscopic characterisation and photodegradation studies of photochromic spiro[fluorene-9,3'-[3'H]-naphtho[2,1-b]pyrans]. *Journal of Photochemistry and Photobiology A: Chemistry*, 168(3), 143–152. <https://doi.org/10.1016/j.jphotochem.2004.05.009>

Dodds, W. K., Bouska, W. W., Eitzmann, J. L., Pilger, T. J., Pitts, K. L., Riley, A. J., Schloesser, J. T., & Thornbrugh, D. J. (2009). Eutrophication of U.S. Freshwaters: Analysis of Potential Economic Damages. *Environmental Science & Technology*, 43(1), 12–19. <https://doi.org/10.1021/es801217q>

Ellis, E. N., Brouhard, B. H., Lynch, R. E., Dawson, E. B., Tisdell, R., Nichols, M. M., & Ramirez, F. (1982). Effects of hemodialysis and dimercaprol in acute dichromate poisoning. *Journal of Toxicology. Clinical Toxicology*, 19(3), 249–258. <https://doi.org/10.3109/15563658209025729>

EPA. (1992). *SW-846 Test Method 7196A: Chromium, Hexavalent (Colorimetric)*. EPA. <https://www.epa.gov/sites/production/files/2015-12/documents/7196a.pdf>

EPA. (1996a). Method 200.9, Revision 2.2: Determination of Trace Elements by Stabilized Temperature Graphite Furnace Atomic Absorption. In *Methods for the Determination of Metals in Environmental Samples* (pp. 146–186). Elsevier. (ISBN 978-0-8155-1398-8) <https://doi.org/10.1016/B978-0-8155-1398-8.50012-4>

EPA. (1996b). Method 6010B Inductively coupled plasma-atomic emission spectrometry. In *Methods for the Determination of Metals in Environmental Samples* (pp. 1–25). Elsevier. (ISBN 978-0-8155-1398-8) <https://www.epa.gov/sites/production/files/documents/6010b.pdf>

EPA. (1998). *Toxicological Review of Hexavalent Chromium*. EPA. https://cfpub.epa.gov/ncea/iris/iris_documents/documents/toxreviews/0144tr.pdf

EPA. (2003). Method 200.5 Revision 4.2 Determination of Trace Elements in Drinking Water by Axially Viewed Inductively Coupled Plasma—Atomic Emission Spectrometry. *U. S. ENVIRONMENTAL PROTECTION AGENCY*, 36.

EPA. (2010). *Chromium-6 in Drinking Water*. EPA. <https://www.bendoregon.gov/home/showdocument?id=2737>

EPA. (2011). Method 218.7: Determination of Hexavalent Chromium in Drinking Water by Ion Chromatography with Post-Column Derivatization and UV-Visible Spectroscopic Detection. *U. S. ENVIRONMENTAL PROTECTION AGENCY*, 31.

EPA, U. (2005). *Technologies and Techniques for Early Warning Systems to Monitor and Evaluate Drinking Water Quality* (p. 236). USEPA.

EPA, U. (2015a). *Recommendations for Public Water Systems to Manage Cyanotoxins in Drinking Water*. <https://www.epa.gov/sites/production/files/2017-06/documents/cyanotoxin-management-drinking-water.pdf>

EPA, U. (2015b). *Drinking Water Health Advisory for the Cyanobacterial Microcystin Toxins*. 75.

Ernstberger, H., & Neubauer, K. (2015). Chromium Speciation in Drinking Water by LC-ICP-MS. *PerkinElmer, Application Note*, 6.

European Commission. (2017). *Directive of the European parliament and of the council on the quality of water intended for human consumption (recast) (753 final)*. https://eur-lex.europa.eu/resource.html?uri=cellar:8c5065b2-074f-11e8-b8f5-01aa75ed71a1.0016.02/DOC_1&format=PDF

Falconer, I. R. (Ed.). (1993). *Algal toxins in seafood and drinking water*. Academic Press. (ISBN 978-0-12-247990-8)

Falconer, I. R. (1999). An Overview of problems caused by toxic blue–green algae (cyanobacteria) in drinking and recreational water. *Environmental Toxicology*, 14(1), 5–12. [https://doi.org/10.1002/\(SICI\)1522-7278\(199902\)14:1<5::AID-TOX3>3.0.CO;2-0](https://doi.org/10.1002/(SICI)1522-7278(199902)14:1<5::AID-TOX3>3.0.CO;2-0)

- Fang, T., Yang, X., Zhang, L., & Gong, J. (2016). Ultrasensitive photoelectrochemical determination of chromium(VI) in water samples by ion-imprinted/formate anion-incorporated graphitic carbon nitride nanostructured hybrid. *Journal of Hazardous Materials*, *312*, 106–113. <https://doi.org/10.1016/j.jhazmat.2016.03.046>
- Fayad, P. B., Roy-Lachapelle, A., Duy, S. V., Prévost, M., & Sauvé, S. (2015). On-line solid-phase extraction coupled to liquid chromatography tandem mass spectrometry for the analysis of cyanotoxins in algal blooms. *Toxicon*, *108*, 167–175. <https://doi.org/10.1016/j.toxicon.2015.10.010>
- Figueiredo, D. R., Azeiteiro, U. M., Esteves, S. M., Gonçalves, F. J. M., & Pereira, M. J. (2004). Microcystin-producing blooms—A serious global public health issue. *Ecotoxicology and Environmental Safety*, *59*(2), 151–163. <https://doi.org/10.1016/j.ecoenv.2004.04.006>
- Furevik, B. R., Durand, D., & Pettersson, L. (2004). Multi-Sensor Synergy for Monitoring of Algal Blooms in the North Sea. *Proceedings of the 2004 Envisat & ERS Symposium (ESA SP-572)*, 7.
- Furukawa, K., Noda, N., Tsuneda, S., Saito, T., Itayama, T., & Inamori, Y. (2006). Highly sensitive real-time PCR assay for quantification of toxic cyanobacteria based on microcystin synthetase a gene. *Journal of Bioscience and Bioengineering*, *102*(2), 90–96. <https://doi.org/10.1263/jbb.102.90>
- Gade, M., Alpers, W., Hühnerfuss, H., Masuko, H., & Kobayashi, T. (1998). Imaging of biogenic and anthropogenic ocean surface films by the multifrequency/multipolarization SIR-C/X-SAR. *Journal of Geophysical Research: Oceans*, *103*(C9), 18851–18866. <https://doi.org/10.1029/97JC01915>
- Garrido, M., Cecchi, P., Malet, N., Bec, B., Torre, F., & Pasqualini, V. (2019). Evaluation of FluoroProbe® performance for the phytoplankton-based assessment of the ecological status of Mediterranean coastal lagoons. *Environmental Monitoring and Assessment*, *191*(4), 204. <https://doi.org/10.1007/s10661-019-7349-8>

- Giddings, M., Aranda-Rodriguez, R., Yasvinski, G., Watson, S. B., & Zura, R. (2012). *Cyanobacterial Toxins: Drinking and Recreational Water Quality Guidelines*. 12.
- Graham, J. L., Loftin, K. A., Meyer, M. T., & Ziegler, A. C. (2010). Cyanotoxin Mixtures and Taste-and-Odor Compounds in Cyanobacterial Blooms from the Midwestern United States. *Environmental Science & Technology*, 44(19), 7361–7368. <https://doi.org/10.1021/es1008938>
- Greenfield, D. I., Marin, R., Doucette, G. J., Mikulski, C., Jones, K., Jensen, S., Roman, B., Alvarado, N., Feldman, J., & Scholin, C. (2008). Field applications of the second-generation Environmental Sample Processor (ESP) for remote detection of harmful algae: 2006-2007: Field applications of the ESP: 2006-2007. *Limnology and Oceanography: Methods*, 6(12), 667–679. <https://doi.org/10.4319/lom.2008.6.667>
- Guertin, J., Jacobs, J. A., Avakian, C. P., & Independent Environmental Technical Evaluation Group (Eds.). (2005). *Chromium (VI) handbook*. CRC Press. (ISBN 978-1-56670-608-7)
- Gürleyük, H., & Wallschläger, D. (2001). Determination of chromium(iii) and chromium(vi) using suppressed ion chromatography inductively coupled plasma mass spectrometry. *J. Anal. At. Spectrom.*, 16(9), 926–930. <https://doi.org/10.1039/B102740A>
- Harris, D. C., & Lucy, C. A. (2015). *Quantative Chemical Analysis* (9th ed.). Kate Parker. (ISBN 978-1-4641-3538-5)
- Health Canada. (2015). *Chromium in Drinking Water*. Federal-Provincial-Territorial Committee on Drinking Water. <https://www.canada.ca/content/dam/canada/health-canada/migration/healthy-canadians/health-system-systeme-sante/consultations/chromium-chrome/alt/chromium-chrome-eng.pdf>
- Health Canada. (2016). Cyanobacterial Toxins in Drinking Water—Document for Public Consultation. *Federal-Provincial-Territorial Committee on Drinking Water*, 1–171. (ISBN 0273-1223)
- Health Canada. (2018). *Guidelines for Canadian drinking water quality: Guideline technical document - chromium*. Federal-Provincial-Territorial Committee on Drinking

Water (Canada). (ISBN 978-0-660-06563-2) http://epe.lac-bac.gc.ca/100/201/301/weekly_acquisitions_list-ef/2018/18-07/publications.gc.ca/collections/collection_2018/sc-hc/H144-36-2017-eng.pdf

Herrero, A., & Flores, E. (2008). *The Cyanobacteria: Molecular Biology, Genomics and Evolution*. Caister Academic Press. (ISBN 978-1-913652-21-0)

Hoshi, S., Konuma, K., Sugawara, K., Uto, M., & Akatsuka, K. (1998). The simple and rapid spectrophotometric determination of trace chromium(VI) after preconcentration as its colored complex on chitin. *Talanta*, 47(3), 659–663. [https://doi.org/10.1016/S0039-9140\(98\)00112-X](https://doi.org/10.1016/S0039-9140(98)00112-X)

Hudnell, H. K. (Ed.). (2008). *Cyanobacterial Harmful Algal Blooms: State of the Science and Research Needs*. Springer. (ISBN 978-0-387-75864-0)

Hwang, E. S., Nam, S. H., & Kim, N. H. (2006). *On-line chromium (Cr³⁺/Cr⁶⁺) Speciation by FI-ICP-OES*. PerkinElmer. <http://citeseerx.ist.psu.edu/viewdoc/download?doi=10.1.1.571.9030&rep=rep1&type=pdf>

Jarczewska, M., Ziółkowski, R., Górski, Ł., & Malinowska, E. (2015). Electrochemical Detection of Chromium(VI): Induced DNA Damage. *Journal of The Electrochemical Society*, 162(12), B326–B331. <https://doi.org/10.1149/2.0401512jes>

Jena, B. K., & Raj, C. R. (2008). Highly sensitive and selective electrochemical detection of sub-ppb level chromium(VI) using nano-sized gold particle. *Talanta*, 76(1), 161–165. <https://doi.org/10.1016/j.talanta.2008.02.027>

Jin, W., & Yan, K. (2015). Recent advances in electrochemical detection of toxic Cr. *RSC Advances*, 5(47), 37440–37450. <https://doi.org/10.1039/C5RA03480A>

Kirman, C. R., Suh, M., Proctor, D. M., & Hays, S. M. (2017). Improved physiologically based pharmacokinetic model for oral exposures to chromium in mice, rats, and humans to address temporal variation and sensitive populations. *Toxicology and Applied Pharmacology*, 325, 9–17. <https://doi.org/10.1016/j.taap.2017.03.023>

Klejdus, B., Kopecký, J., Benešová, L., & Vacek, J. (2009). Solid-phase/supercritical-fluid extraction for liquid chromatography of phenolic compounds in freshwater microalgae and

- selected cyanobacterial species. *Journal of Chromatography A*, 1216(5), 763–771. <https://doi.org/10.1016/j.chroma.2008.11.096>
- Krishna, M., Chandrasekaran, K., Rao, S. V., Karunasagar, D., & Arunachalam, J. (2005). Speciation of Cr(III) and Cr(VI) in waters using immobilized moss and determination by ICP-MS and FAAS. *Talanta*, 65(1), 135–143. <https://doi.org/10.1016/j.talanta.2004.05.051>
- Kubáň, P., Kubáň, P., & Kubáň, V. (2003). Speciation of chromium (III) and chromium (VI) by capillary electrophoresis with contactless conductometric detection and dual opposite end injection. *ELECTROPHORESIS*, 24(9), 1397–1403. <https://doi.org/10.1002/elps.200390179>
- Kurmayer, R., Sivonen, K., Wilmotte, A., & Salmaso, N. (Eds.). (2017). *Molecular Tools for the Detection and Quantification of Toxigenic Cyanobacteria*. John Wiley & Sons, Ltd. (ISBN 978-1-119-33216-9) <https://doi.org/10.1002/9781119332169>
- Lace, A., Ryan, D., Bowkett, M., & Cleary, J. (2019). Chromium Monitoring in Water by Colorimetry Using Optimised 1,5-Diphenylcarbazine Method. *International Journal of Environmental Research and Public Health*, 16(10). <https://doi.org/10.3390/ijerph16101803>
- Lane, C. E., Gutierrez-Wing, M. T., Rusch, K. A., & Benton, M. G. (2012). Homogeneous detection of cyanobacterial DNA via polymerase chain reaction: Uniform cyanobacteria PCR detection. *Letters in Applied Microbiology*, 55(5), 376–383. <https://doi.org/10.1111/j.1472-765X.2012.03304.x>
- Lawton, L. A., Edwards, C., & Codd, G. A. (1994). Extraction and high-performance liquid chromatographic method for the determination of microcystins in raw and treated waters. *The Analyst*, 119(7), 1525. <https://doi.org/10.1039/an9941901525>
- Le, C., Zha, Y., Li, Y., Sun, D., Lu, H., & Yin, B. (2010). Eutrophication of Lake Waters in China: Cost, Causes, and Control. *Environmental Management*, 45(4), 662–668. <https://doi.org/10.1007/s00267-010-9440-3>

- Li, Q., Lian, L., Wang, X., Wang, R., Tian, Y., Guo, X., & Lou, D. (2017). Analysis of microcystins using high-performance liquid chromatography and magnetic solid-phase extraction with silica-coated magnetite with cetylpyridinium chloride. *Journal of Separation Science*, 40(8), 1644–1650. <https://doi.org/10.1002/jssc.201601407>
- Li, W., Duan, J., Niu, C., Qiang, N., & Mulcahy, D. (2011). Determination of Microcystin-LR in Drinking Water Using UPLC Tandem Mass Spectrometry-Matrix Effects and Measurement. *Journal of Chromatographic Science*, 49(9), 665–670. <https://doi.org/10.1093/chrscl/49.9.665>
- Liu, J.-Y., Zeng, L.-H., & Ren, Z.-H. (2020). Recent application of spectroscopy for the detection of microalgae life information: A review. *Applied Spectroscopy Reviews*, 55(1), 26–59. <https://doi.org/10.1080/05704928.2018.1509345>
- Loza, V., Perona, E., & Mateo, P. (2013). Molecular Fingerprinting of Cyanobacteria from River Biofilms as a Water Quality Monitoring Tool. *Applied and Environmental Microbiology*, 79(5), 1459–1472. <https://doi.org/10.1128/AEM.03351-12>
- Ma, J., Yang, B., & Byrne, Robert. H. (2012). Determination of nanomolar chromate in drinking water with solid phase extraction and a portable spectrophotometer. *Journal of Hazardous Materials*, 219–220, 247–252. <https://doi.org/10.1016/j.jhazmat.2012.04.001>
- Mandal, S., & Rath, J. (2015). *Extremophilic Cyanobacteria For Novel Drug Development*. Springer International Publishing. (ISBN 978-3-319-12008-9) <https://doi.org/10.1007/978-3-319-12009-6>
- Mankiewicz-Boczek, J., Izydorczyk, K., Romanowska-Duda, Z., Jurczak, T., Stefaniak, K., & Kokocinski, M. (2006). Detection and monitoring toxigenicity of cyanobacteria by application of molecular methods. *Environmental Toxicology*, 21(4), 380–387. <https://doi.org/10.1002/tox.20200>
- McCullough, G. (2007). *Assessment of bbe Fluoroprobe for algal taxonomic discrimination in Lake Winnipeg* (p. 27) [Report to the Canadian Department of Fisheries and Oceans]. Centre for Earth Observations Science Department of Environment and Geography University of Manitoba.

- McLean, J. E., McNeill, L. S., Edwards, M. A., & Parks, J. L. (2012). Hexavalent chromium review, part 1: Health effects, regulations, and analysis. *Journal - American Water Works Association*, *104*(6), E348–E357. <https://doi.org/10.5942/jawwa.2012.104.0091>
- McNeill, L., McLean, J., Edwards, M., & Parks, J. (2012a). State of the Science of Hexavalent Chromium in Drinking Water. *Water Research Foundation*, 36.
- McNeill, L. S., McLean, J. E., Parks, J. L., & Edwards, M. A. (2012b). Hexavalent chromium review, part 2: Chemistry, occurrence, and treatment. *Journal - American Water Works Association*, *104*(7), E395–E405. <https://doi.org/10.5942/jawwa.2012.104.0092>
- McQuaid, N., Zamyadi, A., Prévost, M., Bird, D. F., & Dorner, S. (2011). Use of in vivo phycoerythrin fluorescence to monitor potential microcystin-producing cyanobacterial biovolume in a drinkingwater source. *J. Environ. Monit.*, *13*(2), 455–463. <https://doi.org/10.1039/C0EM00163E>
- McSheehy, S., Séby, F., & Nash, M. (2010). *The Determination of Trivalent and Hexavalent Chromium in Mineral and Spring Water using HPLC-ICP-MS*. Thermo Scientific. <https://static.thermoscientific.com/images/D02228~.pdf>
- Millie, D. F., Schofield, O. M., Kirkpatrick, G. J., Johnsen, G., & Evens, T. J. (2002). Using absorbance and fluorescence spectra to discriminate microalgae. *European Journal of Phycology*, *37*(3), 313–322. <https://doi.org/10.1017/S0967026202003700>
- Moffat, I., Martinova, N., Seidel, C., & Thompson, C. M. (2018). Hexavalent Chromium in Drinking Water: JOURNAL AWWA. *Journal - American Water Works Association*, *110*(5), E22–E35. <https://doi.org/10.1002/awwa.1044>
- Mohamed, Z. A., Deyab, M. A., Abou-Dobara, M. I., El-Sayed, A. K., & El-Raghi, W. M. (2015). Occurrence of cyanobacteria and microcystin toxins in raw and treated waters of the Nile River, Egypt: Implication for water treatment and human health. *Environmental Science and Pollution Research*, *22*(15), 11716–11727. <https://doi.org/10.1007/s11356-015-4420-z>

- Moreira, C., Martins, A., Azevedo, J., Freitas, M., Regueiras, A., Vale, M., Antunes, A., & Vasconcelos, V. (2011). Application of real-time PCR in the assessment of the toxic cyanobacterium *Cylindrospermopsis raciborskii* abundance and toxicological potential. *Applied Microbiology and Biotechnology*, 92(1), 189–197. <https://doi.org/10.1007/s00253-011-3360-x>
- Moreira, C., Ramos, V., Azevedo, J., & Vasconcelos, V. (2014). Methods to detect cyanobacteria and their toxins in the environment. *Applied Microbiology and Biotechnology*, 98(19), 8073–8082. <https://doi.org/10.1007/s00253-014-5951-9>
- Mulaudzi, L. V., van Staden, J. F., & Stefan, R. I. (2002). Determination of chromium(III) and chromium(VI) by use of a spectrophotometric sequential injection system. *Analytica Chimica Acta*, 467(1–2), 51–60. [https://doi.org/10.1016/S0003-2670\(02\)00188-5](https://doi.org/10.1016/S0003-2670(02)00188-5)
- Mutuyimana, F. P., Liu, J., Nsanzamahoro, S., Na, M., Chen, H., & Chen, X. (2019). Yellow-emissive carbon dots as a fluorescent probe for chromium(VI). *Microchimica Acta*, 186(3), 163. <https://doi.org/10.1007/s00604-019-3284-1>
- Narin, I., Kars, A., & Soylak, M. (2008). A novel solid phase extraction procedure on Amberlite XAD-1180 for speciation of Cr(III), Cr(VI) and total chromium in environmental and pharmaceutical samples. *Journal of Hazardous Materials*, 150(2), 453–458. <https://doi.org/10.1016/j.jhazmat.2007.04.125>
- National Water Quality Management Strategy. (2000). *Australian and New Zealand guidelines for fresh and marine water quality 2000.: Vol. Agriculture and Resource Management Council of Australia and New Zealand*. Australian and New Zealand Environment and Conservation Council. (ISBN 978-0-9578245-0-8)
- Neubauer, K., Reuter, W., & Perrone, P. (2003). Chromium Speciation in Water by HPLC/ICP-MS. *PerkinElmer, Application Note*, 8.
- NHMRC, & NRMCC. (2017). *Australian Drinking Water Guidelines Paper 6 National Water Quality Management Strategy (Version 3.4)*. National Health and Medical Research Council, National Resource Management Ministerial Council. (ISBN 1-86496-511-8)

<https://www.nhmrc.gov.au/sites/default/files/documents/reports/aust-drinking-water-guidelines.pdf>

NTP. (2008). NTP technical report on the toxicology and carcinogenesis studies of sodium dichromate dihydrate (CAS No. 7789-12-0) in F344/N rats and B6C3F1 mice (drinking water studies). *US National Institute of Environmental Health Sciences, National Toxicology Program.*, 7789, 201.

NTP. (2010). NTP toxicology and carcinogenesis studies of chromium picolinate monohydrate (CAS No. 27882-76-4) in F344/N rats and B6C3F1 mice (feed studies). *US National Institute of Environmental Health Sciences, National Toxicology Program.*, 196.

Ölcer, Z., Esen, E., Ersoy, A., Budak, S., Sever Kaya, D., Yağmur Gök, M., Barut, S., Üstek, D., & Uludag, Y. (2015). Microfluidics and nanoparticles based amperometric biosensor for the detection of cyanobacteria (*Planktothrix agardhii* NIVA-CYA 116) DNA. *Biosensors and Bioelectronics*, 70, 426–432. <https://doi.org/10.1016/j.bios.2015.03.052>

Olsson, J., Feng, X. M., Ascue, J., Gentili, F. G., Shabiimam, M. A., Nehrenheim, E., & Thorin, E. (2014). Co-digestion of cultivated microalgae and sewage sludge from municipal waste water treatment. *Bioresource Technology*, 171, 203–210. <https://doi.org/10.1016/j.biortech.2014.08.069>

Onchoke, K. K., & Sasu, S. A. (2016). Determination of Hexavalent Chromium (Cr(VI)) Concentrations via Ion Chromatography and UV-Vis Spectrophotometry in Samples Collected from Nacogdoches Wastewater Treatment Plant, East Texas (USA). *Advances in Environmental Chemistry*, 2016, 1–10. <https://doi.org/10.1155/2016/3468635>

Oren, A. (2014). *Cyanobacteria: An Economic Perspective* (N. K. Sharma, A. K. Rai, & L. J. Stal, Eds.). John Wiley & Sons, Ltd. (ISBN 978-1-118-40223-8) <https://doi.org/10.1002/9781118402238.ch1>

Ortelli, D., Edder, P., Cognard, E., & Jan, P. (2008). Fast screening and quantitation of microcystins in microalgae dietary supplement products and water by liquid chromatography coupled to time of flight mass spectrometry. *Analytica Chimica Acta*, 617(1–2), 230–237. <https://doi.org/10.1016/j.aca.2008.03.033>

- Ortiz, X., Korenkova, E., Jobst, K. J., MacPherson, K. A., & Reiner, E. J. (2017). A high throughput targeted and non-targeted method for the analysis of microcystins and anatoxin-A using on-line solid phase extraction coupled to liquid chromatography–quadrupole time-of-flight high resolution mass spectrometry. *Analytical and Bioanalytical Chemistry*, 409(21), 4959–4969. <https://doi.org/10.1007/s00216-017-0437-0>
- Osaki, S., Osaki, T., & Takashima, Y. (1983). Determination of chromium(vi) in natural waters by the sorption of chromium-diphenylcarbazone with xad-2 resin. *Talanta*, 30(9), 683–686. [https://doi.org/10.1016/0039-9140\(83\)80156-8](https://doi.org/10.1016/0039-9140(83)80156-8)
- Ouyang, R., Bragg, S. A., Chambers, J. Q., & Xue, Z.-L. (2012). Flower-like self-assembly of gold nanoparticles for highly sensitive electrochemical detection of chromium(VI). *Analytica Chimica Acta*, 722, 1–7. <https://doi.org/10.1016/j.aca.2012.01.032>
- Owen, A. J. (1995). *Uses of Derivative Spectroscopy*. Agilent Technologies. https://www.who.edu/cms/files/derivative_spectroscopy_59633940_175744.pdf
- Owen, T. (1998). *Fundamentals of Modern UV-Visible Spectroscopy*. Hewlett-Packard Company. <https://trove.nla.gov.au/work/32688247>
- Pelaez, M., Antoniou, M. G., He, X., Dionysiou, D. D., de la Cruz, A. A., Tsimeli, K., Triantis, T., Hiskia, A., Kaloudis, T., Williams, C., Aubel, M., Chapman, A., Foss, A., Khan, U., O’Shea, K. E., & Westrick, J. (2010). Sources and Occurrence of Cyanotoxins Worldwide. In D. Fatta-Kassinos, K. Bester, & K. Kümmerer (Eds.), *Xenobiotics in the Urban Water Cycle* (Vol. 16, pp. 101–127). Springer Netherlands. (ISBN 978-90-481-3508-0) https://doi.org/10.1007/978-90-481-3509-7_6
- Perkin Elmer. (1996). *Analytical Methods for Atomic Absorption Spectroscopy* (The Perkin-Elmer Corporation). PerkinElmer. http://www1.lasalle.edu/~prushan/Instrumental%20Analysis_files/AA-Perkin%20Elmer%20guide%20to%20all!.pdf
- Perkin Elmer. (2018). Atomic Spectroscopy, A Guide to Selecting the Appropriate Technique and System. *Atomic Spectroscopy*, 16.

- Pressman, M. A. S., & Aldstadt, J. H. (2003). A comparative study of diffusion samplers for the determination of hexavalent chromium by sequential injection spectrophotometry. *Microchemical Journal*, 74(1), 47–57. [https://doi.org/10.1016/S0026-265X\(02\)00156-X](https://doi.org/10.1016/S0026-265X(02)00156-X)
- Pretty, J. N., Mason, C. F., Nedwell, D. B., Hine, R. E., Leaf, S., & Dils, R. (2003). Environmental Costs of Freshwater Eutrophication in England and Wales. *Environmental Science & Technology*, 37(2), 201–208. <https://doi.org/10.1021/es020793k>
- PubChem. (2020a). *Chromate*. National Center for Biotechnology Information. <https://pubchem.ncbi.nlm.nih.gov/compound/24461>
- PubChem. (2020b). *Dichromate*. National Center for Biotechnology Information. <https://pubchem.ncbi.nlm.nih.gov/compound/24503>
- Rajesh, N., Mishra, B. G., & Pareek, P. K. (2008). Solid phase extraction of chromium(VI) from aqueous solutions by adsorption of its diphenylcarbazide complex on a mixed bed adsorbent (acid activated montmorillonite-silica gel) column. *Spectrochimica Acta. Part A, Molecular and Biomolecular Spectroscopy*, 69(2), 612–618. <https://doi.org/10.1016/j.saa.2007.05.011>
- Rakhunde, R., Deshpande, L., & Juneja, H. D. (2012). Chemical Speciation of Chromium in Water: A Review. *Critical Reviews in Environmental Science and Technology*, 42(7), 776–810. <https://doi.org/10.1080/10643389.2010.534029>
- Rice, E. W., Baird, R. B., & Eaton, A. D. (2017). *Standard Methods for the Examination of Water and Wastewater* (23rd ed.). American Public Health Association, American Water Works Association, Water Environment Federation. (ISBN 978-0-87553-287-5)
- Rockett, L., Benson, V., Clementson, A. J., Doyle, T., Hall, T., Harman, M., Jonsson, J., Rumsby, P., Young, W., Wilkinson, D. J., & Warwick, P. (2015). *Understanding the Significance of Chromium in Drinking Water* (p. 187). WRc plc. <http://www.dwi.gov.uk/research/completed-research/reports/DWI70-2-275.pdf>
- Sadeghi, S., & Moghaddam, A. Z. (2015). A new method for separation and determination of Cr(III) and Cr(VI) in water samples by high-performance liquid chromatography based

- on anion exchange stationary phase of ionic liquid modified silica. *Environmental Monitoring and Assessment*, 187(12), 725. <https://doi.org/10.1007/s10661-015-4928-1>
- Saha, R., Nandi, R., & Saha, B. (2011). Sources and toxicity of hexavalent chromium. *Journal of Coordination Chemistry*, 64(10), 1782–1806. <https://doi.org/10.1080/00958972.2011.583646>
- Saini, D. K., Pabbi, S., & Shukla, P. (2018). Cyanobacterial pigments: Perspectives and biotechnological approaches. *Food and Chemical Toxicology*, 120, 616–624. <https://doi.org/10.1016/j.fct.2018.08.002>
- Saker, M., Moreira, C., Martins, J., Neilan, B., & Vasconcelos, V. M. (2009). DNA profiling of complex bacterial populations: Toxic cyanobacterial blooms. *Applied Microbiology and Biotechnology*, 85(2), 237–252. <https://doi.org/10.1007/s00253-009-2180-8>
- Sanchez-Hachair, A., & Hofmann, A. (2018). Hexavalent chromium quantification in solution: Comparing direct UV–visible spectrometry with 1,5-diphenylcarbazide colorimetry. *Comptes Rendus Chimie*, 21(9), 890–896. <https://doi.org/10.1016/j.crci.2018.05.002>
- Sanz-Medel, A., Pereiro, R., & Costa-Fernández, J. M. (2009). Chapter 1. A General Overview of Atomic Spectrometric Techniques. In J. M. Andrade-Garda (Ed.), *Basic Chemometric Techniques in Atomic Spectroscopy* (pp. 1–50). Royal Society of Chemistry. (ISBN 978-0-85404-159-6) <https://doi.org/10.1039/9781847559661-00001>
- Scaife, M. A., Merx-Jacques, A., Woodhall, D. L., & Armenta, R. E. (2015). Algal biofuels in Canada: Status and potential. *Renewable and Sustainable Energy Reviews*, 44, 620–642. <https://doi.org/10.1016/j.rser.2014.12.024>
- Schlüter, L., David, G., Jørgensen, N., Podduturi, R., Tucci, A., Dias, A., & da Silva, R. (2018). Characterization of phytoplankton by pigment analysis and the detection of toxic cyanobacteria in reservoirs with aquaculture production. *Aquaculture Environment Interactions*, 10, 35–48. <https://doi.org/10.3354/aei00256>

- Sedman, R., Beaumont, J., Budroe, J., & Vidair, C. (2011). *California Public Health Goals for Chemicals in Drinking Water—Hexavalent Chromium Cr (VI)*. Office of Environmental Health Hazard Assessment California Environmental Protection Agency. <https://oehha.ca.gov/media/downloads/water/chemicals/phg/cr6phg072911.pdf>
- Sereshti, H., Vasheghani Farahani, M., & Baghdadi, M. (2016). Trace determination of chromium(VI) in environmental water samples using innovative thermally reduced graphene (TRG) modified SiO₂ adsorbent for solid phase extraction and UV–vis spectrophotometry. *Talanta*, *146*, 662–669. <https://doi.org/10.1016/j.talanta.2015.06.051>
- Sharma, N., Choudhary, K., Bajpai, R., & Rai, A. (2010). *Freshwater cyanobacterial (blue-green algae) blooms: Causes, consequences and control*. 24.
- Sharma, P., Bihari, V., Agarwal, S. K., Verma, V., Kesavachandran, C. N., Pangtey, B. S., Mathur, N., Singh, K. P., Srivastava, M., & Goel, S. K. (2012). Groundwater Contaminated with Hexavalent Chromium [Cr (VI)]: A Health Survey and Clinical Examination of Community Inhabitants (Kanpur, India). *PLoS ONE*, *7*(10). <https://doi.org/10.1371/journal.pone.0047877>
- Sherman, B., Lemckert, C., & Zhang, H. (2010). *The Impact of Artificial Destratification on Reservoir Evaporation* (Urban Water Security Research Alliance Technical Report No. 35; p. 25). Urban Water Security Research Alliance (UWSRA). <http://www.urbanwateralliance.org.au/publications/UWSRA-tr35.pdf>
- Singh, B., Baudhdh, K., & Bux, F. (Eds.). (2015). *Algae and Environmental Sustainability*. Springer India. (ISBN 978-81-322-2639-0) <https://doi.org/10.1007/978-81-322-2641-3>
- Son, S., & Wang, M. (2019). VIIRS-Derived Water Turbidity in the Great Lakes. *Remote Sensing*, *11*(12), 1448. <https://doi.org/10.3390/rs11121448>
- Srivastava, A., Singh, S., Ahn, C.-Y., Oh, H.-M., & Asthana, R. K. (2013). Monitoring Approaches for a Toxic Cyanobacterial Bloom. *Environmental Science & Technology*, *47*(16), 8999–9013. <https://doi.org/10.1021/es401245k>
- Stasinakis, A. S., Thomaidis, N. S., & Lekkas, T. D. (2003). Speciation of chromium in wastewater and sludge by extraction with liquid anion exchanger Amberlite LA-2 and

electrothermal atomic absorption spectrometry. *Analytica Chimica Acta*, 478(1), 119–127. [https://doi.org/10.1016/S0003-2670\(02\)01434-4](https://doi.org/10.1016/S0003-2670(02)01434-4)

Stefanelli, M., Vichi, S., Stipa, G., Funari, E., Testai, E., Scardala, S., & Manganelli, M. (2014). Survival, growth and toxicity of *Microcystis aeruginosa* PCC 7806 in experimental conditions mimicking some features of the human gastro-intestinal environment. *Chemico-Biological Interactions*, 215, 54–61. <https://doi.org/10.1016/j.cbi.2014.03.006>

Steffensen, D. A. (2008). Economic cost of cyanobacterial blooms. In H. K. Hudnell (Ed.), *Cyanobacterial Harmful Algal Blooms: State of the Science and Research Needs* (pp. 855–865). Springer. (ISBN 978-0-387-75865-7) https://doi.org/10.1007/978-0-387-75865-7_37

Storey, M. V., van der Gaag, B., & Burns, B. P. (2011). Advances in on-line drinking water quality monitoring and early warning systems. *Water Research*, 45(2), 741–747. <https://doi.org/10.1016/j.watres.2010.08.049>

Sunilkumar, M. N., Ajith, T. A., & Parvathy, V. K. (2014). Acute ammonium dichromate poisoning in a 2 year-old child. *Indian Journal of Critical Care Medicine : Peer-Reviewed, Official Publication of Indian Society of Critical Care Medicine*, 18(11), 757–758. <https://doi.org/10.4103/0972-5229.144024>

Sutton, R. (2010). Chromium-6 in U.S. Tap Water. *Environmental Working Group*, 24.

Swinehart, D. F. (1962). The Beer-Lambert Law. *Journal of Chemical Education*, Vol.39(7), 333. <https://doi.org/10.1021/ed039p333>

Tang, A.-N., Jiang, D.-Q., Jiang, Y., Wang, S.-W., & Yan, X.-P. (2004). Cloud point extraction for high-performance liquid chromatographic speciation of Cr(III) and Cr(VI) in aqueous solutions. *Journal of Chromatography A*, 1036(2), 183–188. <https://doi.org/10.1016/j.chroma.2004.02.065>

Tehrani, M. S., Ebrahimi, A. A., & Rastegar, F. (2004). Chromium Speciation by Surfactant Assisted Solid-Phase Extraction and Flame Atomic Absorption Spectrometric Detection. *Annali Di Chimica*, 94(5–6), 429–435. <https://doi.org/10.1002/adic.200490052>

- Tunçeli, A., & Türker, A. R. (2002). Speciation of Cr(III) and Cr(VI) in water after preconcentration of its 1,5-diphenylcarbazone complex on amberlite XAD-16 resin and determination by FAAS. *Talanta*, 57(6), 1199–1204. [https://doi.org/10.1016/S0039-9140\(02\)00237-0](https://doi.org/10.1016/S0039-9140(02)00237-0)
- Tuzen, M., & Soylak, M. (2006). Chromium speciation in environmental samples by solid phase extraction on Chromosorb 108. *Journal of Hazardous Materials*, 129(1), 266–273. <https://doi.org/10.1016/j.jhazmat.2005.08.046>
- UNESCO. (1996). *Design and Implementation of some Harmful Algal Monitoring Systems*. 44, 116.
- UNESCO, Anderson, D. M., Cembella, A. D., Enevoldsen, H. O., & Hallegraeff, G. M. (2004). *Manual on harmful marine microalgae*. UNESCO. (ISBN 978-92-3-103948-5)
- Van de Waal, D. B., Guillebault, D., Alfonso, A., Rodríguez, I., Botana, L. M., Bijkerk, R., & Medlin, L. K. (2018). Molecular detection of harmful cyanobacteria and expression of their toxin genes in Dutch lakes using multi-probe RNA chips. *Harmful Algae*, 72, 25–35. <https://doi.org/10.1016/j.hal.2017.12.007>
- Vaz, R., Bettini, J., Júnior, J. G. F., Lima, E. D. S., Botero, W. G., Santos, J. C. C., & Schiavon, M. A. (2017). High luminescent carbon dots as an eco-friendly fluorescence sensor for Cr(VI) determination in water and soil samples. *Journal of Photochemistry and Photobiology A: Chemistry*, 346, 502–511. <https://doi.org/10.1016/j.jphotochem.2017.06.047>
- Vincent, W. F. (2009). Cyanobacteria. In G. E. Likens (Ed.), *Encyclopedia of Inland Waters* (pp. 226–232). Academic Press. (ISBN 978-0-12-370626-3) <https://doi.org/10.1016/B978-012370626-3.00127-7>
- Wang, G., Li, J., Zhang, B., Shen, Q., & Zhang, F. (2015). Monitoring cyanobacteria-dominant algal blooms in eutrophicated Taihu Lake in China with synthetic aperture radar images. *Chinese Journal of Oceanology and Limnology*, 33(1), 139–148. <https://doi.org/10.1007/s00343-015-4019-8>

- Wang, N., Wang, L., Yang, H., Xiong, T., Xiao, S., Zhao, J., & Du, W. (2019a). Fluorescent Sensors Based on Organic Polymer-Capped Gold Nanoparticles for the Detection of Cr(VI) in Water. *International Journal of Analytical Chemistry*, 2019, 1–10. <https://doi.org/10.1155/2019/1756014>
- Wang, Y., He, J., Zheng, M., Qin, M., & Wei, W. (2019b). Dual-emission of Eu based metal-organic frameworks hybrids with carbon dots for ratiometric fluorescent detection of Cr(VI). *Talanta*, 191, 519–525. <https://doi.org/10.1016/j.talanta.2018.08.078>
- Weldy, E., Wolff, C., Miao, Z., & Chen, H. (2013). Selective and sensitive detection of chromium(VI) in waters using electrospray ionization mass spectrometry. *Science & Justice*, 53(3), 293–300. <https://doi.org/10.1016/j.scijus.2012.12.003>
- WHO. (2003a). Algae and cyanobacteria in fresh water. In *Guidelines for Safe Recreational Water Environments* (pp. 136–158). WHO Publishing. https://www.who.int/water_sanitation_health/bathing/srwe1-chap8.pdf
- WHO. (2003b). *Guidelines for Safe Recreational Water Environments: Coastal and fresh waters*. World Health Organization. (ISBN 978-92-4-154580-8)
- WHO (Ed.). (2011). *Guidelines for drinking water quality* (4th ed). World Health Organization. (ISBN 978-92-4-154815-1)
- WHO. (2017). *Guidelines for drinking water quality*. World Health Organization. (ISBN 978-92-4-154995-0)
- WHO. (2019). *Chromium in Drinking-water* (p. 34) [Peer review draft]. World Health Organization. https://www.who.int/water_sanitation_health/water-quality/guidelines/chemicals/draft-chromium-190924.pdf
- Wilson, A. E., Gossiaux, D. C., Höök, T. O., Berry, J. P., Landrum, P. F., Dyble, J., & Guildford, S. J. (2008). Evaluation of the human health threat associated with the hepatotoxin microcystin in the muscle and liver tissues of yellow perch (*Perca flavescens*). *Canadian Journal of Fisheries and Aquatic Sciences*, 65(7), 1487–1497. <https://doi.org/10.1139/F08-067>

Winter, J. G., DeSellas, A. M., Fletcher, R., Heintsch, L., Morley, A., Nakamoto, L., & Utsumi, K. (2011). Algal blooms in Ontario, Canada: Increases in reports since 1994. *Lake and Reservoir Management*, 27(2), 107–114. <https://doi.org/10.1080/07438141.2011.557765>

Xie, L., Xie, P., Guo, L., Li, L., Miyabara, Y., & Park, H.-D. (2005). Organ distribution and bioaccumulation of microcystins in freshwater fish at different trophic levels from the eutrophic Lake Chaohu, China. *Environmental Toxicology*, 20(3), 293–300. <https://doi.org/10.1002/tox.20120>

Yarbro, S. K. (1976). *Two photometric methods for the determination of chromium in biological materials* [Georgia Institute of Technology]. <https://smartech.gatech.edu/handle/1853/25982>

Yen, H.-K., Lin, T.-F., & Liao, P.-C. (2011). Simultaneous detection of nine cyanotoxins in drinking water using dual solid-phase extraction and liquid chromatography–mass spectrometry. *Toxicon*, 58(2), 209–218. <https://doi.org/10.1016/j.toxicon.2011.06.003>

Yuan, M., & Carmichael, W. W. (2004). Detection and analysis of the cyanobacterial peptide hepatotoxins microcystin and nodularin using SELDI-TOF mass spectrometry. *Toxicon*, 44(5), 561–570. <https://doi.org/10.1016/j.toxicon.2004.07.015>

Zamyadi, A., Choo, F., Newcombe, G., Stuetz, R., & Henderson, R. K. (2016). A review of monitoring technologies for real-time management of cyanobacteria: Recent advances and future direction. *TrAC Trends in Analytical Chemistry*, 85, 83–96. <https://doi.org/10.1016/j.trac.2016.06.023>

Zamyadi, A., MacLeod, S. L., Fan, Y., McQuaid, N., Dorner, S., Sauv e, S., & Pr evost, M. (2012a). Toxic cyanobacterial breakthrough and accumulation in a drinking water plant: A monitoring and treatment challenge. *Water Research*, 46(5), 1511–1523. <https://doi.org/10.1016/j.watres.2011.11.012>

Zamyadi, A., McQuaid, N., Pr evost, M., & Dorner, S. (2012b). Monitoring of potentially toxic cyanobacteria using an online multi-probe in drinking water sources. *J. Environ. Monit.*, 14(2), 579–588. <https://doi.org/10.1039/C1EM10819K>

Zhang, W., Lou, I., Ung, W. K., Kong, Y., & Mok, K. M. (2014). Application of PCR and real-time PCR for monitoring cyanobacteria, *Microcystis* spp. And *Cylindrospermopsis raciborskii* in Macau freshwater reservoir. *Frontiers of Earth Science*, 8(2), 291–301. <https://doi.org/10.1007/s11707-013-0409-4>

Zinicovscaia, I., & Cepoi, L. (Eds.). (2016). *Cyanobacteria for Bioremediation of Wastewaters*. Springer International Publishing. (ISBN 978-3-319-26749-4) <https://doi.org/10.1007/978-3-319-26751-7>

Appendix A

Table A.9: State Guidelines and Regulations for Cyanobacteria and Cyanobacterial Toxins in Drinking and Recreational Waters in the USA (Chorus, 2005, 2012).

State	Toxin or species	Drinking water	Recreational waters
California	Microcystins (LA, LR, RR, YR)		Action levels Human recreational uses: 0.8 µg/L (water) Human fish consumption: 10 ng/g ww ³ (fish) Livestock: Water 3 µg/L, crusts 0.2 mg/L Pets: Water 7 µg/L, crusts 0.02 mg/Kg Fish: Water 13 ng/g Monitoring Guidance: 40,000 to 10,000 cells/L Microcystin: ≥ 8 µg/L Scum associated with toxigenic species

Florida	Microcystins	1 $\mu\text{g/L}$ chronic; 10 $\mu\text{g/L}$ 90 day	Event Based Response: Common Sense Approach; no recreational activities in blooms.
Indiana	Microcystins		<p>Event-based response: $\geq 20 \mu\text{g/L}$</p> <p>Very low/no risk: $< 4 \mu\text{g/L}$</p> <p>Low to moderate risk of adverse health effects: $4 - 20 \mu\text{g/L}$</p> <p>Seriously consider avoiding contact with water until levels of toxin decrease: $> 20 \mu\text{g/L}$</p>
Iowa	Microcystins		Routine monitoring: Advisory/closure $\geq 20 \mu\text{g/L}$
Kansas	Microcystins		<p>Health advisory: $\geq 4 \mu\text{g/L}$</p> <p>Health warning: $\geq 20 \mu\text{g/L}$</p>
	Total cyanobacteria cells		<p>Health advisory: Cell count $\geq 20,000$ cells/L</p> <p>Health warning: Cell count $\geq 100,000$ cells/L</p>
Maryland	Microcystins or Planktothrix		<p>Routine monitoring:</p> <p>Cell counts: $\geq 40,000$ cells/L</p>

			Only Microcystins: $\geq 14 \mu\text{g/L}$
Massachusetts	Microcystins		Guideline: avoid water contact
			Humans: $14 \mu\text{g/L}$
			Cell counts: $\geq 70,000 \text{ cells/L}$
			Monitoring Guidance: Cell counts: $\geq 70,000 \text{ cells/L}; \geq 8 \mu\text{g/L}$
Michigan			Each county handles incidents on a case-by-case basis
Nebraska	Microcystins		Routine monitoring: Advisory/closure $\geq 20 \mu\text{g/L}$
New Hampshire			Routine Monitoring $> 50\%$ toxigenic cyanobacteria
New York			Each county handles incidents on a case-by-case basis
North Carolina			Routine monitoring in specific waterbodies, monitoring as needed in others
Ohio	Microcystins	$1 \mu\text{g/L}$	Health advisory: $\geq 6 \mu\text{g/L}$
			No contact advisory: $\geq 20 \mu\text{g/L}$

Oklahoma	Total cyanobacteria cells		Action level: Health advisory 100,000 cells/L
	Microcystins		Action level: Health advisory: 20 µg/L
Oregon	Total cyanobacteria cells		Action level: Health advisory ≥ 100,000 cells/L Scum associated with toxigenic species
	Microcystins or Planktothrix		Action level: Health advisory ≥ 40,000 cells/L
	Microcystins	1–12 µg/L	Health advisory: 8 µg/L
Rhode Island	Total cyanobacteria		Health advisory: Evidence of a visible cyanobacteria scum or mat.
	Total cyanobacteria cells		Health advisory: Cell counts: ≥ 70,000 cells/L
	Microcystins		Health advisory: ≥ 14 µg /L
Texas			Health advisory: Cell counts: ≥ 20,000 cells/L

	Any cyanobacteria	Health advisory: Visual identification
Vermont	Microcystins	Health advisory/closure: Microcystin $\geq 6 \mu\text{g/L}$
Virginia	Microcystins	No guidelines
		Decisions are made by the individual charged with assessing the situation.
		Two or more data points from water quality monitoring sites, generally spaced 1–2 miles (1.6–3.2 km) apart in small to medium sized segments, achieving $> 50,000$ cells/L Microcystins and subsequently measuring $> 10 \mu\text{g/L}$ microcystin toxin would suggest an extensive bloom and significant impairment status due to human health risks
Washington	Microcystins	Provisional guideline for warning to avoid exposure (CAUTION): $\leq 6 \mu\text{g/L}$
		Provisional guideline for warning to avoid exposure (WARNING): $\geq 6 \mu\text{g/L}$
		Provisional guideline for warning to avoid exposure (DANGER): $\geq 6 \mu\text{g/L}$ + high toxicity report of illness or pet death
Wisconsin	Any cyanobacteria	May close beach if: Cell counts: $\geq 100,000$ cells/L

Table A.10: National and regional drinking and recreational water quality guidelines and standards currently in place across Canada (Chorus, 2012; Health Canada, 2016).

Jurisdiction	Population	Drinking Water and Cyanobacteria				Water Quality Guidelines		
		Cyanobacteria (as water source issue, %)	Cyanobacteria related to treatment modifications (%)	Amount of surface water treated (m ³ 10 ⁶)	Households on municipal water supply (%)	Drinking MC-LR: 1.5 µg/L	Recreation MC-LR: 20 µg/L Cells: 100,000 cells/L	BRMP in place
Canada	34,278,400	3.9–4.7	–	5186	–	✓	✓	×
Alberta	3,742,800	4.4–5.4	1.8	482	64	✓	✓	✓
British Columbia	4,554,100	6.9–7.4	6.9–7.4	731	69	✓	✓	×
Manitoba	1,243,700	6.2	6	406	50	✓	✓	×

New Brunswick	753,200	0–5	0	80	58	✓	×	×
Newfoundland and Labrador	509,100	–	–	132	72	✓	✓	✓
Nova Scotia	943,400	0	0	101.6	73	✓	×	×
Yukon, NW Territories	43,600 NW 34,300 YK	0	0	6.2	–	✓	×	✓
Ontario	13,282,400	4.6–5.1	4.6–5.1	1733	54	✓	✓	
Prince Edward Island	143,500	0	0	0	–	✓	×	✓
Quebec	7,943,000	1.3–3.7	1.3–3.7	1697	60	✓ (provincial)	×	✓
						MC: 1.5 µg/L	MC: 16 µg/L	
						ATX: 3.7 µg/L	ATX: 340 µg/L	

Saskatchewan	1,052,100	7.6–8.5	6.9–7.1	114	70	✓	✓	×
Nunavut	33,300	–						

Table A.11: Occurrence and characteristics of select algal chlorophylls and their derivatives (Gray, 2010).

Chlorophylls & Derivatives	Occurrence	Specific Coefficient	Extinction (L/g cm); Maximum Absorbance (nm)	Notes
a	all groups (only select prochlorophytes)	87.67; 664		Monovinyl a-a chlorin pigment having a central magnesium ion &, a phytol side chain; a proxy for algal abundance
b	chlorophytes, euglenophytes, prasinophytes, prochlorophytes	51.36; 647		Monovinyl b

Chlorophyllides a & b	a - all groups; b - chlorophytes, euglenophytes, prasinophytes, prochlorophytes	a - 127; 664; b - 74.07; 645	Monovinyl a/b less the phytol chain, senescent processing artifact
Pheophytins a & b	a - all groups; b - chlorophytes, euglenophytes, prasinophytes, prochlorophytes	a - 51.2; 667; b - 31.8; 657	Monovinyl a/b less the magnesium atom
Pheophorbides a & b	a - all groups; b - chlorophytes, euglenophytes, prasinophytes, prochlorophytes	a - 74.2; 667; b - 46.37; 657	Monovinyl a/b less the magnesium atom and phytol chain
Divinyl a & b	prochlorophytes	assume identical to monovinyl chlorophylls	Divinyl a is a proxy for abundance; determined solely by HPLC

Pyropheophytin a	all groups	60.29; 667	Pheophorlide a less the methylated carboxyl group from the isocyclic ring
Mg 2,4 divinylpheoporphylin a ₅ monoethyl ester (MGDVP)	Prochlorophytes, prasinophytes and haptophytes, possibly the cyanobacterium, <i>Acaryochloris marina</i>	select 58.9; 623	–
d	Trace constituents in rhodophytes; major pigment in the cyanobacterium, <i>Acaryochloris marina</i>	N/A; 697	Differs from chlorophyll-a by the precense of a formyl group (instead of a vinyl group) at the c-3 position

Table A.12: Commercial characteristics of eleven in vivo fluorescence cyanobacterial probes (*: For measurement unit, see column raw probe reading unit) (PC: phycocyanin; PE: phycoerythrin, Chla: chlorophyll-a) (Zamyadi et al., 2016).

Manufacturer	In-situ submersible probe/sensor		Excitation wavelength (nm) ± bandpass		Emission wavelength (nm) ± bandpass		Resolution range*	/	Detection limit*	Limit of quantification*	Raw probe reading unit									
			µg Chla/L of cyanobacteria			µg PC/L					ppb			cells/mL			Relative fluorescence unit (RFU)			
bbe Moldaenke	Algal	Online	590		685±5		0.1 / 0 – 200		–	–										
	Analyser (AOA)																			
	Algae Torch		590		680		0.2 / 0 – 200		4	–										
	FluoroProbe		590		680		0.05 / 200		0.3	0.6										
TriOS	MicroFlu-blue		620		655±5		0.1 / 0 – 200		0.7	2.3										
Turner Designs	C3	Submersible	<595		>630		0.1 / 0 – 40,000		2	–										
	fluorometer																			
Hach Hydrolab	DS5x		590		650		20 / 150 – 2×10 ⁵		100	150										
Yellow Springs Instrument	YSI-V6131		590 ±15		660±20		0.1 / 0 – 100		0.2	0.7										

Company								
YSI Inc. (YSI)					1 / 0 – 2.8×10 ⁵	220	–	cells/mL
	EXO		590 ±15	685±20	0.01 / 0 – 100	0.04	–	RFU
WetLabs	ECO FL		630	680	0.03 / 0 – 230	–	–	ppb
Aquaread	Aquaprobe® 2000	AP-	590	655	1 / 0 – 3×10 ⁵	200	200	cells/mL
Chelsea	Unilux & Trilux		610	685	– / 0 to 100	0.01	–	µg PC/L

3. Materials and Methods

3.1 Culture growth and sustenance

Microcystis aeruginosa and *Chlorella vulgaris* were acquired from Canadian Phycological Culture Center (CPCC). Their individual information and culturing information is detailed below (CPCC, 2013).

Algae strain: *Microcystis aeruginosa* CPCC 632

Growth media: Bold's Basal Medium with triple Nitrogen stock (3N-BBM)

Medium preparation: To obtain 1 L of 100% 3N-BBM medium, add 1 mL of K₂HPO₄ stock solution (BBM Stock 5) plus 20 mL of the concentrate to 979 mL of ultrapure D.I. water.

Growth intensity: 1200 lux.

Inoculation and sub-culturing ratio: *Microcystis* can crash if the inoculum is not dense enough. To start the culture, a 1:2 inoculum to medium ratio is employed. For example, 5 mL of 3N-BBM growth medium was added to 5 mL of *M. aeruginosa*. This ensures safe culture growth and avoids potential culture crash. To maintain the microalgal culture, timely sub-culturing is necessary. *M. aeruginosa* required a sub-culture once every 5 – 7 days depending on the cell concentration of the culture (CPCC, 2013; Hellebust et al., 1973). Once the microalgae acclimate to incubator growth conditions, the inoculum to medium ratio was increased to 1:4 and maintained till the completion of experiments pertaining to **Chapters 4 – 7**.

Algae strain: *Chlorella vulgaris* CPCC 90

Growth media: Bold's Basal Medium stock (BBM)

Medium preparation: To obtain 1 L of 100% BBM medium, add 1 mL of K₂HPO₄ stock solution (BBM Stock 5) plus 10 mL of the concentrate to 989 mL of ultrapure D.I. water.

Growth intensity: 1800 lux; higher intensity for *C. vulgaris* was attained by elevating the Erlenmeyer flask using a stand inside the incubator. Higher light intensity was provided to *C. vulgaris* for optimal growth rate.

Inoculation and sub-culturing ratio: To start the culture, a 1:5 inoculum to medium ratio is employed. For example, 8 mL of BBM growth medium was added to 2 mL of *C. vulgaris*. To maintain the viability of the microalgal culture sub-culturing is required step. As *C. vulgaris* is an environmentally sturdy strain, it requires a sub-culture once every 1 – 2 weeks depending on the cell concentration and growth rate of the culture (CPCC, 2013; Hellebust et al., 1973; KBGAWG, 2009). Once the microalgae acclimate to incubator growth conditions, the inoculum to medium ratio was increased to 1:10 and maintained till the completion of the required experiments.

Commonalities for both microalgae

Refer to Table B.2, Table B.3, Table B.4, and Table B.5 for media concentrate preparation information.

Common steps (for 3N-BBM and BBM) during medium preparation: The BBM stock 5 is added during medium preparation separately as it precipitates out when mixed with higher concentration of concentrate stock(s) solution (Hellebust et al., 1973). To ensure that the

medium is sterile, the storage vessel of the prepared medium was sterilized using an autoclave for 30 min at 15 psi and 121 °C.

Storage: The vessel containing the prepared medium was stored in the fridge at 4 °C in the dark until needed to ensure longevity and consistency of the growth media.

Algal culture vessel: Both strains of microalgae were cultured in separate 500 mL Erlenmeyer flasks. To prevent contamination of the microalgal cultures, the flasks were rinsed in D.I. water and the mouths were covered using aluminum foil paper, and sterilized using an autoclave for 30 min at 15 psi and 121 °C. After sterilization, the flasks are let to cool at room temperature before use. All flasks were labeled with the microalgal culture name, strain, growth medium, start date of the culture, dilution ratio, and subsequent sub-culturing date to maintain proper lab- and biosafety.

Growth conditions: The cultures were incubated inside a temperature-controlled incubator (at 24 °C) which was equipped with two daylight fluorescent tube lights to mimic optimal and natural environmental growth conditions. The cultures were maintained under a 24-hour light photoperiod. No supplementary carbon dioxide (CO₂) was supplied to the cultures for growth purposes other than the diffused CO₂ present in ambient air. Sufficient headspace should be maintained in the flasks for gas exchange between the microalgae and the surrounding environment. The flasks were agitated gently and manually twice a day for optimal growth of microalgae.

Sub-culturing equipment: All the cultures were sub-cultured inside a biological safety cabinet equipped with HEPA filter. An automatic pipettor was used with sterile 25 mL pipettes to prevent cross-contamination.

3.2 Sample Preparation and Characterization

3.2.1 Microalgae experiments

For both the microalgal cultures, and all **Chapter 4 – 7** experiments, the initial sample preparation followed the same method to ensure consistency and repeatability. *M. aeruginosa* (cyanobacteria) and *C. vulgaris* (green algae) cultures were separated from their growth medium by centrifugation at 8,000×g for 5 min each using 50 mL tubes for individual experiments. Following centrifugation, the growth medium was discarded, and the collected microalgae were re-suspended in respective mL of water matrices (such as D.I. water, river water, among others). The samples were then gently inverted 5 times to ensure a homogenous concentration of microalgae over the entire volume to obtain the stock culture solution which was then used for subsequent dilutions. Afterwards, the stock cultures were enumerated under a Leitz Laborlux 12 light microscope and quantified using an improved Neubauer hemocytometer. For all experimental purposes, Direct-Q UV Water Purification System (Millipore Sigma, USA) was used for D.I. water.

3.2.1.1 Improved Neubauer hemocytometer

The Neubauer chamber or hemocytometer is a simple counting chamber where the central area is used for counting cells. Commonly, the central area has two counting chamber (upper and lower chamber) containing counting grid of 3 mm x 3 mm in size (Figure 3.1). A glass cover of 22 mm x 22 mm is placed on top of the hemocytometer that covers the central area and is designed so that the distance between the chamber and the cover stays at 0.1 mm (Bastidas, 2013).

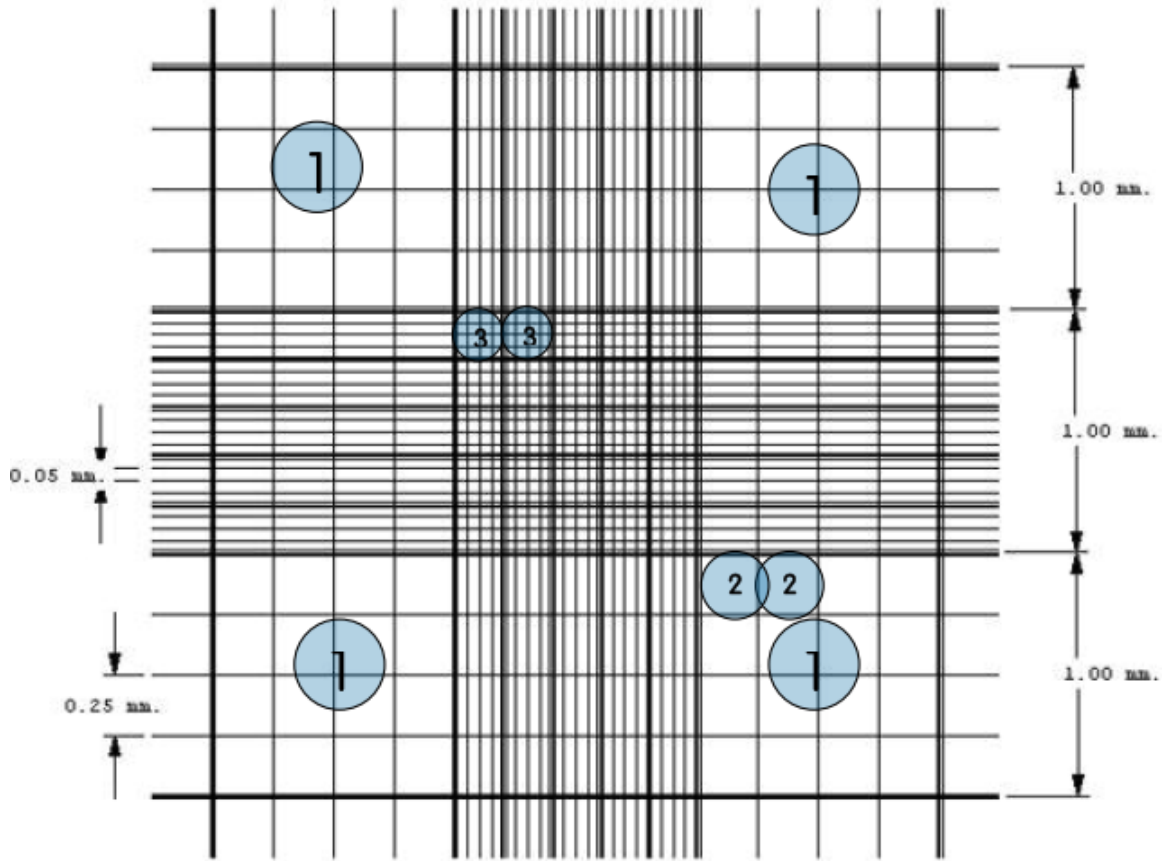


Figure 3.1: Improved Neubauer chamber counting grid details (Bastidas, 2013).

Before cell counting, the hemocytometer and the glass lid are cleaned with ethanol and wiped using kimwipes to minimize error in cell counting. After placing the lid on top of the hemocytometer, the chambers are loaded with 10 μL of the prepared microalgal stock solution by using a sterilized micropipette tip on each side to ensure the balance of the counting chamber. The pipette tip was wetted at least twice using the stock microalgal solution before use. A clean tip was used for each chamber. The hemocytometer preparation is performed in a biological safety cabinet to prevent potential interferences/ errors in the counting process due to aerosols. After each use, the hemocytometer is washed with ethanol and wiped using kimwipes before storing in a safe container.

3.2.1.2 Microscope enumeration

Following the hemocytometer preparation, a Leitz Laborlux 12 light microscope was used for cell enumeration using a 20x magnification objective. The microscope was kept on a stable base that is free from disturbances such as environmental vibration. This helps to avoid cell counting errors. Now, counting can be started with the cells in the first square and as a general rule (which was followed for all microalgal experiments), cells that overlap on the left and top boundary of the selected chamber be counted, while the ones overlapping on the right and the bottom boundary should not be counted (Bastidas, 2013). Furthermore, while counting the zig-zag technique should be used, where the cells inside a square are counted from the top left to the top right, followed by right to left in the next row, and so on (Figure 3.2). This ensures consistency and avoids the overestimation of the concentration of the microalgal stock solution.

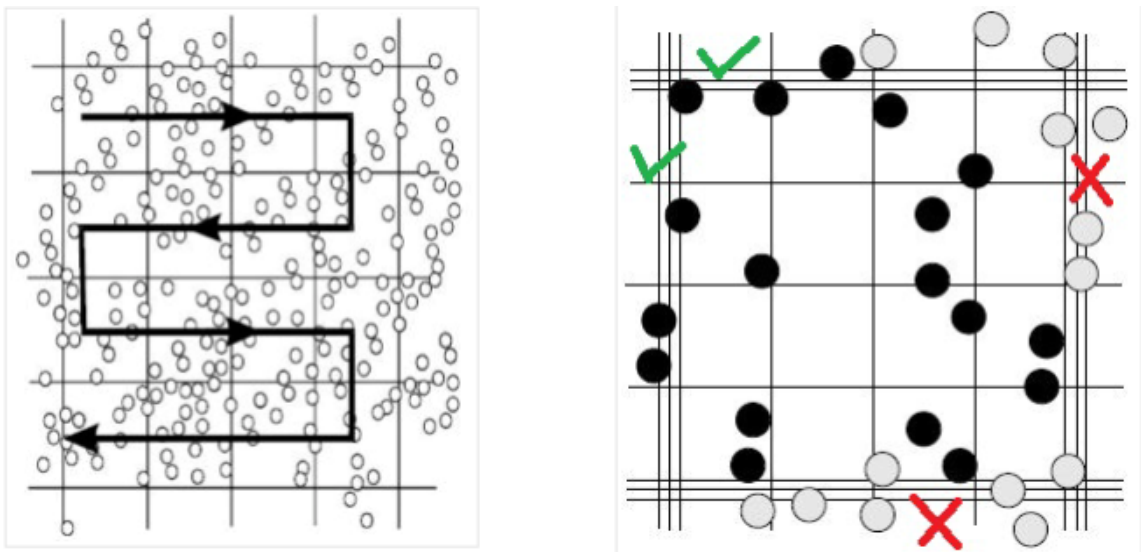


Figure 3.2: Zig-zag counting technique (left) and cells to be counted (right) (Bastidas, 2013).

Concentration calculation (Bastidas, 2013)

$$\text{Concentration (cells/ mL)} = \frac{\text{Number of cells} \times 10^3}{\text{Area counted (mm}^2\text{)} \times \text{Chamber depth (mm)}} \quad 3.1$$

3.2.2 Chromium (VI)

Chromium (VI) was prepared using analytical-reagent grade potassium dichromate (Sigma-Aldrich, $\geq 99.0\%$ purity, ACS reagent grade). To prepare 50 mg/L of stock Cr (VI) solution, dissolve 141.4 mg of dried potassium dichromate ($\text{K}_2\text{Cr}_2\text{O}_7$) crystals in ultrapure D.I. water and dilute to 1000 mL (EPA, 1992). A fresh stock solution was prepared right before experimentation to avoid potential contamination/ interferences in the spectral scan.

3.2.3 Water parameters

The study used the following water matrices for experimental testing purposes: D.I. water, surface water, tap water, salt water, DOC water, turbid water, and pH water. Salt water, DOC water, turbid water and pH water stocks were prepared on the day of the experiment in D.I. water to avoid potentially interfering particles/ decay during testing. These water quality parameters were selected following protocols set by the Alliance for Coastal Technologies (ACT) for the nutrient sensor challenge (Johengen, 2016). ACT is jointly funded by National Oceanic and Atmospheric Administration (NOAA) and EPA to develop, improve, and apply sensor technologies for monitoring purposes. Nutrient sensor challenge was developed to verify sensor technology performance in controlled and field environments, and the same protocols was used to verify the developed UV-Vis SP methodology for microalgal detection (Johengen, 2016). Each concentration level of the microalgae was exposed for 90 mins to the respective water parameter before UV-Vis SP

analysis. A comparative analysis was run by exposing another set of the same microalgal culture using the same concentration levels but with a higher exposure time of 180 mins to each individual water parameter to verify the effect of exposure on detection limit.

3.2.3.1 D.I. water response

Fresh D.I. water from Direct-Q UV Water Purification System (Millipore Sigma, USA) was used to prepare the microalgal/Cr (VI) sample dilutions as necessary on the day of the experiments. No stored water was used for experimentation to avoid possible contamination and change to D.I. water properties.

3.2.3.2 Salinity Response

- Test accuracy and precision over three salinity standards (10, 20, and 30 ppt) at room temperature.
- Salinity was developed using Instant Ocean® sea salt by adding the following amounts to D.I. water matrix in a clean, autoclaved glass container, and mixing thoroughly using a magnetic stirrer till complete solubility is achieved:
 - To make 1 L of 10 ppt of salinity, add 12.37 g of salt in 1000 mL of D.I. water.
 - To make 1 L of 20 ppt of salinity, add 25.02 g of salt in 1000 mL of D.I. water.
 - To make 1 L of 30 ppt of salinity, add 38.37 g of salt in 1000 mL of D.I. water.
- Verify the above standard salinities using a S47 SevenMulti™ dual meter pH / conductivity meter (Mettler Toledo, Ontario, Canada), as shown in Figure 3.3.
 - A minimum of triplicates of each standard solution were measured using the same stock solution but different grab samples.

- The probe sensor was completely immersed in the solution during measurement.
- Note: this measurement is independent of the sample size as the salt is completely solubilized in the stock solution.
- The conductivity meter was calibrated at least once every week using manufacturers standards.
- Individual salinity standards were used to prepare respective microalgal sample dilutions (under constant mixing), as necessary.

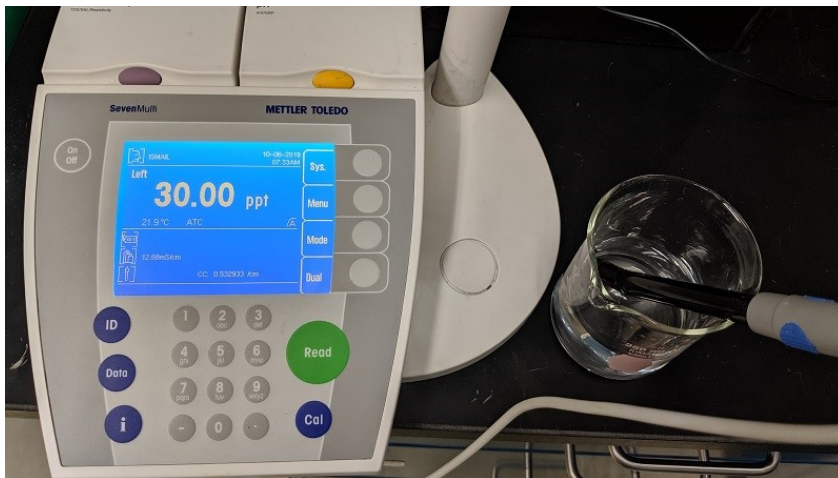


Figure 3.3: An example of 30 ppt salinity using a Mettler Toledo conductivity meter.

Turbidity Response

- Accuracy and precision were tested over three turbidity levels (10, 50, and 100 NTU) at room temperature.

- Turbidity standards were developed using the EPA recommended Elliot Silt Loam reference material (cat # 1B102M), obtained from the International Humic Substance Society (IHSS, 2020).
- The standards were prepared by adding the following amounts to D.I. water matrix in a clean, autoclaved glass container and stirred using a magnetic stirrer:
 - To make 1 L of 10 NTU turbidity, add 45.97 mg of reference material in 1000 mL of D.I. water.
 - To make 1 L of 50 NTU turbidity, add 229.88 mg of reference material in 1000 mL of D.I. water.
 - To make 1 L of 100 NTU turbidity, add 459.78 mg of reference material in 1000 mL of D.I. water.
- The above standards were verified using HACH 2100AN Turbidimeter (Hach, Colorado, USA), shown in Figure 3.4.
 - Place individual 30 mL prepared standards in sample vials and measure using the turbidimeter.
 - Each sample measured was grabbed from the standard containing container (kept under constant stirring), as with turbidity standards, the particles might settle quickly.
 - To ensure accurate measurement, triplicates of each sample were measured using the same vial and same orientation.

- DOC was developed by adding the following amounts to D.I. water matrix in a clean, autoclaved glass container and stirred using a magnetic stirrer:
 - To make 1 L of 1 ppm DOC, add 2 mg of reference material in 1000 mL of D.I. water.
 - To make 1 L of 5 ppm DOC, add 10 mg of reference material in 1000 mL of D.I. water.
 - To make 1 L of 10 ppm DOC, add 20 mg of reference material in 1000 mL of D.I. water.
- The above standards preparation is based on the elemental composition declared by the IHSS where organic carbon is reported at approximately 50% of the total composition and is as follows:

Table 3.1: Elemental composition of Upper Mississippi River Natural Organic Matter standard (IHSS, 2020).

Cat. #	H ₂ O	Ash	C	H	O	N	S	P
1R110N	8.55	8.05	49.98	4.61	41.4	2.36	2.62	–

Where, H₂O content is the %(w/w) of H₂O in the air-equilibrated sample; Ash is the %(w/w) of inorganic residue in a dry sample; and C, H, O, N, S, and P are the elemental composition in %(w/w) of a dry, ash-free sample.

- Individual DOC standards were used to prepare respective microalgal/Cr (VI) sample dilutions (under constant mixing), as necessary.

It should be noted that the DOC, and turbidity for all the microalgal experiments adds to the natural DOC and turbidity produced by microalgae (Singh et al., 2015). Also, each standard was verified on the day of preparation to ensure consistency.

3.2.3.4 Surface water response

For surface water, Rideau River water was used as is and was grabbed from the river using a clean container on the day of the experiment. Before starting the experiment, the river water was allowed to acclimate to room temperature. Particle filtration was not performed on the grabbed river water so as to ensure a better represent realistic water conditions on microalgal/Cr (VI) detection. During sample preparation, the water was constantly stirred at 200 rpm using a magnetic stirrer to avoid particle settling and to maintain a homogenous water matrix. Surface water was analyzed for chemical oxygen demand (COD), hexavalent chromium, turbidity, total organic carbon (TOC), and pH using USEPA Reactor Digestion Method 8000, USEPA 1,5 diphenylcarbohydrazide method 8023, HACH 2100AN Turbidimeter (Hach, USA), Shimadzu TOC-V_{CPH/CPN} analyzer (Shimadzu Scientific Instruments, USA), and pH meter (Orion 5-star, Thermo Scientific, Canada), respectively.

3.2.3.5 pH response

Canadian drinking water quality guidelines recommend that the operational range of pH for finished drinking water should be between 7.0 – 10.5 (Health Canada, 2016). Generally, the pH of drinking water is maintained between 6.5 – 8.5 as most commonly used disinfectants have the highest efficacy between this range, and it avoids corrosion in supply pipes (Barbeau et al., 2005). A survey conducted by Health Canada in 2009 – 2010 reported that raw surface water pH ranged from 4.6 – 8.57; whilst for groundwater, a range of pH between 6.1 – 9.18 was observed (Health Canada, 2016).

Cr (VI) was tested at pH 5, 6, 7, 9, and 10. To prepare stock solutions at the aforementioned pH values, analytical grade sodium hydroxide (NaOH) and hydrochloric acid (HCL) were added to D.I. water matrix in a clean, autoclaved glass container under constant stirring. The pH was be measured using a pH meter (Orion 5-star, Thermo Scientific, Canada), and the pH meter was calibrated at least once a week using manufacturer's standards. Most drinking water samples can be pH adjusted by adding 1 mL or less of adjustment buffer per 100 mL of sample, which introduces an acceptable 1% dilution error (Basumallick & Rohrer, 2016).

3.2.3.6 Tap water response

Tap water was collected on the day of the experiment using clean and sterile 4L HDPE bottles from the sources listed below, which were then used as is (unfiltered) for experimentation purposes. The tap water was analyzed for the following parameters before the tests: COD, Cr (VI), turbidity, TOC, pH, free and total chlorine, using USEPA Reactor Digestion Method 8000, USEPA 1,5 diphenylcarbohydrazide method 8023, HACH 2100AN Turbidimeter (Hach, USA), Shimadzu TOC-V_{CPH/CPN} analyzer (Shimadzu Scientific Instruments, USA), pH meter (Orion 5-star, Thermo Scientific, Canada), USEPA DPD (N,N-diethyl-p-phenylenediamine) method 8021 and 8167, respectively (EPA, 2010a; Rice et al., 2017).

3.2.4 Hexavalent chromium verification

An initial analytical verification at individual concentration levels over the range from 10 – 100 µg/L was performed using HACH method 8023 based on USEPA 1,5 diphenyl carbohydrazide, to ensure that the concentration used for testing purposes is accurate. The test samples for verification were prepared by inoculating Cr (VI) stock solution in D.I.

water and subsequently analyzing them using a DR 2800 Spectrophotometer (HACH, CO, USA). As the method is limited to a minimum sensitivity of 10 $\mu\text{g/L}$, the Cr (VI) concentration levels below 10 $\mu\text{g/L}$ were not verified.

3.3 Experimental design and operation

For **Chapters 4 – 7**, following quantification of required microalgal strains, respective dilutions samples were prepared in their respective water matrix using 50 mL sterile centrifuge tubes. The concentration of the prepared microalgal samples ranged from approximately 7,600,000 cells/mL to 1,855 cells/L. For **Chapter 8**, dilutions using stock Cr (VI) solution were performed by inoculating Cr (VI) in respective water matrices and performing dilutions to get 7 concentration levels ranging from 100 $\mu\text{g/L}$ to 1 $\mu\text{g/L}$. The same dilution ratios were used for all experiments to ensure that the concentration of the samples remained approximately equal between experiments. This was done to make representative and illustrative comparisons between different experimental conditions and the two microalgal cultures. The dilutions used for sample preparation of individual concentration level is shown in Appendix B.

Once the samples were prepared, a desktop laboratory UV-Vis spectrophotometer Cary 100 UV-Vis Spectrophotometer (Agilent Technologies, USA) and Jenway 6850 Double Beam Spectrophotometer (Cole-Parmer, UK) were used for analysis, as shown in Figure 3.5. Before using the spectrophotometer, ensure that the light path is free of any interfering particles by cleaning it with lint free foam swabs, and calibrate the equipment at least once a week using manufacturers calibration. On start-up, the UV-Vis SP was allowed to warm up for a minimum of 30 mins, as this avoids potential fluctuations in energy outputs of the UV (deuterium) and visible light (tungsten) sources while maintaining the appropriate bulb

temperature. Before analysis, the spectrophotometer was zeroed to D.I. water, a minimum of two times (replacing the D.I. water each time) to maintain a standard baseline. A blank run with D.I. water was performed to ensure correct equipment baseline and verify if it is within the equipment manufacturer's error guideline.



Figure 3.5: Left: Cary 100 UV-Vis spectrophotometer (Agilent Technologies); Right: Jenway 6850 Double Beam Spectrophotometer (Cole-Parmer).

The experiments were conducted using a combination of 10-, 50-, and 100-mm pathlength quartz cuvettes, where the cuvettes were filled with a grab sample from the prepared concentration range and measured using a spectrophotometer. The volumes for the grab samples for 10-, 50-, and 100-mm were kept at a constant of 3 mL, 17.5 mL, and 35 mL, respectively. The same volume was used for every experiment to maintain consistency. Making sure to clean the cuvette walls inside, and outside using D.I. water before, and after use. If any visible particles stick to the walls of the cuvette, cleaning it using lint free foam swabs to avoid potential errors in analysis. The cuvettes were inspected regularly for any scratches and if observed, were discarded, and replaced with a new cuvette. All the experiments were conducted using the same cuvette of individual pathlength (as long as there are no visible damages on the cuvette), and the same orientation was employed during analysis for consistency.

As algae are prone to photobleaching, degradation of the photopigment (PC for cyanobacteria, and *Chl-a* for algae/ cyanobacteria) due to frequent excitation, for **Chapters 4 – 7** a grab sample (technical replicate) was not be used more than once during analysis (Gray, 2010). During experimentation, all the samples were analyzed starting from lower concentration to higher concentration to avoid potential overestimation of the low range samples. The cuvettes were rinsed with D.I. water between samples of different concentration levels. Before grabbing the sample for analysis, the sample tube was inverted gently thrice, and then the required volume was grabbed using an automatic pipettor. The same technique was followed for all the experiments. Now, the spectrophotometer was used to measure absorbance at discreet wavelengths, meaning that absorbance measurements were presented at the wavelengths measured by the instrument. The absorbance of the sample measured was at the wavelengths ranging from 190 nm – 800 nm with a constant step interval of 1 nm. The measured quantitative data was extracted using a USB flash drive from the software provided by the equipment manufacturer for post analysis.

3.4 First-order derivative of absorbance

The first-order derivative of absorbance represents the rate of change in absorbance with respect to wavelength ($dA/d\lambda$) (Owen, 1998). This technique was used in pursuit of improving the detection limit of water quality parameters under consideration. First-order derivatives are calculated by taking a difference between each successive absorbance value and dividing it by the wavelength interval separating them (Kus et al., 1996; Owen, 1995). The interval used for change in absorbance values were taken at 1 nm and resulted in $d\lambda$ value of 1. The first derivative corresponds to the slope of the traditional spectrum, where

the maxima correlates with the increase in absorbance with wavelength, while the minima appear after maxima of the normal spectrum. Additionally, the maxima of the normal spectrum correspond to the zero value on the derivative spectra (Burgess & Thomas, 2017). An unwanted effect of the first-order derivative is that as the signal-to-noise ratio decreases, it results in sharper noise features in the spectrum and a higher number of peaks (Kus et al., 1996; Owen, 1995). This can be reduced using alternative techniques as discussed below.

3.5 Savitzky-Golay first derivative of absorbance

Savitzky-Golay (S-G) first-order derivative can be used to simultaneously obtain first-order derivative and smoothen the obtained plot while improving the signal to noise ratio using the following correlation (Savitzky & Golay, 1964):

$$a_j = \frac{\sum_{i=-\frac{m-1}{2}}^{\frac{m-1}{2}} C_i F_{j+i}}{N} \frac{m+1}{2} \leq j \leq n - \frac{m-1}{2} \quad 3.2$$

Where,

a_j = Savitzky-Golay first derivative of absorbance

m = number of data points used

C_i = Savitzky-Golay filter coefficient

F = absorbance value measured at a specific wavelength

j = smoothened data point

N = standardization factor

Each measured absorbance value was smoothed using twenty-three data points so that $i = -11, -10, -9, \dots, 9, 10, 11$; $m = 23$; $N = 1012$; $C_i = -11, -10, -9, \dots, 9, 10, 11$; following S-G first derivative of absorbance (Savitzky & Golay, 1964).

S-G is useful in removing slow-changing baselines and revealing spectral features which are difficult to observe using a first-order derivative. S-G first derivative of absorbance also acts as a filter which reduces the impact of background noise fluctuations on the derivative spectrum. Further, it functions as a better fingerprint identifier than the normal spectrum as it results in a high number of distinct peaks and can function for multicomponent quantitative analysis as well (Burgess & Thomas, 2017; Chen et al., 2014; Ruffin et al., 2008). The biggest advantage of this method is that it can be applied to real-time systems using an algorithm to display traditional spectrum as well as derivative spectrum. However, this technique does come with its potential drawbacks as well. For this technique to work reliably, a minimum of 300 unique wavelengths absorbance data is required. There is no maximum wavelength limit for this method. Further, the resultant derivative spectra differs based on the number of number of wavelengths used for this method and it is critical to be consistent in order to identify the spectral fingerprint of a water contaminant.

Higher derivative spectrums often do not add any supplementary relevant information and hence were not be considered as part of this research. With increasing derivative degree, the spectra become more complex and the intensity of the bands decrease reducing the effectiveness for analysis (Antonov, 1997).

3.6 Method detection limit

Method detection limit (MDL) is the minimum concentration of a component that can be measured with 99% confidence (that the concentration of the compound is greater than zero) using an analytical procedure (Berthouex & Brown, 2002; Kus et al., 1996; WDNR, 1996). All the MDLs for different water quality parameters in this study were calculated according to the Hubaux and Vos (H-V) method, using a tool developed by Chemiasoft with a minimum of 3 spike replicates used for the calculation of detection limit. A statistical method was developed by Hubaux & Vos (1970) for the determination of MDL for linear calibration curves, which states that the sensitivity of the method is proportional to its precision, which can be measured using the standard deviation of the analyzed samples. For spectrophotometric determination, H-V MDL is strongly dependent on the linear regression of the concentration data to that of the measured absorbance

In order to calculate the H-V MDL, a minimum of 3 different concentration standards (J) and spike replicates (K) data must be used. It should be noted that with the increasing number of standards, the sensitivity and confidence of the MDL increases simultaneously (Hubaux & Vos, 1970). For accuracy and repeatability purposes, multiple replicates at individual concentration levels were measured in this study but each replicate was only be measured once. The H-V MDL is calculated based on the assumption that the measured absorbance and the standard concentration are linearly correlated, and form a linear line with the following equation:

$$\hat{y} = bX + a \tag{3.3}$$

Where a, and b are constants calculated via equations 3.4 and 3.5 below:

$$b = \frac{\sum_{i=1}^{i=N} [(x_i - \bar{x})(y_i - \bar{y})]}{\sum_{i=1}^{i=N} (x_i - \bar{x})^2} \quad 3.4$$

$$a = \bar{y} - b\bar{x} \quad 3.5$$

Where, \bar{x} and \bar{y} are the average concentration of the standards measured and their corresponding absorbance measurements, respectively. Subsequently, the standard deviation of regression is calculated as follows:

$$S_{y/x} = \sqrt{\frac{\sum_{i=1}^J \sum_{j=1}^K (\bar{y}_{ij} - \hat{y}_i)^2}{J \times K - 2}} \quad 3.6$$

Where, \hat{y}_i is the value of the calibration standard's response which is calculated from equation 3.3, and \bar{y}_{ij} is the average of the measured absorbance for K number of replicates. The student's t distribution value from one-tail distribution shall be set at $t_{(0.05, N-2)}$ by using a 95% confidence level and considering $N = J \times K$ degrees of freedom. Now, the critical concentration x_c (the concentration at which the estimated concentration can be distinguished from the blank), and the critical response y_c (the instrument response to critical concentration) are estimated as follows:

$$x_c = \frac{t_{(0.05, N-2)} \times S_{y/x}}{b} \times \sqrt{\frac{1}{J \times K} + \frac{\bar{x}^2}{K \times \sum_{i=1}^J (x_i - \bar{x})^2}} \quad 3.7$$

$$y_c = bx_c + a \quad 3.8$$

The final MDL using the H-V method is calculated to be twice the critical concentration and is represented by:

$$MDL = 2x_c \quad 3.9$$

The aforementioned method is implemented using an excel spreadsheet to avoid errors that might arise due to manual calculation and for ease of access. As the MDL methodology is a regression-based methodology, the experimentation design involves replicate spiking at individual concentration level and inclusion of method blanks to improve the confidence of the reported limit (Bernal, 2014; EPA, 2010b). For calculation of the MDL, the wavelengths with the best sensitivity (highest peak) were selected and linearity was verified using standard calibration curves.

3.7 Statistical and analytical analysis

Statistical and analytical analysis of the measured algal concentration was carried out using Microsoft Excel software. Absorbance graphs, the first derivative of absorbance, S-G first derivative of absorbance graphs, and standard calibration curves were plotted. For microalgae, the plots were distributed into higher and lower concentration ranges using the average values of all the technical replicates. For Cr (VI) experiments, graphs were plotted over the entire test concentration range (100 µg/L to 1 µg/L). Standard calibration curves were plotted at the wavelengths of interest and were used to validate whether the absorbance measurements agreed with the Beer-Lambert Law. Coefficient of determination (R^2) and slopes with their individual standard deviations were obtained for an individual parameter of interest, at their respective wavelengths using linear regression analysis.

3.8 References

- Antonov, L. (1997). Fourth derivative spectroscopy—A critical view. *Analytica Chimica Acta*, 349(1–3), 295–301. [https://doi.org/10.1016/S0003-2670\(97\)00210-9](https://doi.org/10.1016/S0003-2670(97)00210-9)
- Barbeau, B., Huffman, D., Mysore, C., Desjardins, R., Clément, B., & Prévost, M. (2005). Examination of discrete and confounding effects of water quality parameters during the inactivation of MS2 phages and *Bacillus subtilis* spores with chlorine dioxide. *Journal of Environmental Engineering and Science*, 4(2), 139–151. <https://doi.org/10.1139/s04-050>
- Bastidas, O. (2013). *Cell counting with Neubauer chamber, basic hemocytometer usage*. Celeromics Technologies, SRL, Grenoble, France. https://www.researchgate.net/profile/Dr_Majid_Azizi/post/How_can_I_measure_the_amount_of_cells_in_a_solution_with_filamentous_fungi/attachment/59d625bfc49f478072e9a7c0/AS%3A272167168610329%401441901117902/download/Cel-l-counting-Neubauer-chamber.pdf
- Basumallick, L., & Rohrer, J. (2016). Sensitive Determination of Hexavalent Chromium in Drinking Water. *Thermo Scientific, Application Update 179*, 6.
- Bernal, E. (2014). Limit of Detection and Limit of Quantification Determination in Gas Chromatography. In X. Guo (Ed.), *Advances in Gas Chromatography*. InTech. <https://doi.org/10.5772/57341>
- Berthouex, P. M., & Brown, L. C. (2002). *Statistics for Environmental Engineers*. 463.
- Burgess, C., & Thomas, O. (2017). UV-Visible Spectrophotometry of Water and Wastewater. In *UV-Visible Spectrophotometry of Water and Wastewater* (pp. 1–524). Elsevier. <https://doi.org/10.1016/B978-0-444-63897-7.00001-9>
- Chen, K., Zhang, H., Wei, H., & Li, Y. (2014). Improved Savitzky–Golay-method-based fluorescence subtraction algorithm for rapid recovery of Raman spectra. *Applied Optics*, 53(24), 5559. <https://doi.org/10.1364/AO.53.005559>
- CPCC. (2013, September 16). *Canadian Psychological Culture Centre*. Canadian Psychological Culture Centre. <https://uwaterloo.ca/canadian-psychological-culture-centre/home>

- EPA, U. (1992). *SW-846 Test Method 7196A: Chromium, Hexavalent (Colorimetric)*. EPA. <https://www.epa.gov/sites/production/files/2015-12/documents/7196a.pdf>
- EPA, U. (2010a). *Chromium-6 in Drinking Water*. EPA. <https://www.bendoregon.gov/home/showdocument?id=2737>
- EPA, U. (2010b). *Technical Basis for the Lowest Concentration Minimum Reporting Level (LCMRL) Calculator* (p. 30) [Technical Report]. United States Environmental Protection Agency. <https://www.epa.gov/dwanalyticalmethods/lowest-concentration-minimum-reporting-level-lcmrl-calculator>
- Gray, M. R. (Ed.). (2010). *Algae: Source to treatment* (1st ed). American Water Works Association.
- Health Canada. (2016). *Guidelines for Canadian drinking water quality: Guideline technical document - pH of drinking water*. <http://oaresource.library.carleton.ca/wcl/2016/20160519/H144-28-2016-eng.pdf>
- Hellebust, J. A., Stein-Taylor, J. R., & Craigie, J. S. (1973). *Handbook of phycological methods: Culture methods and growth measurement*. Cambridge Eng. : University Press.
- Hubaux, Andre., & Vos, Gilbert. (1970). Decision and detection limits for calibration curves. *Analytical Chemistry*, 42(8), 849–855. <https://doi.org/10.1021/ac60290a013>
- IHSS. (2020). *Elemental Compositions and Stable Isotopic Ratios of IHSS Samples* [Natural Organic Matter Research]. International Humic Substances Society. <http://humic-substances.org/elemental-compositions-and-stable-isotopic-ratios-of-ihss-samples/>
- Johengen, T. (2016). *Protocols for the Performance Verification of In Situ Nutrient Analyzers Submitted to the Nutrient Sensor Challenge*. Alliance for Coastal Technologies; 08/08/2020. http://www.act-us.info/nutrients-challenge/Download/Nutrient_Challenge_Test%20Protocols_PV16_01.pdf
- KBGAWG. (2009). *Standard Operating Procedures: Environmental Sampling of Cyanobacteria for Cell Enumeration, Identification and Toxin Analysis*. California Water Board. https://www.waterboards.ca.gov/northcoast/water_issues/programs/tmdls/klamath

_river/klamath_river_khsa_monitoring/pdf/090629/app_a/Cyanobacteria_Sampling_SOP.pdf

- Kus, S., Marzenko, Z., & Obarski, N. (1996). Derivative UV-VIS Spectrophotometry in Analytical Chemistry. *Chern. Anal. (Warsaw)*, Department of Analytical Chemistry, Technical University of Warsaw, 00-664 Warszawa, Poland, 31.
- Owen, A. J. (1995). *Uses of Derivative Spectroscopy*. Agilent Technologies. https://www.who.edu/cms/files/derivative_spectroscopy_59633940_175744.pdf
- Owen, T. (1998). *Fundamentals of Modern UV-Visible Spectroscopy*. Hewlett-Packard Company. <https://trove.nla.gov.au/work/32688247>
- Rice, E. W., Baird, R. B., & Eaton, A. D. (2017). *Standard Methods for the Examination of Water and Wastewater* (23rd ed.). American Public Health Association, American Water Works Association, Water Environment Federation.
- Ruffin, C., King, R. L., & Younan, N. H. (2008). A Combined Derivative Spectroscopy and Savitzky-Golay Filtering Method for the Analysis of Hyperspectral Data. *GIScience & Remote Sensing*, 45(1), 1–15. <https://doi.org/10.2747/1548-1603.45.1.1>
- Savitzky, Abraham., & Golay, M. J. E. (1964). Smoothing and Differentiation of Data by Simplified Least Squares Procedures. *Analytical Chemistry*, 36(8), 1627–1639. <https://doi.org/10.1021/ac60214a047>
- Singh, B., Baudh, K., & Bux, F. (Eds.). (2015). *Algae and Environmental Sustainability*. Springer India. <https://doi.org/10.1007/978-81-322-2641-3>
- WDNR. (1996). *Analytical Detection Limit Guidance & Laboratory Guide for Determining Method Detection Limits* (Analytical Guide PUBL-TS-056-96). Wisconsin Department of Natural Resources Laboratory Certification Program. <https://dnr.wi.gov/regulations/labcert/documents/guidance/-LODguide.pdf>

Appendix B

Culture Media

Bold's Basal Medium with triple Nitrogen stock (3N-BBM) and Bold's Basal Medium (BBM) stock composition and preparation.

Table B.2: Stock concentrate 3N-BBM composition from CPCC at the University of Waterloo (Hellebust et al., 1973).

Substance	Primary Stock	Volume used to prepare 200 mL concentrate (mL)	Concentrated Stock	Final Concentration in Medium (mg/L)
Milli-Q H ₂ O	–	83	–	–
BBM Stock 7: Na ₂ EDTA.2H ₂ O + KOH	10.0 g/L 6.2 g/L	10	0.5 g/L 0.31 g/L	10
BBM Stock 8: FeSO ₄ .7H ₂ O + H ₂ SO ₄ (conc.)	4.98 g/L 1.0 mL	10	0.249 g/L 0.05 mL/L	4.98
BBM Stock 1: KH ₂ PO ₄	175 g/L	10	8.75 g/L	175
BBM Stock 2: CaCl ₂ .2H ₂ O	25 g/L	10	1.25 g/L	25
BBM Stock 3: MgSO ₄ .7H ₂ O	75 g/L	10	3.75 g/L	75

BBM Stock 4:				
NaNO ₃	250 g/L	30	37.5 g/L	750
BBM Stock 5:				
K ₂ HPO ₄	75 g/L	–	–	75
BBM Stock 6:				
NaCl	25 g/L	10	1.25 g/L	25
BBM Stock 9:				
Trace Metal Solution	See below	10	See below	See below
BBM Stock 10:				
H ₃ BO ₃	11.5 g/L	7	0.4025 g/L	8.05
BBM Stock 11:				
F/2 Vitamin Solution	See below	10	See below	See below

Table B.3: Stock concentrate BBM composition from CPCC at the University of Waterloo (Hellebust et al., 1973).

Substance	Primary Stock	Volume used to prepare 100 mL concentrate (mL)	Concentrated Stock	Final Concentration in Medium (mg/L)
Milli-Q H ₂ O	–	3	–	–
BBM Stock 7:				
Na ₂ EDTA.2H ₂ O + KOH	10.0 g/L	10	1 g/L	10

		6.2 g/L		0.62 g/L	
BBM Stock 8:					
FeSO ₄ ·7H ₂ O	+	4.98 g/L	10	0.498 g/L	4.98
H ₂ SO ₄ (conc.)		1.0 mL		0.1 mL/L	
BBM Stock 1:					
KH ₂ PO ₄		175 g/L	10	17.5 g/L	175
BBM Stock 2:					
CaCl ₂ ·2H ₂ O		25 g/L	10	2.5 g/L	25
BBM Stock 3:					
MgSO ₄ ·7H ₂ O		75 g/L	10	7.5 g/L	75
BBM Stock 4:					
NaNO ₃		250 g/L	10	25.0 g/L	250
BBM Stock 5:					
K ₂ HPO ₄		75 g/L	–	–	75
BBM Stock 6:					
NaCl		25 g/L	10	2.5 g/L	25
BBM Stock 9:					
Trace Metal Solution		See below	10	See below	See below
BBM Stock 10:					
H ₃ BO ₃		11.5 g/L	7	0.805 g/L	8.05

BBM Stock 11:
 F/2 Vitamin See below 10 See below See below
 Solution

Table B.4: Trace Metal Solution composition (BBM Stock 9) (Hellebust et al., 1973).

Substance	Primary Stock (g/L)	Concentrated Stock (g/L)	Final concentration in Medium (mg/L)
H ₃ BO ₃	2.86	0.143	2.86
MnCl ₂ .4H ₂ O	1.81	0.0905	1.81
ZnSO ₄ .7H ₂ O	0.222	0.0111	0.222
NaMoO ₄ .5H ₂ O	0.390	0.0195	0.390
CuSO ₄ .5H ₂ O	0.079	0.00395	0.079
Co(NO ₃) ₂ .6H ₂ O	0.049	0.00245	0.049

Table B.5: F/2 Vitamin Solution composition (BBM Stock 11) (Hellebust et al., 1973).

Substance	Primary Stock (g/L)	Concentrated Stock (g/L)	Final concentration in Medium (mg/L)
Vitamin B12 (Cyanocobalamin)	0.001	0.00005	0.001
Biotin	0.001	0.00005	0.001
Thiamine	0.200	0.0100	0.200

To prepare 3N-BBM concentrate, the stocks solutions listed in Table B.2, Table B.4, and Table B.5, were combined in the order listed above. Upon mixing the aforementioned volumes, a 200 mL concentrate was prepared which was stored in the fridge at 4 °C in the dark until needed.

To prepare BBM concentrate, the stocks solutions listed in Table B.3, Table B.4, and Table B.5, were combined in the order listed above. Upon mixing the aforementioned volumes, a 200 mL concentrate was prepared which was be stored in the fridge at 4 °C in the dark until needed.

Note: For preparation of both media concentrates, stock 5 was added during final medium preparation as it precipitates out in the presence of higher stocks solutions (Hellebust et al., 1973).

Microalgae dilution series methodology

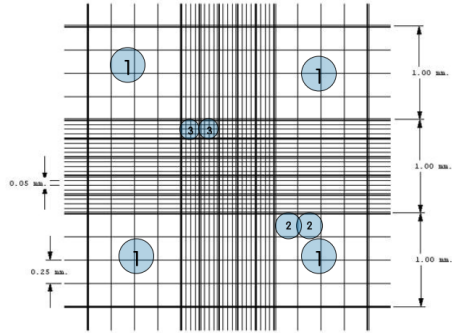
Strain:

Parameter:

- g measured

- NTU/ ppt measured

Date:



$$4 * (1) * (1) * 0.1$$

$$= \text{[cells/ } \mu\text{L]}$$

$$= \text{cells/} \mu\text{l} * 10^3 \text{ [cells/ mL]}$$

0	7,600,000	1:		
1	3,800,000	1:4	12 ml sample	36 ml water
2	1,900,000	1: 2	25 ml	
3	950,000	1: 4	12 ml sample	36 ml water
4	475,000	1: 2		
5	237,000	1: 16	3 ml sample	45 ml water
6	118,750	1: 2		
7	59,686	1: 64	0.8 ml sample	50.4 ml water
8	29,686	1: 2		
9	14,844	1: 256	0.2 ml sample	51 ml water
10	7,422	1: 2		
11	3,711	1: 1024	0.05 ml sample	51.15 ml water
12	1,855	1: 2		

12	4, 5, 6	5	25, 26, 27
11	7, 8, 9	4	28, 29, 30
10	10, 11, 12	3	31, 32, 33
9	13, 14, 15	2	34, 35, 36
8	16, 17, 18	1	37, 38, 39

3	6 ml	Sample	18 ml
5	1.5 ml	Sample	22.5 ml
7	0.4 ml	Sample	25.2 ml
9	0.1	Sample	25.5 ml
11	0.025 ml	Sample	25.575 ml

4. Monitoring of Cyanobacteria using Derivative Spectrophotometry and Improvement of the Method Detection Limit by Changing Pathlength

Amitesh Malhotra and Banu Örmeci*

Department of Civil and Environmental Engineering, Carleton University

1125 Colonel By Drive, Ottawa ON K1S 5B6, Canada

Abstract

Effective monitoring tools and methods are needed for the early detection and management of cyanobacteria in water bodies to minimize their harmful impacts on the environment and public health. This research investigated changing the cuvette pathlength (10-, 50-, and 100-mm) to improve the detection of cyanobacteria using UV-Vis spectrophotometry with subsequent application of derivative spectrophotometry and Savitzky-Golay (S-G) transformation. A non-toxicogenic strain of blue-green cyanobacteria, *Microcystis aeruginosa* (CPCC 632), and a green algae strain for comparison, *Chlorella vulgaris* (CPCC 90), were studied in a wide range of concentrations (955,000 - 1,855 cells/mL). In each concentration range, method detection limits were established with absorbance measurements and S-G first derivative of absorbance using 10-, 50-, and 100-mm cuvette pathlengths. Increasing the cuvette pathlength from 10 mm to 100 mm resulted in a 15-fold improvement in sensitivity with absorbance and a 13-fold improvement with S-G first derivative of absorbance for *M. aeruginosa*. Overall, adoption of 100 mm pathlength and application of S-G derivative spectra improved the method detection limit for *M. aeruginosa* from 337,398 cells /mL to 4,916 cells/mL, which is below the WHO guideline for low probability of adverse health effects (< 20,000 cells/mL). Similarly, the detection

limit for *C. vulgaris* was improved from 650,414 cells /mL to 11,661 cells /mL. The results also showed that spectrophotometry could differentiate *M. aeruginosa* from *C. vulgaris* based on the variations in their pigment absorbance peaks.

Keywords: Cyanobacteria; *Microcystis aeruginosa*; *C. vulgaris*; water; monitoring; derivative spectrophotometry.

4.1 Introduction

The need for better, simple, and affordable early detection systems is imperative with increasing harmful algal blooms (HABs) in water sources worldwide (Hudnell, 2008; Liu et al., 2020; Zamyadi et al., 2016). The presence of HABs creates nuisance from poor water quality, surface scum production and can lead to problems with drinking water treatment such as clogging of filters, increased disinfectant requirements, and in case of extreme events, the need for alternate water sources (Oren, 2014). Cyanobacteria can be toxigenic or non-toxigenic in nature; the toxigenic cyanobacteria can produce highly potent cyanotoxins stored inside the cell walls, which are released upon cell lysis. This poses a potential risk to human health, wildlife, livestock, and the aquatic environment (Al-Sammak et al., 2014; Bukaveckas, 2018; Srivastava et al., 2013). *Anabaena*, *Aphanizomenon*, and *Microcystis* are the three genera of cyanobacteria prominently found in freshwater sources, of which *Microcystis aeruginosa* is the most common toxin-producing species, and microcystins (hepatotoxins) are the most widespread toxins (Mohamed et al., 2015; Stefanelli et al., 2014). Studies have shown that microcystins intoxication can lead to gastroenteritis, liver damage, cancer, and acute poisoning death (Chorus & Bartram, 1999; Hudnell, 2008; Pelaez et al., 2010; Wilson et al., 2008). In addition to toxin production, some cyanobacterial species generate compounds such as

geosmin and 2-methylisoborneol that produce unpleasant tastes and odors, causing water quality deterioration (Graham et al., 2010).

It should be noted that the toxins released when the algal cells are still alive and healthy in freshwater are negligible compared to the toxins released on cell lysis (Bartram & Rees, 2000). Toxins released in freshwater bodies quickly dissolve in water and rapidly dilute and degrade with time. Therefore, cell-bound cyanotoxins are a bigger concern when it comes to drinking water supply and recreational waters due to cell lysis and increased concentration of localized toxins in the conformed area (EPA, 2005; Graham et al., 2010). Therefore, there is an increasing need for monitoring tools and technologies that are sensitive, easy to use, and implementable for the early detection of cyanobacteria before bloom formation.

Due to the harmful effects of cyanobacteria, early detection is crucial and heavily relies upon monitoring programs established by water authorities (EPA, 2005). Several water authorities have developed guidelines based on the guidance values recommended by the World Health Organization (WHO) (Bartram & Rees, 2000; Giddings et al., 2012; WHO, 2017). Examples of national regulations or recommendations based on an alert threshold for relatively mild and/or low probability of adverse health effects of cyanobacteria in drinking and recreational waters are provided in Table 4.1. The ability to monitor cyanobacteria quickly and sensitively prior to bloom formation is a key factor in a successful HAB management strategy and is of utmost importance to water quality managers (Altenburger et al., 2015; EPA, 2015a; Le et al., 2010). This allows authorities to manage blooms and prevent potential harm to the water source.

Table 4.1: Examples of national regulations for managing cyanobacteria/microcystin in water sources.

Country/ Source	Drinking water	Recreational water	Reference
WHO	1 µg/L	≤ 20,000 cells/mL or 10 µg/L <i>Chl-a</i>	(WHO, 2003a)
Canada	1.5 µg/L	≤ 100,000 cells/mL or 20 µg/L <i>Chl-a</i>	(Health Canada, 2016)
USEPA	1.6 µg/L	≤ 20,000 cells/mL or 10 µg/L	(EPA, 2015b)
Brazil	10,000 – 20,000 cells/mL	Not declared	(Chorus, 2012)
France	1 µg/L	≤ 20,000 cells/mL	(Chorus, 2012)
Cuba	< 20,000 cells/mL	20,000 – 100,000 cells/mL	(WHO, 2003a)

Detection technologies for cyanobacteria monitoring are broadly classified into two categories: (1) methods without extraction such as direct counting methods using a microscope, remote sensing, and spectrophotometric, and (2) methods relying on quantification after pigment extraction such as quantitative polymerase chain reaction (qPCR), chromatography based techniques, and biochemical methods/screening assays (AlMamani & Örmeci, 2018; Altenburger et al., 2015; Lane et al., 2012; Moreira et al., 2011, 2014; UNESCO et al., 2004; Wang et al., 2015). However, many of these technologies are not suitable for real-time or near real-time monitoring and often require extensive sample preparation making the methods labor- and time-intensive. For example, real-time qPCR is a promising technology but requires highly skilled personnel for

operation and relies on intrusive pigment extraction (Zhang et al., 2014). Methods like remote sensing enable rapid observation but heavily rely on weather conditions being favorable for monitoring purposes and have a low overall accuracy of detecting a bloom (Wang et al., 2015).

The working principle for estimating cyanobacteria biomass relies on determining primary photopigments present in an algal sample (Bertone et al., 2018). Six different types of chlorophyll (Chl-a, b, d, f, and divinyl-chl a and b) occur naturally in cyanobacteria, but Chl-a predominates accompanied by accessory phycobilin pigments such as phycocyanin and phycoerythrin (Gray, 2010; Shin et al., 2018a, 2018b). Chlorophyll-a is an excellent photoreceptor and thus is the primary pigment for cyanobacteria detection in water sources (Tran Khac et al., 2018). There are some in-situ methods used for real-time monitoring, which mainly rely on fluorometry or infra-red spectral reflectance technology for cyanobacterial quantification (Bertone et al., 2018; Liu et al., 2020; Zamyadi et al., 2016). Fluorometry is the most commonly used method for sensitive in-situ monitoring of cyanobacteria and generally relies on the detection of chlorophyll-a (Chl-a) (Garrido et al., 2019). Studies have reported that the sensitivity of fluorescence measurements for cyanobacterial estimations is affected by factors like varying cells size, cell agglomeration, prior light exposure, presence of other phytoplankton containing Chl-a or phaeopigments, and water turbidity (Bowling et al., 2016; Liu et al., 2020; Zamyadi et al., 2016).

Spectrophotometric analysis is the most well-documented method used to estimate chlorophyll concentrations in the laboratory (Gray, 2010). Spectrophotometry is less sensitive than fluorometry and shares some of the limitations of fluorometry; therefore, it has not been widely employed for cyanobacteria monitoring. The main advantage of the

spectrophotometric method lies in its simplicity, accuracy, rapidness, flexibility to measure multiple pigments with no pigment extraction or reagent requirement. More importantly, spectrophotometry can measure various water quality parameters (such as organic carbon, nitrate, UV absorbance) (Burgess & Thomas, 2017) and transmit data in real-time. Studies have shown that several water quality parameters determine the growth rate and characteristics of bloom formation (Health Canada, 2016; Pelaez et al., 2010), and UV-vis spectrophotometry can measure both cyanobacteria concentrations and water quality parameters simultaneously and offers an advantage in this regard over the other technologies.

Agberien & Örmeci (2019) used derivative spectrophotometry to measure cyanobacteria concentrations in water and reported detection limits of 90,200 cells/mL in surface water and 41,800 cells/mL in deionized water for *M. aeruginosa*, which indicated that the derivative spectrophotometry could be used for the monitoring of cyanobacteria, but the method may not be sensitive enough for early detection (Table 1). The objective of this research was to improve the sensitivity of UV-Vis spectrophotometry for early detection and monitoring of cyanobacteria by increasing cuvette pathlength (10-, 50-, and 100-mm) and applying derivative spectrophotometry. The first derivative of absorbance and complementary statistical tools were investigated with changing pathlengths, and new method detection limits were established that showed substantial improvements. A strain of *Chlorella vulgaris* was used for comparative purposes as green algae are the most prevalent biospheric inhibitors and *Chlorella* is the most common species found in nutrient-rich waters (Borowitzka, 2018; Naselli-Flores & Barone, 2009).

4.2 Materials and Methods

4.2.1 Cultivation of microalgae

A non-toxigenic strain of cyanobacteria, *Microcystis aeruginosa* (CPCC 632) and *Chlorella vulgaris* (CPCC 90), for comparison, were used in this study. *M. aeruginosa* was cultured in sterile 3N-BBM medium while *C. vulgaris* in sterile BBM medium (CPCC, 2013). *M. aeruginosa*, *C. vulgaris* and the growth mediums were purchased from Canadian Phycological Culture Centre (CPCC) at the University of Waterloo (Ontario, Canada). Both strains of microalgae were cultured in separate 500 mL Erlenmeyer flasks. To prevent contamination, the flasks were rinsed in deionized (D.I.) water, the mouth of the flasks were covered using aluminum foil paper and sterilized using an autoclave for 30 min at 15 psi and 121 °C. *M. aeruginosa* and *C. vulgaris* were inoculated in the growth medium using 1:2 and 1:4 dilution ratio, respectively (CPCC, 2013). The cultivation flasks were placed inside a temperature-controlled incubator (24 °C) equipped with two daylight fluorescent tube lights. The cultures were maintained under a 24-hour light photoperiod at an intensity of 1000 lux for *M. aeruginosa* and 1800 lux for *C. vulgaris*, respectively. Higher intensity for *C. vulgaris* was attained by elevating the Erlenmeyer flask using a stand inside the incubator. Higher light intensity was provided to *C. vulgaris* to improve the growth rate (KBGAWG, 2009). No supplementary carbon dioxide CO₂ was supplied to the cultures for growth purposes other than the diffused CO₂ present in ambient air. The flasks were agitated gently and manually twice a day.

4.2.2 Preparation of samples

M. aeruginosa and *C. vulgaris* cultures were separated from their growth medium by centrifugation at 8,000×g for 5 min each using 50 mL tubes. Following centrifugation, the

growth medium was discarded, and the collected microalgae were re-suspended in 50 mL D.I. water (Hellebust et al., 1973). The samples were then gently inverted to ensure a homogenous concentration of algae over the entire volume. The cultures were subsequently enumerated under a Leitz Laborlux 12 light microscope and quantified using an improved Neubauer hemocytometer (Bastidas, 2013). Following quantification of both algal strains, respective dilutions samples were prepared in D.I. water. The same dilution ratios were used for both samples to ensure that the concentration of the samples remained approximately equal to each other. This was done in order to enable meaningful and representative comparisons between both algal cultures. The concentration of samples ranged approximately from 7,612,903 cells/mL to 1,855 cells/mL for *M. aeruginosa*, and 7,627,628 cells/mL to 1,855 cells/mL for *C. vulgaris*.

4.2.3 UV-Visible spectrophotometry

Analysis was performed using a Cary 100 Bio UV-Vis Spectrophotometer (Varian) with 10-, 50-, and 100-mm pathlength quartz cuvettes. The spectral absorbance analysis was carried out between 200 nm to 800 nm wavelength range, and the results were reported in absorbance units (a.u.). For each concentration level, 8 technical replicates were analyzed for both algal strains to avoid photobleaching of the algal photopigments present in the sample. The resultant absorbance spectra were subtracted by absorption blanks (D.I. water) to obtain the final absorbance measurements for both *M. aeruginosa* and *C. vulgaris*. Higher and lower concentration ranges for *M. aeruginosa* were [118,750 - 955,000 cells/mL] and [1,855 - 59,687 cells/mL], and [119,118 - 953,333 cells/mL] and [1,855 - 59,686 cells/mL] for *C. vulgaris*, respectively. To ensure representativeness of the samples, near-similar concentration ranges were maintained for every experiment and the sample

volume for 10-, 50-, and 100-mm cuvettes was kept at 3-, 17.5-, and 35-mL, respectively, for both algal strains.

4.2.4 First derivative of absorbance

The first-order derivative of absorbance represents the rate of change in absorbance with respect to wavelength ($dA/d\lambda$) (Owen, 1998). This technique was used in pursuit of improving the detection limit of microalgae in water. First-order derivatives were calculated by taking a difference between each successive absorbance values and dividing it by the wavelength interval separating them. The interval used for change in absorbance values was taken at 1 nm and resulted in $d\lambda$ value of 1.

4.2.5 Savitzky-Golay first derivative of absorbance

Savitzky-Golay (S-G) first order derivative was used to smoothen the plot of first order derivative and improve the signal to noise ratio using the following correlation (Savitzky & Golay, 1964).

$$a_j = \frac{\sum_{i=-\frac{m-1}{2}}^{\frac{m-1}{2}} C_i F_{j+i}}{N} \frac{m+1}{2} \leq j \leq n - \frac{m-1}{2}$$

Where a_j = Savitzky-Golay first derivative of absorbance; m = number of data points used; C_i = Savitzky-Golay filter coefficient; F = absorbance value measured at a specific wavelength; j = smoothened data point; N = standardization factor.

Each measured absorbance value was smoothened using twenty-three data points such that $i = -11, -10, -9, \dots, 9, 10, 11$; $m = 23$; $N = 1012$; $C_i = -11, -10, -9, \dots, 9, 10, 11$; following S-G first derivative of absorbance (Savitzky & Golay, 1964).

4.2.6 Method detection limit

The minimum concentration of a component measured using an analytical procedure with 99% confidence, where the concentration of the component is greater than zero is known as the method detection limit (MDL) (WDNR, 1996). The MDLs were calculated according to the Hubaux and Vos method, using a tool developed by Chemiasoft, with a minimum of 8 technical spike replicates for MDL calculation of individual algal strain (Hubaux & Vos, 1970).

4.2.7 Statistical analysis

Statistical analysis of the measured algal concentration was carried out using Microsoft Excel software. Absorbance graphs, S-G first derivative of absorbance graphs and standard calibration curves were plotted for higher and lower concentration ranges (for both algae) using the average values of the 8 technical replicates. Standard calibration curves were used to validate whether the absorbance measurements agreed with the Beer-Lambert Law. Coefficient of determination (R^2) and slopes with their individual standard deviations were obtained for both *M. aeruginosa* and *C. vulgaris* at their individual wavelengths of interest.

4.3 Results

4.3.1 Absorbance measurements

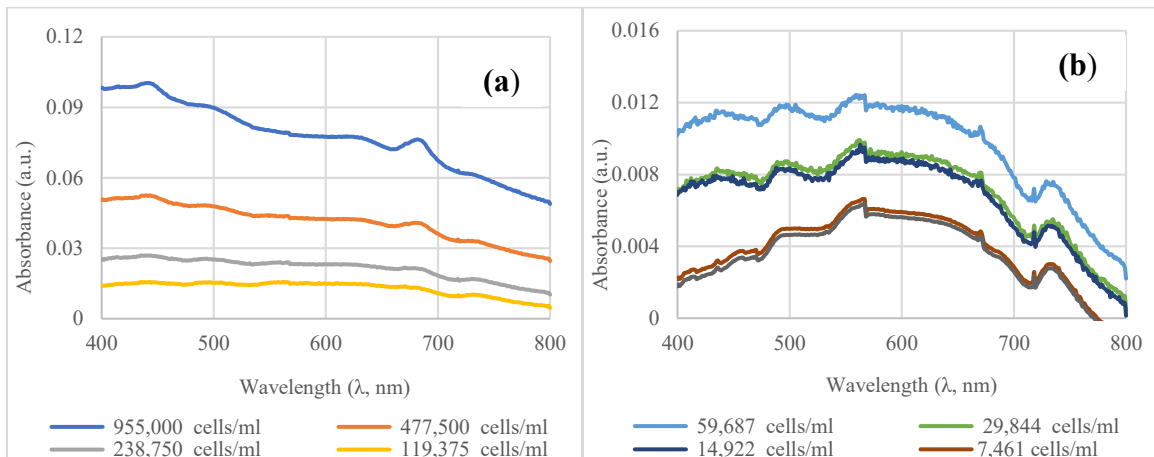
Experiments were carried out in D.I. water to establish interference-free spectral lines for cyanobacterial analysis. At a higher concentration range, *M. aeruginosa* resulted in three peaks at approximately 442, 636, and 682 nm, with 682 nm being the most prominent peak, which was used for analysis (Figure 4.1). The absorbance peaks near 440 and 680 nm are the primary characteristics of the photopigment chlorophyll-a, while the peak at 636 nm corresponds to phycocyanin. This explains the peaks observed for *M. aeruginosa* as

cyanobacteria carry both *Chl-a* and phycocyanin photopigments (LeBlanc Renaud et al., 2011). Considering the aforementioned peaks, the primary analysis focused on wavelengths between 400 – 800 nm.

Comparison of absorbance spectra of *M. aeruginosa*, indicates an increase in absorbance with growing cyanobacterial concentration for each individual pathlength used (Figure 4.1). With longer cuvette pathlength, higher absorbance measurements were observed, which is expected as more light is absorbed by a larger photosensitive sample volume (Burgess & Thomas, 2017). For 10 mm pathlength analysis, no significant peak was observed for the lower concentration range test (Figure 4.1 b), but peaks corresponding to *Chl-a* can be observed for the higher concentration (Figure 4.1 a). For 50- and 100-mm pathlength tests, solely *Chl-a* peaks were clearly observed at lower concentration range (Figure 4.1 d,f); meanwhile, at higher concentration range (Figure 4.1 c,e), both *Chl-a* and Phycocyanin peaks were prominently visible. It was observed that the sensitivity from 10 mm to 50 mm pathlength increased approximately 9-fold, with the detection limit improving from 337,398 cells/mL to 36,354 cells/mL for 50 mm pathlength. On the other hand, with 100 mm pathlength, the MDL improved further to 22,038 cells/mL for cyanobacterial detection, but the improvement was not as significant as the change from 10 to 50 mm pathlength. From the results obtained, 100 mm pathlength cuvette displayed the highest sensitivity.

To validate the analysis, standard calibration curves at 682 nm were generated for higher and lower concentration range tests to ensure that the data followed the Beer-Bouguer-Lambert Law (refer to Figure C.5). All higher concentration range results conformed with Beer-Bouguer-Lambert Law, validating the analysis. As the focus of this study is for

sensitive detection of cyanobacteria, the discussion from here on focuses on the lower concentration results, and the high concentration results are also presented. For all low concentration range results, a strong correlation between cyanobacterial concentration and absorbance was observed ($R^2 = 0.9137, 0.9491, \text{ and } 0.9995$, for 10-, 50-, and 100-mm pathlengths, respectively). There was a positive linear trend for the entire concentration range of absorbance measurements ranging from 1,855 – 955,000 cells/mL. Further, the slopes obtained at 636 nm and 682 nm were approximately the same [$8.6637 \times 10^{-07} \pm 1.1741 \times 10^{-08} \text{ au}/(\text{cells}/\text{mL})$ and $8.6234 \times 10^{-07} \pm 1.0036 \times 10^{-08} \text{ au}/(\text{cells}/\text{mL})$, respectively], with a strong correlation maintained between concentration and absorbance ($R^2 > 0.99$) at 636 nm. However, even with higher pathlengths, it is difficult to distinguish the peaks at 636 nm from background noise at the lower concentration range. Despite that, for 50-, and 100-mm pathlengths, the peaks at 682 nm can be readily observed at a concentration of approximately 60,000 cells/mL, with a diminishing peak at around 30,000 cells/mL.



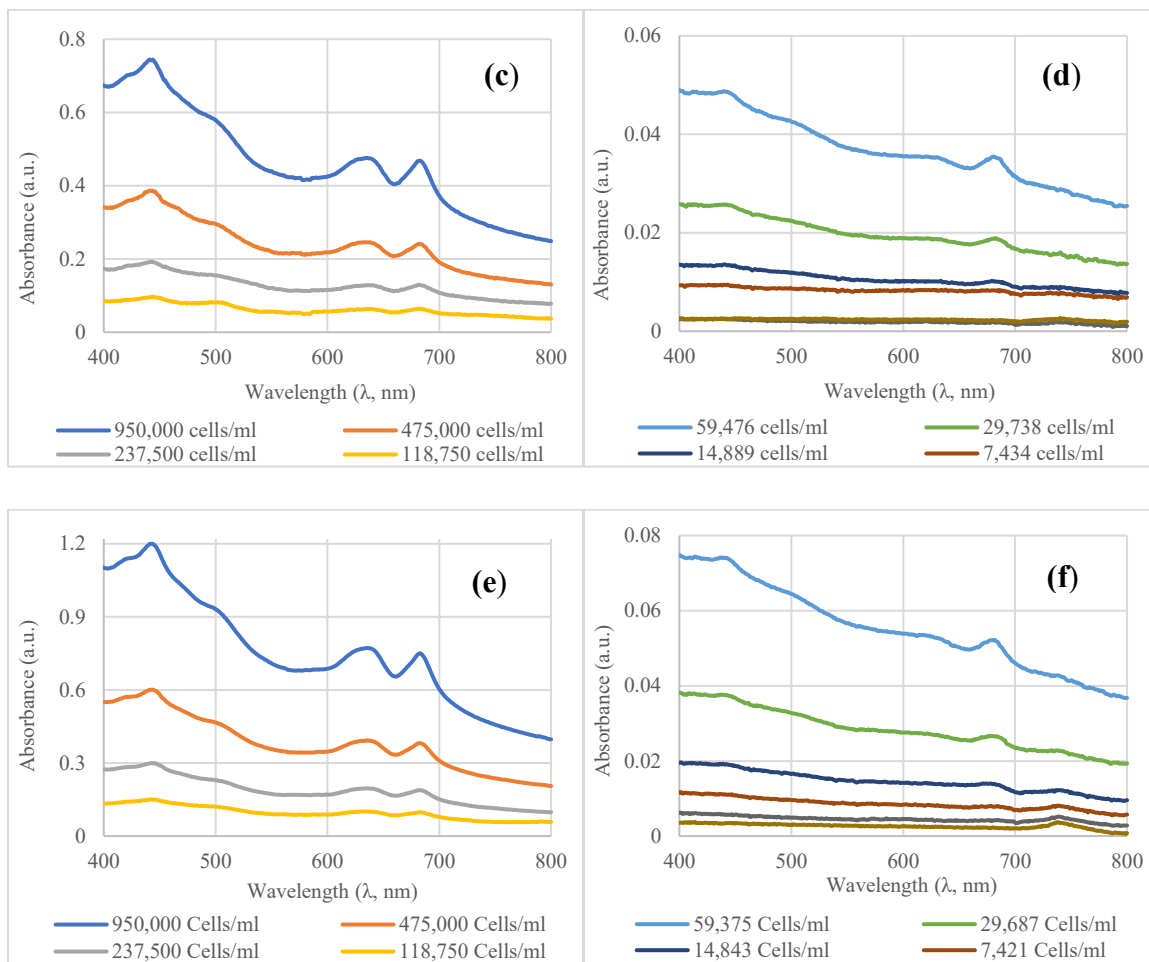


Figure 4.1: Absorbance spectra at higher and lower concentration ranges of *M. aeruginosa* for 10 mm (a, b), 50 mm (c, d), and 100 mm (e, f) cuvette pathlengths, respectively.

4.3.2 First derivative of absorbance

The first derivative corresponds to the slope of the traditional spectrum, where the maxima correlate with the increase in absorbance with wavelength, while the minima appear after maxima of the normal spectrum. Additionally, the maxima of the normal spectrum correspond to the zero value on the derivative spectra (Burgess & Thomas, 2017). First-order derivative of absorbance was implemented in a study to identify key wavelengths to improve the signal-to-noise ratio and reduce background noise while reducing issues that arise from shifting water baseline and overlapping spectral peaks (AlMomani & Örmeci,

2018). A similar technique was applied in this study to investigate the effect of the first derivative on the detection of cyanobacteria. Figure 4.2 illustrates a plot of the first derivative of absorbance versus concentration for *M. aeruginosa* at higher and lower concentrations. For higher concentration tests, a peak close to 670 nm can be observed for 50- and 100-mm pathlengths (Figure 4.2 c, e), while no peak is observed for 10 mm pathlength test (Figure 4.2 a). At the same time, the signal cannot be readily differentiated from background noise at lower concentrations (as seen from Figure 4.2 b, d), and an increase in noise can be observed. Moreover, even with increasing cuvette pathlength, no significant peak was observed at lower concentration making further analysis and detection of cyanobacteria difficult (Figure 4.2 f).

Upon comparison of the normal absorbance spectra to the first-order derivative of absorbance spectra, it was observed that the number of peaks increased drastically (increasing noise), but there were no prominent peaks observed unlike the peaks readily observed in the normal absorbance spectra. Besides, the absorbance values observed upon application of the first derivative of absorbance were lower than the normal absorbance spectra, which is an attribute of the first derivative of absorbance, as it plots the rate of change in absorbance against wavelength, instead of a plot of absorbance versus wavelength. An unwanted effect of the first-order derivative is that as the signal-to-noise ratio decreases, it results in sharper noise features in the spectrum and a higher number of peaks due to rapid changes in amplitude under the presence of random noise (Kus et al., 1996). This can be reduced using alternatives techniques such as Savitzky-Golay derivative as discussed below.

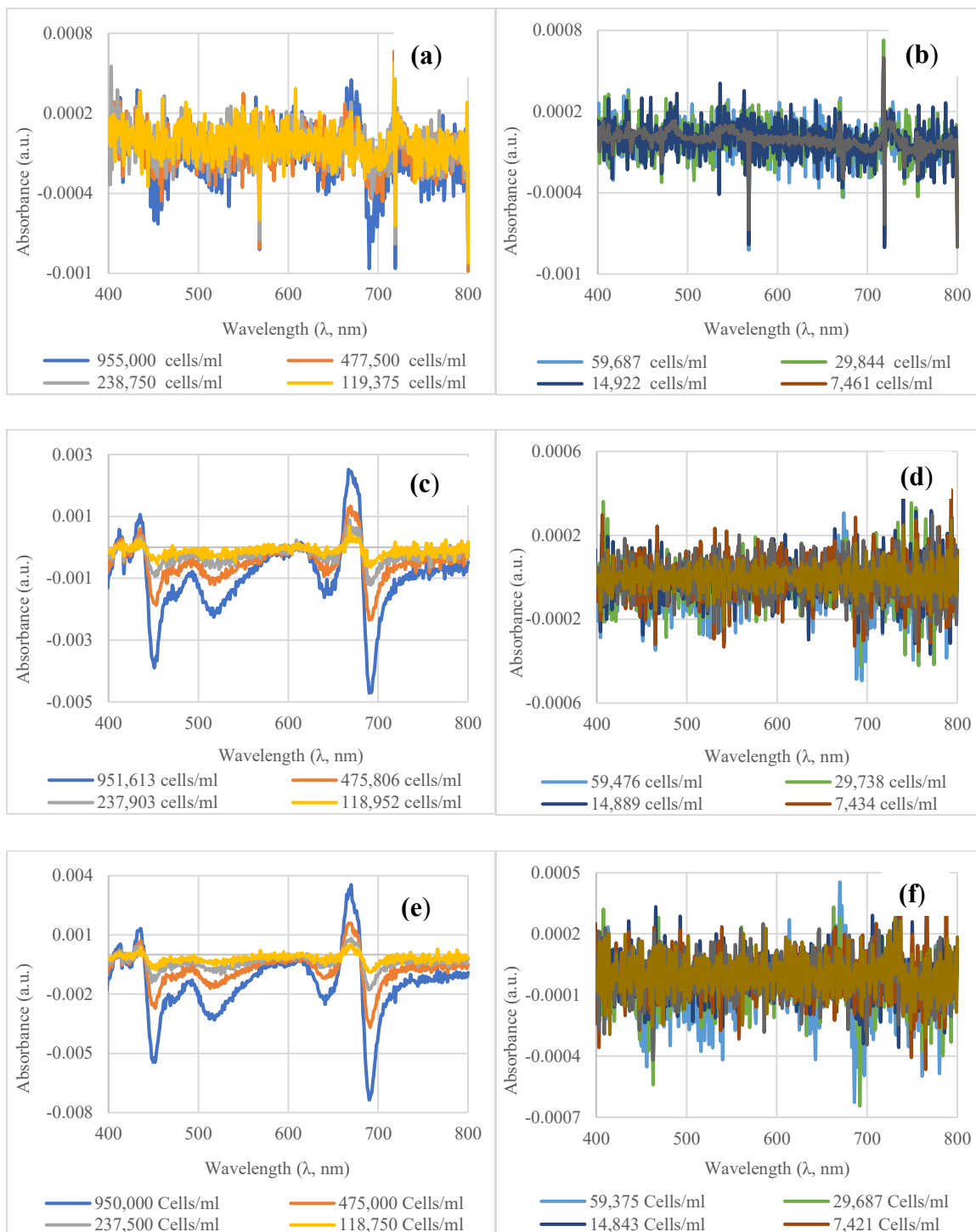


Figure 4.2: First derivative of absorbance spectra of *M. aeruginosa* at higher and lower concentrations for 10 mm (a, b), 50 mm (c, d), and 100 mm (e, f) cuvette pathlength, respectively.

4.3.3 Savitzky-Golay first derivative of absorbance

Savitzky-Golay (S-G) first derivative of absorbance was applied to simultaneously obtain first-order derivative and smoothen the plot obtained by derivative absorbance, which reduces the enhanced background noise obtained due to the first derivative of absorbance (Ruffin et al., 2008). This resulted in sharp and distinct peaks for *M. aeruginosa* at higher as well as lower concentrations for 50 mm and 100 mm pathlengths (lower concentration illustrated in Figure 4.3 c, e). Conversely, for *C. vulgaris*, 50 mm pathlength tests revealed sharp peaks at higher concentrations (supplementary information Figure C.7), while lower concentrations displayed peaks accompanied with added noise features (Figure 4.3 d). Nonetheless, distinct peaks can be observed for 100 mm pathlength tests at higher as well as lower concentration ranges (lower concentration illustrated in Figure 4.3 f) for *C. vulgaris*. However, similar to the normal absorbance spectra, it is difficult to differentiate between signal and noise on the Savitzky-Golay spectral scan using 10 mm pathlength for both cyanobacterial and non-cyanobacterial algae strain at lower concentrations (as illustrated in Figure 4.3 a,b).

Upon application of the derivative spectrophotometry method, a shift in the primary peak of interest (at 704 nm) was observed for *M. aeruginosa* when compared to the normal absorbance spectra (at 682 nm). This is an attribute of the derivative spectrophotometry as it plots the rate of change of absorbance against wavelength (Agberien & Örmeci, 2019). Both 50-and 100-mm pathlength results revealed analogous spectral patterns at higher and lower concentration ranges. The standard calibration curves (illustrated in Figure C.6), plotted at 704 nm showed a linear trend

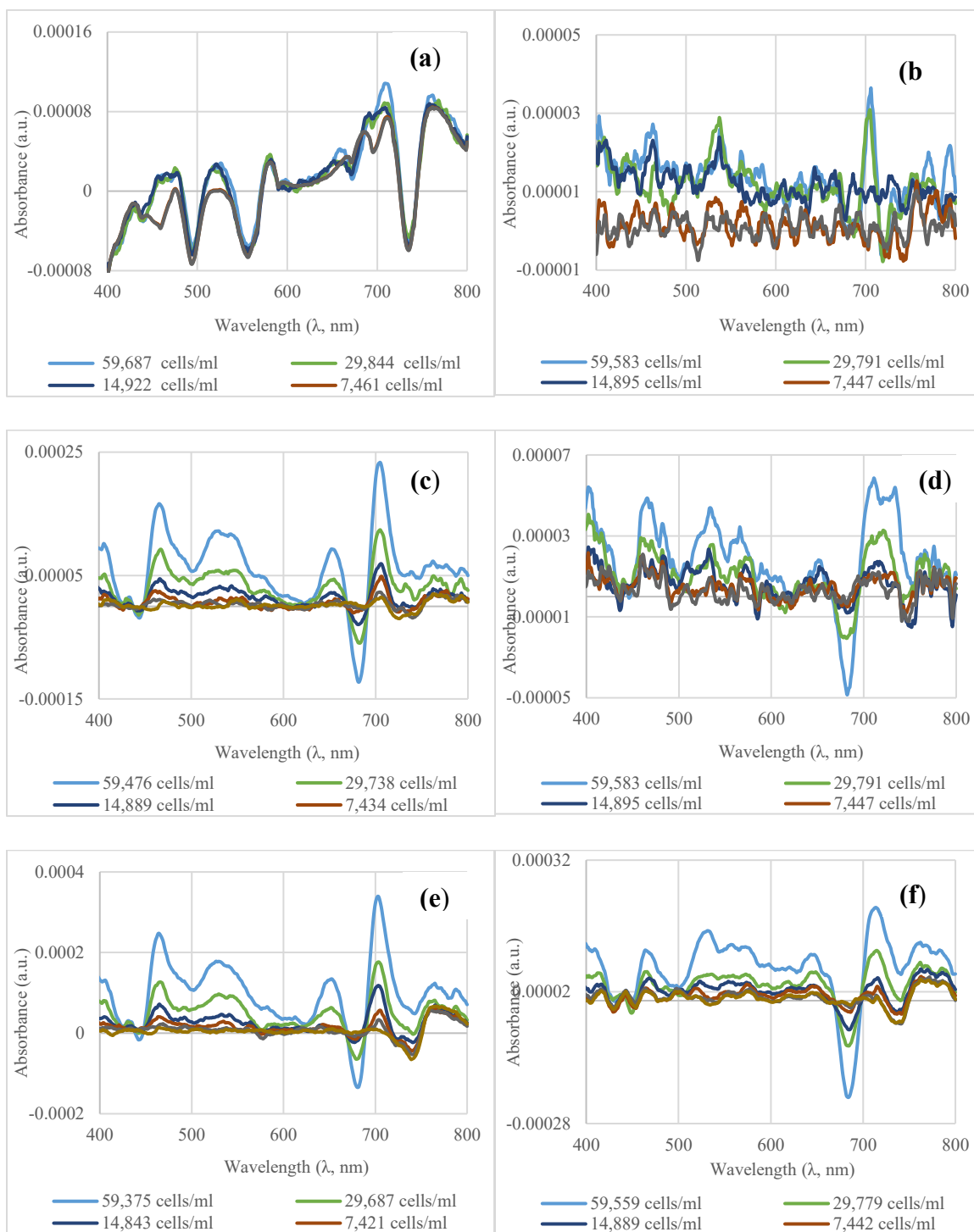


Figure 4.3: Savitzky-Golay first derivative of absorbance spectra of *M. aeruginosa* and *C. Vulgaris* at lower concentrations for 10 mm (a, b), 50 mm (c, d), and 100 mm (e, f) cuvette pathlength, respectively.

and a strong positive correlation between the S-G first derivative of absorbance and concentration ($R^2 = 0.8381, 0.9981, \text{ and } 0.9943$, for 10, 50, and 100 mm pathlength, respectively). The MDL using S-G first derivative of absorbance for 10, 50, and 100 mm pathlength was calculated to be 65,312 cells/mL, 9,005 cells/mL, and 4,916 cells/mL, respectively. Approximately 7-fold improvement in detection was observed between 10 and 50 mm pathlength; at the same time, a 13-fold improvement was observed between 10 and 100 mm pathlength. A summary of the results obtained for both algal strains from the above experiments, including pathlength and detection limits, are shown in Table 4.2.

Table 4.2: Summary of experimental results for *Microcystis aeruginosa* and *Chlorella vulgaris* for higher and lower concentration ranges.

Test	Pathlength (mm)	Concentration range (cells/mL)	Slope \pm standard deviation	R^2	MDL (cells/mL)	
<i>M. aeruginosa</i>						
Absorbance at 682 nm	10	3,731 – 59,687	$1.0843 \times 10^{-07} \pm 1.9245 \times 10^{-08}$	0.9136	337,398	
		119,375 – 955,000	$7.8861 \times 10^{-08} \pm 2.27084 \times 10^{-09}$	0.9981		
	50	1,859 – 59,476	$5.4483 \times 10^{-07} \pm 6.3111 \times 10^{-08}$	0.9491	36,354	
		118,952 – 951,613	$5.7188 \times 10^{-07} \pm 6.6346 \times 10^{-09}$	0.9997		
	100	1,859 – 59,375	$8.6234 \times 10^{-07} \pm 1.0036 \times 10^{-08}$	0.9995	22,038	
		118,750 – 950,000	$9.1702 \times 10^{-07} \pm 1.2518 \times 10^{-09}$	0.9999		
	S-G first derivative	10	3,731 – 59,687	$7.5988 \times 10^{-10} \pm 1.9284 \times 10^{-10}$	0.8381	65,312

of absorbance at 706 nm		119,375 – 955,000	$5.0784 \times 10^{-10} \pm 6.5253 \times 10^{-12}$	0.9951		
	50	1,859 – 59,476	$3.6577 \times 10^{-09} \pm 7.9187 \times 10^{-11}$	0.9981	9,005	
		118,952 – 951,613	$3.8234 \times 10^{-09} \pm 8.5669 \times 10^{-12}$	0.9999		
	100	1,859 – 59,375	$5.5873 \times 10^{-09} \pm 2.1122 \times 10^{-10}$	0.9943	4,916	
		118,750 – 950,000	$6.0763 \times 10^{-09} \pm 1.6246 \times 10^{-11}$	0.9999		
	<i>C. vulgaris</i>					
Absorbance at 684 nm	10	3,723 – 59,583	$1.1652 \times 10^{-07} \pm 4.6621 \times 10^{-08}$	0.6756	650,414	
		119,166 – 953,333	$2.6319 \times 10^{-08} \pm 1.6184 \times 10^{-09}$	0.9924		
	50	3,723 – 59,583	$1.8628 \times 10^{-07} \pm 1.3855 \times 10^{-09}$	0.9931	84,312	
		119,166 – 953,333	$1.8497 \times 10^{-07} \pm 1.4197 \times 10^{-09}$	0.9998		
	100	1,861 – 59,559	$9.6102 \times 10^{-07} \pm 1.2770 \times 10^{-08}$	0.9992	41,361	
		119,118 – 952,941	$8.1156 \times 10^{-07} \pm 8.3307 \times 10^{-08}$	0.9997		
	S-G first derivative of absorbance at 708 nm	10	3,723 – 59,583	$5.6416 \times 10^{-10} \pm 7.9760 \times 10^{-11}$	0.9434	145,289
			119,166 – 953,333	$1.6681 \times 10^{-10} \pm 9.7520 \times 10^{-12}$	0.9932	
50		3,723 – 59,583	$8.3759 \times 10^{-10} \pm 3.6126 \times 10^{-11}$	0.9945	45,449	
		119,166 – 953,333	$9.0879 \times 10^{-10} \pm$	0.9987		

			2.2396×10^{-11}		
	100	1,861 – 59,559	$3.6620 \times 10^{-09} \pm$ 1.0246×10^{-10}	0.9969	11,661
		119,118 – 952,941	$3.8160 \times 10^{-09} \pm$ 7.6739×10^{-11}	0.9991	

4.3.4 Spectral comparison of *M. aeruginosa* and *C. vulgaris*

Investigating the potential differences between the absorbance spectra of a blue-green cyanobacteria (*M. aeruginosa*) and a non-cyanobacterial green algae (*C. vulgaris*) is critical to determine whether cyanobacteria can be differentiated from non-cyanobacterial algae for detection purposes. *M. aeruginosa* and *C. vulgaris* have similar structural morphologies where cells are spherical or ovoidal in shape and can be present in the form of single cells and/or mucilaginous colonies (Álvarez et al., 2020; Safi, 2014). However, the organisms have varying cell sizes with *M. aeruginosa* ranging from 3 – 5 µm in diameter, while *C. vulgaris* cells range between 3 – 10 µm in diameter, which may potentially impact the absorbance measurements due to physical characteristics (Bañares-España et al., 2016; Li et al., 2016; Safi, 2014; Wilson et al., 2006). In addition, *M. aeruginosa* is known to form colonies of variable size (10 – 1000 µm) under natural conditions (as a response to prevailing environmental conditions), and studies have reported that the size of the colonies can increase by a factor of 2.7 in less than a week (Gan et al., 2012; Kurmayer et al., 2003; Yang et al., 2008). This aggregation behavior can potentially impact the normal absorbance spectra.

For comparison purposes, the absorbance spectra using 50 mm pathlength of *M. aeruginosa* and *C. vulgaris* at similar concentrations are illustrated in Figure 4.4 (a,b,

respectively). *C. vulgaris* absorbance spectra resulted in two peaks at 444 nm and 684 nm. These peaks are characteristic of *C. vulgaris* as it is known to carry photopigments chlorophyll-a and chlorophyll-b (*Chl-b*) (Miazek et al., 2015). On the other hand, as discussed before, *M. aeruginosa* carries both *Chl-a* and Phycocyanin photopigments, which resulted in three peaks on the absorption spectra. Phycocyanin is an accessory pigment of chlorophyll and is predominantly found in cyanobacteria, which allows differentiating cyanobacteria from other algae for detection (Cotterill et al., 2019). Additionally, experimental results indicate a significant difference in the absorbance value between *M. aeruginosa* and *C. vulgaris* at the chlorophyll peaks (near 440 nm and 680 nm). For example, at the peak close to 680 nm and approximately 1,900,000 cells/mL concentration: *M. aeruginosa* exhibits an absorbance value of 0.8740 (a.u.), while *C. vulgaris* has an absorbance value of 0.3492 (a.u.). The likely reason *C. vulgaris* displays a lower overall absorbance when compared to *M. aeruginosa* is because of the presence of photopigments chlorophyll-a and chlorophyll-b. While *Chl-a* is known to absorb light strongly, *Chl-b* on the other hand absorbs light weakly, which results in lower overall absorbance (Gray, 2010). This indicates that the cyanobacterial and non-cyanobacterial algae could be differentiated based on the differences of their absorbance spectra, and the application of mathematical and statistical tools can increase the specificity of detection further.

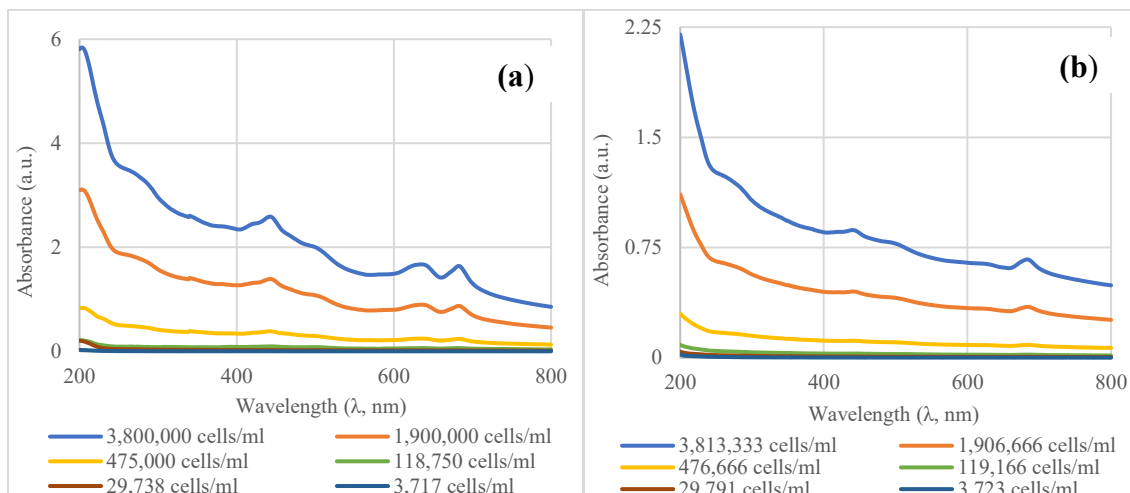


Figure 4.4: Absorbance spectra of *M. aeruginosa* (a) and *C. vulgaris* (b) using 50 mm pathlength cuvette.

4.4 Discussion

The presented results indicate that spectrophotometry when employed in tandem with mathematical and statistical tools such as Savitzky-Golay first derivative of absorbance, can be used for sensitive detection and early-monitoring of cyanobacteria in source waters. By increasing the cuvette pathlength and implementing derivative spectrophotometry, a significant improvement in the detection limit for *M. aeruginosa* and *C. vulgaris* was observed. Comparing the detection limit obtained by normal absorbance spectra to S-G derivative spectra for *M. aeruginosa* (cyanobacteria), 10 mm pathlength showed a 5-fold approximate increase in sensitivity (from 337,398 to 65,312 cells /mL); while a 4-fold improvement was observed for the 50-, and 100-mm pathlength (from 36,354 to 9,005 cells /mL, and 22,038 to 4,916 cells /mL, respectively). In addition, *C. vulgaris* resulted in an approximate 4-fold improvement in detection for the 10 mm pathlength (from 650,414 to 145,289 cells /mL); while 50-, and 100-mm pathlength followed a 2-fold (from 84,312 to 45,449 cells /mL), and 3-fold (from 41,361 to 11,661 cells /mL) improvement in detection

between the normal absorbance spectra and S-G derivative spectra. A higher increase in sensitivity was found with increasing pathlength for *C. vulgaris* in comparison to *M. aeruginosa*, as *C. vulgaris* does not absorb light as strongly due to the presence of Chl-b (Gray, 2010). For all the tests conducted, 100 mm pathlength results showed the highest sensitivity for detection. Compared to the 10 mm pathlength conventionally used for absorbance measurements in the field, adoption of 100 mm pathlength and application of S-G derivative spectra improved the detection limits from 337,398 cells /mL to 4,916 cells/mL for *M. aeruginosa*, and from 650,414 cells /mL to 11,661 cells /mL for *C. vulgaris*.

A previous study conducted by Agberien & Örmeci (2019) reported an approximately 4-fold improvement in detection using derivative spectrophotometry, but the method was not sensitive enough to lower the detection limit to the WHO guidelines. The method presented in this study successfully improved the method detection limit to approximately 5,000 cells/mL for monitoring cyanobacteria, which is well below the WHO and USEPA established guidelines (< 20,000 cells/mL) for low probability of adverse health effects in recreational waters (EPA, 2015b; WHO, 2003b). Further research is recommended to test the detection limits in surface waters under realistic conditions and determine its applicability to the real-time monitoring of cyanobacteria. Future testing utilizing different signal processing and mathematical tools should also be investigated to improve the sensitivity of detection further.

The primary advantage of using spectrophotometry is the readiness of the technology for real-time water monitoring applications. In-line and real-time spectrophotometers are widely used for water monitoring applications, such as at water and wastewater treatment

plants, and they can also transmit data in real-time. A wide range of water quality parameters can either be directly measured or calculated (i.e., UVT, UV254, dissolved and total organic carbon, biochemical and chemical oxygen demand, nitrate, nitrite, total suspended solids), and the results of this study show that cyanobacteria can be added to these parameters. Measuring multiple parameters simultaneously is critical for monitoring cyanobacteria as nutrient concentrations and water quality have a considerable impact on cyanobacteria dominance in source waters (Ha et al., 2009; Srivastava et al., 2013). In addition, the method presented in this study requires no sample processing, reagent use, or pigment extraction required by traditional approaches for cyanobacterial monitoring. The results of this study also indicate that spectrophotometry could differentiate the cyanobacterial algae from non-cyanobacterial algae based on the variations in their pigment absorbance peaks, and this could be a useful tool. Previously, Agberien & Örmeci (2019) reported that spectrophotometry was not able to differentiate between a toxigenic and non-toxigenic strain of *M. aeruginosa*, which were morphologically identical and carry the same photopigments.

Spectrophotometry also carries some limitations. It can overestimate chlorophyll concentration in the presence of other interfering pigments such as phaeopigments, which are the degradation products of algal chlorophyll pigments (Dos Santos et al., 2003). Furthermore, green-sulfur bacteria present in freshwater and marine systems can cause interference in the estimation and interpretation of algae chlorophyll concentration (Gray, 2010). Spectrophotometry is also susceptible to background noise in the presence of other constituents such as turbidity and baseline shift due to changing water characteristics (Burgess & Thomas, 2017). However, the derivative of absorbance can be used to identify

critical wavelengths while improving signal-to-noise ratio and the interference caused due to baseline shift (Demetriades-Shah et al., 1990; Wiggins et al., 2007). Finally, spectrophotometry does not have the sensitivity or specificity of fluorometry. In fluorometric scans, concentrations are estimated via excitation and emission characteristics and each phytoplankton compound has a distinct signal in fluorescence (Liu et al., 2020). Fluorometry is capable of monitoring cyanobacterial concentrations within the WHO established guidelines; however, the maximum operational capability is limited to 200,000 cells/mL (Zamyadi et al., 2016). Furthermore, fluorometric sensors have to be calibrated to a known biological entity and temperature to be able to measure a specific bloom of interest and do not quantify data on cyanobacterial biomass or concentration but rather provide relative phytoplankton concentration (Bowling et al., 2016). This can potentially lead to over or under-estimation of algal concentration. Contrary to this, spectrophotometry has a wider working range, which allows it to be employed at highly eutrophic lakes (Gray, 2010).

4.5 Conclusion

This study improved the sensitivity of UV-Vis spectrophotometry for early detection and monitoring of cyanobacteria by increasing cuvette pathlength from conventional 10-mm to 50- and 100-mm and applying S-G derivative spectrophotometry. The first derivative of absorbance and complementary statistical tools were investigated with changing pathlengths in lower and higher concentration ranges, and new method detection limits were established that showed substantial improvements. Compared to the 10 mm pathlength conventionally used for absorbance measurements in the field, adoption of 100 mm pathlength and application of S-G derivative spectra improved the detection limit from

337,398 cells /mL to 4,916 cells/mL for *M. aeruginosa*, successfully lowering the detection limit below the WHO guideline (< 20,000 cells/mL) for low probability of adverse health effects. *C. vulgaris* was also studied to compare against *M. aeruginosa*, and similarly the detection limit was improved from 650,414 cells /mL to 11,661 cells /mL. The results also showed that spectrophotometry could differentiate *M. aeruginosa* from *C. vulgaris* based on the variations in their pigment absorbance peaks, which could provide a useful tool in identifying blooms of interest.

Acknowledgment

This research was funded by the Natural Sciences Engineering Research Council of Canada (NSERC) and CREATE grant (TEDGIEER) program. The authors would also like to thank Real Tech Inc. (Whitby, Ontario).

Declaration of authors contributions

A.M. and B.O. conceived and planned the experimental design. A.M. carried out the experiments and data evaluation. A.M. and B.O. contributed to the interpretation and assessment of the results. A.M. took the lead in writing the manuscript. All authors provided critical feedback and helped shape the research, analysis and manuscript.

Statement of informed consent

No conflicts, informed consent, or human or animal rights are applicable to this study.

4.6 References

Agberien, A. V., & Örmeci, B. (2019). Monitoring of Cyanobacteria in Water Using Spectrophotometry and First Derivative of Absorbance. *Water*, *12*(1), 124. <https://doi.org/10.3390/w12010124>

AlMomani, F. A., & Örmeci, B. (2018). Monitoring and measurement of microalgae using the first derivative of absorbance and comparison with chlorophyll extraction method. *Environmental Monitoring and Assessment*, *190*(2), 90. <https://doi.org/10.1007/s10661-018-6468-y>

Al-Sammak, M., Hoagland, K., Cassada, D., & Snow, D. (2014). Co-occurrence of the Cyanotoxins BMAA, DABA and Anatoxin-a in Nebraska Reservoirs, Fish, and Aquatic Plants. *Toxins*, *6*(2), 488–508. <https://doi.org/10.3390/toxins6020488>

Altenburger R, Ait-Aissa S, Antczak P, Backhaus T, Barceló D, Seiler TB, Brion F, Busch W, Chipman K, de Alda ML, de Aragão Umbuzeiro G, Escher BI, Falciani F, Faust M, Focks A, Hilscherova K, Hollender J, Hollert H, Jäger F, Jahnke A, Kortenkamp A, Krauss M, Lemkine GF, Munthe J, Neumann S, Schymanski EL, Scrimshaw M, Segner H, Slobodnik J, Smedes F, Kughathas S, Teodorovic I, Tindall AJ, Tollefsen KE, Walz KH, Williams TD, Van den Brink PJ, van Gils J, Vrana B, Zhang X, Brack W. (2015). Future water quality monitoring—Adapting tools to deal with mixtures of pollutants in water resource management. *Science of The Total Environment*, *512–513*, 540–551. <https://doi.org/10.1016/j.scitotenv.2014.12.057>

Álvarez, S. D., Kruk, C., Martínez de la Escalera, G., Montes, M. A., Segura, A. M., & Piccini, C. (2020). Morphology captures toxicity in *Microcystis aeruginosa* complex:

Evidence from a wide environmental gradient☆. *Harmful Algae*, 97, 101854.

<https://doi.org/10.1016/j.hal.2020.101854>

Bañares-España, E., del Mar Fernández-Arjona, M., García-Sánchez, M. J., Hernández-López, M., Reul, A., Mariné, M. H., & Flores-Moya, A. (2016). Sulphide Resistance in the Cyanobacterium *Microcystis aeruginosa*: A Comparative Study of Morphology and Photosynthetic Performance Between the Sulphide-Resistant Mutant and the Wild-Type Strain. *Microbial Ecology*, 71(4), 860–872. <https://doi.org/10.1007/s00248-015-0715-3>

Bartram, J., & Rees, G. (Eds.). (2000). *Monitoring Bathing Waters: A Practical Guide to the Design and Implementation of Assessments and Monitoring Programmes* (0 ed.). CRC Press - WHO. <https://doi.org/10.4324/9780203478264>

Bastidas, O. (2013). *Cell counting with Neubauer chamber, basic hemocytometer usage*. Celeromics Technologies, SRL, Grenoble, France. https://www.researchgate.net/profile/Dr_Majid_Azizi/post/How_can_I_measure_the_amount_of_cells_in_a_solution_with_filamentous_fungi/attachment/59d625bfc49f478072e9a7c0/AS%3A272167168610329%401441901117902/download/Cell-counting-Neubauer-chamber.pdf

Beijerinck, M. W. (1890). *Chlorella vulgaris* Beijerinck 1890. *Culturversuche mit Zoochlorellen, Lichenengonidien und anderen niederen Algen.*, *Botanische Zeitung* 47: 725-739, 741-754, 757-768, 781-785, 1–29. AlgaeBase.

Bertone, E., Burford, M. A., & Hamilton, D. P. (2018). Fluorescence probes for real-time remote cyanobacteria monitoring: A review of challenges and opportunities. *Water Research*, 141, 152–162. <https://doi.org/10.1016/j.watres.2018.05.001>

Borowitzka, M. A. (2018). Chapter 3—Biology of Microalgae. In I. A. Levine & J. Fleurence (Eds.), *Microalgae in Health and Disease Prevention* (pp. 23–72). Academic Press. <https://doi.org/10.1016/B978-0-12-811405-6.00003-7>

Bowling, L. C., Zamyadi, A., & Henderson, R. K. (2016). Assessment of in situ fluorometry to measure cyanobacterial presence in water bodies with diverse cyanobacterial populations. *Water Research*, *105*, 22–33. <https://doi.org/10.1016/j.watres.2016.08.051>

Bukaveckas PA, Franklin R, Tassone S, Trache B, Egerton T. Cyanobacteria and cyanotoxins at the river-estuarine transition. *Harmful Algae*. 2018 Jun;76:11-21. doi: 10.1016/j.hal.2018.04.012. PMID: 29887201.

Burgess, C., & Thomas, O. (2017). UV-Visible Spectrophotometry of Water and Wastewater. In *UV-Visible Spectrophotometry of Water and Wastewater* (pp. 1–524). Elsevier. <https://doi.org/10.1016/B978-0-444-63897-7.00001-9>

Chorus, I. (2012). Current approaches to Cyanotoxin risk assessment, risk management and regulations in different countries. *Federal Environment Agency, (Umweltbundesamt), Dessau-Roßlau, Germany*. (Texte | 63/2012, p. 151). ISSN 1862-4804 <https://www.umweltbundesamt.de/sites/default/files/medien/374/publikationen/4390pdf>

Chorus, I., & Bartram, J. (Eds.). (1999). *Toxic cyanobacteria in water: A guide to their public health consequences, monitoring, and management*. E & FN Spon. London, United Kingdom. ISBN 0-419-23930-8

Cotterill, V., Hamilton, D. P., Puddick, J., Suren, A., & Wood, S. A. (2019). Phycocyanin sensors as an early warning system for cyanobacteria blooms concentrations: A case study in the Rotorua lakes. *New Zealand Journal of Marine and Freshwater Research*, 53(4), 555–570. <https://doi.org/10.1080/00288330.2019.1617322>

CPCC. (2013, September 16). *Canadian Phycological Culture Centre*. Canadian Phycological Culture Centre. <https://uwaterloo.ca/canadian-phycological-culture-centre/home>

Demetriades-Shah, T. H., Steven, M. D., & Clark, J. A. (1990). High resolution derivative spectra in remote sensing. *Remote Sensing of Environment*, 33(1), 55–64. [https://doi.org/10.1016/0034-4257\(90\)90055-Q](https://doi.org/10.1016/0034-4257(90)90055-Q)

Dos Santos, A., Calijuri, M., Moraes, E. M., Adorno, M. A., Falco, P., Carvalho, D. P., Debert, G. L. B., & Benassi, S. F. (2003). Comparison of three methods for Chlorophyll determination: Spectrophotometry and Fluorimetry in samples containing pigment mixtures and spectrophotometry in samples with separate pigments through High Performance Liquid Chromatography. *Acta Limnologica Brasiliensia*, 15, 12.

EPA, U. (2005). *Technologies and Techniques for Early Warning Systems to Monitor and Evaluate Drinking Water Quality* (p. 236). Washington, DC, USEPA.

EPA, U. (2015a). *Recommendations for Public Water Systems to Manage Cyanotoxins in Drinking Water*. Washington, DC. <https://www.epa.gov/sites/production/files/2017-06/documents/cyanotoxin-management-drinking-water.pdf>

EPA, U. (2015b). *Drinking Water Health Advisory for the Cyanobacterial Microcystin Toxins*. 75. USEPA, Washington, DC <https://www.epa.gov/sites/default/files/2017-06/documents/microcystins-report-2015.pdf>

Gan, N., Xiao, Y., Zhu, L., Wu, Z., Liu, J., Hu, C., & Song, L. (2012). The role of microcystins in maintaining colonies of bloom-forming *Microcystis* spp.: *Microcystis* colony maintenance by microcystins. *Environmental Microbiology*, *14*(3), 730–742. <https://doi.org/10.1111/j.1462-2920.2011.02624.x>

Garrido, M., Cecchi, P., Malet, N., Bec, B., Torre, F., & Pasqualini, V. (2019). Evaluation of FluoroProbe® performance for the phytoplankton-based assessment of the ecological status of Mediterranean coastal lagoons. *Environmental Monitoring and Assessment*, *191*(4), 204. <https://doi.org/10.1007/s10661-019-7349-8>

Giddings, M., Aranda-Rodriguez, R., Yasvinski, G., Watson, S. B., & Zura, R. (2012).. *Cyanobacterial Toxins: Drinking and Recreational Water Quality Guidelines*. Federal Environment Agency (Umweltbundesamt), Ottawa, ON, Canada. 12.

Graham, J. L., Loftin, K. A., Meyer, M. T., & Ziegler, A. C. (2010). Cyanotoxin Mixtures and Taste-and-Odor Compounds in Cyanobacterial Blooms from the Midwestern United States. *Environmental Science & Technology*, *44*(19), 7361–7368. <https://doi.org/10.1021/es1008938>

Gray, M. R. (Ed.). (2010). *Algae: Source to treatment* (1st ed). American Water Works Association. Denver, CO, United States. ISBN 9781615837939

Ha, J. H., Hidaka, T., & Tsuno, H. (2009). Quantification of Toxic Microcystis and Evaluation of Its Dominance Ratio in Blooms Using Real-Time PCR. *Environmental Science & Technology*, 43(3), 812–818. <https://doi.org/10.1021/es801265f>

Health Canada. (2016). Cyanobacterial Toxins in Drinking Water—Document for Public Consultation. *Federal-Provincial-Territorial Committee on Drinking Water*, 1–171. <https://www.canada.ca/content/dam/canada/health-canada/migration/healthy-canadians/health-system-systeme-sante/consultations/cyanobacteria-cyanobacterie/alt/cyanobacteria-cyanobacterie-eng.pdf>

Hellebust, J. A., Stein-Taylor, J. R., & Craigie, J. S. (1973). *Handbook of phycological methods: Culture methods and growth measurement*. Cambridge Eng. : University Press. Cambridge, United Kingdom.

Hubaux, Andre., & Vos, Gilbert. (1970). Decision and detection limits for calibration curves. *Analytical Chemistry*, 42(8), 849–855. <https://doi.org/10.1021/ac60290a013>

Hudnell, H. K. (Ed.). (2008). *Cyanobacterial harmful algal blooms: State of the science and research needs*. Springer. Research Triangle Park, NC, United States. ISBN 978-0-387-75865-7

KBGAWG. (2009). *Standard Operating Procedures: Environmental Sampling of Cyanobacteria for Cell Enumeration, Identification and Toxin Analysis*. California Water Board.

https://www.waterboards.ca.gov/northcoast/water_issues/programs/tmdls/klamath_river/klamath_river_khsa_monitoring/pdf/090629/app_a/Cyanobacteria_Sampling_SOP.pdf

- Kurmayer, R., Christiansen, G., & Chorus, I. (2003). The Abundance of Microcystin-Producing Genotypes Correlates Positively with Colony Size in *Microcystis* sp. And Determines Its Microcystin Net Production in Lake Wannsee. *Applied and Environmental Microbiology*, 69(2), 787–795. <https://doi.org/10.1128/AEM.69.2.787-795.2003>
- Kus, S., Marczenko, Z., & Obarski, N. (1996). Derivative UV-VIS Spectrophotometry in Analytical Chemistry. *Chern. Anal. (Warsaw)*, Department of Analytical Chemistry, Technical University of Warsaw, 00-664 Warszawa, Poland, 31.
- Kützing, F. T. (1846). *Microcystis aeruginosa* (Kützing) Kützing 1846: 6. *Tabulae phycologicae, oder, Abbildungen der Tange. Vol. I, fasc. 1 pp. 1–8, pls 1-10.* (Nordhausen: Gedruckt auf kosten des Verfassers in commission bei W. Köhne), 1–160. AlgaeBase.
- Lane, C. E., Gutierrez-Wing, M. T., Rusch, K. A., & Benton, M. G. (2012). Homogeneous detection of cyanobacterial DNA via polymerase chain reaction: Uniform cyanobacteria PCR detection. *Letters in Applied Microbiology*, 55(5), 376–383. <https://doi.org/10.1111/j.1472-765X.2012.03304.x>
- Le, C., Zha, Y., Li, Y., Sun, D., Lu, H., & Yin, B. (2010). Eutrophication of Lake Waters in China: Cost, Causes, and Control. *Environmental Management*, 45(4), 662–668. <https://doi.org/10.1007/s00267-010-9440-3>
- LeBlanc Renaud, S., Pick, F. R., & Fortin, N. (2011). Effect of Light Intensity on the Relative Dominance of Toxigenic and Nontoxigenic Strains of *Microcystis aeruginosa* ▽. *Applied and Environmental Microbiology*, 77(19), 7016–7022. <https://doi.org/10.1128/AEM.05246-11>

Li, T., Xu, J., Gao, B., Xiang, W., Li, A., & Zhang, C. (2016). Morphology, growth, biochemical composition and photosynthetic performance of *Chlorella vulgaris* (Trebouxiophyceae) under low and high nitrogen supplies. *Algal Research*, 16, 481-491. doi:10.1016/j.algal.2016.04.008

Liu, J.-Y., Zeng, L.-H., & Ren, Z.-H. (2020). Recent application of spectroscopy for the detection of microalgae life information: A review. *Applied Spectroscopy Reviews*, 55(1), 26–59. <https://doi.org/10.1080/05704928.2018.1509345>

Miazek, K., Iwanek, W., Remacle, C., Richel, A., & Goffin, D. (2015). Effect of Metals, Metalloids and Metallic Nanoparticles on Microalgae Growth and Industrial Product Biosynthesis: A Review. *International Journal of Molecular Sciences*, 16(10), 23929–23969. <https://doi.org/10.3390/ijms161023929>

Mohamed, Z. A., Deyab, M. A., Abou-Dobara, M. I., El-Sayed, A. K., & El-Raghi, W. M. (2015). Occurrence of cyanobacteria and microcystin toxins in raw and treated waters of the Nile River, Egypt: Implication for water treatment and human health. *Environmental Science and Pollution Research*, 22(15), 11716–11727. <https://doi.org/10.1007/s11356-015-4420-z>

Moreira, C., Martins, A., Azevedo, J., Freitas, M., Regueiras, A., Vale, M., Antunes, A., & Vasconcelos, V. (2011). Application of real-time PCR in the assessment of the toxic cyanobacterium *Cylindrospermopsis raciborskii* abundance and toxicological potential. *Applied Microbiology and Biotechnology*, 92(1), 189–197. <https://doi.org/10.1007/s00253-011-3360-x>

Moreira, C., Ramos, V., Azevedo, J., & Vasconcelos, V. (2014). Methods to detect cyanobacteria and their toxins in the environment. *Applied Microbiology and Biotechnology*, 98(19), 8073–8082. <https://doi.org/10.1007/s00253-014-5951-9>

Naselli-Flores, L., & Barone, R. (2009). Green Algae. In G. E. Likens (Ed.), *Encyclopedia of Inland Waters* (pp. 166–173). Academic Press. <https://doi.org/10.1016/B978-012370626-3.00134-4>

Oren, A. (2014). *Cyanobacteria: An Economic Perspective* (N. K. Sharma, A. K. Rai, & L. J. Stal, Eds.). John Wiley & Sons, Ltd. <https://doi.org/10.1002/9781118402238.ch1>

Owen, T. (1998). *Fundamentals of Modern UV-Visible Spectroscopy*. Hewlett-Packard Company. <https://trove.nla.gov.au/work/32688247>

Pelaez, M., Antoniou, M. G., He, X., Dionysiou, D. D., de la Cruz, A. A., Tsimeli, K., Triantis, T., Hiskia, A., Kaloudis, T., Williams, C., Aubel, M., Chapman, A., Foss, A., Khan, U., O’Shea, K. E., & Westrick, J. (2010). Sources and Occurrence of Cyanotoxins Worldwide. In D. Fatta-Kassinos, K. Bester, & K. Kümmerer (Eds.), *Xenobiotics in the Urban Water Cycle* (Vol. 16, pp. 101–127). Springer Netherlands. https://doi.org/10.1007/978-90-481-3509-7_6

Ruffin, C., King, R. L., & Younan, N. H. (2008). A Combined Derivative Spectroscopy and Savitzky-Golay Filtering Method for the Analysis of Hyperspectral Data. *GIScience & Remote Sensing*, 45(1), 1–15. <https://doi.org/10.2747/1548-1603.45.1.1>

Safi, C., Zebib, B., Merah, O., Pontalier, P., Vaca-Garcia, C., Morphology, composition, production, processing and applications of *Chlorella vulgaris*: A review, Renewable and

Sustainable Energy Reviews, Volume 35, 2014, Pages 265-278, ISSN 1364-0321, <https://doi.org/10.1016/j.rser.2014.04.007>.

Savitzky, Abraham., & Golay, M. J. E. (1964). Smoothing and Differentiation of Data by Simplified Least Squares Procedures. *Analytical Chemistry*, 36(8), 1627–1639. <https://doi.org/10.1021/ac60214a047>

Shin, Y.-H., Barnett, J. Z., Gutierrez-Wing, M. T., Rusch, K. A., & Choi, J.-W. (2018a). A hand-held fluorescent sensor platform for selectively estimating green algae and cyanobacteria biomass. *Sensors and Actuators B: Chemical*, 262, 938–946. <https://doi.org/10.1016/j.snb.2018.02.045>

Shin, Y.-H., Gutierrez-Wing, M. T., & Choi, J.-W. (2018b). A field-deployable and handheld fluorometer for environmental water quality monitoring. *Micro and Nano Systems Letters*, 6(1), 16. <https://doi.org/10.1186/s40486-018-0078-x>

Srivastava, A., Singh, S., Ahn, C.-Y., Oh, H.-M., & Asthana, R. K. (2013). Monitoring Approaches for a Toxic Cyanobacterial Bloom. *Environmental Science & Technology*, 47(16), 8999–9013. <https://doi.org/10.1021/es401245k>

Stefanelli, M., Vichi, S., Stipa, G., Funari, E., Testai, E., Scardala, S., & Manganelli, M. (2014). Survival, growth and toxicity of *Microcystis aeruginosa* PCC 7806 in experimental conditions mimicking some features of the human gastro-intestinal environment. *Chemo-Biological Interactions*, 215, 54–61. <https://doi.org/10.1016/j.cbi.2014.03.006>

Tran Khac, V., Hong, Y., Plec, D., Lemaire, B., Dubois, P., Saad, M., & Vinçon-Leite, B. (2018). An Automatic Monitoring System for High-Frequency Measuring and Real-Time

Management of Cyanobacterial Blooms in Urban Water Bodies. *Processes*, 6(2), 11.
<https://doi.org/10.3390/pr6020011>

UNESCO, Anderson, D. M., Cembella, A. D., Enevoldsen, H. O., & Hallegraeff, G. M. (2004). *Manual on harmful marine microalgae*. UNESCO. Paris, France, 793pp. DOI:
<https://doi.org/10.25607/OBP-1370>

Wang, G., Li, J., Zhang, B., Shen, Q., & Zhang, F. (2015). Monitoring cyanobacteria-dominant algal blooms in eutrophicated Taihu Lake in China with synthetic aperture radar images. *Chinese Journal of Oceanology and Limnology*, 33(1), 139–148.
<https://doi.org/10.1007/s00343-015-4019-8>

WDNR. (1996). *Analytical Detection Limit Guidance & Laboratory Guide for Determining Method Detection Limits* (Analytical Guide PUBL-TS-056-96). Wisconsin Department of Natural Resources Laboratory Certification Program.
<https://dnr.wi.gov/regulations/labcert/documents/guidance/-LODguide.pdf>

WHO. (2003). *Guidelines for Safe Recreational Water Environments: Coastal and fresh waters*. World Health Organization. 219 p., Geneva, Switzerland ISBN 9241545801

WHO. (2017). *Guidelines for drinking-water quality*. Geneva, Switzerland, World Health Organization ISBN 978-92-4-154995-0

Wiggins, K., Palmer, R., Hutchinson, W., & Drummond, P. (2007). An investigation into the use of calculating the first derivative of absorbance spectra as a tool for forensic fibre analysis. *Science & Justice*, 47(1), 9–18. <https://doi.org/10.1016/j.scijus.2006.11.001>

Wilson, A. E., Gossiaux, D. C., Höök, T. O., Berry, J. P., Landrum, P. F., Dyble, J., & Guildford, S. J. (2008). Evaluation of the human health threat associated with the hepatotoxin microcystin in the muscle and liver tissues of yellow perch (*Perca flavescens*). *Canadian Journal of Fisheries and Aquatic Sciences*, 65(7), 1487–1497. <https://doi.org/10.1139/F08-067>

Wilson, A. E., Wilson, W. A., & Hay, M. E. (2006). Intraspecific Variation in Growth and Morphology of the Bloom-Forming Cyanobacterium *Microcystis aeruginosa*. *Applied and Environmental Microbiology*, 72(11), 7386–7389. <https://doi.org/10.1128/AEM.00834-06>

Yang, Z., Kong, F., Shi, X., Zhang, M., Xing, P., & Cao, H. (2008). *CHANGES IN THE MORPHOLOGY AND POLYSACCHARIDE CONTENT OF MICROCYSTIS AERUGINOSA (CYANOBACTERIA) DURING FLAGELLATE GRAZING*. 5. <https://doi.org/10.1111/j.1529-8817.2008.00502.x>

Zamyadi, A., Choo, F., Newcombe, G., Stuetz, R., & Henderson, R. K. (2016). A review of monitoring technologies for real-time management of cyanobacteria: Recent advances and future direction. *TrAC Trends in Analytical Chemistry*, 85, 83–96. <https://doi.org/10.1016/j.trac.2016.06.023>

Zhang, W., Lou, I., Ung, W. K., Kong, Y., & Mok, K. M. (2014). Application of PCR and real-time PCR for monitoring cyanobacteria, *Microcystis* spp. And *Cylindrospermopsis raciborskii* in Macau freshwater reservoir. *Frontiers of Earth Science*, 8(2), 291–301. <https://doi.org/10.1007/s11707-013-0409-4>

Appendix C

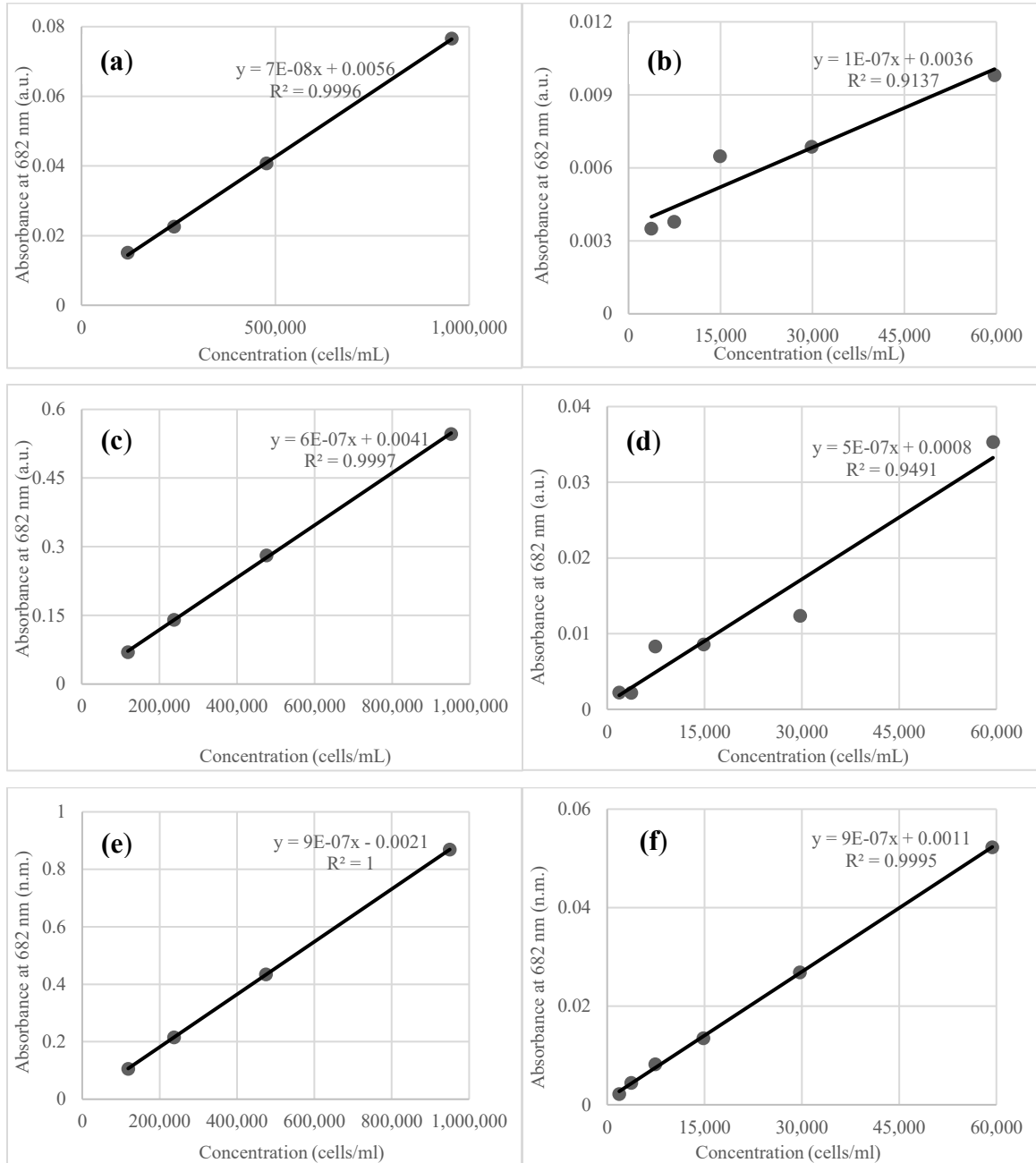


Figure C.5: Standard calibration curves for absorbance spectra at higher and lower concentration ranges of *M. aeruginosa* for 10 mm (a, b), 50 mm (c, d), and 100 mm (e, f) cuvette pathlengths, respectively.

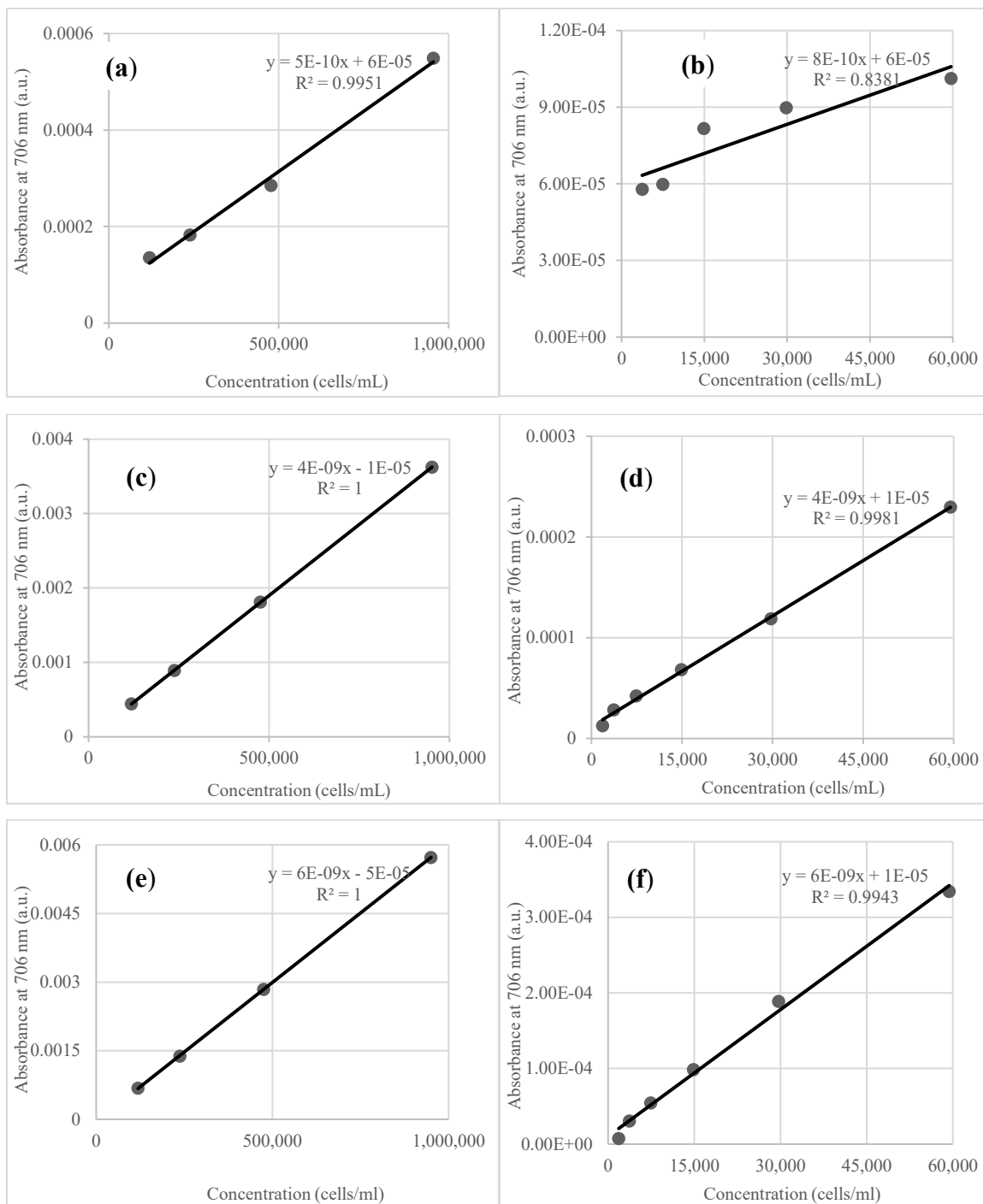


Figure C.6: Standard calibration curves for Savitzky-Golay first derivative of absorbance at higher and lower concentration ranges of *M. aeruginosa* for 10 mm (a, b), 50 mm (c, d), and 100 mm (e, f) cuvette pathlengths, respectively.

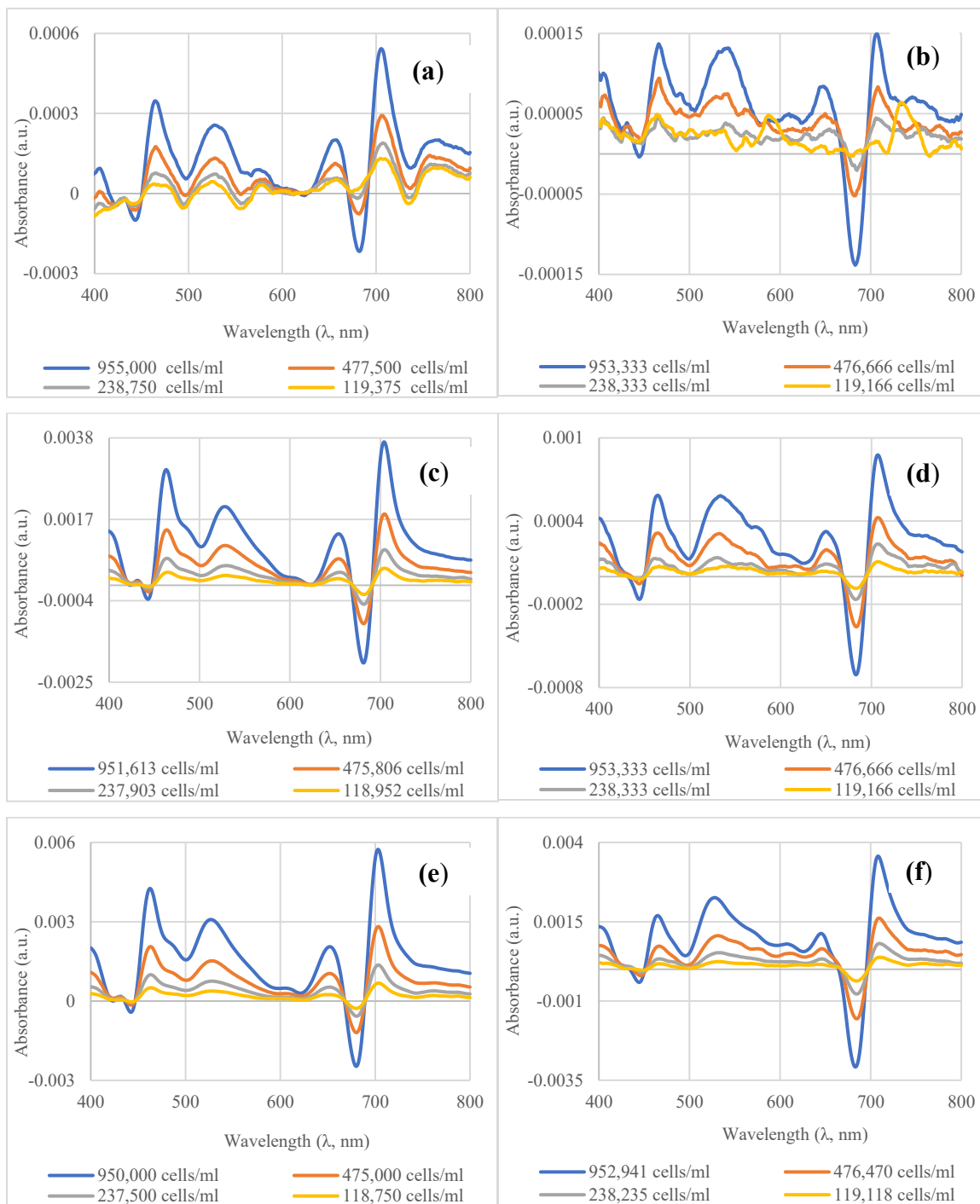


Figure C.7: Savitzky-Golay first derivative of absorbance spectra of *M. aeruginosa* and *C. Vulgaris* at higher concentrations for 10 mm (a, b), 50 mm (c, d), and 100 mm (e, f) cuvette pathlength, respectively.

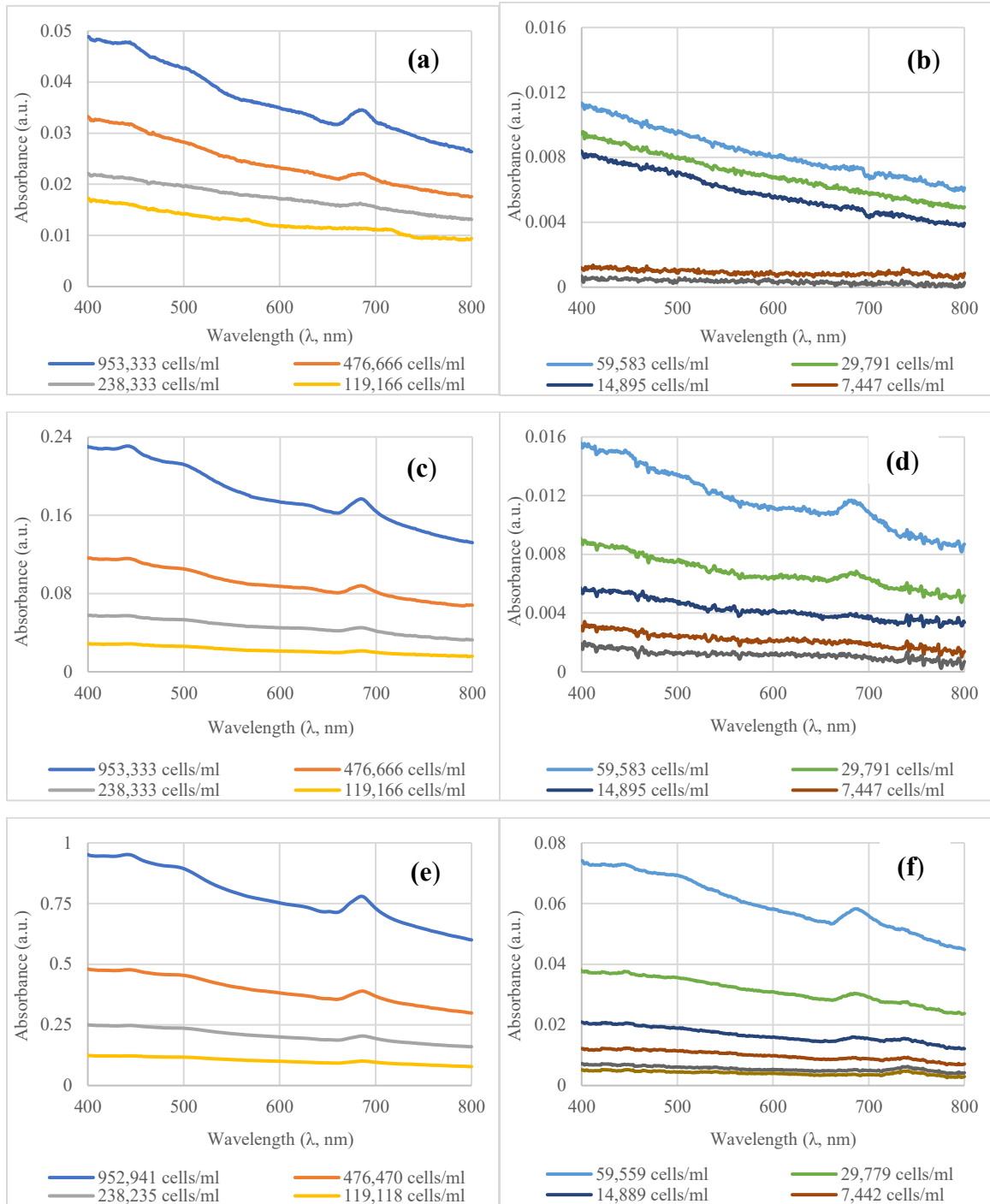


Figure C.8: Absorbance spectra at higher and lower concentration ranges of *C. vulgaris* for 10 mm (a, b), 50 mm (c, d), and 100 mm (e, f) cuvette pathlengths, respectively.

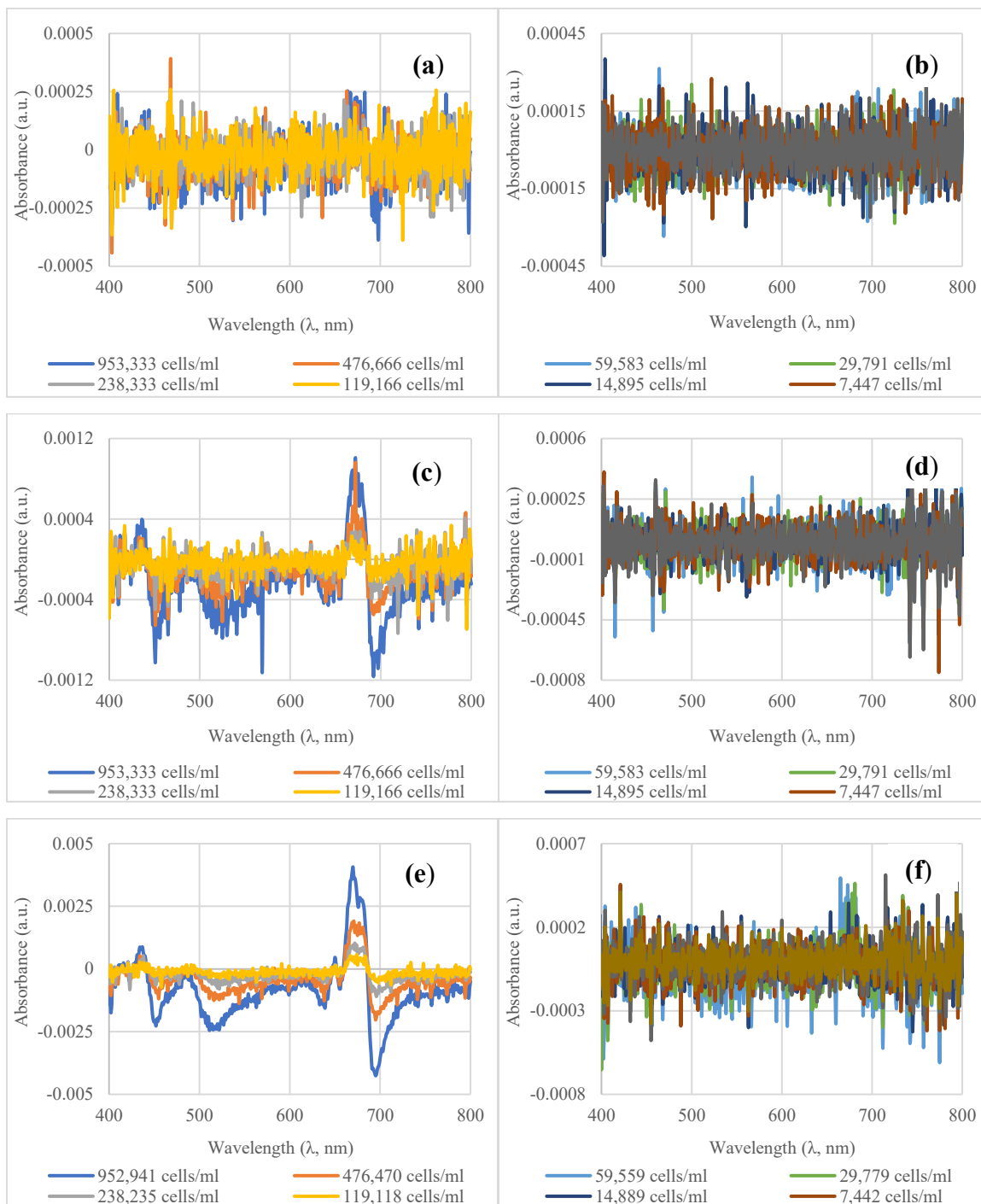


Figure C.9: First derivative of absorbance spectra of *C. vulgaris* at higher and lower concentrations for 10 mm (a, b), 50 mm (c, d), and 100 mm (e, f) cuvette pathlength, respectively.

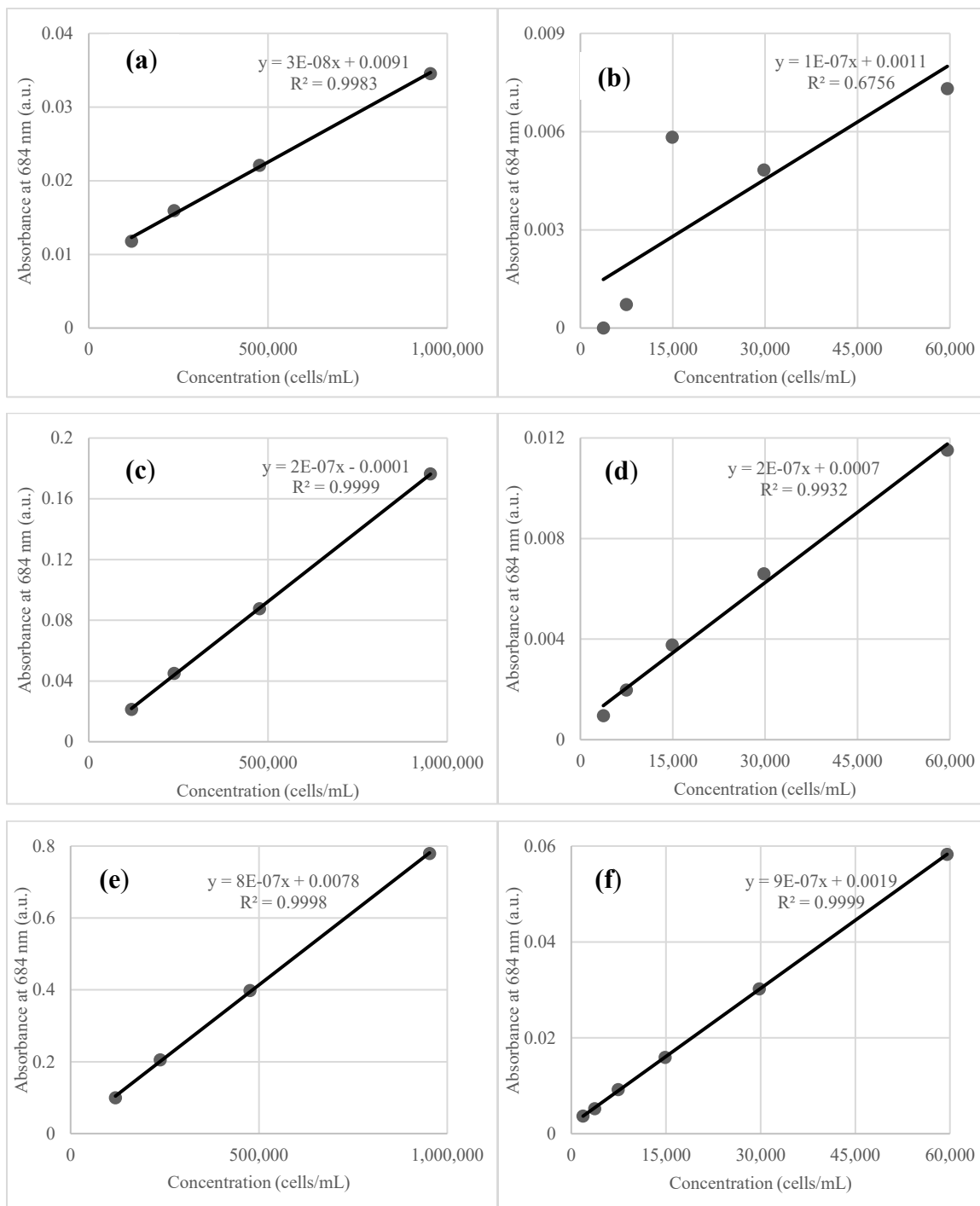


Figure C.10: Standard calibration curves for absorbance spectra at higher and lower concentration ranges of *C. vulgaris* for 10 mm (a, b), 50 mm (c, d), and 100 mm (e, f) cuvette pathlengths, respectively.

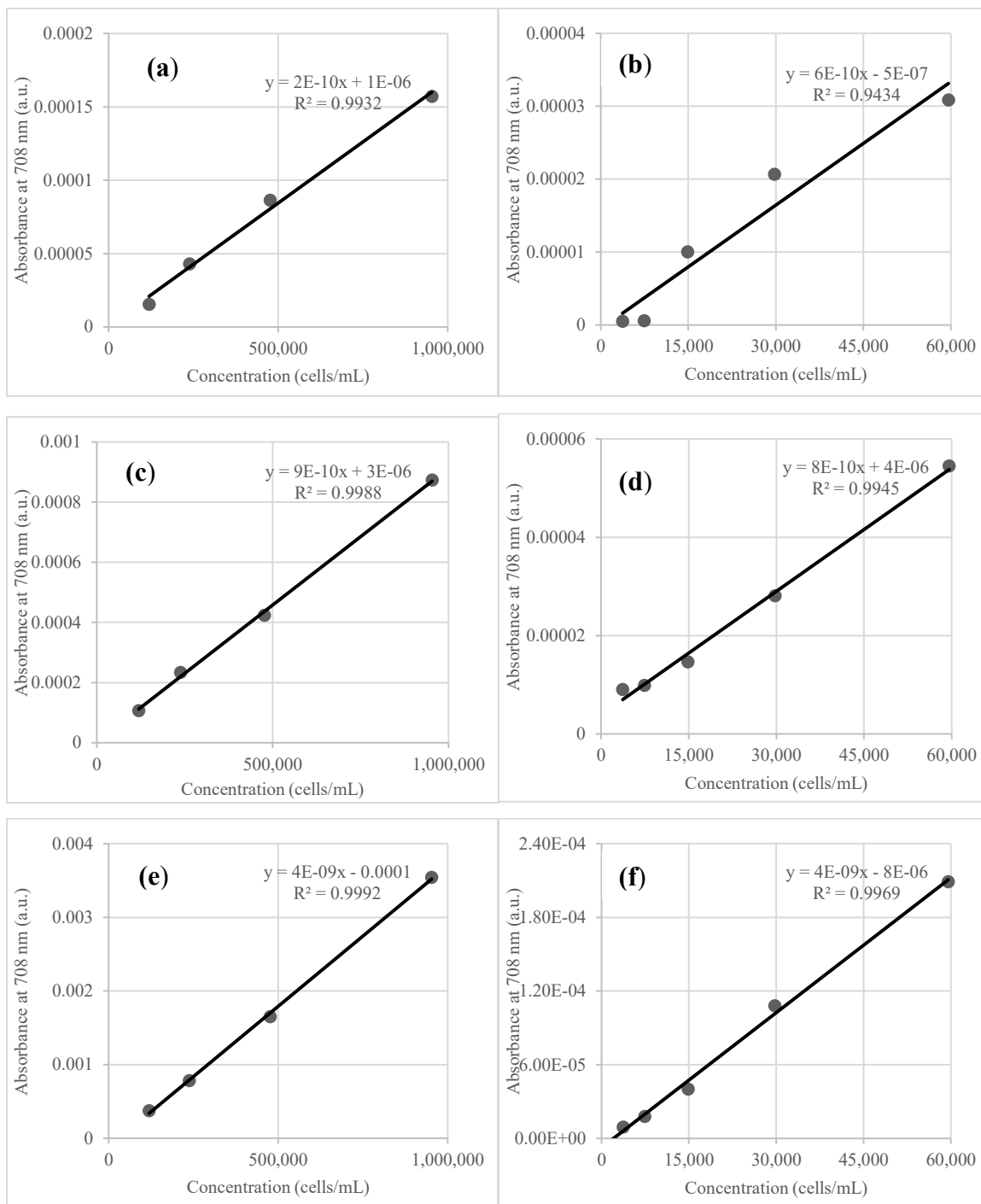


Figure C.11: Standard calibration curves for Savitzky-Golay first derivative of absorbance at higher and lower concentration ranges of *C. vulgaris* for 10 mm (a, b), 50 mm (c, d), and 100 mm (e, f) cuvette pathlengths, respectively.

5. Detection and Identification of a Mixed Cyanobacteria and Microalgae Culture using Derivative Spectrophotometry

Amitesh Malhotra and Banu Örmeci*

Department of Civil and Environmental Engineering, Carleton University
1125 Colonel By Drive, Ottawa ON K1S 5B6, Canada

Abstract

Early detection and monitoring of algal blooms and potentially toxic cyanobacteria in source waters are becoming increasingly important with rising climate change and industrialization. There is a growing need to be able to measure the mixed microalgae cultures sensitively and accurately, as in nature multiple algae species are present in source waters. This study investigated the detection of an equal concentration, mixed culture of cyanobacteria (*Microcystis aeruginosa*) and a common green algae (*Chlorella vulgaris*) in water using UV-Vis spectrophotometry, while employing longer pathlengths and derivative spectrophotometry to improve the detection limit. A strong linear relationship ($R^2 > 0.99$) was found between the concentration and absorbance of the mixed culture at 682 nm using 50-, and 100-mm pathlengths. This study showed that cyanobacterial (phycocyanin) peak could be separately identified in mixed culture setting, while the chlorophyll peaks of both algae overlapped each other. The lowest detection limit of the mixed algal culture using traditional spectrophotometry and derivative spectrophotometry was calculated to be 25,997 cells/mL and 5,505 cells/mL using a 100 mm cuvette pathlength. Lastly, the performance of mixed culture and individual algal cultures were compared, and analyses were carried out to evaluate differences in slopes which can be

used for quantification purposes. The results indicate that derivative spectrophotometry significantly improved the detection limit making the method potentially viable for early-detection of mixed algal cultures.

Keywords: *Chlorella vulgaris*; *Microcystis aeruginosa*; cyanobacteria; derivative spectrophotometry; monitoring; water.

5.1 Introduction

With worsening global climate change and ever-increasing industrialization, source water body quality is deteriorating worldwide, which often leads to eutrophication (Dodds et al., 2009). Eutrophication, in turn, promotes phytoplankton growth such as algae, which under the right conditions proliferates and results in a bloom formation. Of which, cyanobacterial blooms are of particular concern due to the capability of some species to produce harmful toxins and taste and odor compounds (Bajpai et al., 2011; Graham et al., 2010). Some cyanobacteria (CB), commonly known as blue-green algae, can produce toxins known as cyanotoxins, which if consumed, pose a severe health risk to humans, as well as animals including aquatic animals (Bukaveckas, 2018; EPA, 2015).

Microcystis aeruginosa is the most prominent and widespread CB found throughout the world in eutrophic water bodies (Stefanelli et al., 2014). Several *Microcystis* can produce microcystins (hepatotoxins), which could lead to liver damage, gastroenteritis, bioaccumulation, cancer, and in case of extreme intoxication, even death (Al-Ammar et al., 2013; Berry et al., 2011; Health Canada, 2016). On the other hand, *Chlorella* (green algae) is widely prevalent in natural water sources such as lakes, streams, and rivers and is often found in conjunction with CB blooms (American Water Works Association, 2011; Li et

al., 2016; Safi, 2014). *Chlorella* is a resilient algae and proliferates easily because of its low nutrient requirement and ability to survive in harsh conditions, which can result in nuisance such as surface scum formation and reduction of dissolved oxygen in source water, among others (Dong et al., 2018). Due to the aforementioned reasons, it is critical for water authorities across the globe to be able to detect algae before bloom formation, so that correct management strategies can be applied to handle events (Boyer, 2007; Chorus, 2005, 2012). These strategies heavily rely on threshold levels identified by governing bodies that define alert levels for management purposes. Different countries have varying recreational and drinking water regulations which makes selecting a single technique for monitoring difficult. Countries without their own guidance values tend to follow WHO recommendations (Giddings et al., 2012; WHO, 2003a). For safety purposes, while monitoring blooms, these values assume that any algae present is potentially toxic. Table 5.1 shows a few examples of regulations and guidance values in water sources around the world.

Table 5.1: Examples of regulations/ guidance values for recreational and drinking water sources.

Country/ Source	Recreational water	Drinking water	Reference
USEPA	$\leq 20,000$ cells/mL or 10 $\mu\text{g/L}$ <i>Chl-a</i>	1.6 $\mu\text{g/L}$ Microcystin	(EPA, 2015)
Canada	$\leq 100,000$ cells/mL or 20 $\mu\text{g/L}$ <i>Chl-a</i>	1.5 $\mu\text{g/L}$ Microcystin	(Health Canada, 2020)
WHO	$\leq 20,000$ cells/mL or 10 $\mu\text{g/L}$ <i>Chl-a</i>	1 $\mu\text{g/L}$ Microcystin	(WHO, 2003a)

Cuba	20,000 – 100,000 cells/mL	< 20,000 cells/mL	(WHO, 2003b)
Australia	≤ 50,000 cells/L <i>M. aeruginosa</i>	6,500 cells/L 1 µg/L Microcystin	(NRMMC, 2017; NWQMS, 2000)

Various technologies are currently employed to quantify microalgae and cyanobacteria, and they rely either on pigment or toxin detection. The oldest method is based on microscopic enumeration but is labor-intensive and prone to errors (Chorus & Bartram, 1999). Newer techniques are based on chromatography (such as HPLC and LC-MS), molecular-based methods (for example, qPCR, RAPD, and microarrays), and fluorometry (Azevedo et al., 2011; Balest et al., 2016; Baxa et al., 2010; Furukawa et al., 2006; Kim et al., 2017; Liu et al., 2020; Quansah et al., 2010). Although molecular and chromatography based methods are highly selective and sensitive, they require extraction of toxins and pigments from the sample before detection, making them intrusive in nature, time-intensive, and require skilled personnel for operation and analysis purposes (Balest et al., 2016; EPA, 2005; Moreira et al., 2011). In-situ fluorometry is the most common technology used for on-site monitoring of cyanobacteria due to its sensitivity and relies primarily on detecting chlorophyll-a (*Chl-a*). However, fluorescence-based methods require high caution while quantifying algae, as the data reported is in relative fluorescence units in comparison to standard methods (American Water Works Association, 2011; McCullough, 2007).

The use of real-time spectrophotometers to measure different water quality parameters such as but not limited to chemical oxygen demand (COD), biological oxygen demand (BOD),

dissolved organic matter (DOM), UV transmittance (UVT), and total suspended solids (TSS), has grown tremendously over the last decade (Burgess & Thomas, 2017). Spectrophotometric measurements are rapid, simple, can be performed with or without extraction, and have the capacity to work in real-time (Agberien & Örmeci, 2019). But spectrophotometers have not been widely used for monitoring microalgae or cyanobacteria (AlMamani & Örmeci, 2018). Studies have shown the capability of spectrophotometry to measure various microalgae species, and most algae are quantified by selecting a wavelength of interest in the range from 540 – 685 nm (American Water Works Association, 2011; Craig & Carr, 1968; Lichtenthaler & Buschmann, 2001; Liu et al., 2020). The main limitation of UV-Vis spectrophotometry is that the sensitivity of measurements is affected by the presence of organic matter and turbidity in source water, which might lead to higher noise than signal recorded in the absorbance measurements (Agberien & Örmeci, 2019; Burgess & Thomas, 2017).

Most current methods focus on detection of a single photopigment at a time. Detection of multiple photopigments simultaneously is a complex process, which results in increased cost making it undesirable. It is of great advantage to be able to detect multiple photopigments using existing technology, as that reduces the cost required for estimation and early-detection of cyanobacteria. Previous studies have focused on the spectrophotometric detection of individual cyanobacteria or microalgae strains. The aim of this study was to investigate the use of spectrophotometry for early detection and monitoring of mixed algal blooms, with a focus on the detection of cyanobacteria in a mixed-culture setting. This is how cyanobacteria would naturally be present in surface waters and it would also be more challenging to detect and differentiate cyanobacteria in a

mixed culture. It should be noted that the potentially toxic CB release minimal amount of toxins during the growth phase (before cell lysis) and thus the focus of this study is on early detection (Dodds et al., 2009; EPA, 2015). Furthermore, different cuvette pathlengths were examined, and derivative of absorbance was applied to improve the method detection limit (MDL). Finally, MDLs were calculated, and analyses were carried out between the mixed culture and the individual axenic cultures to establish performance differences.

5.2 Materials and Methods

5.2.1 Cultivation of microalgae

A green algae strain (*Chlorella vulgaris*) and a non-toxigenic blue-green cyanobacteria strain (*Microcystis aeruginosa*) were used for this study. *C. vulgaris* CPCC90 and *M. aeruginosa* CPCC 632 algal cultures were obtained from Canadian Phycological Culture Centre (CPCC) at the University of Waterloo (Ontario, Canada) and cultured in sterile BBM and 3N-BBM mediums, respectively. The algal cultures were grown and sustained in separate 500 mL Erlenmeyer flasks. To prevent contamination and maintain the axenic cultures, the flasks were rinsed with deionized (D.I.) water and sterilized using an autoclave for 30 mins at 15 psi and 121 °C. A dilution ratio of 1:2 and 1:4 was maintained during cultivation using 3N-BBM and BBM growth mediums for *M. aeruginosa* and *C. vulgaris*, respectively.

The flasks were incubated inside a temperature-controlled incubator (at 24 °C), equipped with fluorescent tube light blubs emitting daylight, 24-hours daily. The algal cultures were maintained at a light intensity of 1,800 lux and 1,000 lux for *C. vulgaris* and *M. aeruginosa*, respectively. *C. vulgaris* was cultured at a higher intensity due to its higher photo-intensity requirement for optimal growth (Canadian Phycological Culture Centre, 2013). The culture

flasks were stirred gently and manually twice a day to promote homogenous distribution within the growth medium, and no additional carbon dioxide (CO₂) was supplied to the algal cultures other than the natural diffusion of CO₂ present in ambient air.

5.2.2 Preparation of mixed algal samples

C. vulgaris and *M. aeruginosa* were individually pipetted from their growth flasks and separated from their growth medium using 50 mL centrifuge tubes via centrifugation at 8,000 x g for 5 mins. The separated growth medium for both the algal tubes was then discarded, and the concentrated algal cells were re-suspended in 40 mL D.I. water, individually. The samples were gently inverted thrice to obtain a homogenous cell mixture. The two algal cultures were then enumerated using a Leitz Laborlux 12 light microscope to quantify the concentration of the separated cultures using an improved Neubauer hemocytometer. Once the cultures were quantified, an initial dilution was performed on both the algal samples to obtain equal initial concentration (7,600,040 cells/mL). Subsequently, a 50 mL stock of the mixed culture was prepared by mixing 25 mL of equalized concentration of *M. aeruginosa* with 25 mL of *C. vulgaris*, so that the overall concentration of the stock solution remained at approximately 7,600,000 cells/mL. The concentration of the mixed culture was verified by direct counting using the previously mentioned microscope and hemocytometer technique. Dilutions using the stock culture were performed to obtain sample concentration ranging from 7,614,678 cells/mL to 3,710 cells/mL. Fresh samples were prepared on the day of the experiment from the growth cultures for individual cuvette pathlengths used. The concentration range developed for the analysis using varying pathlength was kept approximately equal to each other to perform a representative comparison.

5.2.3 Spectrophotometry

A Cary 100 Bio UV-Vis Spectrophotometer (Varian) was used for analysis with varying pathlengths (using 10-, 50-, and 100-mm quartz cuvettes). The spectrophotometer was zeroed to D.I. water and calibrated before use. The spectral scan was performed over the wavelength range between 200 nm to 800 nm with a spectral scan step set at 1 nm. The results were reported in terms of absorbance units (a.u.). Four unique replicates were analyzed at each concentration level to avoid potential errors due to photobleaching of pigments present in the sample. The scanned absorbance values were subtracted by an absorption blank (performed using D.I. water) to obtain resultant absorbance measurements for the mixed culture sample. The analysis was performed by distributing the scanned concentration range into higher [i.e., 951,834 – 118,750 cells/mL] and lower [i.e., 59,490 – 3,710 cells/mL] concentration ranges. Standard calibration curves were plotted for the mixed culture sample to verify that the measured absorbance values agreed with Beer-Bouguer-Lambert Law. The sample volume for all the experiments was kept at 3-, 17.5-, and 35-mL for 10-, 50-, and 100-mm pathlengths, respectively. The entire experiment was replicated twice to ensure consistency and repeatability.

5.2.4 Derivative of absorbance

Derivative spectrophotometry offers the ability to check a sample quality in a robust way (Burgess & Thomas, 2017). Derivative spectra do not increase the information content of the traditional spectra; rather it allows the information to be analyzed in a better manner. Derivative spectra provide information about the slope of the spectrum, as well as the shoulder and inflexion points allowing for a better characterisation of a compound. Savitzky-Golay (S-G) first-order derivative can be used to simultaneously obtain first-

order derivative and smoothen the obtained plot while improving the signal to noise ratio using the following correlation (Savitzky & Golay, 1964):

$$a_j = \frac{\sum_{i=-\frac{m-1}{2}}^{\frac{m-1}{2}} C_i F_{j+i}}{N} \quad \frac{m+1}{2} \leq j \leq n - \frac{m-1}{2}$$

Where a_j = Savitzky-Golay first derivative of absorbance; m = number of data points used; C_i = Savitzky-Golay filter coefficient; F = absorbance value measured at a specific wavelength; j = smoothened data point; N = standardization factor.

Each measured absorbance value was smoothened over twenty-three data points so that $i = -11, -10, \dots, 10, 11$; $C_i = -11, -10, \dots, 10, 11$; $m = 23$; $N = 1012$; following first derivative of absorbance developed by Savitzky and Golay (Savitzky & Golay, 1964).

5.2.5 Method detection limit

Method detection limit (MDL) is the minimum concentration of a component that can be measured with 99% confidence, that the concentration of the compound is greater than zero, using an analytical procedure (Kus et al., 1996; WDNR, 1996). The MDLs for this study were calculated using a tool developed by Chemiasoft based on the Hubaux and Vos method. The Hubaux and Vos method is strongly dependent on the linear regression of the concentration data to that of the measured absorbance (Hubaux & Vos, 1970). The method requires a minimum of 3 replicates at each concentration to calculate the detection limit.

5.3 Results

5.3.1 Absorbance measurements

The cyanobacterial and green-algae, mixed culture experiments, were conducted using D.I. water to characterize the effect on the spectral scan (interference-free) for cyanobacterial

detection. The scanned spectra (as illustrated in Figure 5.1) resulted in three peaks at 682-, 632-, and 444-nm, of which 682 nm was most prominently observed. The photopigment chlorophyll-a (*Chl-a*) characteristically results in peaks proximate to 680- and 440-nm; while chlorophyll-b (*Chl-b*) peaks close to 650- and 450-nm (Dos Santos et al., 2003; Saini et al., 2018). It should be noted that *Chl-b* weakly absorbs around 650 nm (Miazek et al., 2015). Further, the peak at 632 nm corresponds to the accessory photopigment phycocyanin which is an accessory photopigment present in cyanobacteria. Typically, phycocyanin (PC) absorption peak is located between 612 – 626 nm, but small peak shifts are often observed with changing water characteristics and between different cyanobacterial algae (Lichtenthaler & Buschmann, 2001; Simis & Kauko, 2012; Sobiechowska-Sasim et al., 2014). Considering the above, the peak at 682 nm and the spectral range between 400 – 800 nm were selected as the primary area for analysis and detection.

With increasing cuvette pathlength and cell concentration, an overall increase in absorbance was observed (Figure 5.1), as is expected considering the Beer–Lambert–Bouguer Law (Swinehart, 1962). The primary reason for the increase is because longer pathlengths require larger sample volume, resulting in higher area and number of sample cells being exposed which in turn absorb more light (Burgess & Thomas, 2017). From the results, it was observed that no significant peak could be detected using 10 mm pathlength at lower concentrations (Figure 5.1 b), while peaks of interest were observed using 50-, and 100-mm cuvette pathlengths (Figure 5.1 d, f) even at lower concentrations. Smoother and more distinct peaks of interest could be observed with increasing pathlength at lower concentration range with *Chl-a* being the most prominent. The results showed a 7-fold

improvement in sensitivity from 10- to 50-mm pathlength, while an approximate 12-fold improvement in detection limit was observed between 10-, and 100-mm pathlength. The lowest MDL for mixed-algal culture using normal absorbance values at 682 nm was calculated to be 25,997 cells/mL, using a 100-mm cell pathlength, in D.I. water. Similarly, a 13-fold improvement was observed with increasing pathlength for the mixed-culture at 632 nm (PC peak), which resulted in a MDL of 36,227 cells/mL using 100-mm pathlength (Table 5.2).

Standard calibration curves generated at 682- and 632-nm verified that the results followed Beer-Bouguer-Lambert Law for both, higher and lower concentration ranges. Lower concentration results will be discussed henceforth as the aim of the study was for sensitive analysis of mixed-algal culture. A positive linear trend and strong correspondence was observed between the mixed-culture concentration and absorbance at lower concentrations ($R^2 > 0.9$ for 10-, 50-, and 100-mm pathlengths) for both *Chl-a* and PC peaks. Standard calibration curves are presented in supplementary material (Figure D.5 and Figure D.7). Additionally, at 632 nm, the strong correspondence was maintained between mixed-culture concentration and absorbance ($R^2 > 0.95$), and similar slopes were observed for 682 nm and 632 nm [$8.9927 \times 10^{-07} \pm 5.7847 \times 10^{-08}$ au/(cells/mL) and $8.8187 \times 10^{-07} \pm 1.3199 \times 10^{-08}$ au/(cells/mL), respectively, for 100-mm pathlength]. It is worth noting that at low cell concentrations ($< 40,000$ cells/mL), it is difficult to distinguish the peak at 632 nm from background noise despite higher cuvette pathlength.

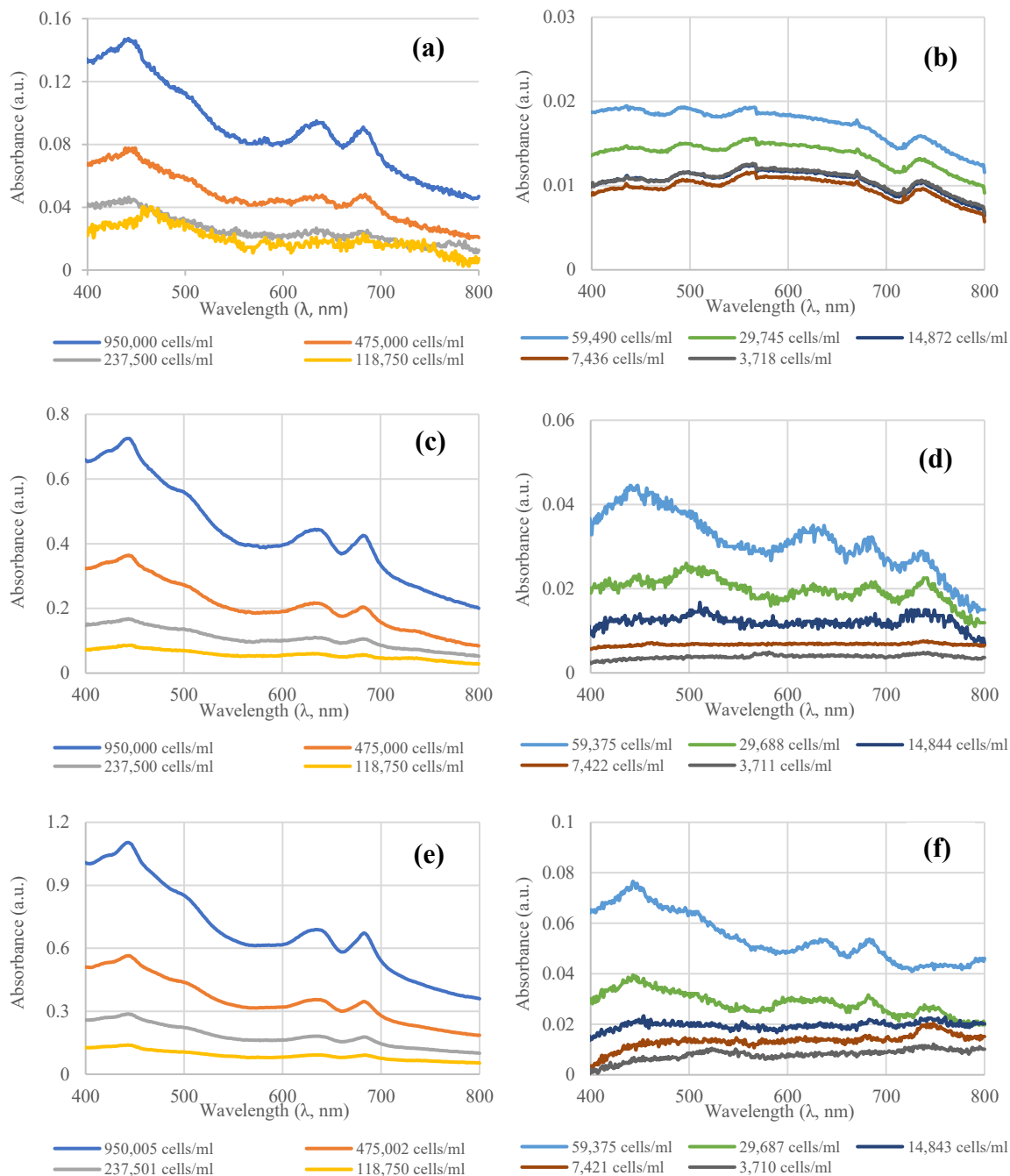


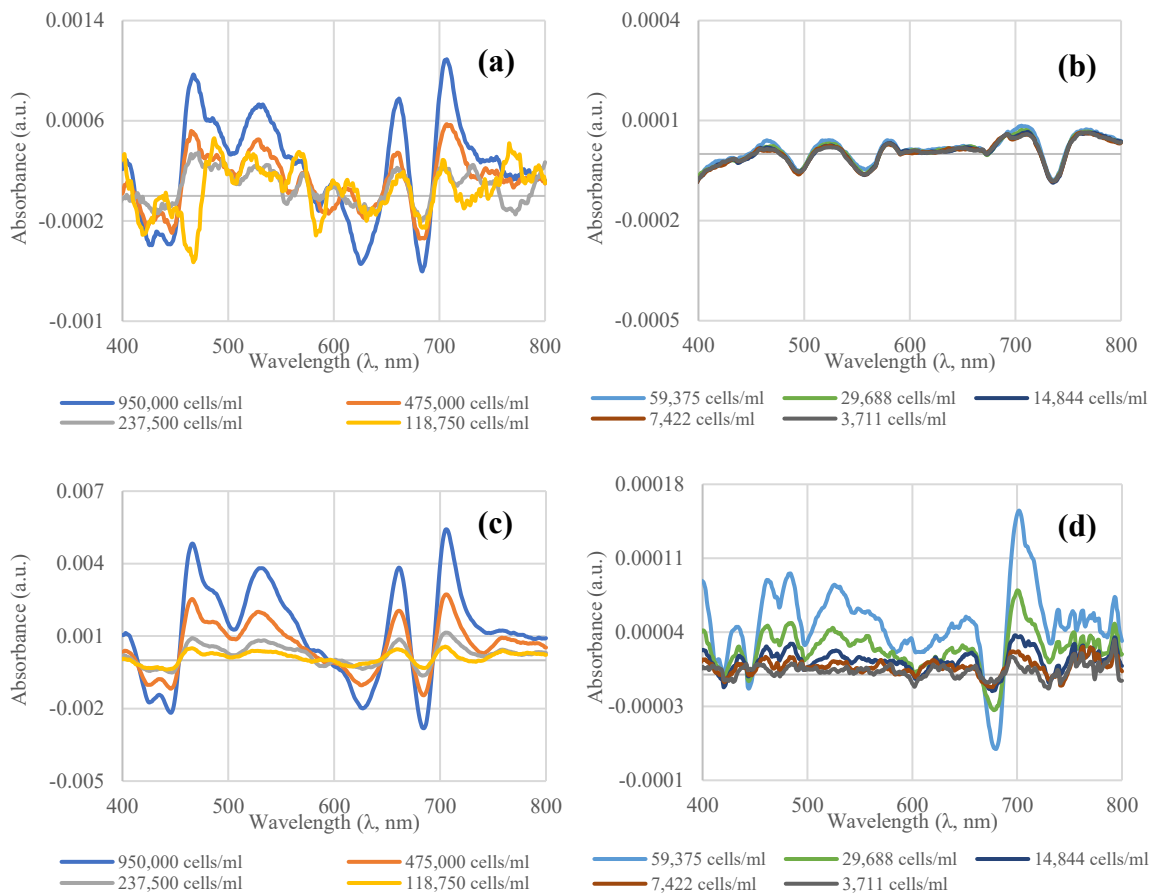
Figure 5.1: Absorbance spectra at higher and lower concentration ranges of mixed *M. aeruginosa* and *C. vulgaris* cultures at 10 mm (a, b), 50 mm (c, d), and 100 mm (e, f) cuvette pathlengths, respectively.

5.3.2 Savitzky-Golay first derivative of absorbance measurements

Savitzky-Golay (S-G) first derivative of absorbance is an analytical tool which allows for the simultaneous obtainment of first order derivative of absorbance, while applying a smoothing filter (Ruffin et al., 2008). This technique helped enhance the signal while reducing background noise, which in turn resulted in sharp and distinct peaks for both concentration ranges, except for 10 mm pathlength at lower concentrations (see Figure 5.2). However, it was difficult to distinguish between signal and noise at very low cell concentrations ($< 10,000$ cells/mL) using 10-, and 50-mm pathlengths. Considering the above, the results obtained from 50-, and 100-mm pathlength will be discussed.

Upon comparison of the normal absorbance spectra (Figure 5.1) and S-G first derivative (Figure 5.2), shift in peaks is observed from 682-, 632-, and 444-nm to 706-, 662-, and 466-nm, respectively. This is a characteristic of first order derivative of absorbance and corresponds to the rate of change of absorbance against wavelength (Kus et al., 1996). Figure 5.2 shows that 50-, and 100-mm pathlength spectral curves are comparable at both concentration ranges. Standard calibration curves plotted at 706- and 660- nm displayed a good linear relationship ($R^2 > 0.9$) between the mixed-culture concentration and corresponding derivative of absorbance for all 3 pathlengths, except for 10 mm at lower concentration (see Table 5.2, Figure D.6 and Figure D.8). A slight change in the slope of the calibration curve was observed between the higher and the lower concentration ranges for the mixed-algal culture. For example, the slope for 50 mm pathlength for lower and higher concentrations at 706 nm was found to be $2.3317 \times 10^{-09} \pm 2.3292 \times 10^{-11}$ and $2.8288 \times 10^{-09} \pm 3.0028 \times 10^{-11}$, respectively. The MDL of mixed culture in D.I. water at *Chl-a* peak using S-G first derivative of absorbance for 10-, 50-, and 100-mm pathlength was

calculated to be 90,449 cells/mL, 11,820 cells/mL, and 5,505 cells/mL, respectively. An approximate 7-fold improvement in MDL was observed between 10-, and 50-mm pathlength, while a 16-fold improvement in detection was observed between 10-, and 100-mm pathlength. Similar improvements were observed for PC peak between 10-, and 50-mm pathlength, whilst an 8-fold improvement was seen from 10- to 100-mm pathlength (Table 5.2).



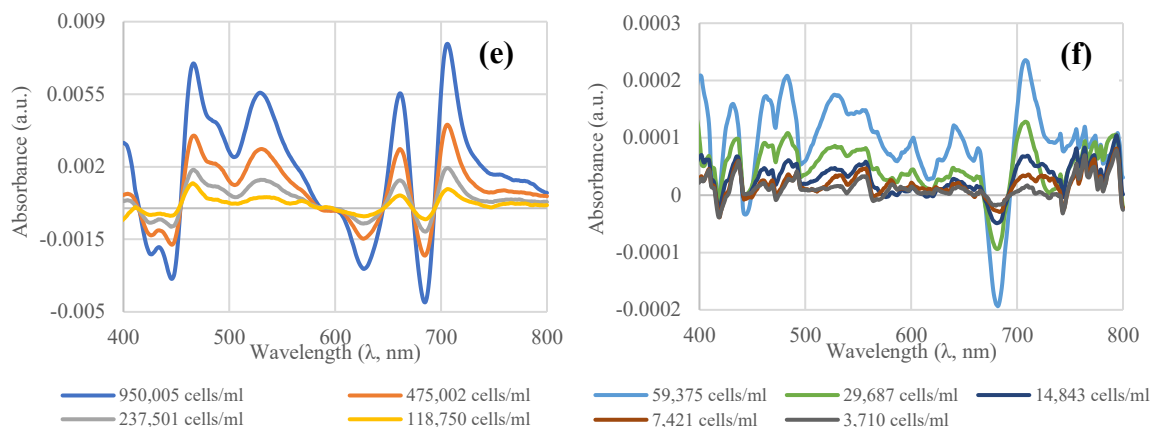


Figure 5.2: Savitzky-Golay first derivative of absorbance spectra at higher and lower concentration ranges of mixed *M. aeruginosa* and *C. vulgaris* cultures at 10 mm (a, b), 50 mm (c, d), and 100 mm (e, f) cuvette pathlengths, respectively.

A summary of the experimental results obtained for the mixed algal culture in D.I. water including varying pathlength and MDLs are shown in Table 5.2.

Table 5.2: Summary of experimental results for mixed equal concentration of *Microcystis aeruginosa* and *Chlorella vulgaris* in D.I. water for higher and lower concentration ranges.

Test	Pathlength (mm)	Concentration Range (cells/mL)	Slope	R ²	MDL (cells/mL)
<i>M. aeruginosa</i> and <i>C. vulgaris</i> equal concentration (<i>Chl-a</i> peak)					
Absorbance at 682 nm	10	3,711 – 59,375	$1.2611 \times 10^{-07} \pm 1.6392 \times 10^{-08}$	0.9517	308,962
		118,750 – 950,000	$1.0869 \times 10^{-07} \pm 1.6577 \times 10^{-09}$	0.9995	
	50	3,711 – 59,375	$5.4239 \times 10^{-07} \pm 1.0162 \times 10^{-08}$	0.9989	41,259
		118,750 – 950,000	$5.7816 \times 10^{-07} \pm$	0.9998	

			4.1485×10^{-09}		
	100	3,710 – 59,375	$8.9927 \times 10^{-07} \pm$ 5.7847×10^{-08}	0.9998	25,997
		118,750 – 950,005	$8.4497 \times 10^{-07} \pm$ 4.6359×10^{-09}	0.9999	
S-G first derivative of absorbance at 706 nm	10	3,711 – 59,375	$5.8425 \times 10^{-10} \pm$ 4.1112×10^{-11}	0.9853	90,449
		118,750 – 950,000	$5.4258 \times 10^{-10} \pm$ 9.4576×10^{-12}	0.9993	
	50	3,711 – 59,375	$2.3317 \times 10^{-09} \pm$ 2.3292×10^{-11}	0.9997	11,820
		118,750 – 950,000	$2.8288 \times 10^{-09} \pm$ 3.0028×10^{-11}	0.9997	
	100	3,710 – 59,375	$4.0634 \times 10^{-09} \pm$ 4.6983×10^{-11}	0.9995	5,505
		118,750 – 950,005	$4.5383 \times 10^{-09} \pm$ 1.1569×10^{-10}	0.9987	
<i>M. aeruginosa</i> and <i>C. vulgaris</i> equal concentration (PC peak)					
Absorbance at 632 nm	10	3,711 – 59,375	$1.2682 \times 10^{-07} \pm$ 1.6786×10^{-08}	0.9500	474,335
		118,750 – 950,000	$1.0871 \times 10^{-07} \pm$ 3.1043×10^{-09}	0.9983	

	50	3,711 – 59,375	$5.3680 \times 10^{-07} \pm$ 8.8240×10^{-09}	0.9991	52,613
		118,750 – 950,000	$5.7713 \times 10^{-07} \pm$ 6.6004×10^{-09}	0.9997	
	100	3,710 – 59,375	$8.8187 \times 10^{-07} \pm$ 1.3199×10^{-08}	0.9993	36,227
		118,750 – 950,005	$8.0134 \times 10^{-07} \pm$ 1.0528×10^{-08}	0.9996	
S-G first derivative of absorbance at 660 nm	10	3,711 – 59,375	$2.6602 \times 10^{-10} \pm$ 7.3097×10^{-11}	0.8153	127,084
		118,750 – 950,000	$7.3157 \times 10^{-10} \pm$ 5.6211×10^{-11}	0.9883	
	50	3,711 – 59,375	$5.5599 \times 10^{-10} \pm$ 5.8670×10^{-11}	0.9676	18,418
		118,750 – 950,000	$5.2513 \times 10^{-10} \pm$ 8.8348×10^{-12}	0.9994	
	100	3,710 – 59,375	$1.1397 \times 10^{-09} \pm$ 4.2211×10^{-11}	0.9959	14,697
		118,750 – 950,005	$5.8276 \times 10^{-09} \pm$ 1.0666×10^{-10}	0.9993	

5.3.3 Spectral comparison of mixed-culture with *M. aeruginosa* and *C. vulgaris* cultures

In the last phase of the study, the spectral curves of both individual algae were compared to that of the mixed-culture to investigate potential differences and overlaps. This allows us to determine whether cyanobacteria can be identified and detected in the presence of non-cyanobacterial algae and validate its application for monitoring purposes. *M. aeruginosa* and *C. vulgaris* share similar spherical and/or ovoidal cell structures, with the exception that *M. aeruginosa* contain gas vacuoles, which allows them to naturally change their location in water (Li et al., 2016; Reynolds, 2007; Wilson et al., 2006). Nonetheless, both algal cultures have diverse cell diameter which ranges from 3 – 10 µm for *C. vulgaris* and from 3 – 5 µm for *M. aeruginosa* (Álvarez et al., 2020; Bañares-España et al., 2016; Safi, 2014). Under natural conditions, *M. aeruginosa* tends to form colonies which ranges from 10 – 1000 µm in size and can aggregate at a high rate in response to harsher environmental conditions (as part of their natural survival instinct) (Gan et al., 2012; Kurmayer et al., 2003). On the other hand, *C. vulgaris* usually lives in unicellular populations but can potentially form colonies in presence of competing predatory algae (Dong et al., 2018; Fisher et al., 2016). It should be noted that the aforementioned factors can potentially affect the spectral absorbance response.

The absorbance spectra of *M. aeruginosa*, *C. vulgaris*, and equal concentration mixed culture algae at near similar concentrations using 50-mm pathlength are shown in Figure 5.3 for comparative purposes. The algal culture *M. aeruginosa* contains photopigments *Chl-a* and PC; whilst *C. vulgaris* carries both *Chl-a* and *Chl-b* photopigments (CPCC, 2013). Observing Figure 5.3, *M. aeruginosa* exhibited peaks at 442-, 632-, and 682 nm

(Figure 5.3 a); *C. vulgaris* peaked at 446-, and 684-nm (Figure 5.3 b); and the mixed culture displayed peaks at 444-, 632-, and 682-nm (Figure 5.3 c). The mixed culture showed a slight variation in peaks close to 440-, and 680-nm due to the presence of *Chl-a* and *Chl-b* together, but the PC peak at 632-nm remained constant. As outlined earlier (refer to 5.3.1), photopigment *Chl-a* peaks around 680-, and 440-nm; *Chl-b* peaks around 650-, and 450-nm; and PC peaks at 632 nm (Craig & Carr, 1968; Dos Santos et al., 2003; Gray, 2010). PC is predominantly present in cyanobacteria which allows cyanobacterial algae to be differentiated from other algae in a mixed culture environment (Cotterill et al., 2019; Schneider et al., 1991). A comparison using the S-G derivative spectra was performed using 50-mm pathlength as shown in Figure 5.4 and similar results were observed. *M. aeruginosa* exhibited peaks relevant to *Chl-a* and PC photopigments at 660-, and 706-nm, respectively (Figure 5.4 a); *C. vulgaris* peaked at 708-nm, corresponding to *Chl-a* (Figure 5.4 b); and the mixed culture displayed peaks at 660-, and 706-nm for *Chl-a* and PC, respectively (Figure 5.4 c).

From the results, it was observed that the equal concentration mixed culture (Figure 5.3 c) resulted in an overall reduction in overall absorbance when compared to *M. aeruginosa* absorbance spectra (Figure 5.3 a), but was higher than the absorbance observed for axenic *C. vulgaris* (Figure 5.3 b). This can be attributed to the fact that the photopigment *Chl-a* is known to absorb more strongly when compared to *Chl-b* (Gray, 2010). Regardless, a strong and clear peak for the photopigment PC was observed in the mixed culture (Figure 5.3 c and Figure 5.4 c), despite the presence of a foreign, non-cyanobacterial algae. This exhibits the potential detection capability of cyanobacteria in a mixed culture environment using the method outlined in this study.

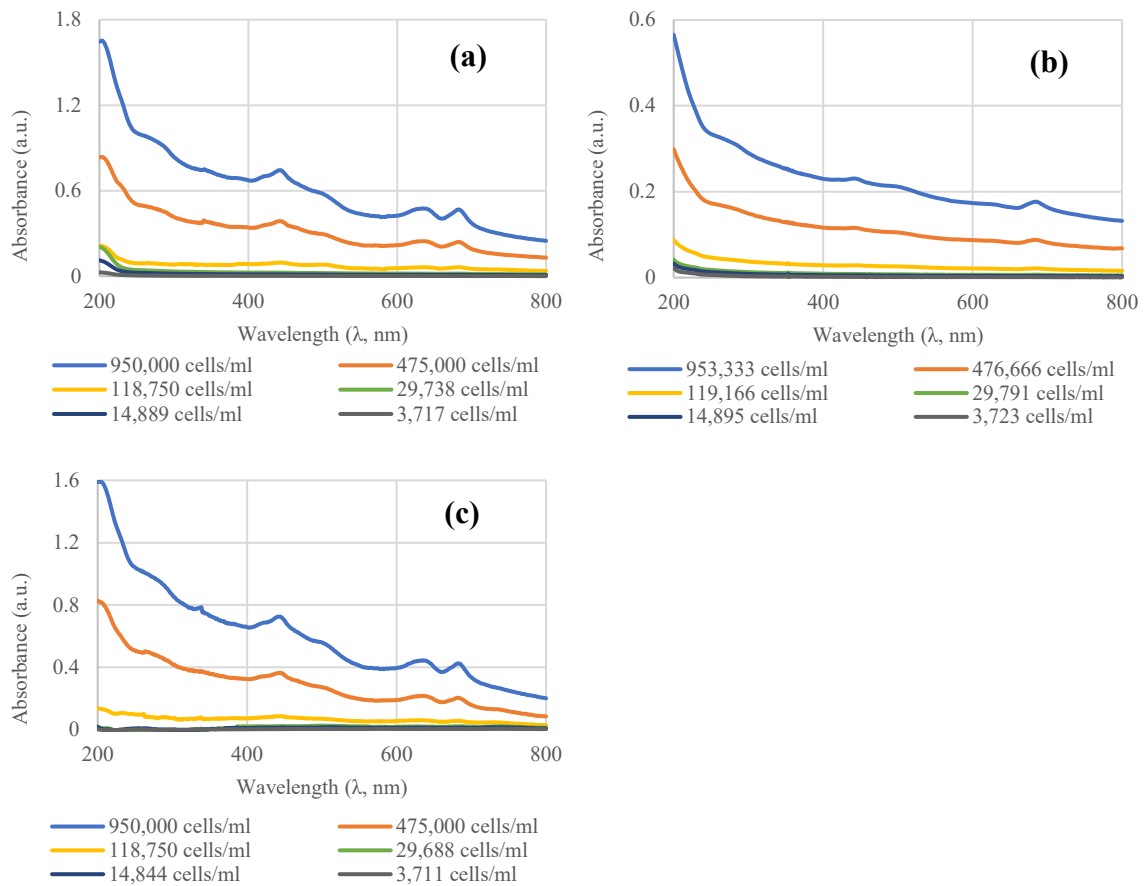
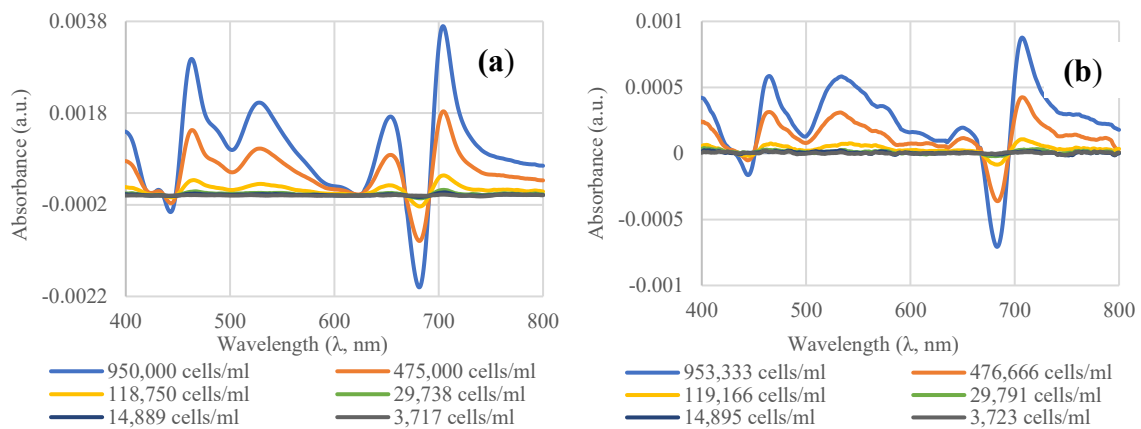


Figure 5.3: Absorbance spectra of *M. aeruginosa* (a), *C. vulgaris* (b), and mixed-culture (c) using 50 mm pathlength cuvette.



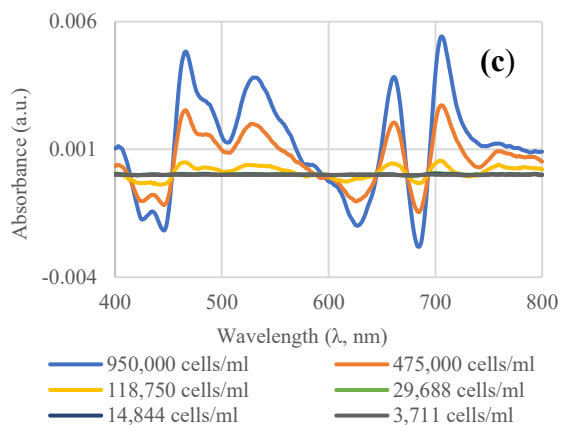


Figure 5.4: Savitzky-Golay first order derivative of absorbance spectra of *M. aeruginosa* (a), *C. vulgaris* (b), and mixed-culture (c) using 50 mm pathlength cuvette.

5.4 Discussion

The results shown in this study indicate that, it is possible to detect cyanobacteria in a mixed-culture using longer pathlengths, while employing derivative spectrophotometry, in the presence of equally concentrated non-cyanobacterial algae. Comparing the MDL obtained by the normal absorbance to that of the S-G first order derivative of absorbance, 10-, 50-, and 100-mm results showed an approximate 3-, 3-, and 5-fold improvement in detection, respectively (see Table 5.2). As previously shown in a study by Malhotra & Örmeci (2021), using 100 mm cell pathlength in conjunction with derivative spectrophotometry, the MDL for *M. aeruginosa* was reported to be 4,916 cells/mL, while *C. vulgaris* had an MDL of 11,661 cells/mL. This study showed that it was possible to detect a mixture of both algae to as low as 5,505 cells/mL concentration. The MDL obtained using the method described in this study is well within (< 20,000 cells/mL) the WHO recommended guideline for low probability of negative health effects from cyanobacteria in recreational waters (WHO, 2003a, 2003b). To be able to identify

cyanobacteria in a mixed population is considered extremely beneficial from a water monitoring and management perspective (Altenburger et al., 2015; Bowling et al., 2017).

To reiterate the results, in this mixed algal culture, we observe both Chlorophylls (a&b) and PC peaks which allows us to determine that cyanobacteria are present. But the presence of Chlorophyll alone does not allow us to distinguish between the type of algae present in source water (Lichtenthaler & Buschmann, 2001; Simis & Kauko, 2012; Sobiechowska-Sasim et al., 2014). The absorbance values itself differs with varying algae as seen with *M. aeruginosa*, *C. vulgaris*, and mixed culture (refer 5.3.3), therefore, the measurement of *Chl-a* photopigment is most commonly employed to estimate a potential bloom formation for water monitoring purposes (Bowling et al., 2016; Friedrichs et al., 2017; Lichtenthaler & Buschmann, 2001; Liu et al., 2020). To quantify unknown concentration of algae in source water, calibration curves between the concentration and sample absorbance (at a wavelength of interest) are universally used (AlMomani & Örmeci, 2018; Dos Santos et al., 2003; Millie et al., 2002). So, comparing slopes at similar concentrations is critical in determining whether the linear relationship to quantify unknown concentration holds true under mixed-culture condition.

This part of the discussion will focus on slopes of regression lines using 50 mm cell pathlength, over the approximate concentration range from 3,710 – 950,000 cells/mL. The slope from the absorbance spectra at 682 nm for mixed culture, *M. aeruginosa*, and *C. vulgaris*, were calculated as $5.6937 \times 10^{-07} \pm 3.7337 \times 10^{-09}$, $5.6618 \times 10^{-07} \pm 4.8373 \times 10^{-09}$, $1.8695 \times 10^{-07} \pm 5.3264 \times 10^{-09}$, respectively, for the whole concentration range (Malhotra & Örmeci, 2021). A strong linear relationship between the concentration and absorbance was observed for three algal samples ($R^2 > 0.99$). The slopes for mixed culture

and *M. aeruginosa* were found to be close to each other, while *C. vulgaris* had a slope that was uniquely associable to it (AlMamani & Örmeci, 2016; Shin et al., 2018). Despite the equal concentration mixed culture, the slope indicates that the cyanobacteria, *M. aeruginosa* might be predominating in the culture sample. Further research is needed to understand the interactions between different algae in a mixed culture environment which might impact culture dominance and change of peaks due to presence of multiple photopigments. Likewise, the slope at 632 nm for mixed culture and *M. aeruginosa* were calculated as $5.6786 \times 10^{-07} \pm 4.3607 \times 10^{-09}$ and $5.6290 \times 10^{-07} \pm 3.4260 \times 10^{-09}$ respectively, for the concentration ranging from 3,710 – 950,000 cells/mL. The slopes were found to be comparable and had a strong linear relationship ($R^2 > 0.99$).

Current techniques for algal detection include chromatography based (such as HPLC) methods, Polymerase Chain Reaction (PCR), spectroscopy-based methods, fluorometry and remote sensing (Al-Tebrineh et al., 2011; Azevedo et al., 2011; Catherine et al., 2012; Greenfield et al., 2008; Lichtenthaler & Buschmann, 2001). Although these techniques are sensitive, most of these methods are labor-intensive, require skilled personnel, and often require extraction prior to detection, making them time-consuming processes. Spectrophotometry is one of the most common and historic methods that can be used to estimate photopigment (such as *Chl-a* and PC) concentrations in samples. The dominant advantage of the spectrophotometric method described is that it is simple, rapid, does not require pigment extraction or reagent use, and can potentially be used for in-line monitoring to measure potential bloom formation (cyanobacterial and non-cyanobacterial) (Mukhopadhyay & Mason, 2013; Tran Khac et al., 2018). Further, spectrophotometry can be employed to simultaneously quantify multiple water quality parameters (such as DOM,

UVT, DOC, TSS, BOD, and N-compounds, among others), in conjunction with algal photopigments making this method really attractive to water quality managers (Burgess & Thomas, 2017; Lichtenthaler & Buschmann, 2001; Schneider et al., 1991, 1991).

The main drawback of spectrophotometry is that it is less specific and sensitive when compared to fluorometry and chromatography based methods (Beltrán et al., 2012; Bertone et al., 2018). Additionally, fluorometry does not rely on cuvettes and estimates concentration based on the ability of a pigment to fluoresce (as each phytoplankton compound has a distinct signal in fluorescence) (Liu et al., 2020). Regardless, fluorometry has a limited working range (typically below 200,000 cells/mL) and is not capable of measuring multiple water quality parameters simultaneously limiting its application for highly eutrophic source water bodies (Zamyadi et al., 2016). Moreover, fluorometers have to be calibrated to a known photopigment concentration range which is typically expected at a particular water source for algal monitoring purposes (Bertone et al., 2018).

Fluorometry and spectrophotometry are both analytical processes which work on the principal of pigment interaction with light and are susceptible to similar interference factors. Some of the major factors include the presence of degradation and VBNC products, turbidity, varying algal morphologies, and bias resulting from instrumentation, which might lead to improper quantification of algal concentration (Liu et al., 2020; Sobiechowska-Sasim et al., 2014; Zamyadi et al., 2016). Regardless, this study shows that using longer pathlengths and employing derivative spectrophotometry, the spectrophotometric method described could be a potentially valuable monitoring tool. It should be noted that this study was conducted in D.I. water and had equal concentrations

of both algae, which might not hold true in the natural environment and can result in potential differences in absorbance patterns.

5.5 Conclusion

This study indicates that it is possible to sensitively detect cyanobacteria with UV-vis spectrophotometry in a mixed-culture environment. An increase in cuvette pathlength, enhanced the detection limit of normal absorbance spectra from 308,967 cells/mL to 25,997 cells/mL for 10-, and 100-mm, respectively, for a mixed *M. aeruginosa* and *C. vulgaris* culture, without any application of statistical or mathematical techniques. Upon applying the Savitzky-Golay first derivative of absorbance (derivative spectrophotometry method), the peaks smoothed by improving the signal-to-noise typically observed in traditional spectrophotometry, making analysis and detection easier. The MDL for *Chl-a* peak in a mixed *M. aeruginosa* and *C. vulgaris* culture after applying the derivative method was calculated to be 5,505 cells/mL using 100-mm pathlength, which is well below the limit for low probability of adverse health effects in recreational water according to the EPA guideline (< 20,000 cells/mL). In addition, this study was able to separately identify cyanobacterial (PC) peak from chlorophyll peak in a mixed-culture setting, while the chlorophyll peaks of both algae overlapped each other. The MDL for PC peak with 100-mm pathlength and derivative spectrophotometry was found to be 14,697 cell/mL indicating method viability. This method can also be implemented as an early warning system for water monitoring purposes to detect potential bloom formation of common algae, as well as HABs. The proposed method is simple, straight-forward, non-destructive, requires no sample processing (reagent or extraction), and can be applied to monitor broad array of source water quality parameters due to its wide concentration working range.

Acknowledgment

This research was funded by the Natural Sciences Engineering Research Council of Canada (NSERC) and CREATE grant (TEDGIEER) program. The authors would also like to thank Real Tech Inc. (Whitby, Ontario).

Conflicts of interest: The authors declare no conflict of interest.

5.6 References

- Agberien, A. V., & Örmeci, B. (2019). Monitoring of Cyanobacteria in Water Using Spectrophotometry and First Derivative of Absorbance. *Water*, *12*(1), 124. <https://doi.org/10.3390/w12010124>
- Al-Ammar, R., Nabok, A., Hashim, A., & Smith, T. (2013). Optical detection of microcystin produced by cyanobacteria. *Journal of Physics: Conference Series*, *450*, 012006. <https://doi.org/10.1088/1742-6596/450/1/012006>
- AlMomani, F. A., & Örmeci, B. (2016). Performance Of *Chlorella Vulgaris*, *Neochloris Oleoabundans*, and mixed indigenous microalgae for treatment of primary effluent, secondary effluent and centrate. *Ecological Engineering*, *95*, 280–289. <https://doi.org/10.1016/j.ecoleng.2016.06.038>
- AlMomani, F. A., & Örmeci, B. (2018). Monitoring and measurement of microalgae using the first derivative of absorbance and comparison with chlorophyll extraction method. *Environmental Monitoring and Assessment*, *190*(2), 90. <https://doi.org/10.1007/s10661-018-6468-y>
- Al-Tebrineh, J., Gehringer, M. M., Akcaalan, R., & Neilan, B. A. (2011). A new quantitative PCR assay for the detection of hepatotoxigenic cyanobacteria. *Toxicon*, *57*(4), 546–554. <https://doi.org/10.1016/j.toxicon.2010.12.018>
- Altenburger, R., Ait-Aissa, S., Antczak, P., Backhaus, T., Barceló, D., Seiler, T.-B., Brion, F., Busch, W., Chipman, K., de Alda, M. L., de Aragão Umbuzeiro, G., Escher, B. I., Falciani, F., Faust, M., Focks, A., Hilscherova, K., Hollender, J., Hollert, H., Jäger, F., ... Brack, W. (2015). Future water quality monitoring—Adapting tools to deal with mixtures of pollutants in water resource management. *Science of The Total Environment*, *512–513*, 540–551. <https://doi.org/10.1016/j.scitotenv.2014.12.057>
- Álvarez, S. D., Kruk, C., Martínez de la Escalera, G., Montes, M. A., Segura, A. M., & Piccini, C. (2020). Morphology captures toxicity in *Microcystis aeruginosa* complex: Evidence from a wide environmental gradient☆. *Harmful Algae*, *97*, 101854. <https://doi.org/10.1016/j.hal.2020.101854>

- American Water Works Association (Ed.). (2011). *Algae: Source to Treatment* (1st ed.). American Water Works Association. (ISBN 1-58321-787-8)
- Azevedo, J., Osswald, J., Guilhermino, L., & Vasconcelos, V. (2011). Development and Validation of an SPE-HPLC-FL Method for the Determination of Anatoxin-a in Water and Trout (*Oncorhincus mykiss*). *Analytical Letters*, *44*(8), 1431–1441. <https://doi.org/10.1080/00032719.2010.512682>
- Bajpai, R., Sharma, N. K., & Rai, A. K. (2011). Cyanotoxins: An Emerging Environmental Concern. *Advances in Life Science*, 187–211.
- Balest, L., Murgolo, S., Sciancalepore, L., Montemurro, P., Abis, P. P., Pastore, C., & Mascolo, G. (2016). Ultra-trace levels analysis of microcystins and nodularin in surface water by on-line solid-phase extraction with high-performance liquid chromatography tandem mass spectrometry. *Analytical and Bioanalytical Chemistry*, *408*(15), 4063–4071. <https://doi.org/10.1007/s00216-016-9495-y>
- Bañares-España, E., del Mar Fernández-Arjona, M., García-Sánchez, M. J., Hernández-López, M., Reul, A., Mariné, M. H., & Flores-Moya, A. (2016). Sulphide Resistance in the Cyanobacterium *Microcystis aeruginosa*: A Comparative Study of Morphology and Photosynthetic Performance Between the Sulphide-Resistant Mutant and the Wild-Type Strain. *Microbial Ecology*, *71*(4), 860–872. <https://doi.org/10.1007/s00248-015-0715-3>
- Baxa, D. V., Kurobe, T., Ger, K. A., Lehman, P. W., & Teh, S. J. (2010). Estimating the abundance of toxic *Microcystis* in the San Francisco Estuary using quantitative real-time PCR. *Harmful Algae*, *9*(3), 342–349. <https://doi.org/10.1016/j.hal.2010.01.001>
- Beltrán, E., Ibáñez, M., Sancho, J. V., & Hernández, F. (2012). Determination of six microcystins and nodularin in surface and drinking waters by on-line solid phase extraction–ultra high pressure liquid chromatography tandem mass spectrometry. *Journal of Chromatography A*, *1266*, 61–68. <https://doi.org/10.1016/j.chroma.2012.10.017>
- Berry, J. P., Lee, E., Walton, K., Wilson, A. E., & Bernal-Brooks, F. (2011). Bioaccumulation of microcystins by fish associated with a persistent cyanobacterial

- bloom in Lago de Patzcuaro (Michoacan, Mexico). *Environmental Toxicology and Chemistry*, 30(7), 1621–1628. <https://doi.org/10.1002/etc.548>
- Bertone, E., Burford, M. A., & Hamilton, D. P. (2018). Fluorescence probes for real-time remote cyanobacteria monitoring: A review of challenges and opportunities. *Water Research*, 141, 152–162. <https://doi.org/10.1016/j.watres.2018.05.001>
- Bowling, L. C., Shaikh, M., Brayan, J., & Malthus, T. (2017). An evaluation of a handheld spectroradiometer for the near real-time measurement of cyanobacteria for bloom management purposes. *Environmental Monitoring and Assessment*, 189(10), 495. <https://doi.org/10.1007/s10661-017-6205-y>
- Bowling, L. C., Zamyadi, A., & Henderson, R. K. (2016). Assessment of in situ fluorometry to measure cyanobacterial presence in water bodies with diverse cyanobacterial populations. *Water Research*, 105, 22–33. <https://doi.org/10.1016/j.watres.2016.08.051>
- Boyer, G. L. (2007). The occurrence of cyanobacterial toxins in New York lakes: Lessons from the MERHAB-Lower Great Lakes program. *Lake and Reservoir Management*, 23(2), 153–160. <https://doi.org/10.1080/07438140709353918>
- Bukaveckas, P. A. (2018). Cyanobacteria and cyanotoxins at the river-estuarine transition. *Harmful Algae*, 11.
- Burgess, C., & Thomas, O. (2017). UV-Visible Spectrophotometry of Water and Wastewater. In *UV-Visible Spectrophotometry of Water and Wastewater* (pp. 1–524). Elsevier. (ISBN 978-0-444-63897-7) <https://doi.org/10.1016/B978-0-444-63897-7.00001-9>
- Canadian Phycological Culture Centre. (2013, September 16). *Canadian Phycological Culture Centre*. Canadian Phycological Culture Centre. <https://uwaterloo.ca/canadian-phycological-culture-centre/home>
- Catherine, A., Escoffier, N., Belhocine, A., Nasri, A. B., Hamlaoui, S., Yéprémian, C., Bernard, C., & Troussellier, M. (2012). On the use of the FluoroProbe®, a phytoplankton quantification method based on fluorescence excitation spectra for large-scale surveys of lakes and reservoirs. *Water Research*, 46(6), 1771–1784. <https://doi.org/10.1016/j.watres.2011.12.056>

- Chorus, I. (2005). Current approaches to cyanotoxin risk assessment, risk management and regulations in different countries. *Federal Environmental Agency, 1*, 122.
- Chorus, I. (2012). Current approaches to Cyanotoxin risk assessment, risk management and regulations in different countries. *Federal Environment Agency, 2*, 151.
- Chorus, I., & Bartram, J. (Eds.). (1999). *Toxic cyanobacteria in water: A guide to their public health consequences, monitoring, and management*. E & FN Spon. (ISBN 978-0-419-23930-7)
- Cotterill, V., Hamilton, D. P., Puddick, J., Suren, A., & Wood, S. A. (2019). Phycocyanin sensors as an early warning system for cyanobacteria blooms concentrations: A case study in the Rotorua lakes. *New Zealand Journal of Marine and Freshwater Research, 53*(4), 555–570. <https://doi.org/10.1080/00288330.2019.1617322>
- Craig, I. W., & Carr, N. G. (1968). C-phycocyanin and allophycocyanin in two species of blue-green algae. *Biochemical Journal, 106*(2), 361–366. <https://doi.org/10.1042/bj1060361>
- Dodds, W. K., Bouska, W. W., Eitzmann, J. L., Pilger, T. J., Pitts, K. L., Riley, A. J., Schloesser, J. T., & Thornbrugh, D. J. (2009). Eutrophication of U.S. Freshwaters: Analysis of Potential Economic Damages. *Environmental Science & Technology, 43*(1), 12–19. <https://doi.org/10.1021/es801217q>
- Dong, J., Gao, Y., Chang, M., Ma, H., Han, K., Tao, X., & Li, Y. (2018). Colony formation by the green alga *Chlorella vulgaris* in response to the competitor *Ceratophyllum demersum*. *Hydrobiologia, 805*(1), 177–187. <https://doi.org/10.1007/s10750-017-3294-0>
- Dos Santos, A., Calijuri, M., Moraes, E. M., Adorno, M. A., Falco, P., Carvalho, D. P., Debert, G. L. B., & Benassi, S. F. (2003). Comparison of three methods for Chlorophyll determination: Spectrophotometry and Fluorimetry in samples containing pigment mixtures and spectrophotometry in samples with separate pigments through High Performance Liquid Chromatography. *Acta Limnologica Brasiliensia, 15*, 12.
- EPA, U. (2005). *Technologies and Techniques for Early Warning Systems to Monitor and Evaluate Drinking Water Quality* (p. 236). USEPA.

- EPA, U. (2015). *Drinking Water Health Advisory for the Cyanobacterial Microcystin Toxins*. 75.
- Fisher, R. M., Bell, T., & West, S. A. (2016). Multicellular group formation in response to predators in the alga *Chlorella vulgaris*. *Journal of Evolutionary Biology*, 29(3), 551–559. <https://doi.org/10.1111/jeb.12804>
- Friedrichs, A., Busch, J., van der Woerd, H., & Zielinski, O. (2017). SmartFluo: A Method and Affordable Adapter to Measure Chlorophyll a Fluorescence with Smartphones. *Sensors*, 17(4), 678. <https://doi.org/10.3390/s17040678>
- Furukawa, K., Noda, N., Tsuneda, S., Saito, T., Itayama, T., & Inamori, Y. (2006). Highly sensitive real-time PCR assay for quantification of toxic cyanobacteria based on microcystin synthetase a gene. *Journal of Bioscience and Bioengineering*, 102(2), 90–96. <https://doi.org/10.1263/jbb.102.90>
- Gan, N., Xiao, Y., Zhu, L., Wu, Z., Liu, J., Hu, C., & Song, L. (2012). The role of microcystins in maintaining colonies of bloom-forming *Microcystis* spp.: *Microcystis* colony maintenance by microcystins. *Environmental Microbiology*, 14(3), 730–742. <https://doi.org/10.1111/j.1462-2920.2011.02624.x>
- Giddings, M., Aranda-Rodriguez, R., Yasvinski, G., Watson, S. B., & Zura, R. (2012). *Cyanobacterial Toxins: Drinking and Recreational Water Quality Guidelines*. 12.
- Graham, J. L., Loftin, K. A., Meyer, M. T., & Ziegler, A. C. (2010). Cyanotoxin Mixtures and Taste-and-Odor Compounds in Cyanobacterial Blooms from the Midwestern United States. *Environmental Science & Technology*, 44(19), 7361–7368. <https://doi.org/10.1021/es1008938>
- Greenfield, D. I., Marin, R., Doucette, G. J., Mikulski, C., Jones, K., Jensen, S., Roman, B., Alvarado, N., Feldman, J., & Scholin, C. (2008). Field applications of the second-generation Environmental Sample Processor (ESP) for remote detection of harmful algae: 2006-2007: Field applications of the ESP: 2006-2007. *Limnology and Oceanography: Methods*, 6(12), 667–679. <https://doi.org/10.4319/lom.2008.6.667>
- Health Canada. (2016). Cyanobacterial Toxins in Drinking Water—Document for Public Consultation. *Federal-Provincial-Territorial Committee on Drinking Water*, 1–171. (ISBN 0273-1223)

- Health Canada. (2020). *Guidelines for Canadian Drinking Water Quality Summary Table*. Federal-Provincial-Territorial Committee on Drinking Water of the Federal-Provincial-Territorial Committee on Health and the Environment. https://www.canada.ca/content/dam/hc-sc/migration/hc-sc/ewh-semt/alt_formats/pdf/pubs/water-eau/sum_guide-res_recom/summary-table-EN-2020-02-11.pdf
- Hubaux, Andre., & Vos, Gilbert. (1970). Decision and detection limits for calibration curves. *Analytical Chemistry*, 42(8), 849–855. <https://doi.org/10.1021/ac60290a013>
- Kim, S.-H., He, Y., Lee, E.-H., Kim, J.-H., & Park, S. M. (2017). Portable Fluorometer for Cyanobacteria Detection. *IEEE Sensors Journal*, 17(8), 2377–2384. <https://doi.org/10.1109/JSEN.2017.2672993>
- Kurmayer, R., Christiansen, G., & Chorus, I. (2003). The Abundance of Microcystin-Producing Genotypes Correlates Positively with Colony Size in *Microcystis* sp. And Determines Its Microcystin Net Production in Lake Wannsee. *Applied and Environmental Microbiology*, 69(2), 787–795. <https://doi.org/10.1128/AEM.69.2.787-795.2003>
- Kus, S., Marczenko, Z., & Obarski, N. (1996). Derivative UV-VIS Spectrophotometry in Analytical Chemistry. *Chern. Anal. (Warsaw)*, Department of Analytical Chemistry, Technical University of Warsaw, 00-664 Warszawa, Poland, 31.
- Li, T., Xu, J., Gao, B., Xiang, W., Li, A., & Zhang, C. (2016). Morphology, growth, biochemical composition and photosynthetic performance of *Chlorella vulgaris* (Trebouxiophyceae) under low and high nitrogen supplies. *Algal Research*, 11.
- Lichtenthaler, H. K., & Buschmann, C. (2001). Chlorophylls and Carotenoids: Measurement and Characterization by UV-VIS Spectroscopy. *Current Protocols in Food Analytical Chemistry*, 1(1), F4.3.1-F4.3.8. <https://doi.org/10.1002/0471142913.faf0403s01>
- Liu, J.-Y., Zeng, L.-H., & Ren, Z.-H. (2020). Recent application of spectroscopy for the detection of microalgae life information: A review. *Applied Spectroscopy Reviews*, 55(1), 26–59. <https://doi.org/10.1080/05704928.2018.1509345>

- Malhotra, A., & Örmeci, B. (2021). Monitoring of Cyanobacteria using Derivative Spectrophotometry and improvement of the method detection limit by changing pathlength. *Manuscript Submitted for Publication, Department of Civil and Environmental Engineering, Carleton University*, 1–46.
- McCullough, G. (2007). *Assessment of bbe Fluoroprobe for algal taxonomic discrimination in Lake Winnipeg* (p. 27) [Report to the Canadian Department of Fisheries and Oceans]. Centre for Earth Observations Science Department of Environment and Geography University of Manitoba.
- Miazek, K., Iwanek, W., Remacle, C., Richel, A., & Goffin, D. (2015). Effect of Metals, Metalloids and Metallic Nanoparticles on Microalgae Growth and Industrial Product Biosynthesis: A Review. *International Journal of Molecular Sciences*, *16*(10), 23929–23969. <https://doi.org/10.3390/ijms161023929>
- Millie, D. F., Schofield, O. M., ??E., Kirkpatrick, G. J., Johnsen, G., & Evens, T. J. (2002). Using absorbance and fluorescence spectra to discriminate microalgae. *European Journal of Phycology*, *37*(3), 313–322. <https://doi.org/10.1017/S0967026202003700>
- Moreira, C., Martins, A., Azevedo, J., Freitas, M., Regueiras, A., Vale, M., Antunes, A., & Vasconcelos, V. (2011). Application of real-time PCR in the assessment of the toxic cyanobacterium *Cylindrospermopsis raciborskii* abundance and toxicological potential. *Applied Microbiology and Biotechnology*, *92*(1), 189–197. <https://doi.org/10.1007/s00253-011-3360-x>
- Mukhopadhyay, S. C., & Mason, A. (Eds.). (2013). *Smart Sensors for Real-Time Water Quality Monitoring* (Vol. 4). Springer Berlin Heidelberg. (ISBN 978-3-642-37005-2) <https://doi.org/10.1007/978-3-642-37006-9>
- National Water Quality Management Strategy. (2000). *Australian and New Zealand guidelines for fresh and marine water quality 2000.: Vol. Agriculture and Resource Management Council of Australia and New Zealand*. Australian and New Zealand Environment and Conservation Council. (ISBN 978-0-9578245-0-8)
- NHMRC, & NRMCC. (2017). *Australian Drinking Water Guidelines Paper 6 National Water Quality Management Strategy* (Version 3.4). National Health and Medical Research Council, National Resource Management Ministerial Council. (ISBN 1-

86496-511-8)

<https://www.nhmrc.gov.au/sites/default/files/documents/reports/aust-drinking-water-guidelines.pdf>

- Quansah, J. E., Engel, B., & Rochon, G. L. (2010). *Early Warning Systems: A Review*. 2(2), 22.
- Reynolds, C. S. (2007). Variability in the provision and function of mucilage in phytoplankton: Facultative responses to the environment. *Hydrobiologia*, 578(1), 37–45. <https://doi.org/10.1007/s10750-006-0431-6>
- Ruffin, C., King, R. L., & Younan, N. H. (2008). A Combined Derivative Spectroscopy and Savitzky-Golay Filtering Method for the Analysis of Hyperspectral Data. *GIScience & Remote Sensing*, 45(1), 1–15. <https://doi.org/10.2747/1548-1603.45.1.1>
- Safi, C. (2014). Morphology, composition, production, processing and applications of *Chlorella vulgaris*_ A review. *Renewable and Sustainable Energy Reviews*, 14.
- Saini, D. K., Pabbi, S., & Shukla, P. (2018). Cyanobacterial pigments: Perspectives and biotechnological approaches. *Food and Chemical Toxicology*, 120, 616–624. <https://doi.org/10.1016/j.fct.2018.08.002>
- Savitzky, Abraham., & Golay, M. J. E. (1964). Smoothing and Differentiation of Data by Simplified Least Squares Procedures. *Analytical Chemistry*, 36(8), 1627–1639. <https://doi.org/10.1021/ac60214a047>
- Schneider, S., Wokusch, Th., Tiltscher, H., Fischer, R., & Scheer, H. (1991). UV-VIS Absorption Spectra at High Pressure of C-Phycocyanin and Allophycocyanin from *Mastigocladus laminosus*. *Zeitschrift Für Naturforschung C*, 46(9–10), 717–724. <https://doi.org/10.1515/znc-1991-9-1002>
- Shin, Y.-H., Barnett, J. Z., Gutierrez-Wing, M. T., Rusch, K. A., & Choi, J.-W. (2018). A hand-held fluorescent sensor platform for selectively estimating green algae and cyanobacteria biomass. *Sensors and Actuators B: Chemical*, 262, 938–946. <https://doi.org/10.1016/j.snb.2018.02.045>
- Simis, S. G. H., & Kauko, H. M. (2012). In vivo mass-specific absorption spectra of phycobilipigments through selective bleaching: Selective bleaching of

- phytoplankton pigments. *Limnology and Oceanography: Methods*, 10(4), 214–226. <https://doi.org/10.4319/lom.2012.10.214>
- Sobiechowska-Sasim, M., Stoń-Egiert, J., & Kosakowska, A. (2014). Quantitative analysis of extracted phycobilin pigments in cyanobacteria—An assessment of spectrophotometric and spectrofluorometric methods. *Journal of Applied Phycology*, 26(5), 2065–2074. <https://doi.org/10.1007/s10811-014-0244-3>
- Stefanelli, M., Vichi, S., Stipa, G., Funari, E., Testai, E., Scardala, S., & Manganelli, M. (2014). Survival, growth and toxicity of *Microcystis aeruginosa* PCC 7806 in experimental conditions mimicking some features of the human gastro-intestinal environment. *Chemico-Biological Interactions*, 215, 54–61. <https://doi.org/10.1016/j.cbi.2014.03.006>
- Swinehart, D. F. (1962). The Beer-Lambert Law. *Journal of Chemical Education*, Vol.39(7), 333. <https://doi.org/10.1021/ed039p333>
- Tran Khac, V., Hong, Y., Plec, D., Lemaire, B., Dubois, P., Saad, M., & Vinçon-Leite, B. (2018). An Automatic Monitoring System for High-Frequency Measuring and Real-Time Management of Cyanobacterial Blooms in Urban Water Bodies. *Processes*, 6(2), 11. <https://doi.org/10.3390/pr6020011>
- WDNR. (1996). *Analytical Detection Limit Guidance & Laboratory Guide for Determining Method Detection Limits* (Analytical Guide PUBL-TS-056-96). Wisconsin Department of Natural Resources Laboratory Certification Program. <https://dnr.wi.gov/regulations/labcert/documents/guidance/-LODguide.pdf>
- WHO. (2003a). Algae and cyanobacteria in fresh water. In *Guidelines for Safe Recreational Water Environments* (pp. 136–158). WHO Publishing. https://www.who.int/water_sanitation_health/bathing/srwe1-chap8.pdf
- WHO. (2003b). *Guidelines for Safe Recreational Water Environments: Coastal and fresh waters*. World Health Organization. (ISBN 978-92-4-154580-8)
- Wilson, A. E., Wilson, W. A., & Hay, M. E. (2006). Intraspecific Variation in Growth and Morphology of the Bloom-Forming Cyanobacterium *Microcystis aeruginosa*. *Applied and Environmental Microbiology*, 72(11), 7386–7389. <https://doi.org/10.1128/AEM.00834-06>

Zamyadi, A., Choo, F., Newcombe, G., Stuetz, R., & Henderson, R. K. (2016). A review of monitoring technologies for real-time management of cyanobacteria: Recent advances and future direction. *TrAC Trends in Analytical Chemistry*, 85, 83–96. <https://doi.org/10.1016/j.trac.2016.06.023>

Appendix D

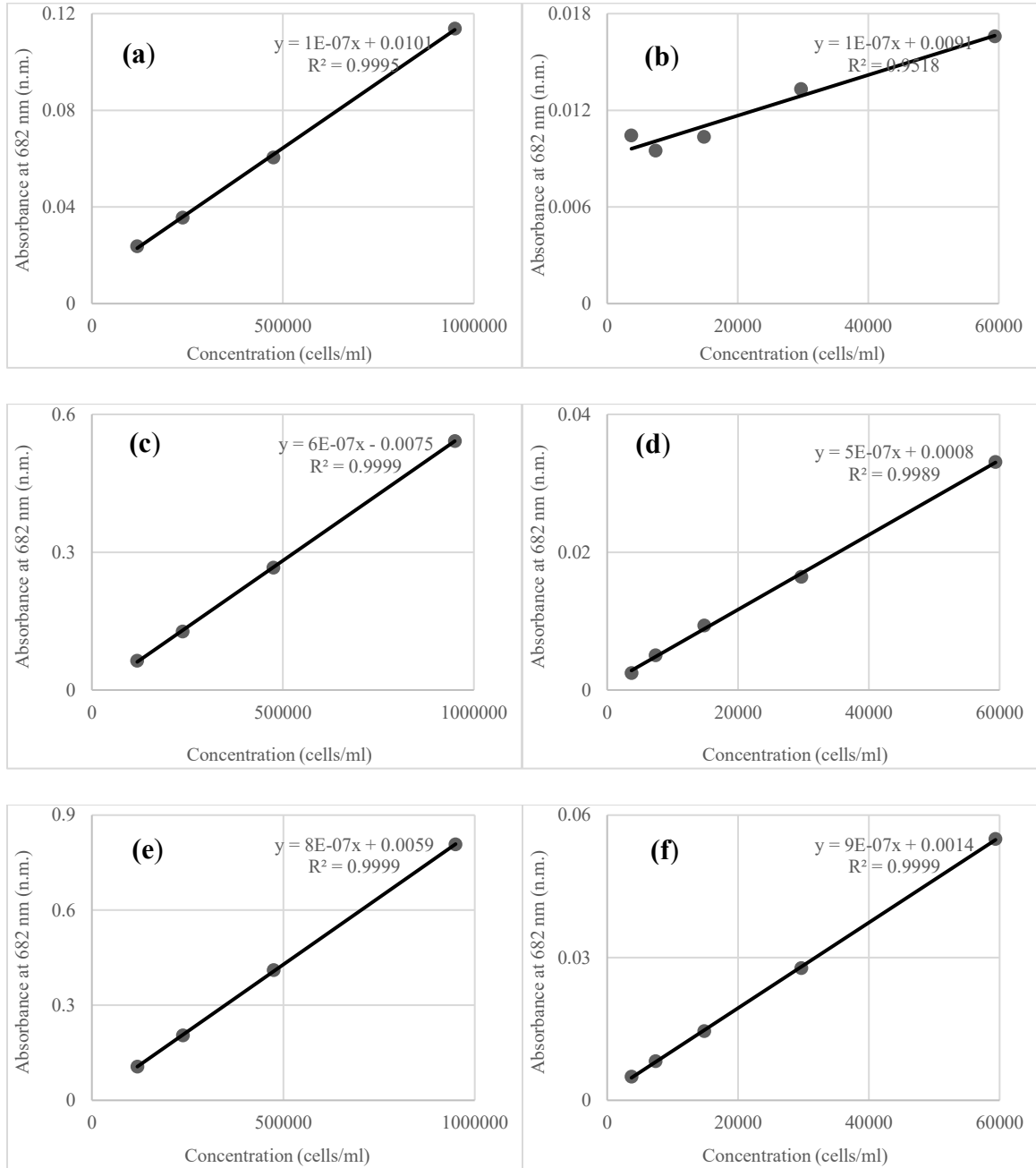


Figure D.5: Standard calibration curves for absorbance spectra at *Chl-a* peak at higher and lower concentration ranges of mixed-culture for 10 mm (a, b), 50 mm (c, d), and 100 mm (e, f) cuvette pathlengths, respectively.

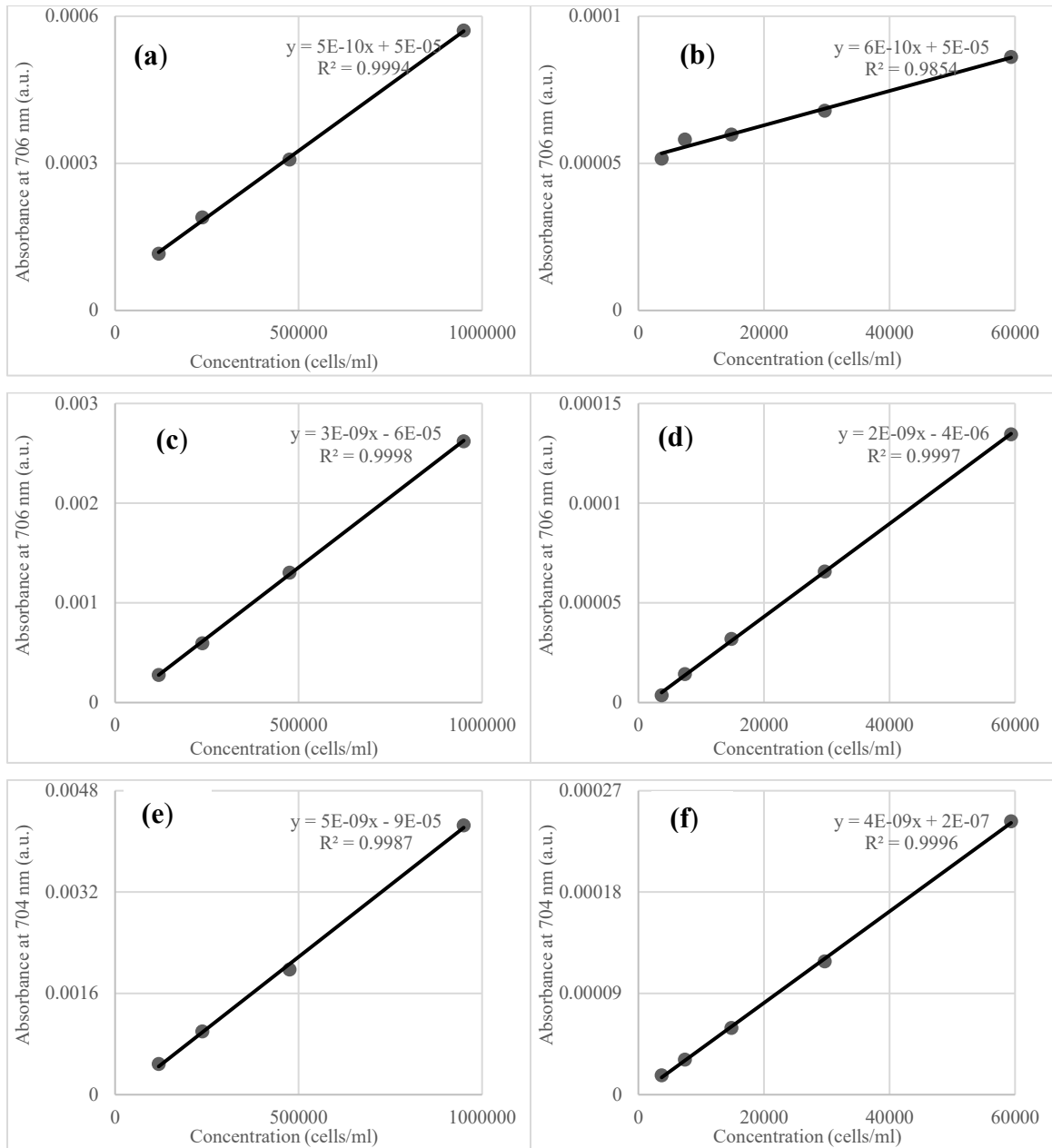


Figure D.6: Standard calibration curves for Savitzky-Golay first derivative of absorbance at *Chl-a* peak at higher and lower concentration ranges of mixed-culture for 10 mm (a, b), 50 mm (c, d), and 100 mm (e, f) cuvette pathlengths, respectively.

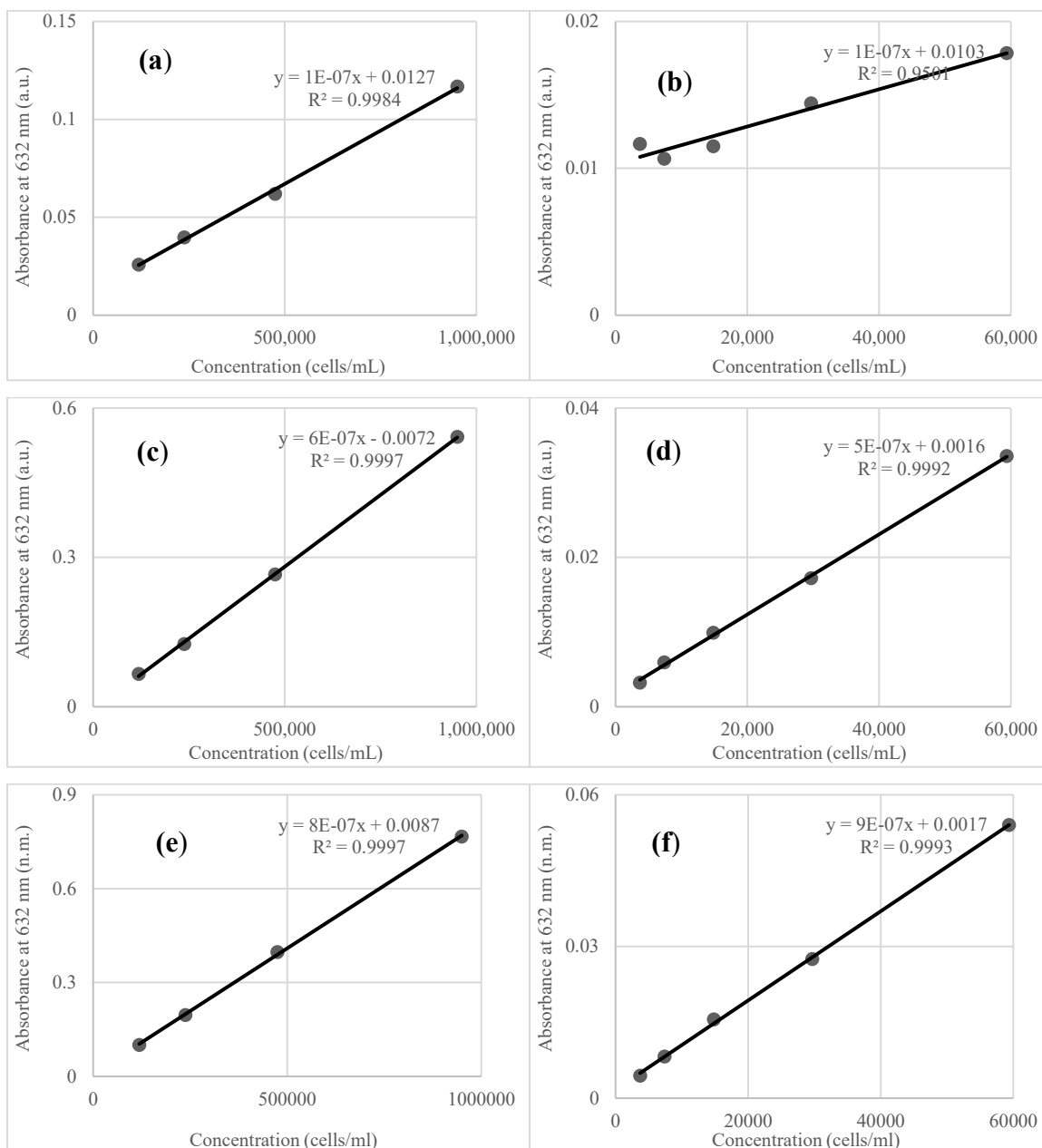


Figure D.7: Standard calibration curves for absorbance spectra at PC peak at higher and lower concentration ranges of mixed-culture for 10 mm (a, b), 50 mm (c, d), and 100 mm (e, f) cuvette pathlengths, respectively.

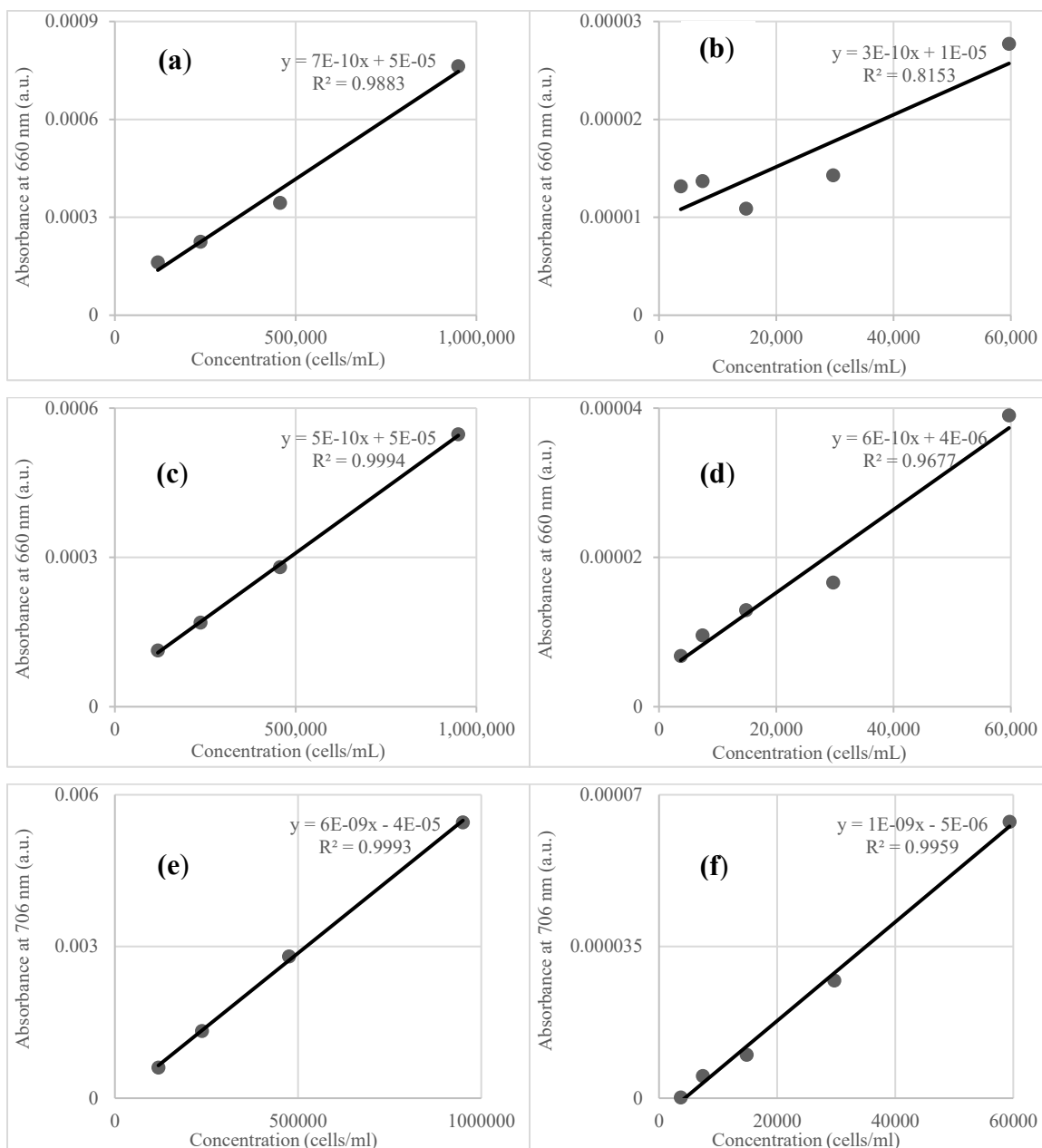


Figure D.8: Standard calibration curves for Savitzky-Golay first derivative of absorbance at PC peak at higher and lower concentration ranges of mixed-culture for 10 mm (a, b), 50 mm (c, d), and 100 mm (e, f) cuvette pathlengths, respectively.

6. Detection and Monitoring of Cyanobacteria and Green Algae in River Water using Derivative Spectrophotometry

Amitesh Malhotra and Banu Örmeci*

Department of Civil and Environmental Engineering, Carleton University

1125 Colonel By Drive, Ottawa ON K1S 5B6, Canada

Abstract

Monitoring of microalgae in source water has become more important than ever, especially due to worsening eutrophication as well as global warming and an increase in potentially toxic cyanobacterial bloom formation. This research investigated using longer cuvette pathlengths (50-, and 100-mm) and Savitzky-Golay (S-G) first derivative of absorbance for detection and monitoring of *Microcystis aeruginosa* (cyanobacteria) and *Chlorella vulgaris* (green algae) in river water to provide realistic conditions in determining the method performance. Further, differences between the absorbance spectra of cyanobacterial and green algae were analyzed to identify key peaks from different photopigments for monitoring purposes. For both microalgae, correlations between cell concentrations, absorbance, and derivative of absorbance measurements were investigated. In addition, method detection limits (MDLs) were established, and calibration curves were made to carry out sensitivity analyses. A strong linear relationship ($R^2 > 0.9$) was observed between concentration and absorbance for all peaks of interest (such as 682 nm for photopigment *Chl-a* and 632 nm for phycocyanin). Finally, the performance and MDLs were compared for both microalgae in river water with deionized water. Results obtained using 100 mm pathlength and S-G derivative were found to be the most sensitive and had

the lowest MDLs of 12,798 cells/mL and 8,546 cells/mL for *M. aeruginosa* for phycocyanin and *Chl-a* peaks in river water; whilst *C. vulgaris* had the lowest MDL of 13,695 cells/mL for *Chl-a* peak in river water. These results indicate that using longer cuvette pathlengths and employing derivative spectrophotometry, the method described can be potentially used for early detection and monitoring of cyanobacteria and green algae in real environmental samples.

Keywords: *Chlorella vulgaris*; *Microcystis aeruginosa*; cyanobacteria; derivative spectrophotometry; water; monitoring.

6.1 Introduction

Monitoring of source waters for algae proliferation is essential, with worsening water quality and increasing eutrophication (Altenburger et al., 2015; Dodds et al., 2009). Global climate warming in combination with eutrophication supports microalgal growth by increasing water column stability and facilitating bloom formation (Figueiredo et al., 2004; Ibelings et al., 2014). Microalgae in source waters are increasing globally and can cause nuisance by producing taste and odor (T&O) compounds, reducing natural dissolved oxygen (DO), impacting natural aquatic habitat, forming scum, and increasing treatment cost if source water is used for drinking or recreational purposes) (Bajpai et al., 2011; Oren, 2014; Sharma et al., 2010). In regard to microalgae, of particular concern are potentially toxic cyanobacteria (CB) which have the capability of producing harmful toxins, known as cyanotoxins in addition to T&O compounds (Al-Sammak et al., 2013; Bukaveckas, 2018). CB blooms pose a major hazard to human and animal health, as well as to the environment (Falconer, 1999; Health Canada, 2016).

Amongst cyanobacteria, *Microcystis* sp. is a bloom-forming genus which is found all over the world in highly eutrophic source water bodies (Pelaez et al., 2010). Species within this genus can be toxic or non-toxic in nature and but several species produce hepatoxins, which upon ingestion can cause gastroenteritis, liver damage, cancer, and/or bioaccumulation (Berry et al., 2011; Health Canada, 2016; Winter et al., 2011). Likewise, *Chlorella* sp. is a common green algae genera that is found in eutrophic source waters around the globe (AlMamani & Örmeci, 2016; Safi, 2014). Therefore, *Microcystis aeruginosa* (cyanobacteria) and *Chlorella vulgaris* (non-cyanobacterial algae) were selected for monitoring and detection purposes in this study.

Due to reasons mentioned before, the early detection of bloom in source water is a requirement in many countries (Bowling et al., 2017; Bukaveckas, 2018). Some water authorities around the world have developed their own drinking and recreational water regulations for source water containing algae with a prime focus on cyanobacteria, but the great majority follow guidance values recommended by the World Health Organization (WHO) (Bartram & Rees, 2000; Chorus, 2012; WHO, 2017a). With varying regulations and management practices, selecting a single technology for monitoring purposes becomes a challenging task (Giddings et al., 2012). A few examples of regulations and guidance values for source waters are shown in Table 6.1. It is important to be aware that for public safety, while monitoring potential blooms in drinking water sources, any detected cyanobacteria is assumed to be potentially toxic in nature (EPA, 2005, 2015). This makes early detection a key for the management of blooms. It should also be mentioned that minimal to no guidelines exist for non-toxic algae in source waters.

Table 6.1: Regulations/ guidance value examples for low probability of adverse health effects in drinking and recreational water sources around the world for cyanobacteria.

Regulatory Body	Drinking water	Recreational water	Reference
Canada	1.5 µg/L Microcystin	≤ 100,000 cells/mL or 20 µg/L <i>Chl-a</i>	(Health Canada, 2020)
WHO	1 µg/L Microcystin	≤ 20,000 cells/mL or 10 µg/L <i>Chl-a</i>	(WHO, 2003a)
USEPA	1.6 µg/L Microcystin	≤ 20,000 cells/mL or 10 µg/L <i>Chl-a</i>	(EPA, 2015)
Cuba	< 20,000 cells/mL	20,000 – 100,000 cells/mL	(WHO, 2003b)
Brazil	10,000 – 20,000 cells/mL	Not declared	(Chorus, 2005)
Turkey	> 5,000 cells/L > 1 µg/L <i>Chl-a</i>	< 20,000 cells/L < 10 µg/L <i>Chl-a</i>	(Chorus, 2012)

Detection and monitoring techniques for cyanobacteria and other microalgae are broadly based on either pigment or toxin estimation (Moreira et al., 2014; UNESCO, 1996). Traditional methods are based on direct counting and microscopic estimation, which are highly prone to errors but cost-effective (Chorus & Bartram, 1999). Current techniques are based on molecular methods (such as qPCR and biochemical assays), fluorometry, spectrophotometry, remote sensing, and chromatography (Agberien & Örmeci, 2019; Balest et al., 2016; Greenfield et al., 2008; Kim et al., 2017; Moreira et al., 2011; Quansah

et al., 2010). Techniques based on chromatography and molecular methods are highly selective and sensitive in detection with a limit of detection as low as 1 ng/L, but are intrusive in nature, require extensive sample preparation before analysis, and skilled personnel for operation (Balest et al., 2016; Dos Santos et al., 2003; EPA, 2005). Spectrophotometric, fluorometric, and remote sensing methods can be used for intrusive or non-intrusive monitoring based on the methods applied. Typically, non-intrusive methods are selected to reduce analysis time and environmental waste produced by relying on reagent/pigment or toxin extraction (Gray, 2010; McCullough, 2007). Remote sensing, although an attractive alternative monitoring technique, is highly dependent on weather and cannot distinguish between the type of microalgal bloom present (Furevik et al., 2004; Wang et al., 2015). Fluorometry is presently the most common technology applied for on-line monitoring of microalgae and cyanobacteria due to its high sensitivity and low detection limit (Zamyadi et al., 2016). However, studies have shown that the sensitivity is susceptible to changing microalgal physical properties, intensity of fluorescent light, presence of non-algal phytoplankton, and fluctuating pigment content (Bertone et al., 2018; Bowling et al., 2016, 2017).

Using spectrophotometry for on-line monitoring of water quality parameters such as total organic carbon (TOC), chemical oxygen demand (COD), biological oxygen demand (BOD), nitrates, nitrites, benzene, total suspended solids (TSS), among others, has increased dramatically (Burgess & Thomas, 2017). The ability to measure different water parameters is beneficial for microalgae monitoring as multiple factors contribute to bloom proliferation (such as a mix of nutrients and favorable environmental conditions) (Health Canada, 2016). The main advantage of spectrophotometry is that it is easily available,

simple, rapid, can measure extracted and unextracted pigment concentration, and can transmit data in real-time (AlMamani & Örmeci, 2018). However, spectrophotometry has not been widely used for real-time monitoring of cyanobacteria and microalgae. The main limitation of spectrophotometry is that it is vulnerable to baseline shifts of water and measurements are altered in the presence of different water contaminants, and turbidity (Owen, 1995). To correct this, derivative spectrophotometry can be applied to reduce background noise and improve spectra for analysis while reducing issues with baseline shifts (Kus et al., 1996). A study by Agberien & Örmeci (2019) investigated the use of derivative spectrophotometry for monitoring cyanobacteria (*M. aeruginosa*) and reported a detection limit of 90,231 cells/mL in surface water using 10 mm pathlength. Another study that tested derivative spectrophotometry for monitoring microalgae reported a detection limit of 0.56 TVS/L in surface water (AlMamani & Örmeci, 2018). These studies indicate that spectrophotometry has potential for monitoring but might not be as sensitive as other methods.

The objective of this study was to demonstrate the potential of using readily available UV-Vis spectrophotometer technology while implementing derivative spectrophotometry as an analytical tool in order to develop an early detection system to be used for monitoring of cyanobacteria and microalgae in surface waters. Studies using environmental samples are limited in nature but critical for understanding applicability for real-time microalgae monitoring. Unfiltered river water was used in order to provide realistic and challenging conditions in determining the performance and limitations of the method. Most of the traditional techniques require pre-processing to analyze environmental samples resulting in a key drawback and raising a need for better monitoring technique, which can analyze

samples in a robust manner without relying on sample processing. Cuvette pathlengths of 50- and 100-mm were used to improve the detection and sensitivity compared to traditional spectrophotometry. To compare Rideau River water to typical source waters where cyanobacterial blooms occur, it was tested for pH, turbidity and COD for characterisation and representative purposes. Lastly, detection limits were established, and sensitivity analyses were conducted between inoculated microalgae in river water and deionized water while comparing their performance.

6.2 Materials and Methods

6.2.1 Microalgae growth and cultivation

Microcystis aeruginosa CPCC632 (non-toxic cyanobacteria) and *Chlorella vulgaris* CPCC90 (common green algae) were selected for this study and acquired from the Canadian Phycological Culture Center (CPCC) at the University of Waterloo (Ontario, Canada). These microalgae were cultured using sterile growth media of Bold's Basal Medium with triple Nitrogen stock (3N-BBM) and Bold's Basal Medium (BBM), respectively (CPCC, 2013). *M. aeruginosa* and *C. vulgaris* were cultured in their corresponding growth medium using 1:2 and 1:3 dilution factors for the duration of this study. The microalgae were cultured in individual 1,000 mL clean Erlenmeyer flasks, which were rinsed using deionized (D.I.) water and sterilized using an autoclave for 30 min at 15 psi and 121 °C, before use. This was done to prevent potential cross-contamination from foreign sources, which might impact algal growth and properties.

The Erlenmeyer flasks containing the cultures were cultivated in a temperature-controlled incubator (kept at 24 °C), under 24-hour photoperiod using two fluorescent tube lights emitting daylight, to mimic optimal natural growth conditions. *M. aeruginosa* was kept at

an intensity of 1,000 lux inside the incubator, while *C. vulgaris* was exposed to 1,800 lux for optimal growth (CPCC, 2013). The cultures sourced carbon dioxide diffused from natural air for growth purposes. To maintain a homogenous mixture and promote higher gas exchange rate, both culture flasks were manually stirred twice a day.

6.2.2 Characterization of river water

A clean high-density polyethylene container was used to grab surface water from Rideau River (Ottawa, Ontario). Fresh river water was collected on the day of the experiment and the collected water was allowed to acclimate to room temperature for experimental consistency purposes following standard operating procedures (KBGAWG, 2009). The raw water was analyzed for chemical oxygen demand (COD), turbidity, and pH in triplicates according to Standard Methods, 5220 D. Closed Reflux Colorimetric Method, 2130 B. Nephelometric Method, and 4500-H⁺ B. Electrometric Method, respectively (Rice et al., 2017). A DR 2800 Spectrophotometer (HACH, CO, USA) using USEPA Reactor Digestion Method 8000 was used for COD measurement; while a HACH 2100AN Turbidimeter (Hach, CO, USA) and a pH meter (Orion 5-star, Thermo Scientific, Canada) were used to measure turbidity and pH, respectively. The instruments were calibrated daily using manufacturer's standards, before use.

6.2.3 Sample preparation for spectrophotometric analysis

The cultivated *M. aeruginosa* and *C. vulgaris* cultures were separated from their respective growth mediums by centrifugation at 8,000×g for 5 mins using 50 mL centrifuge tubes. Subsequently, the separated media was discarded, and the microalgae was resuspended in 45 mL river water. Then the samples were gently inverted 5 times to ensure a homogenous mixture of microalgae which was used as stock for sample dilutions (for both cultures).

Afterward, the stock cultures were enumerated under a Leitz Laborlux 12 light microscope, and an improved Neubauer hemocytometer was used for quantification purposes. Following quantification of both algal strains, sample preparation was carried out using the same dilution ratios to achieve near similar cell concentrations between each concentration range. The prepared samples ranged from 3,800,000 cells/mL to 1,855 cells/mL with 12 concentration levels for both *M. aeruginosa* and *C. vulgaris* cultures. This consistency allowed for an accurate comparison between different tests. Note that the raw water for sample preparation was used as is (without any particulate filtration) from the source and was kept under constant mixing using a magnetic stirrer to avoid particulate settlement. This was done to ensure a better representation of realistic water conditions on microalgal detection limit.

6.2.4 UV-Vis Spectrophotometry

A laboratory UV-Vis spectrophotometer Cary 100 (Agilent Technologies, USA) was used for analysis, while varying pathlengths using 50-, and 100-mm quartz cuvettes. Before each test, the spectrophotometer was calibrated and zeroed to D.I. water using respective cuvettes. The absorbance measurements were carried over the spectral range from 200 nm to 800 nm, with a 1 nm set spectral scan step. Absorbance measurements for both *M. aeruginosa* and *C. vulgaris* in water samples were repeated at least four times using a freshly prepared microalgae solution, and the absorbance values were measured in absorbance units (a.u.). A higher number of replicates were used to ensure repeatability between samples while minimizing error and avoiding potential issues associated with photobleaching of microalgae (Hudnell, 2008; UNESCO et al., 2004). The resultant absorbance values for each test sample were subtracted by a blank river water measurement

to obtain the final absorbance for both *M. aeruginosa* and *C. vulgaris* tests independently. This was done for both 50-and 100-mm pathlengths before the experiment. The same cuvette orientation was consistently used between individual measurements, and the cuvettes were regularly inspected for any damage that might impact analyzed values. Between each test, the cuvettes were thoroughly cleaned using D.I. water, and the samples were scanned starting from lowest concentration to highest concentration. To simplify the analysis, the measured samples were distributed into lower [i.e., 59,375 – 1,855 cells/mL] and higher [i.e., 950,000 – 118,750 cells /mL] concentration ranges. To verify whether the samples followed Beer-Bouguer-Lambert law, standard calibration curves were plotted, and each test was performed twice to verify applicability and repeatability. The volumes for the prepared grab samples for 50 mm, and 100 mm were kept at 17.5 mL and 35 mL, respectively.

6.2.5 Calculation of Savitzky-Golay first-order derivative of absorbance

Derivative spectrophotometry is the use of first or higher derivatives of observed absorbance with respect to the recorded wavelength. It is used for qualitative and quantitative analysis (Owen, 1995). Savitzky-Golay (S-G) first-order derivative is a technique that allows to simultaneously smoothen the observed data and attain first-order derivative of absorbance. This improves the signal-to-noise ratio in comparison to the zero-order absorbance, resulting in sharper and clearer peaks for better analysis (Ruffin et al., 2008). It is calculated using the following correlation:

$$a_j = \frac{\sum_{i=-\frac{m-1}{2}}^{\frac{m-1}{2}} C_i F_{j+i}}{N} \frac{m+1}{2} \leq j \leq n - \frac{m-1}{2}$$

Where, a_j = Savitzky-Golay first derivative of absorbance; C_i = Savitzky-Golay filter coefficient; F = absorbance value measured at a specific wavelength; m = number of data points used; j = smoothened data point; N = standardization factor. Each measured absorbance value was smoothened over twenty-three data points so that $i = -11, -10, \dots, 10, 11$; $C_i = -11, -10, \dots, 10, 11$; $m = 23$; $N = 1012$; following S-G table of coefficients for first derivative of absorbance (Savitzky & Golay, 1964).

6.2.6 Establishing detection limit

The minimum detection limit for microalgae concentration was determined using Hubaux and Vos method, which is a widely accepted statistical method for calculating method detection limit (MDL) (Voigtman, 2017). At least 10 data points were recorded and used to determine the MDL as the method requires a minimum of 3 data points and 3 replicates (Hubaux & Vos, 1970). An excel-based calculator developed by Chemiasoft for Hubaux and Vos method was used to calculate the MDL. All the MDLs for all both microalgal concentrations were determined at a 99% confidence level indicating that the analyte concentration is greater than zero (Berthouex & Brown, 2002).

6.3 Results

6.3.1 Spectrophotometric measurements of *M. aeruginosa* in river water

Spectrophotometric measurements were carried out to determine the viability of spectrophotometry for cyanobacterial detection in a natural water sample. Since the river water was used as-is, without any filtration, the absorbance measurements are susceptible to variations due to organic and inorganic contaminants present in the source water. The river water was characterized for its chemical oxygen demand (COD), turbidity, pH, and the results are shown in Table 6.2. The absorbance spectra of *M. aeruginosa*

(cyanobacteria) was determined in river water in two major concentration ranges: higher (118,750 – 950,000 cells/mL) and lower (1,855 – 59,375 cells/mL) ranges. The absorbance measurements (illustrated in Figure 6.1) resulted in three major peaks to be observed at 442-, 632-, and 682-nm, with the sharpest peak being observed at 682 nm. This correlates well considering that *M. aeruginosa* are known to carry the primary photopigment chlorophyll-a (*Chl-a*) and an accessory photopigment known as phycocyanin (PC) which is unique to cyanobacteria (Dos Santos et al., 2003; Saini et al., 2018). Typically, the photopigment *Chl-a* peaks close to 440-, and 680-nm; while the peak at 632 nm correlates to PC. The phycocyanin peak is traditionally located between 612 – 626 nm, but the peak is prone to shifts with different cyanobacteria and changing water characteristics (Craig & Carr, 1968; McQuaid et al., 2011; Raps et al., 1985; Sobiechowska-Sasim et al., 2014). It should be noted that the objective of this research was not to study the impact of individual water quality parameters on detection, rather the effectiveness of this method under realistic water monitoring conditions. Lastly, as all the identified peaks fell between the range of 400 – 800 nm of the spectrum, and therefore the study focused on that range for analysis purposes.

Table 6.2: Results from Rideau River characterization.

Parameter	Measurement (Mean)
COD (mg/L)	24 ± 1.8
Turbidity (NTU)	12 ± 2.0
pH	7.84
Temperature (°C)	20.5 ± 0.5

Following the Beer-Lambert Law, both 50-, and 100-mm results saw an incremental increase in absorbance values with increasing concentration (Figure 6.1). With increasing cuvette pathlength, the observed absorbance values increased for samples with the same cell concentration. This is expected as a larger pathlength holds a bigger volume, which in turn results in more light being absorbed by the sample (Burgess & Thomas, 2017). At the higher concentration range for both pathlengths, all peaks were clearly observed (Figure 6.1 a,c). At lower concentrations, for 50 mm pathlength (Figure 6.1 b), results indicated that a clear peak could not be readily identified for *Chl-a* and PC below 30,000 cells/mL and 60,000 cells/mL concentration, respectively. On the other hand, lower concentration 100 mm pathlength (Figure 6.1 d) results showed no clear peak for *Chl-a* and PC below 15,000 cells/mL and 30,000 cells/mL, respectively. The detection limit was calculated at both *Chl-a* and PC peak at 682-, and 632-nm, respectively. Changing cuvette pathlength from 50-, to 100-mm improved the sensitivity by approximately 2-fold, reducing the detection limit to 26,788 cells/mL and 36,705 cells/mL using 100 mm pathlength for *Chl-a* and PC, respectively from 44,248 cells/mL and 62,660 cells/mL (Table 6.3).

Calibration curves were generated at 682-, and 632-nm for higher and lower ranges to validate coherency of the data with Beer-Lambert Law and are illustrated in supplementary information Figure E.4 and Figure E.6. A strong linear relationship was observed between absorbance and concentration at both the wavelengths ($R^2 > 0.9$), and the slopes at 682-, and 632-nm were approximately the same for 50-, and 100-mm pathlengths over the entire concentration range (Table 6.3). For example, at 682-, and 632-nm, the slopes for lower concentration range for 50 mm were $3.8336 \times 10^{-07} \pm 3.0833 \times 10^{-08}$ au/(cells/mL) and $3.7430 \times 10^{-07} \pm 2.7904 \times 10^{-08}$ au/(cells/mL), respectively. Similarly, for 100 mm at 682-

, and 632-nm, the slopes for lower concentration range were $6.6302 \times 10^{-07} \pm 1.0201 \times 10^{-08}$ au/(cells/mL) and $6.4778 \times 10^{-07} \pm 1.0084 \times 10^{-08}$ au/(cells/mL), respectively. However, even with 100 mm pathlength, at concentrations lower than 30,000 cells/mL, it was difficult to clearly distinguish cyanobacterial peaks from background noise in river water.

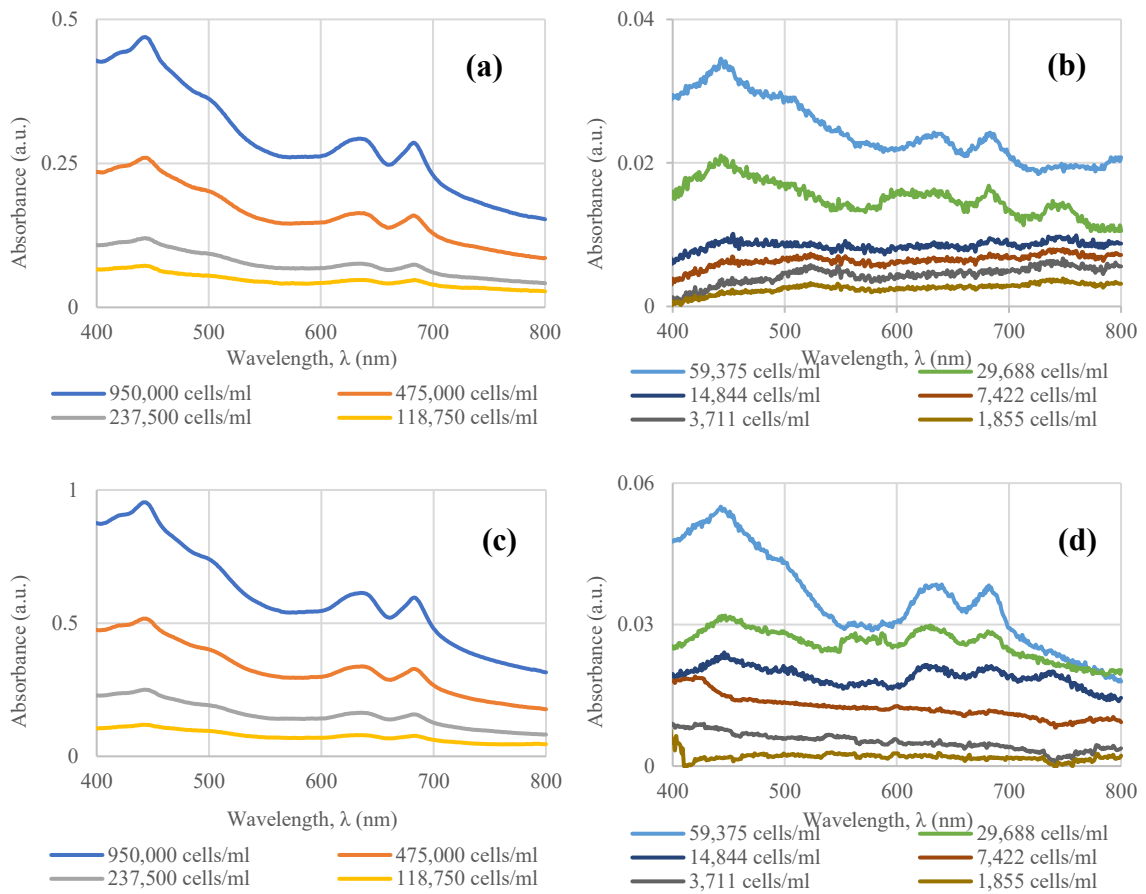


Figure 6.1: Absorbance spectra at higher and lower concentration ranges of *M. aeruginosa* for 50 mm (a, b), and 100 mm (c, d) cuvette pathlengths, respectively.

6.3.2 Savitzky-Golay first derivative of absorbance of *M. aeruginosa* in river water

Savitzky-Golay (S-G) first derivative of absorbance was implemented to concurrently calculate the first-order derivative of absorbance, while smoothening the plot obtained

using predefined polynomial coefficients (Chen et al., 2014; Ruffin et al., 2008). This analytical tool facilitated in reducing random background noise while amplifying absorbance signal, which resulted in sharp and readily identifiable peaks for *M. aeruginosa* (Figure 6.2).

Comparing the zero-order absorbance spectra (Figure 6.1) to S-G derivative spectra (Figure 6.2), a shift in primary peaks of interest was observed at 706-, and 660-nm from 682-, and 632-nm, which correspond to *Chl-a* and PC, respectively. This is a characteristic and an expected shift in peak as the first-order derivative of absorbance corresponds to the rate of change of absorbance with wavelength (Agberien & Örmeci, 2019; Kus et al., 1996). With changing *M. aeruginosa* concentration, these wavelengths exhibited the most noticeable changes as well. At the lower concentration range, the PC peak showed a lower response in absorbance. This is likely due to interferences from water constituents such as turbidity, which might have a significant impact on lower cyanobacterial concentrations. Similar spectral curves could be observed for 50- and 100-mm pathlengths at similar concentration ranges (Figure 6.2). An approximate 2-fold improvement in detection was observed by increasing the cuvette pathlength from 50 mm to 100 mm. The MDL of *M. aeruginosa* in river water using S-G first derivative of absorbance for 50 mm pathlength was found to be 22,457 cells/mL for PC and 18,324 cells/mL for *Chl-a* peaks, while the MDL using 100 mm pathlength was found to be 12,798 cells/mL for PC and 8,546 cells/mL for *Chl-a*.

Standard calibration curves were plotted at 660-, and 706-nm wavelengths indicating a strong linear relationship ($R^2 > 0.94$) between *M. aeruginosa* concentration and the S-G first derivative of absorbance for both cuvette pathlengths and are illustrated in supplementary information Figure E.7 and Figure E.5, respectively. The slopes of the

calibration curves were similar between different concentration ranges. For example, the slope for 100 mm pathlength at 706 nm at lower and higher concentration range was estimated to be $4.2421 \times 10^{-09} \pm 4.5723 \times 10^{-10}$ and $4.4338 \times 10^{-09} \pm 1.5224 \times 10^{-10}$, respectively (see Table 6.3). However, at concentrations below 7,500 cells/mL, it was difficult to differentiate between signal with noise for both 50-, and 100-mm pathlengths (Figure 6.2 **Error! Reference source not found.** b,d).

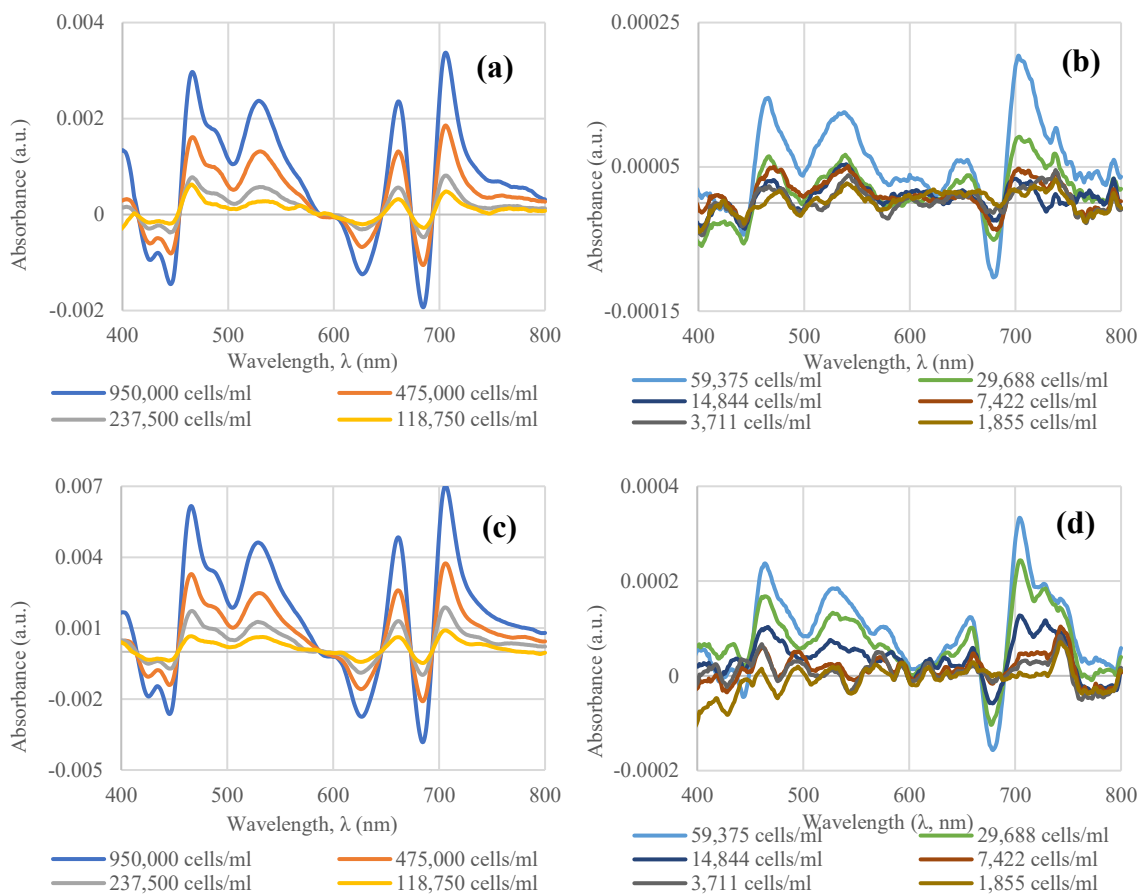


Figure 6.2: Savitzky-Golay first derivative of absorbance spectra at higher and lower concentration ranges of *M. aeruginosa* for 50 mm (a, b), and 100 mm (c, d) cuvette pathlengths, respectively.

A summary of experimental results obtained from river water testing using different pathlengths is shown for *Microcystis aeruginosa* and *Chlorella vulgaris* in Table 6.3.

Table 6.3: Critical data for *Microcystis aeruginosa* and *Chlorella vulgaris* in river water for higher (118,750 – 950,000 cells/mL) and lower (1,855 – 59,375 cells/mL) concentration ranges.

Test	Pathlength (mm)	Concentration Range (cells/mL)	Slope	R ²	MDL (cells/mL)
<i>M. aeruginosa</i> (Phycocyanin peak)					
Absorbance 632 nm	50	1,855 – 59,375	$3.7430 \times 10^{-07} \pm$ 2.7904×10^{-08}	0.9782	62,660
		118,750 – 950,000	$3.4729 \times 10^{-07} \pm$ 2.1838×10^{-08}	0.9921	
	100	1,855 – 59,375	$6.4778 \times 10^{-07} \pm$ 1.0084×10^{-08}	0.9116	36,705
		118,750 – 950,005	$7.3408 \times 10^{-07} \pm$ 4.2665×10^{-08}	0.9932	
S-G first derivative of absorbance 660 nm	50	1,855 – 59,375	$4.0325 \times 10^{-10} \pm$ 9.0640×10^{-11}	0.9590	22,457
		118,750 – 950,000	$4.9574 \times 10^{-10} \pm$ 2.7866×10^{-11}	0.9937	
	100	1,855 – 59,375	$1.3138 \times 10^{-09} \pm$ 1.5133×10^{-10}	0.9445	12,798
		118,750 – 950,005	$1.0965 \times 10^{-09} \pm$ 6.3494×10^{-11}	0.9933	

<i>M. aeruginosa</i> (Chlorophyll peak)					
Absorbance 682 nm	50	1,855 – 59,375	$3.8336 \times 10^{-07} \pm$ 3.0833×10^{-08}	0.9747	44,248
		118,750 – 950,000	$3.5300 \times 10^{-07} \pm$ 2.0612×10^{-09}	0.9932	
	100	1,855 – 59,375	$6.6302 \times 10^{-07} \pm$ 1.0201×10^{-08}	0.9134	26,788
		118,750 – 950,005	$7.4297 \times 10^{-07} \pm$ 4.2146×10^{-08}	0.9936	
S-G first derivative of absorbance 706 nm	50	1,855 – 59,375	$2.2093 \times 10^{-09} \pm$ 1.4560×10^{-10}	0.9829	18,324
		118,750 – 950,000	$2.1409 \times 10^{-09} \pm$ 9.6281×10^{-11}	0.9959	
	100	1,855 – 59,375	$4.2421 \times 10^{-09} \pm$ 4.5723×10^{-10}	0.9555	8,546
		118,750 – 950,005	$4.4338 \times 10^{-09} \pm$ 1.5224×10^{-10}	0.9976	
<i>C. vulgaris</i> (Chlorophyll peak)					
Absorbance 684 nm	50	1,855 – 59,375	$4.0230 \times 10^{-07} \pm$ 2.2721×10^{-08}	0.9874	65,489
		118,750 – 950,000	$3.4216 \times 10^{-07} \pm$ 2.8811×10^{-08}	0.9860	

	100	1,855 – 59,375	$9.0934 \times 10^{-07} \pm$ 3.0517×10^{-08}	0.9955	40,369
		118,750 – 950,005	$7.1222 \times 10^{-07} \pm$ 4.7140×10^{-08}	0.9913	
S-G first derivative of absorbance	50	1,855 – 59,375	$2.0380 \times 10^{-09} \pm$ 1.0649×10^{-10}	0.9891	24,509
		118,750 – 950,000	$1.9404 \times 10^{-09} \pm$ 1.5834×10^{-10}	0.9868	
708 nm	100	1,855 – 59,375	$5.0128 \times 10^{-09} \pm$ 8.0320×10^{-11}	0.9989	13,695
		118,750 – 950,005	$4.0864 \times 10^{-09} \pm$ 2.1265×10^{-10}	0.9946	

6.3.3 Comparison of *M. aeruginosa* and *C. vulgaris* cultures spectra in river water and D.I. water

The final phase of this study involved comparing the zero-order and derivative spectra of *M. aeruginosa* and *C. vulgaris*, to determine the potential differences based on their absorbance characteristics and impact on detection. *M. aeruginosa* and *C. vulgaris* share similar structural morphologies where cells can be present in spherical and ovoidal shapes but have varying cell sizes which range from 3 – 5 μm in diameter and 3 – 10 μm in diameter for *M. aeruginosa* and *C. vulgaris*, respectively (Álvarez et al., 2020; Bañares-España et al., 2016; Safi, 2014). One key difference is that *M. aeruginosa* contains natural

gas vacuoles allowing them to freely alter their location in source waters based on their nutrient/ light requirements (Reynolds, 2007; Wilson et al., 2006). Additionally, *M. aeruginosa* are known to form mucilaginous colonies in natural environments ranging from 10 – 1000 µm in diameter, usually in response to harsh growth conditions but can also be found in nature as unicellular organisms (Gan et al., 2012; Yang et al., 2008). On the other hand, *C. vulgaris* are generally present in unicellular populations; nevertheless, there have been some studies showing potential colony formation behavior of *C. vulgaris* for survival in the presence of competing algae (Dong et al., 2018; Fisher et al., 2016). It should be noted that these varying environmental factors can potentially impact the absorbance spectra.

Similar concentrations of *M. aeruginosa* and *C. vulgaris* were tested for comparative purposes and the resultant spectra in river water and D.I. water using 100 mm pathlength are illustrated in Figure 6.3. *C. vulgaris* absorbance spectra resulted in two peaks at 446-, and 684-nm (Figure 6.3 b), of which 684 nm is the most prominent. *C. vulgaris* are known to carry two photopigments, *Chl-a* and chlorophyll-b (*Chl-b*) (Safi, 2014). It is known that *Chl-a* peaks close to 440- and 680-nm (refer 6.3.1), while *Chl-b* peaks close to 650-, and 450-nm (Dos Santos et al., 2003; Miazek et al., 2015; Saini et al., 2018). However, *Chl-b* peaks weakly at 450 nm when compared to peak close to 680 nm due to its naturally weak absorbance at that wavelength (Gray, 2010; Millie et al., 2002). The primary difference between absorbance spectra of *M. aeruginosa* and *C. vulgaris* is that *M. aeruginosa* contains an additional peak at 632 nm, which is due to the presence of the pigment PC and differentiates cyanobacterial algae from non-cyanobacterial algae (Cotterill et al., 2019). Comparing the zero-order absorbance results of *M. aeruginosa* and *C. vulgaris* in

D.I. water (Figure 6.3 c,d) to river water (Figure 6.3 a,b), no significant visual differences could be observed and the peaks for both algal cultures remained at the same wavelengths. However, at lower concentrations, small and frequent fluctuations in absorbance were observed for river water tests (Figure 6.1 b,d). This can be potentially attributed to the presence of organic and inorganic contaminants present in source river water, leading to interferences being observed in the absorbance spectra. A slightly lower detection limit was found in D.I. water results for both *M. aeruginosa* and *C. vulgaris* than in river water. The MDL for *M. aeruginosa* at *Chl-a* peak (682 nm), using 100 mm pathlength in river water and D.I. water was calculated to be 26,788 cells/mL (Table 6.3) and 22,038 cells/mL, respectively. The lowest MDL for *C. vulgaris* using 100 mm at *Chl-a* peak (684 nm) was calculated to be 40,369 cells/mL in river water (Table 6.3) and 37,413 cells/mL in D.I. water.

Further, the Savitzky-Golay first-order derivative of absorbance spectra of *M. aeruginosa* and *C. vulgaris* were compared in river water to investigate the differences in peaks between cyanobacterial and non-cyanobacterial algae (Figure 6.3 e,f). As previously discussed, *M. aeruginosa* resulted in two peaks of interest at 706 nm and 660 nm which corresponds to the photopigments *Chl-a* (682 nm) and PC (632 nm), respectively in the zero-order absorbance spectra (refer 6.3.2). Meanwhile, for *C. vulgaris*, the primary peak of interest was observed at 708 nm, which corresponds to *Chl-a* (684 nm) peak observed in the zero-order absorbance spectra (Figure 6.3 b,f). Between the two algal cultures, *M. aeruginosa* derivative spectra had an additional peak at 660 nm which can be potentially used to identify cyanobacteria from non-cyanobacterial algae. The MDL for S-G first-order derivative of absorbance using 100 mm pathlength was calculated to be 8,546 cells/mL and

13,695 cells/mL for *M. aeruginosa* and *C. vulgaris* at 706- and 708-nm, respectively, in river water.

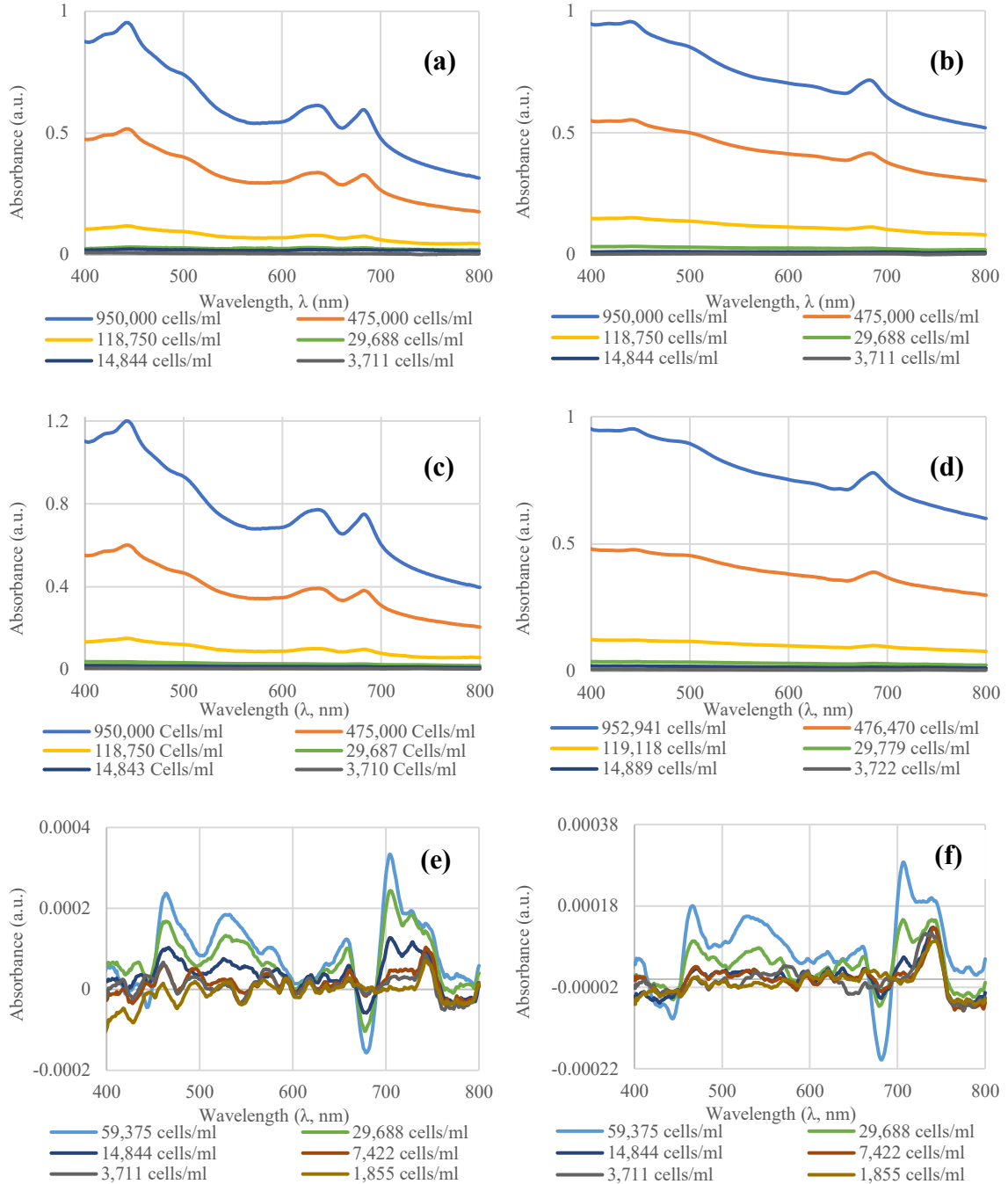


Figure 6.3: Absorbance spectra of *M. aeruginosa* and *C. vulgaris* in river water (a, b), in D.I. water (c, d), and Savitzky-Golay first derivative of absorbance spectra in river water (e, f) using 100 mm cuvette pathlengths, respectively.

6.4 Discussion

The results indicate that using spectrophotometry would be extremely beneficial for sensitive monitoring of microalgae with a focus on potentially toxic cyanobacteria in source river water. Coupled together with derivative spectrophotometry, this method could be beneficial for potential bloom management, providing data that can be used for an early warning system. The detection limit calculated for the zero-order absorbance spectra and the S-G first derivative of absorbance showed higher sensitivity (approximately 3-fold improvement) with increasing cuvette pathlength from 50 mm to 100 mm for both *M. aeruginosa* and *C. vulgaris*. For example, the MDL for *M. aeruginosa* from zero-order absorbance to S-G derivative of absorbance using 100 mm pathlength for *Chl-a* reduced from 26,788 cells/mL to 8,546 cells/mL (ref. Table 6.3). The MDLs for both microalgae using the longest pathlength resulted in a concentration below 20,000 cells/mL, which is well within the WHO recommendation for low probability of negative health effects in recreational waters from cyanobacterial algae (WHO, 2003a, 2017b). Lake and low-flowing rivers with high nutrient loading have a high chance of algal proliferation. Typically, surface water characteristics vary from as low as 2 mg/L to 30 mg/L in unpolluted water (used for drinking water purposes) for COD; turbidity is usually reported to be < 20 NTU but high turbidity (> 40 NTU) is reported during weather events (for rivers); and pH varies between 6.8 – 8.6 (Boyer, 2008; Jain & Singh, 2003; Mohamed et al., 2015; Puig et al., 2016; Zamyadi et al., 2012a). The properties analyzed for Rideau River water falls within the typical characteristics observed for source waters, making this method viable for monitoring purposes.

The technique applied in this paper provides data on cyanobacterial and green algae concentrations in terms of the photopigments *chlorophyll-a* and phycocyanin. The PC peak observed in the cyanobacterial sample is what allows us to distinguish between cyanobacterial and non-cyanobacterial algae (Cotterill et al., 2019; Simis & Kauko, 2012). Results suggest that by monitoring multiple peaks for data, better insight into the algal population can be obtained. Universally, to measure unknown concentrations of microalgae in sample water, calibration curves are made using existing concentration data and sample absorbance (Burgess & Thomas, 2017; Dos Santos et al., 2003; Millie et al., 2002). Comparing and analyzing slopes at similar concentrations in D.I. water and river water is critical to understanding the applicability of the method for realistic monitoring purposes. For consistency purposes, the following part focuses on slopes of regression lines related to the PC peak for *M. aeruginosa* over the concentration range from 1,855 – 950,000 cells/mL. The slopes at 632 nm for zero-order absorbance using 100 mm pathlength were calculated to be $7.9489 \times 10^{-07} \pm 1.6140 \times 10^{-08}$ and $7.4757 \times 10^{-07} \pm 1.6194 \times 10^{-08}$ for river water and D.I. water, respectively. Similarly, for S-G derivative, slopes at 660 nm using 100 mm pathlength were found to be $1.1750 \times 10^{-09} \pm 6.2721 \times 10^{-11}$ and $1.1221 \times 10^{-09} \pm 2.7632 \times 10^{-11}$ for river water and D.I. water, respectively. The slopes for 100 mm pathlength for the PC peak were similar between different experiments demonstrating applicability for monitoring use. However, slopes at the same wavelengths were estimated using 50 mm pathlengths for similar concentrations, and a slight change in slope was observed. For example, at 632 nm, the slopes were calculated to be $4.8 \times 10^{-07} \pm 8.0200 \times 10^{-09}$ and $3.7411 \times 10^{-07} \pm 2.0307 \times 10^{-09}$ for river water and D.I. water, respectively using zero-order absorbance data. This could be explained due to the presence of unknown water

constituents potentially causing interferences and impacting the absorbance scan, which has been demonstrated in several studies before (AlMomani & Örmeci, 2018; Burgess & Thomas, 2017; Mukhopadhyay & Mason, 2013; Sobiechowska-Sasim et al., 2014). Slopes calculated using *Chl-a* peaks for *M. aeruginosa* and *C. vulgaris* exhibited similar characteristics between the two pathlengths as well. Nonetheless, a strong linear relationship between absorbance data and concentration was observed ($R^2 > 0.99$) over the concentration range from 1,855 – 950,000 cells/mL.

Although a number of sensitive techniques (based on chromatography, immunoassay, or PCR, for example) are currently used for monitoring of microalgae and cyanotoxin detection, most require high skill to operate, pigment/toxin extraction prior to analysis, and are time-consuming in nature (Al-Ammar et al., 2013; Al-Tebrineh et al., 2011; Azevedo et al., 2011; Campàs & Marty, 2007; Liu et al., 2020). The main advantage of the spectrophotometric method is the capability to simultaneously monitor multiple photopigments for algal detection while monitoring different important water quality parameters such as biological oxygen demand (BOD), ultraviolet transmittance (UVT), total suspended solids (TSS), and but not limited to, nitrogen compounds (Burgess & Thomas, 2017; Mukhopadhyay & Mason, 2013; Schneider et al., 1991; Tran Khac et al., 2018). Further, spectrophotometry is simple, rapid, can be applied for on-line monitoring, does not require pigment extraction for quantification, and has a broad working range (up to 3,800,000 cells/mL) (Agberien & Örmeci, 2019; AlMomani & Örmeci, 2018). In addition to these abilities, the potential of the spectrophotometric method to distinguish cyanobacteria from non-cyanobacterial algae in a realistic environment can prove to be a valuable tool to municipal water managers around the world (Altenburger et al., 2015;

Bowling et al., 2017). However, for real-time applications, fluorometry is more sensitive and specific than spectrophotometry for algal monitoring and does not rely on cuvette for sample analysis (Zamyadi et al., 2016). The high specificity of fluorometry is based on measuring both excitation and emission spectra from a photopigment to quantify based on its distinct fluorescence signature (Bowling et al., 2016; Liu et al., 2020). Fluorometers have been reported to be able to estimate cell concentration below 2,000 cells/mL, but sufficient studies verifying the detection limits have not been published (Bowling et al., 2016; Garrido et al., 2019; Kim et al., 2017; Zamyadi et al., 2012b). Nonetheless, fluorometry has a significantly lower working range in comparison to spectrophotometry (< 200,000 cells/mL) and is incapable of multi-water parameters measurement, limiting the applicability of the single instrument (Bowling et al., 2016, 2016). Both spectrophotometry and fluorometry are analytical processes that are susceptible to some similar sources of inferences. For example, when measuring *Chl-a*, these methods can over/under-estimate cell concentration with varying algal cell properties (such as size, agglomeration, and pigment content), presence of non-algal phytoplankton containing *Chl-a*, other phycobilin proteins or degradation products, and water properties (such as turbidity, color, temperature, and organic matter) (Burgess & Thomas, 2017; Catherine et al., 2012; Kim et al., 2017; Lichtenthaler & Buschmann, 2001; Schneider et al., 1991).

6.5 Conclusion

Considering that eutrophication is a growing issue around the world, algal blooms, including potentially toxic cyanobacterial blooms, are here to stay. As it is well known that blooms pose a hazard to human and aquatic life, this increases the need for better monitoring technology. The method used in this study for monitoring of microalgae

performed adequately when using higher pathlengths with derivative spectrophotometry for early detection of cyanobacterial and non-cyanobacterial algae in river water. The lowest method detection limit for *M. aeruginosa* for the photopigment PC was calculated to be 12,798 cells/mL; whilst the photopigment Chl-a resulted in a detection limit of 8,546 cells/mL and 13,695 cells/mL for *M. aeruginosa* and *C. vulgaris*, respectively, using Savitzky-Golay first derivative of absorbance and 100 mm cuvette pathlength. The MDLs calculated were below the WHO recommendation of 20,000 cells/mL cyanobacterial concentration in source water for low probability of adverse health effects. In addition, spectral comparison of *M. aeruginosa* and *C. vulgaris* showed that cyanobacteria could be differentiated from common green microalgae in river water, based on the presence of different photopigments present in sample water.

Further, spectrophotometry can be used to measure multiple water parameters (such as TSS, BOD, N-compounds) while monitoring microalgae which is a great asset from a source monitoring perspective. Having a single piece of equipment for monitoring saves cost as well as space requirements. However, spectrophotometry is prone to fluctuations in the presence of water constituents (such as turbidity, dissolved organic carbon, phytoplankton containing the same photopigment as algae, to name a few), warranting further research to check the potential impact of individual water quality parameters, on spectral interferences that might impact algal detection. Nonetheless, the use of spectrophotometry has considerable potential for early detection and monitoring of microalgae in realistic conditions (i.e., river water monitoring), which can greatly aid water professionals and decision-makers in making early management decisions.

Acknowledgment

This research was funded by the Natural Sciences Engineering Research Council of Canada (NSERC) and CREATE grant (TEDGIEER) program. The authors would also like to thank Real Tech Inc. (Whitby, Ontario).

Conflicts of interest: The authors declare no conflict of interest.

6.6 References

- Agberien, A. V., & Örmeci, B. (2019). Monitoring of Cyanobacteria in Water Using Spectrophotometry and First Derivative of Absorbance. *Water*, *12*(1), 124. <https://doi.org/10.3390/w12010124>
- Al-Ammar, R., Nabok, A., Hashim, A., & Smith, T. (2013). Optical detection of microcystin produced by cyanobacteria. *Journal of Physics: Conference Series*, *450*, 012006. <https://doi.org/10.1088/1742-6596/450/1/012006>
- AlMomani, F. A., & Örmeci, B. (2016). Performance Of *Chlorella Vulgaris*, *Neochloris Oleoabundans*, and mixed indigenous microalgae for treatment of primary effluent, secondary effluent and centrate. *Ecological Engineering*, *95*, 280–289. <https://doi.org/10.1016/j.ecoleng.2016.06.038>
- AlMomani, F. A., & Örmeci, B. (2018). Monitoring and measurement of microalgae using the first derivative of absorbance and comparison with chlorophyll extraction method. *Environmental Monitoring and Assessment*, *190*(2), 90. <https://doi.org/10.1007/s10661-018-6468-y>
- Al-Sammak, M., Hoagland, K. D., Snow, D. D., & Cassada, D. (2013). Methods for simultaneous detection of the cyanotoxins BMAA, DABA, and anatoxin-a in environmental samples. *Toxicon*, *76*, 316–325. <https://doi.org/10.1016/j.toxicon.2013.10.015>
- Al-Tebrineh, J., Gehringer, M. M., Akcaalan, R., & Neilan, B. A. (2011). A new quantitative PCR assay for the detection of hepatotoxigenic cyanobacteria. *Toxicon*, *57*(4), 546–554. <https://doi.org/10.1016/j.toxicon.2010.12.018>
- Altenburger, R., Ait-Aissa, S., Antczak, P., Backhaus, T., Barceló, D., Seiler, T.-B., Brion, F., Busch, W., Chipman, K., de Alda, M. L., de Aragão Umbuzeiro, G., Escher, B. I., Falciani, F., Faust, M., Focks, A., Hilscherova, K., Hollender, J., Hollert, H., Jäger, F., ... Brack, W. (2015). Future water quality monitoring—Adapting tools to deal with mixtures of pollutants in water resource management. *Science of The Total Environment*, *512–513*, 540–551. <https://doi.org/10.1016/j.scitotenv.2014.12.057>

Álvarez, S. D., Kruk, C., Martínez de la Escalera, G., Montes, M. A., Segura, A. M., & Piccini, C. (2020). Morphology captures toxicity in *Microcystis aeruginosa* complex: Evidence from a wide environmental gradient☆. *Harmful Algae*, 97, 101854. <https://doi.org/10.1016/j.hal.2020.101854>

American Water Works Association (Ed.). (2011). *Algae: Source to Treatment* (1st ed.). American Water Works Association. (ISBN 1-58321-787-8)

Azevedo, J., Osswald, J., Guilhermino, L., & Vasconcelos, V. (2011). Development and Validation of an SPE-HPLC-FL Method for the Determination of Anatoxin-a in Water and Trout (*Oncorhincus mykiss*). *Analytical Letters*, 44(8), 1431–1441. <https://doi.org/10.1080/00032719.2010.512682>

Bajpai, R., Sharma, N. K., & Rai, A. K. (2011). Cyanotoxins: An Emerging Environmental Concern. *Advances in Life Science*, 187–211.

Balest, L., Murgolo, S., Sciancalepore, L., Montemurro, P., Abis, P. P., Pastore, C., & Mascolo, G. (2016). Ultra-trace levels analysis of microcystins and nodularin in surface water by on-line solid-phase extraction with high-performance liquid chromatography tandem mass spectrometry. *Analytical and Bioanalytical Chemistry*, 408(15), 4063–4071. <https://doi.org/10.1007/s00216-016-9495-y>

Bañares-España, E., del Mar Fernández-Arjona, M., García-Sánchez, M. J., Hernández-López, M., Reul, A., Mariné, M. H., & Flores-Moya, A. (2016). Sulphide Resistance in the Cyanobacterium *Microcystis aeruginosa*: A Comparative Study of Morphology and Photosynthetic Performance Between the Sulphide-Resistant Mutant and the Wild-Type Strain. *Microbial Ecology*, 71(4), 860–872. <https://doi.org/10.1007/s00248-015-0715-3>

Bartram, J., & Rees, G. (Eds.). (2000). *Monitoring Bathing Waters: A Practical Guide to the Design and Implementation of Assessments and Monitoring Programmes* (0 ed.). CRC Press - WHO. (ISBN 978-0-429-20430-2) <https://doi.org/10.4324/9780203478264>

Berry, J. P., Lee, E., Walton, K., Wilson, A. E., & Bernal-Brooks, F. (2011). Bioaccumulation of microcystins by fish associated with a persistent cyanobacterial bloom

- in Lago de Patzcuaro (Michoacan, Mexico). *Environmental Toxicology and Chemistry*, 30(7), 1621–1628. <https://doi.org/10.1002/etc.548>
- Berthouex, P. M., & Brown, L. C. (2002). *Statistics for Environmental Engineers*. 463.
- Bertone, E., Burford, M. A., & Hamilton, D. P. (2018). Fluorescence probes for real-time remote cyanobacteria monitoring: A review of challenges and opportunities. *Water Research*, 141, 152–162. <https://doi.org/10.1016/j.watres.2018.05.001>
- Bowling, L. C., Shaikh, M., Brayon, J., & Malthus, T. (2017). An evaluation of a handheld spectroradiometer for the near real-time measurement of cyanobacteria for bloom management purposes. *Environmental Monitoring and Assessment*, 189(10), 495. <https://doi.org/10.1007/s10661-017-6205-y>
- Bowling, L. C., Zamyadi, A., & Henderson, R. K. (2016). Assessment of in situ fluorometry to measure cyanobacterial presence in water bodies with diverse cyanobacterial populations. *Water Research*, 105, 22–33. <https://doi.org/10.1016/j.watres.2016.08.051>
- Boyer, G. L. (2008). *Chapter 7: Cyanobacterial Toxins in New York and the Lower Great Lakes Ecosystems*.
- Bukaveckas, P. A. (2018). Cyanobacteria and cyanotoxins at the river-estuarine transition. *Harmful Algae*, 11.
- Burgess, C., & Thomas, O. (2017). UV-Visible Spectrophotometry of Water and Wastewater. In *UV-Visible Spectrophotometry of Water and Wastewater* (pp. 1–524). Elsevier. (ISBN 978-0-444-63897-7) <https://doi.org/10.1016/B978-0-444-63897-7.00001-9>
- Campàs, M., & Marty, J.-L. (2007). Highly sensitive amperometric immunosensors for microcystin detection in algae. *Biosensors and Bioelectronics*, 22(6), 1034–1040. <https://doi.org/10.1016/j.bios.2006.04.025>

Canadian Phycological Culture Centre. (2013, September 16). *Canadian Phycological Culture Centre*. Canadian Phycological Culture Centre. <https://uwaterloo.ca/canadian-phycological-culture-centre/home>

Catherine, A., Escoffier, N., Belhocine, A., Nasri, A. B., Hamlaoui, S., Yéprémian, C., Bernard, C., & Troussellier, M. (2012). On the use of the FluoroProbe®, a phytoplankton quantification method based on fluorescence excitation spectra for large-scale surveys of lakes and reservoirs. *Water Research*, *46*(6), 1771–1784. <https://doi.org/10.1016/j.watres.2011.12.056>

Chen, K., Zhang, H., Wei, H., & Li, Y. (2014). Improved Savitzky–Golay-method-based fluorescence subtraction algorithm for rapid recovery of Raman spectra. *Applied Optics*, *53*(24), 5559. <https://doi.org/10.1364/AO.53.005559>

Chorus, I. (2005). Current approaches to cyanotoxin risk assessment, risk management and regulations in different countries. *Federal Environmental Agency*, *1*, 122.

Chorus, I. (2012). Current approaches to Cyanotoxin risk assessment, risk management and regulations in different countries. *Federal Environment Agency*, *2*, 151.

Chorus, I., & Bartram, J. (Eds.). (1999). *Toxic cyanobacteria in water: A guide to their public health consequences, monitoring, and management*. E & FN Spon. (ISBN 978-0-419-23930-7)

Cotterill, V., Hamilton, D. P., Puddick, J., Suren, A., & Wood, S. A. (2019). Phycocyanin sensors as an early warning system for cyanobacteria blooms concentrations: A case study in the Rotorua lakes. *New Zealand Journal of Marine and Freshwater Research*, *53*(4), 555–570. <https://doi.org/10.1080/00288330.2019.1617322>

Craig, I. W., & Carr, N. G. (1968). C-phycocyanin and allophycocyanin in two species of blue-green algae. *Biochemical Journal*, *106*(2), 361–366. <https://doi.org/10.1042/bj1060361>

Dodds, W. K., Bouska, W. W., Eitzmann, J. L., Pilger, T. J., Pitts, K. L., Riley, A. J., Schloesser, J. T., & Thornbrugh, D. J. (2009). Eutrophication of U.S. Freshwaters:

- Analysis of Potential Economic Damages. *Environmental Science & Technology*, 43(1), 12–19. <https://doi.org/10.1021/es801217q>
- Dong, J., Gao, Y., Chang, M., Ma, H., Han, K., Tao, X., & Li, Y. (2018). Colony formation by the green alga *Chlorella vulgaris* in response to the competitor *Ceratophyllum demersum*. *Hydrobiologia*, 805(1), 177–187. <https://doi.org/10.1007/s10750-017-3294-0>
- Dos Santos, A., Calijuri, M., Moraes, E. M., Adorno, M. A., Falco, P., Carvalho, D. P., Debert, G. L. B., & Benassi, S. F. (2003). Comparison of three methods for Chlorophyll determination: Spectrophotometry and Fluorimetry in samples containing pigment mixtures and spectrophotometry in samples with separate pigments through High Performance Liquid Chromatography. *Acta Limnologica Brasiliensia*, 15, 12.
- EPA, U. (2005). *Technologies and Techniques for Early Warning Systems to Monitor and Evaluate Drinking Water Quality* (p. 236). USEPA.
- EPA, U. (2015). *Drinking Water Health Advisory for the Cyanobacterial Microcystin Toxins*. 75.
- Falconer, I. R. (1999). An Overview of problems caused by toxic blue–green algae (cyanobacteria) in drinking and recreational water. *Environmental Toxicology*, 14(1), 5–12. [https://doi.org/10.1002/\(SICI\)1522-7278\(199902\)14:1<5::AID-TOX3>3.0.CO;2-0](https://doi.org/10.1002/(SICI)1522-7278(199902)14:1<5::AID-TOX3>3.0.CO;2-0)
- Figueiredo, D. R., Azeiteiro, U. M., Esteves, S. M., Gonçalves, F. J. M., & Pereira, M. J. (2004). Microcystin-producing blooms—A serious global public health issue. *Ecotoxicology and Environmental Safety*, 59(2), 151–163. <https://doi.org/10.1016/j.ecoenv.2004.04.006>
- Fisher, R. M., Bell, T., & West, S. A. (2016). Multicellular group formation in response to predators in the alga *Chlorella vulgaris*. *Journal of Evolutionary Biology*, 29(3), 551–559. <https://doi.org/10.1111/jeb.12804>
- Furevik, B. R., Durand, D., & Pettersson, L. (2004). Multi-Sensor Synergy for Monitoring of Algal Blooms in the North Sea. *Proceedings of the 2004 Envisat & ERS Symposium (ESA SP-572)*, 7.

- Gan, N., Xiao, Y., Zhu, L., Wu, Z., Liu, J., Hu, C., & Song, L. (2012). The role of microcystins in maintaining colonies of bloom-forming *Microcystis* spp.: *Microcystis* colony maintenance by microcystins. *Environmental Microbiology*, *14*(3), 730–742. <https://doi.org/10.1111/j.1462-2920.2011.02624.x>
- Garrido, M., Cecchi, P., Malet, N., Bec, B., Torre, F., & Pasqualini, V. (2019). Evaluation of FluoroProbe® performance for the phytoplankton-based assessment of the ecological status of Mediterranean coastal lagoons. *Environmental Monitoring and Assessment*, *191*(4), 204. <https://doi.org/10.1007/s10661-019-7349-8>
- Giddings, M., Aranda-Rodriguez, R., Yasvinski, G., Watson, S. B., & Zura, R. (2012). *Cyanobacterial Toxins: Drinking and Recreational Water Quality Guidelines*. 12.
- Greenfield, D. I., Marin, R., Doucette, G. J., Mikulski, C., Jones, K., Jensen, S., Roman, B., Alvarado, N., Feldman, J., & Scholin, C. (2008). Field applications of the second-generation Environmental Sample Processor (ESP) for remote detection of harmful algae: 2006-2007: Field applications of the ESP: 2006-2007. *Limnology and Oceanography: Methods*, *6*(12), 667–679. <https://doi.org/10.4319/lom.2008.6.667>
- Health Canada. (2016). Cyanobacterial Toxins in Drinking Water—Document for Public Consultation. *Federal-Provincial-Territorial Committee on Drinking Water*, 1–171. (ISBN 0273-1223)
- Health Canada. (2020). *Guidelines for Canadian Drinking Water Quality Summary Table*. Federal-Provincial-Territorial Committee on Drinking Water of the Federal-Provincial-Territorial Committee on Health and the Environment. https://www.canada.ca/content/dam/hc-sc/migration/hc-sc/ewh-semt/alt_formats/pdf/pubs/water-eau/sum_guide-res_recom/summary-table-EN-2020-02-11.pdf
- Hubaux, Andre., & Vos, Gilbert. (1970). Decision and detection limits for calibration curves. *Analytical Chemistry*, *42*(8), 849–855. <https://doi.org/10.1021/ac60290a013>
- Hudnell, H. K. (Ed.). (2008). *Cyanobacterial Harmful Algal Blooms: State of the Science and Research Needs*. Springer. (ISBN 978-0-387-75864-0)

- Ibelings, B. W., Backer, L. C., Kardinaal, W. E. A., & Chorus, I. (2014). Current approaches to cyanotoxin risk assessment and risk management around the globe. *Harmful Algae*, 40, 63–74. <https://doi.org/10.1016/j.hal.2014.10.002>
- Jain, S. K., & Singh, V. P. (2003). Chapter 13—Water Quality Modeling. In S. K. Jain & V. P. Singh (Eds.), *Developments in Water Science* (Vol. 51, pp. 743–786). Elsevier. [https://doi.org/10.1016/S0167-5648\(03\)80067-9](https://doi.org/10.1016/S0167-5648(03)80067-9)
- Kim, S.-H., He, Y., Lee, E.-H., Kim, J.-H., & Park, S. M. (2017). Portable Fluorometer for Cyanobacteria Detection. *IEEE Sensors Journal*, 17(8), 2377–2384. <https://doi.org/10.1109/JSEN.2017.2672993>
- Klamath Blue Green Algae Working Group. (2009). *Standard Operating Procedures: Environmental Sampling of Cyanobacteria for Cell Enumeration, Identification and Toxin Analysis*. California Water Board. https://www.waterboards.ca.gov/northcoast/water_issues/programs/tmdls/klamath_river/klamath_river_khsa_monitoring/pdf/090629/app_a/Cyanobacteria_Sampling_SOP.pdf
- Kus, S., Marczenko, Z., & Obarski, N. (1996). Derivative UV-VIS Spectrophotometry in Analytical Chemistry. *Chern. Anal. (Warsaw)*, Department of Analytical Chemistry, Technical University of Warsaw, 00-664 Warszawa, Poland, 31.
- Lichtenthaler, H. K., & Buschmann, C. (2001). Chlorophylls and Carotenoids: Measurement and Characterization by UV-VIS Spectroscopy. *Current Protocols in Food Analytical Chemistry*, 1(1), F4.3.1-F4.3.8. <https://doi.org/10.1002/0471142913.faf0403s01>
- Liu, J.-Y., Zeng, L.-H., & Ren, Z.-H. (2020). Recent application of spectroscopy for the detection of microalgae life information: A review. *Applied Spectroscopy Reviews*, 55(1), 26–59. <https://doi.org/10.1080/05704928.2018.1509345>
- McCullough, G. (2007). *Assessment of bbe Fluoroprobe for algal taxonomic discrimination in Lake Winnipeg* (p. 27) [Report to the Canadian Department of Fisheries and Oceans]. Centre for Earth Observations Science Department of Environment and Geography University of Manitoba.

- McQuaid, N., Zamyadi, A., Prévost, M., Bird, D. F., & Dorner, S. (2011). Use of in vivo phycoerythrin fluorescence to monitor potential microcystin-producing cyanobacterial biovolume in a drinking water source. *J. Environ. Monit.*, *13*(2), 455–463. <https://doi.org/10.1039/C0EM00163E>
- Miazek, K., Iwanek, W., Remacle, C., Richel, A., & Goffin, D. (2015). Effect of Metals, Metalloids and Metallic Nanoparticles on Microalgae Growth and Industrial Product Biosynthesis: A Review. *International Journal of Molecular Sciences*, *16*(10), 23929–23969. <https://doi.org/10.3390/ijms161023929>
- Millie, D. F., Schofield, O. M., ??E., Kirkpatrick, G. J., Johnsen, G., & Evens, T. J. (2002). Using absorbance and fluorescence spectra to discriminate microalgae. *European Journal of Phycology*, *37*(3), 313–322. <https://doi.org/10.1017/S0967026202003700>
- Mohamed, Z. A., Deyab, M. A., Abou-Dobara, M. I., El-Sayed, A. K., & El-Raghi, W. M. (2015). Occurrence of cyanobacteria and microcystin toxins in raw and treated waters of the Nile River, Egypt: Implication for water treatment and human health. *Environmental Science and Pollution Research*, *22*(15), 11716–11727. <https://doi.org/10.1007/s11356-015-4420-z>
- Moreira, C., Martins, A., Azevedo, J., Freitas, M., Regueiras, A., Vale, M., Antunes, A., & Vasconcelos, V. (2011). Application of real-time PCR in the assessment of the toxic cyanobacterium *Cylindrospermopsis raciborskii* abundance and toxicological potential. *Applied Microbiology and Biotechnology*, *92*(1), 189–197. <https://doi.org/10.1007/s00253-011-3360-x>
- Moreira, C., Ramos, V., Azevedo, J., & Vasconcelos, V. (2014). Methods to detect cyanobacteria and their toxins in the environment. *Applied Microbiology and Biotechnology*, *98*(19), 8073–8082. <https://doi.org/10.1007/s00253-014-5951-9>
- Mukhopadhyay, S. C., & Mason, A. (Eds.). (2013). *Smart Sensors for Real-Time Water Quality Monitoring* (Vol. 4). Springer Berlin Heidelberg. (ISBN 978-3-642-37005-2) <https://doi.org/10.1007/978-3-642-37006-9>

- Oren, A. (2014). *Cyanobacteria: An Economic Perspective* (N. K. Sharma, A. K. Rai, & L. J. Stal, Eds.). John Wiley & Sons, Ltd. (ISBN 978-1-118-40223-8) <https://doi.org/10.1002/9781118402238.ch1>
- Owen, A. J. (1995). *Uses of Derivative Spectroscopy*. Agilent Technologies. https://www.who.edu/cms/files/derivative_spectroscopy_59633940_175744.pdf
- Pelaez, M., Antoniou, M. G., He, X., Dionysiou, D. D., de la Cruz, A. A., Tsimeli, K., Triantis, T., Hiskia, A., Kaloudis, T., Williams, C., Aubel, M., Chapman, A., Foss, A., Khan, U., O'Shea, K. E., & Westrick, J. (2010). Sources and Occurrence of Cyanotoxins Worldwide. In D. Fatta-Kassinos, K. Bester, & K. Kümmerer (Eds.), *Xenobiotics in the Urban Water Cycle* (Vol. 16, pp. 101–127). Springer Netherlands. (ISBN 978-90-481-3508-0) https://doi.org/10.1007/978-90-481-3509-7_6
- Puig, A., Olguín Salinas, H. F., & Borús, J. A. (2016). Relevance of the Paraná River hydrology on the fluvial water quality of the Delta Biosphere Reserve. *Environmental Science and Pollution Research*, 23(12), 11430–11447. <https://doi.org/10.1007/s11356-015-5744-4>
- Quansah, J. E., Engel, B., & Rochon, G. L. (2010). *Early Warning Systems: A Review*. 2(2), 22.
- Raps, S., Kycia, J. H., Ledbetter, M. C., & Siegelman, H. W. (1985). Light Intensity Adaptation and Phycobilisome Composition of *Microcystis aeruginosa*. *Plant Physiology*, 79(4), 983–987. <https://doi.org/10.1104/pp.79.4.983>
- Reynolds, C. S. (2007). Variability in the provision and function of mucilage in phytoplankton: Facultative responses to the environment. *Hydrobiologia*, 578(1), 37–45. <https://doi.org/10.1007/s10750-006-0431-6>
- Rice, E. W., Baird, R. B., & Eaton, A. D. (2017). *Standard Methods for the Examination of Water and Wastewater* (23rd ed.). American Public Health Association, American Water Works Association, Water Environment Federation. (ISBN 978-0-87553-287-5)

- Ruffin, C., King, R. L., & Younan, N. H. (2008). A Combined Derivative Spectroscopy and Savitzky-Golay Filtering Method for the Analysis of Hyperspectral Data. *GIScience & Remote Sensing*, 45(1), 1–15. <https://doi.org/10.2747/1548-1603.45.1.1>
- Safi, C. (2014). Morphology, composition, production, processing and applications of *Chlorella vulgaris*_ A review. *Renewable and Sustainable Energy Reviews*, 14.
- Saini, D. K., Pabbi, S., & Shukla, P. (2018). Cyanobacterial pigments: Perspectives and biotechnological approaches. *Food and Chemical Toxicology*, 120, 616–624. <https://doi.org/10.1016/j.fct.2018.08.002>
- Savitzky, Abraham., & Golay, M. J. E. (1964). Smoothing and Differentiation of Data by Simplified Least Squares Procedures. *Analytical Chemistry*, 36(8), 1627–1639. <https://doi.org/10.1021/ac60214a047>
- Schneider, S., Wokusch, Th., Tiltcher, H., Fischer, R., & Scheer, H. (1991). UV-VIS Absorption Spectra at High Pressure of C-Phycocyanin and Allophycocyanin from *Mastigocladus laminosus*. *Zeitschrift Für Naturforschung C*, 46(9–10), 717–724. <https://doi.org/10.1515/znc-1991-9-1002>
- Sharma, N., Choudhary, K., Bajpai, R., & Rai, A. (2010). *Freshwater cyanobacterial (blue-green algae) blooms: Causes, consequences and control*. 24.
- Simis, S. G. H., & Kauko, H. M. (2012). In vivo mass-specific absorption spectra of phycobilipigments through selective bleaching: Selective bleaching of phytoplankton pigments. *Limnology and Oceanography: Methods*, 10(4), 214–226. <https://doi.org/10.4319/lom.2012.10.214>
- Sobiechowska-Sasim, M., Stoń-Egiert, J., & Kosakowska, A. (2014). Quantitative analysis of extracted phycobilin pigments in cyanobacteria—An assessment of spectrophotometric and spectrofluorometric methods. *Journal of Applied Phycology*, 26(5), 2065–2074. <https://doi.org/10.1007/s10811-014-0244-3>
- Tran Khac, V., Hong, Y., Plec, D., Lemaire, B., Dubois, P., Saad, M., & Vinçon-Leite, B. (2018). An Automatic Monitoring System for High-Frequency Measuring and Real-Time

- Management of Cyanobacterial Blooms in Urban Water Bodies. *Processes*, 6(2), 11. <https://doi.org/10.3390/pr6020011>
- UNESCO. (1996). *Design and Implementation of some Harmful Algal Monitoring Systems*. 44, 116.
- UNESCO, Anderson, D. M., Cembella, A. D., Enevoldsen, H. O., & Hallegraeff, G. M. (2004). *Manual on harmful marine microalgae*. UNESCO. (ISBN 978-92-3-103948-5)
- Voigtman, E. (2017). The Hubaux and Vos Method. In *Limits of Detection in Chemical Analysis* (pp. 325–329). John Wiley & Sons, Inc. (ISBN 978-1-119-18900-8) <https://doi.org/10.1002/9781119189008.app5>
- Wang, G., Li, J., Zhang, B., Shen, Q., & Zhang, F. (2015). Monitoring cyanobacteria-dominant algal blooms in eutrophicated Taihu Lake in China with synthetic aperture radar images. *Chinese Journal of Oceanology and Limnology*, 33(1), 139–148. <https://doi.org/10.1007/s00343-015-4019-8>
- WHO. (2003a). Algae and cyanobacteria in fresh water. In *Guidelines for Safe Recreational Water Environments* (pp. 136–158). WHO Publishing. https://www.who.int/water_sanitation_health/bathing/srwe1-chap8.pdf
- WHO. (2003b). *Guidelines for Safe Recreational Water Environments: Coastal and fresh waters*. World Health Organization. (ISBN 978-92-4-154580-8)
- WHO. (2017a). *Guidelines for drinking water quality*. World Health Organization. (ISBN 978-92-4-154995-0)
- WHO. (2017b). *Guidelines for drinking-water quality*. (ISBN 978-92-4-154995-0)
- Wilson, A. E., Wilson, W. A., & Hay, M. E. (2006). Intraspecific Variation in Growth and Morphology of the Bloom-Forming Cyanobacterium *Microcystis aeruginosa*. *Applied and Environmental Microbiology*, 72(11), 7386–7389. <https://doi.org/10.1128/AEM.00834-06>
- Winter, J. G., DeSellas, A. M., Fletcher, R., Heintsch, L., Morley, A., Nakamoto, L., & Utsumi, K. (2011). Algal blooms in Ontario, Canada: Increases in reports since 1994. *Lake*

and Reservoir Management, 27(2), 107–114.
<https://doi.org/10.1080/07438141.2011.557765>

Yang, Z., Kong, F., Shi, X., Zhang, M., Xing, P., & Cao, H. (2008). *Changes in the Morphology and Polysaccharide Content of Microcystis aeruginosa (Cyanobacteria) during Flagellate Grazing*. 5. <https://doi.org/10.1111/j.1529-8817.2008.00502.x>

Zamyadi, A., Choo, F., Newcombe, G., Stuetz, R., & Henderson, R. K. (2016). A review of monitoring technologies for real-time management of cyanobacteria: Recent advances and future direction. *TrAC Trends in Analytical Chemistry*, 85, 83–96.
<https://doi.org/10.1016/j.trac.2016.06.023>

Zamyadi, A., MacLeod, S. L., Fan, Y., McQuaid, N., Dorner, S., Sauv e, S., & Pr evost, M. (2012a). Toxic cyanobacterial breakthrough and accumulation in a drinking water plant: A monitoring and treatment challenge. *Water Research*, 46(5), 1511–1523.
<https://doi.org/10.1016/j.watres.2011.11.012>

Zamyadi, A., McQuaid, N., Pr evost, M., & Dorner, S. (2012b). Monitoring of potentially toxic cyanobacteria using an online multi-probe in drinking water sources. *J. Environ. Monit.*, 14(2), 579–588. <https://doi.org/10.1039/C1EM10819K>

Appendix E

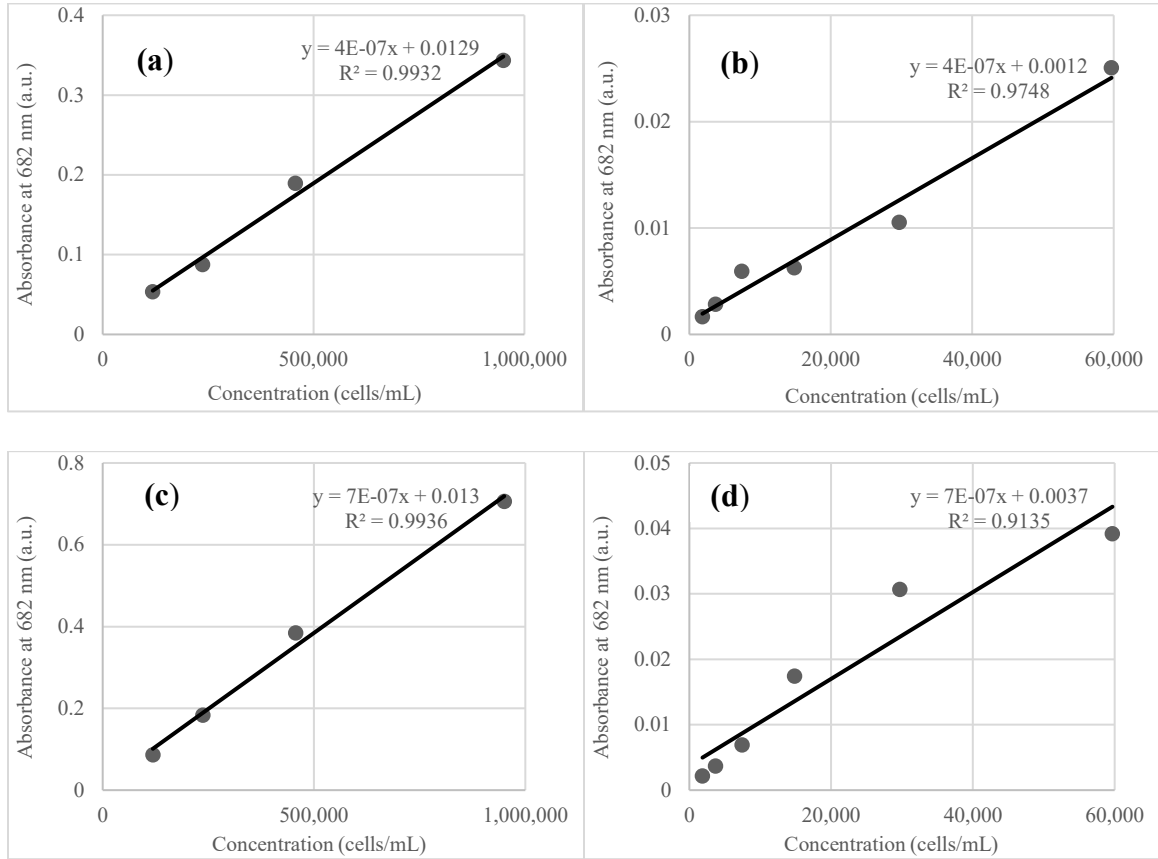
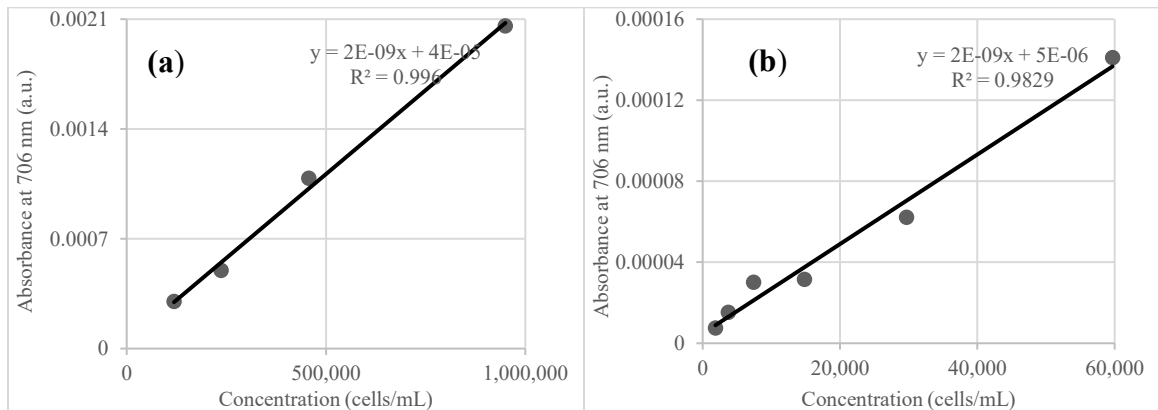


Figure E.4: Standard calibration curves for absorbance spectra at *Chl-a* peak at higher and lower concentration ranges of *M. aeruginosa* in river water for 50 mm (a, b) and 100 mm (c, d) cuvette pathlengths, respectively.



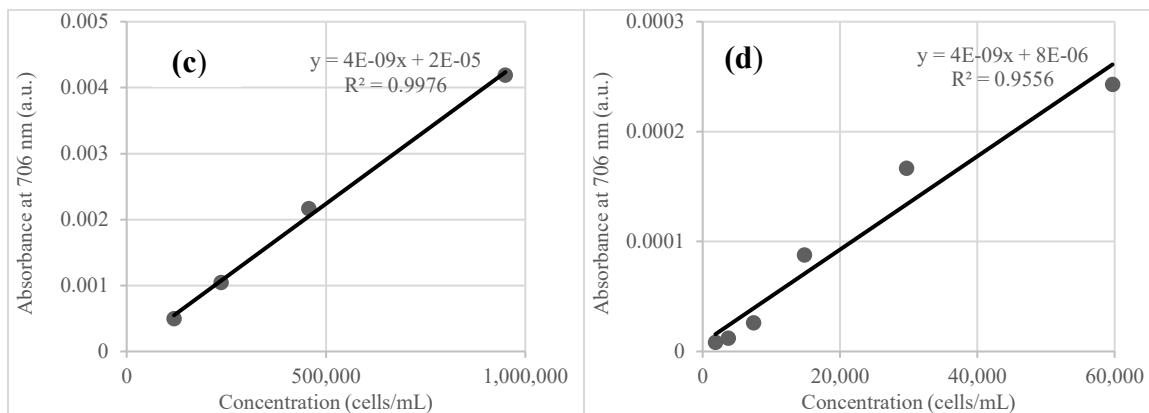


Figure E.5: Standard calibration curves for Savitzky-Golay first derivative of absorbance at *Chl-a* peak at higher and lower concentration ranges of *M. aeruginosa* in river water for 50 mm (a, b) and 100 mm (c, d) cuvette pathlengths, respectively.

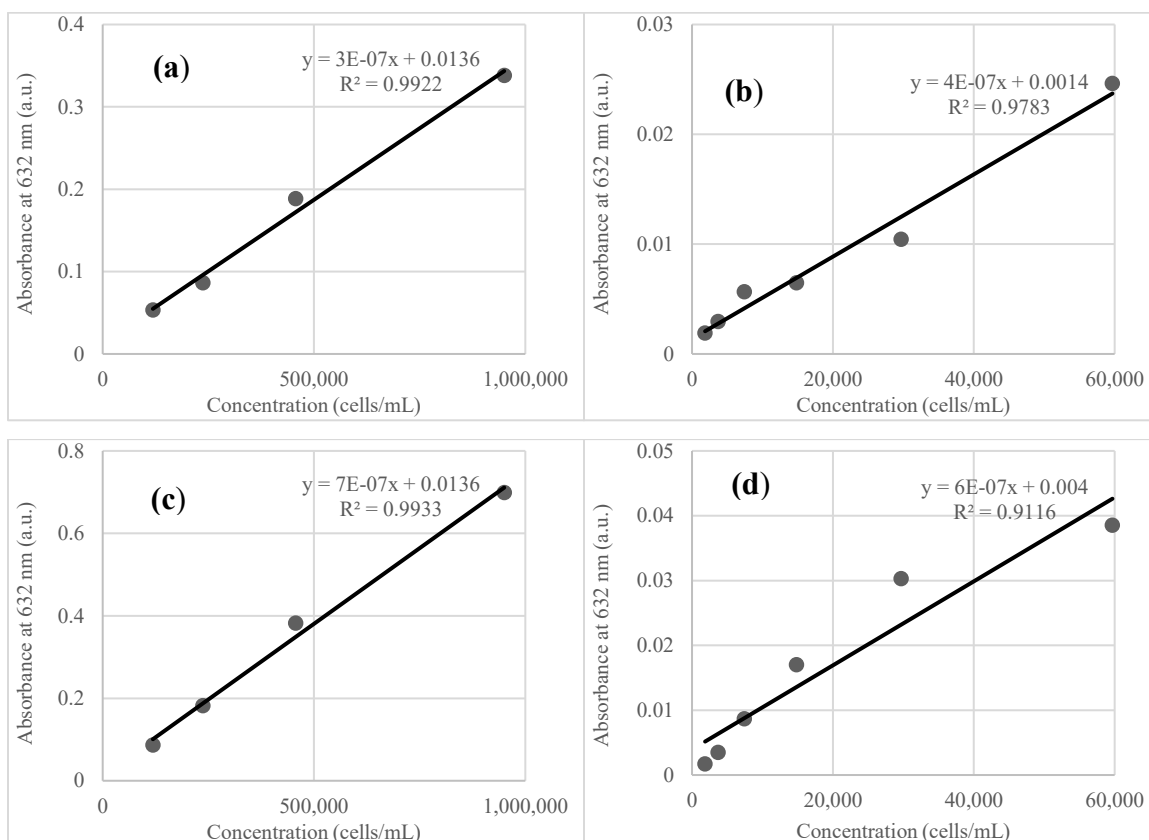


Figure E.6: Standard calibration curves for absorbance spectra at PC peak at higher and lower concentration ranges of *M. aeruginosa* in river water for 50 mm (a, b) and 100 mm (c, d) cuvette pathlengths, respectively.

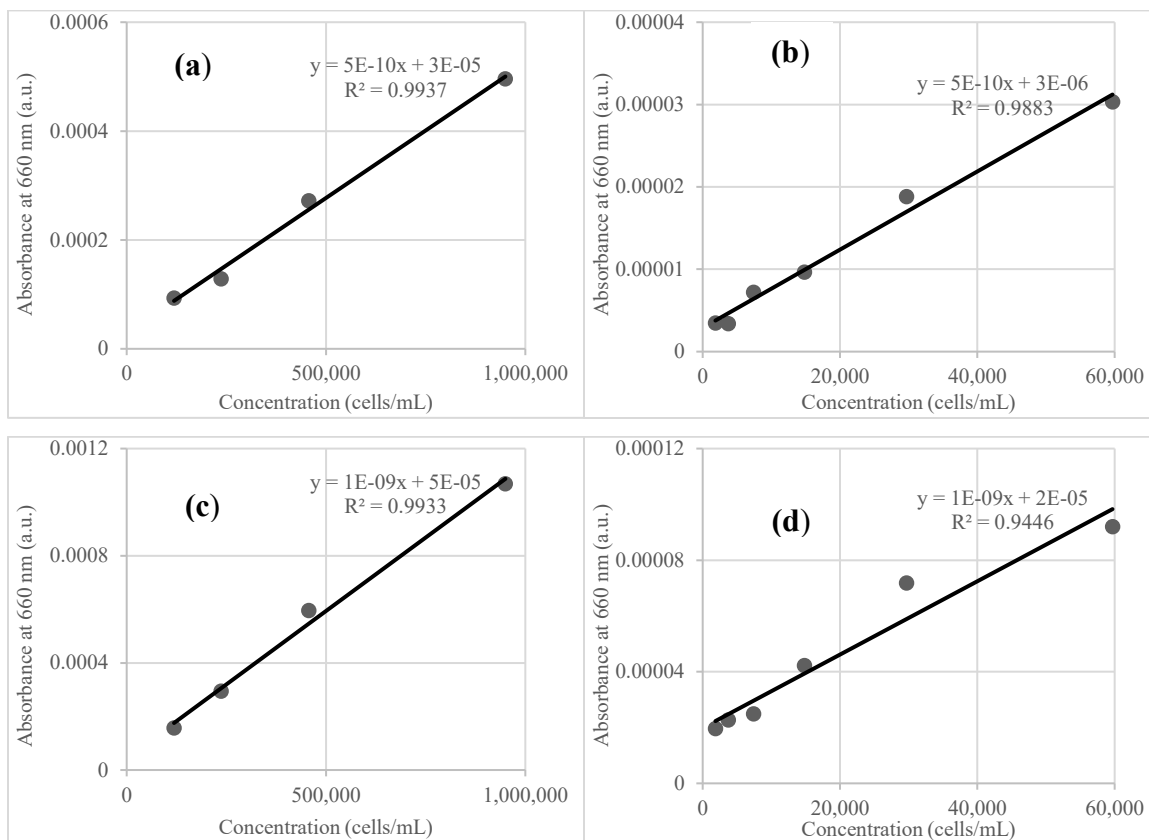
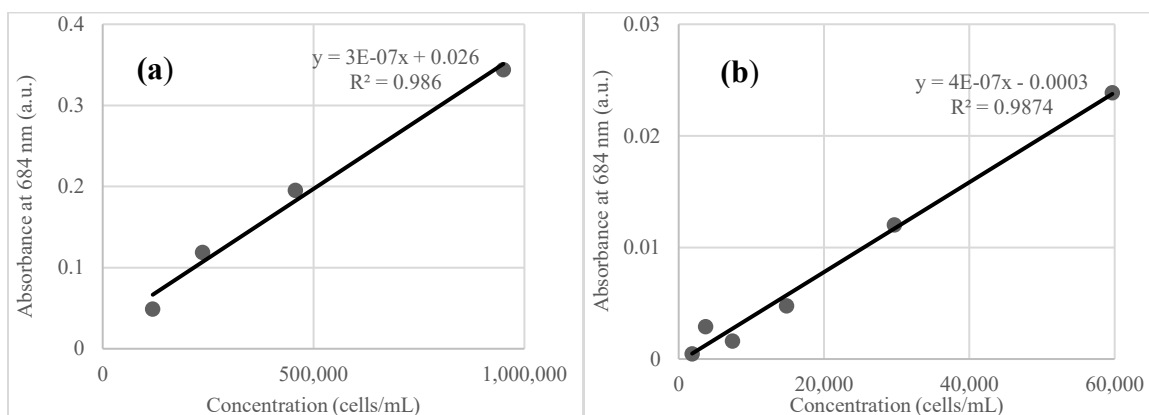


Figure E.7: Standard calibration curves for Savitzky-Golay first derivative of absorbance at PC peak at higher and lower concentration ranges of *M. aeruginosa* in river water for 50 mm (a, b) and 100 mm (c, d) cuvette pathlengths, respectively.



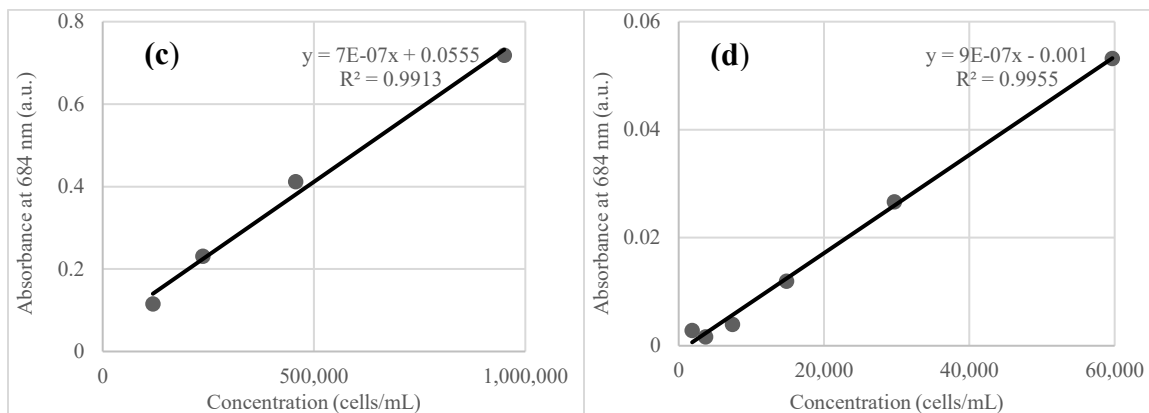


Figure E.8: Standard calibration curves for absorbance spectra at *Chl-a* peak at higher and lower concentration ranges of *C. vulgaris* in river water for 50 mm (a, b) and 100 mm (c, d) cuvette pathlengths, respectively.

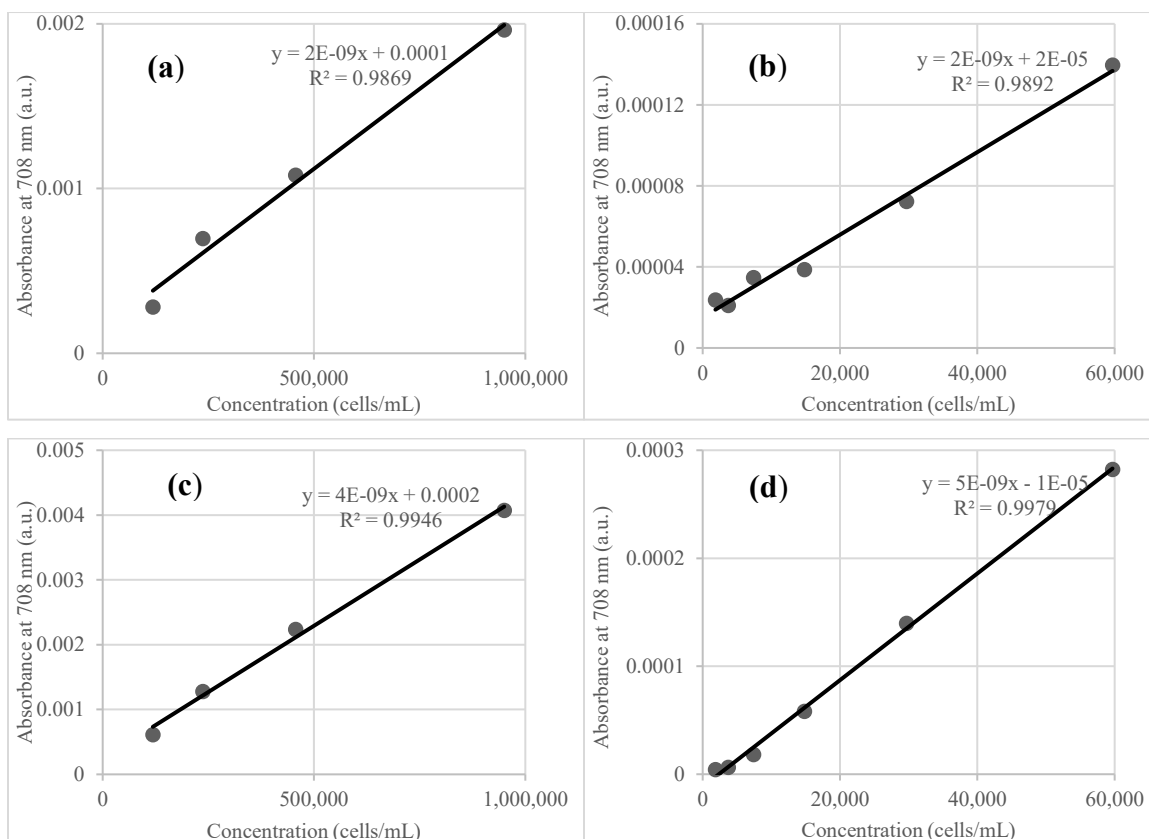


Figure E.9: Standard calibration curves for Savitzky-Golay first derivative of absorbance at *Chl-a* peak at higher and lower concentration ranges of *C. vulgaris* in river water for 50 mm (a, b) and 100 mm (c, d) cuvette pathlengths, respectively.

7. Implications of Water Quality Parameters on Detection and Monitoring of Cyanobacteria using UV-Vis Derivative Spectrophotometry

Amitesh Malhotra and Banu Örmeci*

Department of Civil and Environmental Engineering, Carleton University

1125 Colonel By Drive, Ottawa ON K1S 5B6, Canada

Abstract

Cyanobacterial blooms are now a long-standing and recurring environmental issue around the globe due to their potential toxicity and accompanying negative impacts such as the formation of taste and odor compounds, water discoloration, scum formation, to name a few. Early detection and routine monitoring of source water is, therefore, an increasing need, and methods to promptly identify cyanobacterial presence are critical. In this study, *M. aeruginosa* was used to test the impact of three water quality parameters (WQP), including salinity, DOC (dissolved organic carbon), and turbidity, on the detection and monitoring of cyanobacteria using UV-Vis derivative spectrophotometry. The study established the method detection limits under a wide range of WQP. Further, the effect of two cuvette pathlengths (50-, and 100-mm) and two exposure times (90 and 180 mins) at two peaks, corresponding to photopigments chlorophyll-a (*Chl-a*) and phycocyanin (PC), were investigated while applying and Savitzky-Golay (S-G) first derivative of absorbance technique to improve sensitivity. Results indicate that the relationship between the two photopigments and absorbance was generally strong ($R^2 > 0.9$), except for higher turbidity tests ($R^2 > 0.8$), and 100 mm pathlength was found to be the most sensitive in terms of

detection. Additionally, there was no significant change in absorbance, detection limit, or slope observed between the two exposure times. The lowest detection limits using the established method was found to be 11,083 cells/mL and 12,632 cells/mL for 1 mg/L DOC for *Chl-a* and PC, respectively. Sensitivity analyses revealed slight variations in slopes of regression with increasing WQP concentration, which was expected with increasing interfering contaminants. Overall, the results demonstrate that despite varying WQPs, with the aid of derivate spectrophotometry and longer cuvette pathlength (100 mm), the method can be successfully used for potential detection and monitoring of cyanobacteria in different source waters.

Keywords: *Microcystis aeruginosa*; cyanobacteria; derivative spectrophotometry; early detection, water, monitoring.

7.1 Introduction

Cyanobacteria (CB), also referred to as blue-green algae, are photosynthetic prokaryotes that use various photopigments, primarily chlorophyll-a (*Chl-a*), to capture sunlight for energy production (WHO, 2003). They are commonly found in freshwater lakes, ponds, wetlands, rivers, and streams but can even occur in oceans (Bowling et al., 2017; Chorus, 2012; Winter et al., 2011). It is often assumed that when cyanobacteria from freshwater sources reach saline estuaries, they stop growing after some period of time, but studies have shown that some cyanobacteria can survive saline conditions (Rosen et al., 2018). However, salinity tolerance varies between different cyanobacteria, and the study by Rosen et al. (2018) using *Microcystis aeruginosa* reported a maximum tolerance of 18 ppt salinity, above which, toxins were found to leak from the cells into the water. Further, Álvarez et

al. (2020) reported that salinity can have a direct impact on the morphology and colony forming behavior of *M. aeruginosa*.

In addition to this, dissolved organic carbon (DOC) is another critical parameter that affects cyanobacteria. Following cell lysis, when CB biomass undergoes decomposition, research has shown that CB releases DOC and nutrients corresponding to the differences of Nitrogen-based compounds and total phosphorous in source water (Li et al., 2018; Ye et al., 2011). This in response adds to existing dissolved organic matter (DOM) in source water and supports microorganism growth (Li et al., 2018). Moreover, Ye et al. (2011) reported that nitrate depletion causes CB to undergo cell lysis and cause release of DOC, significantly increasing carbon to nitrogen (C/N) ratio in water. Additionally, after a bloom collapse, Ye et al. (2011) reported that the C/N ratio declines as DOC is biologically reactive, changing the DOM pool from carbon enriched to nitrogen enriched caused by bacterial respiration. Furthermore, experimentation conducted by Zhao et al. (2019) has shown that in presence of DOC extracted from biochar, paddy soil and rice husks, an increase in photosynthesis of *M. aeruginosa* was observed at carbon concentrations ranging from 0 to 10 mg/L. However, inhibition of *M. aeruginosa* growth rate was reported in excess presence of humic-acid like substances and high carbon concentrations of biochar (Zhao et al., 2019). Non-algal turbidity is another parameter which impacts CB growth in source waters. Research suggests that CB biomass yield per unit total phosphorous is higher in presence of natural turbidity and turbidity can impact relationship between CB biomass and total phosphorous in a given water system (Dzialowski et al., 2011). Nevertheless, Dzialowski et al. (2011) also reported that high levels of natural turbidity can lower CB predicted yield, which might be caused by reduced amount of light reaching CB

biomass. Supplimentarily, turbidity and DOC are known to cause optical interference with spectrophotometric measurements, increasing importance of these water quality parameters (WQPs) as potential impact factors on CB detection (Burgess & Thomas, 2017).

There are three groups of CB commonly observed in the aquatic environments: bloom-formers, mat-forming, and picocyanobacteria (Vincent, 2009). Bloom-formers flourish in warm, stable, and nutrient-rich lakes. *Anabaena*, *Aphanizomenon*, and *Microcystis* are the three genera of cyanobacteria commonly present in surface waters, and *Microcystis spp.* is the most prevalent genera around the world (Stefanelli et al., 2014). Studies show that a single factor does not necessarily determine bloom formation, rather a mixture of nutrients (nitrogen and phosphorous) and environmental conditions (warm temperature, light intensity, growth rate, and stability) present together influence cyanobacterial growth (Health Canada, 2016; Pelaez et al., 2010). In addition, studies have shown that cyanobacteria can adjust their depth in water using gas vacuoles to enhance growth conditions and can survive extreme water conditions, for example, at high temperatures (74 °C) and low pH (4) (Oren, 2014). These properties of bloom-formers suggest that with warming global temperatures, the frequency and severity of blooms will become increasingly prevalent. Thus, there is a need to be able to monitor the source water body for different water quality parameters in tandem with cyanobacteria to ensure the protection and safe use of water bodies.

Cyanobacteria can be toxigenic or non-toxigenic in nature; the toxigenic species release toxins known as cyanotoxins stored inside the cell walls, on cell lysis. The toxins released during the growth phase are minimal, and they quickly dissolve in water and rapidly dilute

and degrade with time (EPA, 2015). Species within the *Microcystis* sp. genus can be toxigenic or non-toxigenic. Toxic species produce hepatoxins, which upon ingestion can cause gastroenteritis, liver damage, cancer, and/or tissue bioaccumulation (Berry et al., 2011; Health Canada, 2016). Additionally, cyanobacterial blooms also lead to lower source dissolved oxygen content, production of taste and odor compounds (i.e., 2-methylisoborneol and Geosmin), and scum formation, which can lead to overall deterioration of source water quality (Graham et al., 2010). Studies have shown that source water impacted by toxic blooms can cost millions of additional dollars in operational costs to water and wastewater treatment plants (Oren, 2014). This increasing global issue gives rise to the need for the early detection of cyanobacteria in source waters. It should be noted that both toxigenic and non-toxigenic *M. aeruginosa* carry the same photopigment markers phycocyanin (PC) and *Chl-a* (American Water Works Association, 2011; Saini et al., 2018). Current monitoring and detection techniques for cyanobacteria rely on quantitative estimation of toxin amount, pigment present, or methods relying on direct counting (Moreira et al., 2014). However, due to high variability of water quality and cyanobacteria present in source water, technologies have difficulties quantifying amount accurately and lack repeatability (Srivastava et al., 2013). For example, direct counting methods which use microscopic enumeration are incapable of providing in-situ results and require skilled technicians for sampling and quantification to avoid measurement bias (Falconer, 1999). Other promising techniques rely on real-time quantitative polymerase chain reaction (qPCR), remote sensing, and probe technology (based on fluorometry) which can theoretically provide an estimation of cell/toxin concentration (Baxa et al., 2010; Bertone et al., 2018; Furevik et al., 2004; Lane et al., 2012). Currently, fluorometry-based

instruments are the most used for real-time monitoring of cyanobacteria because of their specificity and sensitivity (Zamyadi et al., 2012). Despite that, research shows that the reported sensitivity of fluorometry is vulnerable to sources of interferences such as the presence of target photopigment in mixed phytoplanktonic populations, fluctuating water quality and column optics, uncertain cell pigment content, and prior cyanobacterial exposure to light (Bertone et al., 2018; Zamyadi et al., 2016).

Spectrophotometry depends on recording and reporting absorbance values of different photopigments (such as *Chl-a*) at individual wavelengths for cyanobacterial quantification (Hudnell, 2008; Saini et al., 2018). Furthermore, it is a readily available, rapid, flexible, and non-intrusive technique that can be used for the detection of cyanobacteria without relying on reagents and/or sample preparation/extraction (Burgess & Thomas, 2017). Recently, the use of spectrophotometers for real-time monitoring of different water quality parameters (such as TSS, BOD, COD, N-compounds, UVT, and Benzene, among others) has increased drastically (Altenburger et al., 2015; Burgess & Thomas, 2017). However, its use for cyanobacterial detection has not been widely studied due to its vulnerability to shifting baseline with seasonal changes and absorbance impact with changing water quality (such as turbidity, interfering phaeopigments, organic and inorganic contaminants) (AlMomani & Örmeci, 2018). Recent studies have investigated the use of derivative spectrophotometry for detection of microalgae (including cyanobacteria) and the results reported that baseline shifts were minimized and there was an improvement in signal to noise ratio of the resultant derivative spectra (Agberien & Örmeci, 2019; Malhotra & Örmeci, 2021).

In light of this present scenario, it becomes vital to develop and apply techniques that can assist in early detection and routine monitoring of cyanobacterial blooms in source waters. This study focused on non-toxicogenic bloom-forming variety of cyanobacteria aka *M. aeruginosa* under different water quality parameters using UV-Vis spectrophotometry. The main goal of this study was to examine the performance and effectiveness of derivative spectrophotometry, as a potential tool for early detection of cyanobacteria under varying water quality parameters (lowest to highest concentration levels). The effect of controlled water quality parameters on cyanobacterial detection using spectrophotometry has not been studied before. Understanding the impact of individual parameters allows for evaluating the field monitoring application of derivative spectrophotometry. Varying cuvette pathlengths (50-, and 100-mm) and water quality parameter exposure times were investigated to check the impact on cyanobacterial absorbance. Linear relationships and coefficient of determinations were established using absorbance measurements, derivative of absorbance, and cyanobacterial concentration. Finally, sensitivity analyses were carried out between different water matrices to confidently determine the lowest cyanobacterial concentrations that can be detected under varying water quality conditions.

7.2 Materials and Methods

7.2.1 Cyanobacteria cultivation and growth

Microcystis aeruginosa CPCC632 (cyanobacteria) and its growth media were acquired from Canadian Phycological Culture Center (CPCC) at the University of Waterloo (Ontario, Canada). *M. aeruginosa* was grown using sterile Bold's Basal Medium with triple Nitrogen stock (3N-BBM) media with a dilution factor of 1:2 for the duration of this study and was cultured in 500 mL Erlenmeyer flasks (Canadian Phycological Culture

Centre, 2013). The Erlenmeyer flasks were thoroughly cleansed using deionized (D.I.) water and autoclaved for 30 mins at 15 psi and 121 °C to achieve sterilization. Sterilization was performed and the mouths of the flasks were covered using aluminum foil to prevent potential culture contamination.

For each batch experiment, 200 mL of synthetic growth medium (3N-BBM) was inoculated with *M. aeruginosa* in the sterile Erlenmeyer flask and was placed inside an incubator at a constant temperature (of 24 °C). The microalgae were grown under continuous 24-hour light photoperiod, using 2 daylight emitting fluorescent tube-lights, and were kept at an intensity of 1,000 lux to obtain optimal growth rate (Canadian Phycological Culture Centre, 2013). Additional carbon dioxide (CO₂) was not supplied to the culture and the cultivation relied on natural diffusion of the CO₂ from ambient air. Sufficient headspace was maintained in the flasks for gas exchange between the microalgae and ambient air. The cultivation flasks were stirred gently and manually, twice daily, to maintain a homogenous growth and promote a healthy culture.

7.2.2 Sample preparation for spectrophotometric analysis

M. aeruginosa was separated from its growth medium by centrifugation at 8,000×g for 5 mins using 50 mL centrifuge tubes for individual experiments. Following centrifugation, the growth medium was discarded and the collected microalgal pellet was resuspended in 45 mL of respective water matrices as needed. To obtain a homogenous stock culture, the resuspended sample was gently inverted 5-times and was subsequently used for sample preparation. The prepared stock culture was then quantified using an improved Neubauer hemocytometer by enumerating it under a Leitz Laborlux 12 light microscope, equipped with a 20x magnification objective. The microscope was kept on a stable base that is free

from disturbances such as environmental vibration. Following quantification, dilutions were performed to get 12 concentration levels where the cell concentration ranged from 3,800,000 cells/mL to 1,855 cells/mL for *M. aeruginosa*. Constant dilution ratios were maintained between different WQPs tests to achieve consistency in concentration ranges and aid in comparative analyses. Fresh D.I. water from Direct-Q UV Water Purification System (Millipore Sigma, USA) and clean glass containers were used to prepare standard water matrices as necessary on the day of the experiments. No stored water was used for experimentation to avoid possible contamination and change to D.I. water properties.

The following water quality parameters were used for experimental testing purposes: saline water, DOC water, and turbid water; and were prepared on the day of the experiment in D.I. water. These WQPs were selected following protocols set by the Alliance for Coastal Technologies (ACT) for the nutrient sensor challenge (Johengen, 2016). ACT is jointly funded by National Oceanic and Atmospheric Administration (NOAA) and EPA to develop, improve, and apply sensor technologies for monitoring purposes. Nutrient sensor challenge was developed to verify sensor technology performance in controlled and field environments, and the same protocols were used to verify the developed UV-Vis spectrophotometry methodology for cyanobacterial detection (Johengen, 2016). Salinity, DOC, and turbidity waters matrices were developed using Instant Ocean® sea salt, EPA recommended Upper Mississippi River Natural Organic Matter standard (cat # 1R110N), and Elliot Silt Loam reference material (cat # 1B102M), respectively, obtained from the International Humic Substance Society (IHSS, 2020). All tests were performed at three concentration levels following ACT protocols and the preparation information using the aforementioned reference material is shown in Table 7.1 (Johengen, 2016).

Table 7.1: Water quality parameters preparation information.

Parameter	Value	Reference material added per 1000 mL of D.I. water
Salinity	10 ppt	12.37 g
	20 ppt	25.02 g
	30 ppt	38.37 g
DOC	1 ppm	2 mg
	5 ppm	10 mg
	10 ppm	20 mg
Turbidity	10 NTU	45.97 mg
	50 NTU	229.88 mg
	100 NTU	459.78 mg

*Where, ppt = parts per thousand; ppm = parts per million, NTU = Nephelometric Turbidity unit; g = grams; mg = milligrams.

Each water matrix was constantly stirred (at 350 rpm) using a magnetic stirrer during sample preparation to avoid particle settling and maintain a homogenous mixture. Based on the ACT protocols, each concentration level of cyanobacteria was exposed for 90 mins to the respective water parameter before UV-Vis spectrophotometric analysis. A comparative analysis was run by exposing another set of the same cyanobacterial culture using the same concentration levels, but with a higher exposure time of 180 mins to each individual water parameter, to examine the potential impact of exposure on detection limit (Johengen, 2016).

7.2.3 Verification of water quality parameters

The prepared WQP solutions to be used for inoculation were tested and verified on the day of the experiments for accuracy purposes. All instruments were calibrated using the manufacturer's standards before use. Salinity was verified using a S47 SevenMulti™ dual

meter pH / conductivity meter (Mettler Toledo, Ontario, Canada); while turbidity was verified using HACH 2100AN Turbidimeter (Hach, Colorado, USA). A minimum of triplicates of each standard solution was measured using the same flask and different grab samples to ensure consistency. On the other hand, DOC preparation was based on the elemental composition declared by the IHSS where organic carbon is reported at approximately 50% of the total composition (IHSS, 2020) and is as follows:

Table 7.2: Elemental composition of Upper Mississippi River Natural Organic Matter standard (IHSS, 2020).

Cat. #	H ₂ O	Ash	C	H	O	N	S	P
1R110N	8.55	8.05	49.98	4.61	41.4	2.36	2.62	–

Where, H₂O content is the %(w/w) of H₂O in the air-equilibrated sample; Ash is the %(w/w) of inorganic residue in a dry sample; and C, H, O, N, S, and P are the elemental composition in %(w/w) of a dry, ash-free sample.

7.2.4 UV-Vis Spectrophotometry

Sample analysis was performed using a Jenway 6850 Double Beam Spectrophotometer (Cole-Parmer, UK) and quartz cuvettes of pathlengths 10-, 50-, and 100-mm. The spectrophotometer was calibrated before use and was zeroed to D.I. water to maintain a consistent baseline. The absorbance scan for each WQP was performed with a spectral scan step of 1 nm and over the wavelength range of 190 nm to 800 nm. The resultant absorbance values were reported as absorbance units (a.u.). Cyanobacterial samples were analyzed in triplicates by using another sample for each run to avoid photobleaching of cyanobacteria and minimize scanning error (American Water Works Association, 2011; Hudnell, 2008). A blank water matrix absorbance scan was subtracted from the absorbance of cyanobacterial inoculated sample to attain final absorbance values. Constant cuvette

orientation was maintained between different experiments to ensure consistency. Cuvettes were cleaned using foam swabs and D.I. water between experiments, and the test was performed starting from the lower concentration going towards the highest concentration.

Standard calibration curves were plotted to verify whether the data followed Beer-Lambert Law. The analyzed cyanobacterial samples were segregated into lower [59,375 – 1,855 cells/mL] and higher [950,000 – 118,750 cells/mL] concentration ranges to facilitate data analysis. At each individual WQP value, two individual tests were performed at cyanobacterial exposure times of 90 mins and 180 mins based on the ACT guideline for sensor testing (Johengen, 2016). Similar sample concentrations were maintained between each test to establish representative results, and a consistent sample volume of 3-, 17.5-, and 35-mL was maintained for 10-, 50-, and 100-mm pathlength cuvettes, respectively.

7.2.5 Savitzky-Golay first-order derivative of absorbance

Derivative spectrophotometry is a method which offers the ability to check sample quality in a robust way (Burgess & Thomas, 2017). It is based on the use of first or higher derivatives of absorbance with respect to wavelength. A derivative spectrum does not increase the information content of the traditional spectrum; rather it allows the information to be analyzed in a better manner (Owen, 1995). Savitzky-Golay (S-G) first-order derivative of absorbance is an analytical tool which upon application results in simultaneous first-order derivative of absorbance and smoothing of the recorded data, boosting the observed signal while reducing noise (Savitzky & Golay, 1964). Further, it functions as a better fingerprint identifier than the normal spectrum as it results in more distinct peaks and can function for multicomponent quantitative analysis (Ruffin et al., 2008). It is calculated as follows:

$$a_j = \frac{\sum_{i=-\frac{m-1}{2}}^{\frac{m-1}{2}} C_i F_{j+i}}{N} \quad \frac{m+1}{2} \leq j \leq n - \frac{m-1}{2}$$

Where, a_j = Savitzky-Golay first derivative of absorbance; m = number of data points used; C_i = Savitzky-Golay filter coefficient; F = absorbance value measured at a specific wavelength; N = standardization factor; j = smoothed data point. Each measured absorbance value was smoothed over twenty-three data points so that $i = -11, -10, \dots, 10, 11$; $C_i = -11, -10, \dots, 10, 11$; $m = 23$; $N = 1012$; following Savitzky-Golay recommended guideline and coefficients for first derivative of absorbance (Savitzky & Golay, 1964). Higher derivative spectrums often do not add any supplementary relevant information and hence were not be considered as part of this research (Owen, 1998).

7.2.6 Establishing method detection limit

Method detection limit (MDL) is the lowest concentration of a sample substance that can be statistically determined using an analytical procedure, with 99% confidence to be different from a blank sample (WDNR, 1996). For this study, the MDLs were calculated according to Hubaux and Vos (H-V) method which relies on a minimum of 3 data points for the calculation of detection limit (Voigtman, 2017). H-V method states that the sensitivity of the method is proportional to its precision, which can be measured using the standard deviation of the analyzed samples and is strongly dependent on the linear regression of the observed data (Voigtman, 2017). For accuracy and repeatability purposes, three replicates at 10 individual concentration levels were measured in this study and used for the calculation of the MDL.

7.3 Results

7.3.1 Spectrophotometric measurements of *M. aeruginosa* in water matrices

The absorbance spectra of *M. aeruginosa* were determined at individual concentrations (ranging from 950,000 – 1,855 cells/mL) in saline, DOC, and turbid water using three levels of WQPs (see Table 7.1). The test was conducted twice by varying exposure times (90 and 180 mins) and changing cuvette pathlength (50 and 100 mm) in order to check the effect of some important WQPs (from low impact to high impact) on the MDL of cyanobacteria. This allowed for sensitivity determination of the developed method at varying cyanobacterial concentrations. The absorbance spectra of *M. aeruginosa* under 20 ppt salinity, 5 ppm DOC, and 50 NTU turbidity water matrices are presented in Figure 7.1; while 10 and 30 ppt salinity, 1 and 10 ppm DOC, and 10 and 100 NTU turbidity are shown in supplementary Figure F.5. Intermediate WQPs results using 100 mm cuvette pathlength and 180 mins exposure are shown here for visual representation. 90 mins exposure results for both pathlengths are tabulated in Table F.5 for reference. Higher exposure results (180 mins) will be discussed here onwards as a minimal change in absorbance values were observed between the two exposure times and 180 mins provides more exposure between cyanobacteria and individual WQPs. For example, *M. aeruginosa* in 5 ppm DOC water matrix for 59,375 cells/mL concentration and at 682-nm, resulted in the absorbance values of 0.008033 a.u. and 0.007967 a.u. for 180- and 90-mins exposure, respectively.

Three absorbance peaks were observed in these spectra (as illustrated in Figure 7.1) at 442-, 632-, and 682-nm, with the most distinguished peak and the highest absorbance values observed at 682-nm. The peaks at 442- and 682-nm correspond to photopigment *Chlorophyll-a* (*Chl-a*), while the peak at 632-nm correlates to phycocyanin (PC), an

accessory photopigment found in cyanobacteria (Saini et al., 2018). It should be noted that phycocyanin peak is prone to slight variations within different cyanobacterial species and with fluctuating water properties (Craig & Carr, 1968; Sobiechowska-Sasim et al., 2014). The cyanobacteria *M. aeruginosa* is known to carry both photopigments, which are conventionally used for identification purposes, of which PC acts as a marker unique to cyanobacteria (Agberien & Örmeci, 2019; American Water Works Association, 2011; Bowling et al., 2016). The analysis focused on 400 – 800 nm spectral range as all peaks of interest fall in the middle of that range. For *Chl-a*, 682-nm peak was studied in detail because of its higher absorbance response. With higher WQPs levels, a decrease in absorbance at PC peak was observed, which is likely due to interferences from water constituents that contribute to overall absorbance value. Contrastingly, *Chl-a* peak was minimally affected in the presence of water constituents.

Incremental increases in *M. aeruginosa* cell concentrations resulted in incremental increases in absorbance for both pathlength tests and exposures, indicating that the results followed Beer-Lambert Law. Except for 50 and 100 NTU results, a strong linear relationship between cyanobacterial concentration and absorbance at the peaks 632- and 682-nm were observed ($R^2 > 0.9$). Nonetheless, 50 and 100 NTU results still held a positive linear relationship ($R^2 > 0.8$). With increasing WQP concentrations, the linearity of data showed a decrease in value, as did the slopes of regression lines. This, in turn, resulted in increasing MDL with a higher value of WQP water matrix. This is expected as with increasing interfering constituents that absorb or scatter light, it becomes harder to differentiate between signal and noise (Burgess & Thomas, 2017). Furthermore, with increasing WQP value, *Chl-a* peak continued showing a strong response, but the PC peak

absorbance decreased. It should be noted that the final absorbance values of the graphs (see Figure 7.1) differ with changing WQP because the blank water matrix is subtracted from the recorded absorbance to attain the final absorbance value. Moreover, turbidity displays a decreasing absorbance trend towards near-UV wavelengths as most organic and inorganic matter absorbs strongly with decreasing wavelength (Burgess & Thomas, 2017). The MDLs obtained for 50 mm pathlength were lower in sensitivity in comparison to 100 mm results. 100 mm pathlength results showed the highest sensitivity and their MDL are discussed hereafter. The highest MDL for absorbance with 180 mins exposure at 682- and 632-nm was observed for 100 NTU turbidity at 268,626 and 308,530 cells/mL, respectively. On the other hand, the lowest MDL with 180 mins exposure at 682- and 632-nm was observed for 1 ppm DOC at 33,113 cells/mL and 36,127 cells/mL, respectively (Table 7.3 and Table 7.4). Similar MDLs were observed for 90 mins exposure as well and are tabulated in Table F.5.

Calibration curves for *M. aeruginosa* in different water matrices were generated at 682- and 632-nm. The slopes for 90- and 180-mins exposure were found to be close to each other for both 50- and 100-mm pathlengths (see Table 7.1, Table 7.4 and Table F.5). For instance, considering 20 ppt salinity test using 100 mm pathlength at 682 nm wavelength, the 90 mins exposure displayed a slope of $7.3056 \times 10^{-8} \pm 1.8412 \times 10^{-9}$ while 180 mins exposure had a slope of $7.2840 \times 10^{-8} \pm 1.8038 \times 10^{-9}$. Similarly, at 632 nm wavelength for 20 ppt salinity test, the 90-, and 180-mins exposure had a slope of $7.3391 \times 10^{-8} \pm 1.8927 \times 10^{-9}$ and $7.3441 \times 10^{-8} \pm 2.0372 \times 10^{-9}$, respectively. Correspondingly, the MDLs between the two exposures at 682-, and 632-nm wavelengths were also found to be approximately the same.

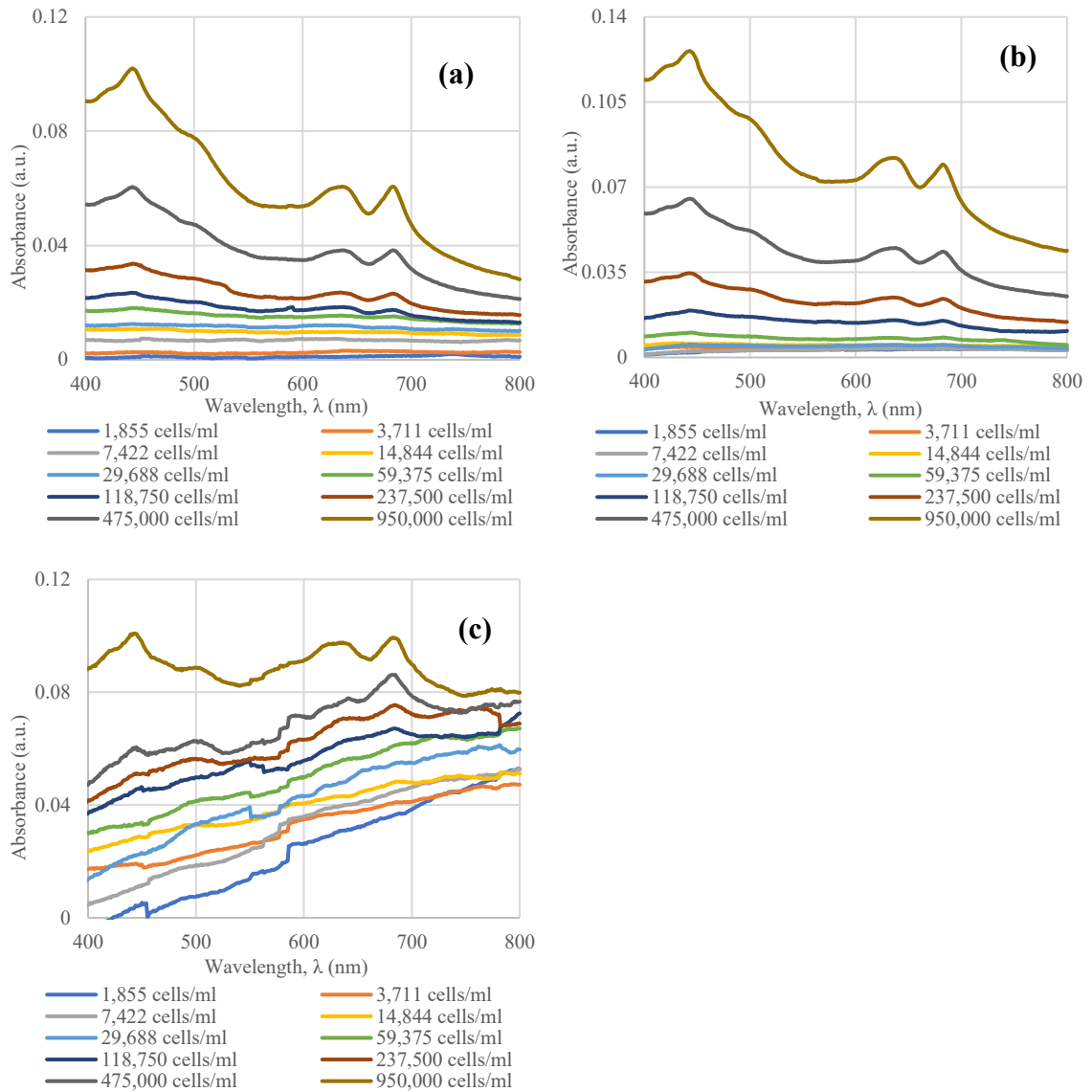


Figure 7.1: Absorbance spectra of *M. aeruginosa* using 100 mm cuvette pathlength for 20 ppt salinity (a), 5 ppm DOC (b), and 50 NTU turbidity (c).

7.3.2 Savitzky-Golay first derivative of absorbance of *M. aeruginosa* in water matrices

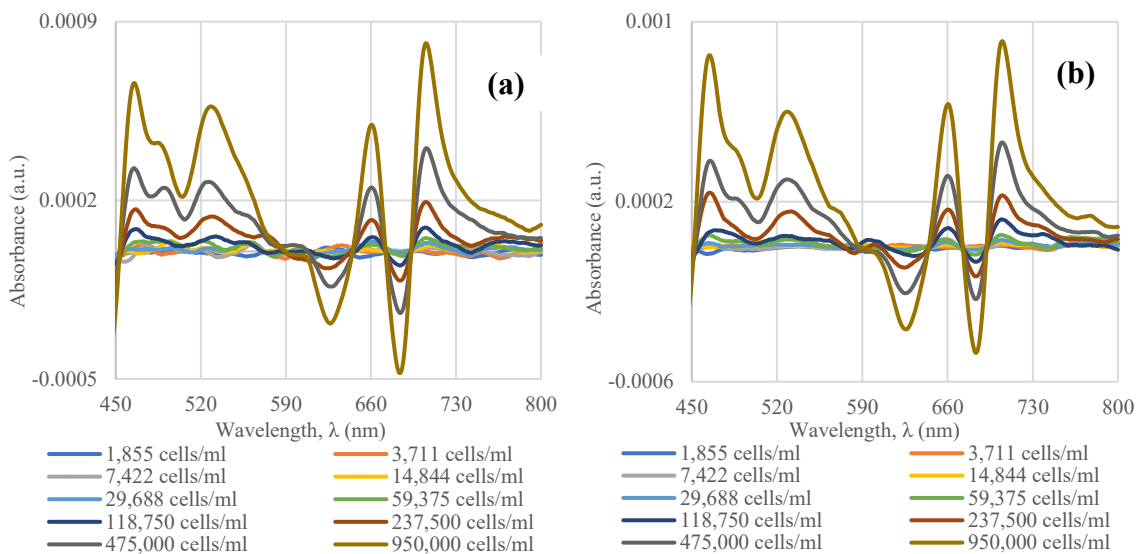
To simultaneously obtain the first-order derivative of absorbance and smoothen the data, Savitzky-Golay first derivative of absorbance was applied to zero-order absorbance of the same concentration range (from 950,000 – 1,855 cells/mL). Predefined S-G polynomial

coefficients were used to smoothen the plot as a means to amplify observed absorbance signal and reduce background noise (Ruffin et al., 2008). This resulted in the attainment of distinct and sharp peaks of photopigments of interest in terms of derivative of absorbance for *M. aeruginosa* under 20 ppt salinity, 5 ppm DOC, and 50 NTU turbidity water matrices (as illustrated in Figure 7.2). As it is known that the peaks of interest for *M. aeruginosa* lie within the wavelength range of 400 to 800 nm, the S-G analytical tool was applied specifically to that range, starting from 800 nm going towards 400 nm.

A shift in peaks of interest was observed for the S-G derivative spectra (Figure 7.2) when compared to the zero-order absorbance graphs (Figure 7.1). The new peaks of interest for S-G derivative were observed at 660- and 706-nm wavelengths, which correspond to 632- and 706-nm wavelengths observed in the zero-order absorbance spectra. This shift in peak is characteristic of the derivative of absorbance technique as the derivative absorbance represents the rate of change in zero-order absorbance with respect to wavelength (Agberien & Örmeci, 2019; Kus et al., 1996). Similar to the zero-order absorbance, at higher turbidity levels (50 and 100 NTU), the PC peak at 660 nm absorbed lower when compared to the *Chl-a* peak (for example, Figure 7.2 c). However, for other WQP tests, both *Chl-a* and PC peaks showed a stronger absorbance response after application of S-G derivative technique than zero-order absorbance for 90 mins as well as 180 mins exposure (Figure 7.2 a, b). In character with zero-order absorbance, 100 mm results were much higher in sensitivity as compared to 50 mm and the MDLs for both peaks at 660- and 706-nm wavelengths, and were found to be proximate to each other with changing exposure times (refer Table 7.3, Table 7.4 and Table F.5). The highest and the lowest MDL at 706- and 660-nm using 100 mm pathlength were observed for 100 NTU turbidity and 1 ppm

DOC, respectively at 67,577 and 76,775 cells/mL; and 13,632 and 13,966 cells/mL (Table 7.3 and Table 7.4). A minimum of 2-fold improvement in detection limit was observed for all WQP tests upon application of S-G derivative technique to zero-order absorbance data.

To verify the previous results, calibration curves at 660- and 706-nm wavelengths were plotted to test the linear relationship between the Savitzky-Golay first derivative of absorbance and *M. aeruginosa* cell concentration. The results indicate a strong linear relationship ($R^2 > 0.9$) for all WQP tests at 660- and 706-nm except for higher turbidity results (50 and 100 NTU) at 660 nm ($R^2 > 0.8$) for both exposure times (Table 7.3, Table 7.4 and Table F.5). 50- and 100-mm pathlengths at 90- and 180-mins exposure revealed analogous slopes. To give an example, consider 5 ppm DOC test results using 100 mm pathlength at 660 nm wavelength; the slope was found to be $7.1655 \times 10^{-10} \pm 7.6877 \times 10^{-12}$ and $7.2790 \times 10^{-10} \pm 9.9051 \times 10^{-12}$ for 90-, and 180-mins exposure, respectively. The results indicate that S-G first derivative of absorbance can be a useful analytical tool for the detection of cyanobacteria.



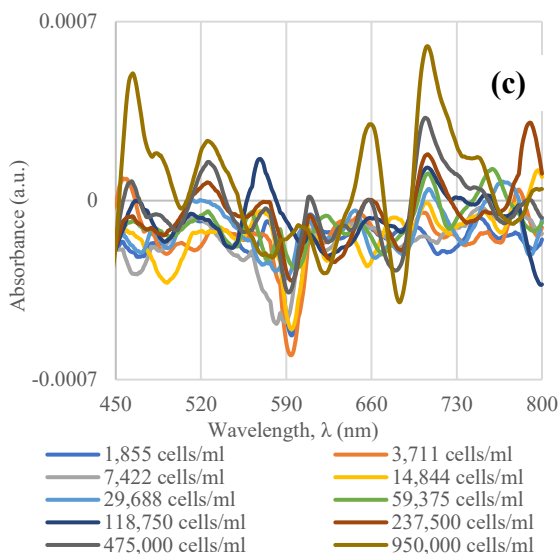


Figure 7.2: Savitzky-Golay first derivative of absorbance spectra of *M. aeruginosa* using 100 mm cuvette pathlength for 20 ppt salinity (a), 5 ppm DOC (b), and 50 NTU turbidity (c).

7.3.3 Modified application of Savitzky-Golay first derivative of absorbance

In pursuit of further improving the detection limit for cyanobacteria under different WQPs, Savitzky-Golay technique was applied to a narrower range of wavelengths. This was done in order to reduce background noise and enhance the relevant signal response. It should be noted that derivative absorbance does not increase the amount of information present but rather amplifies relevant information for better analysis (Kus et al., 1996). As the peaks of interest lie at 632- and 682-nm wavelengths for zero-order spectra, the S-G technique was applied to two narrower sections of wavelengths starting from 800 – 600 nm and 750 – 450 nm, respectively. The peaks for these two narrower sections for 5 ppm DOC (as illustrated in Figure 7.3) were observed at the same wavelengths of 660- and 706-nm corresponding to the S-G previously applied to a broader range of 800 – 400 nm (refer 7.3.2). Despite the modified wavelength range application of S-G, no improvement in detection limit was observed for *M. aeruginosa*.

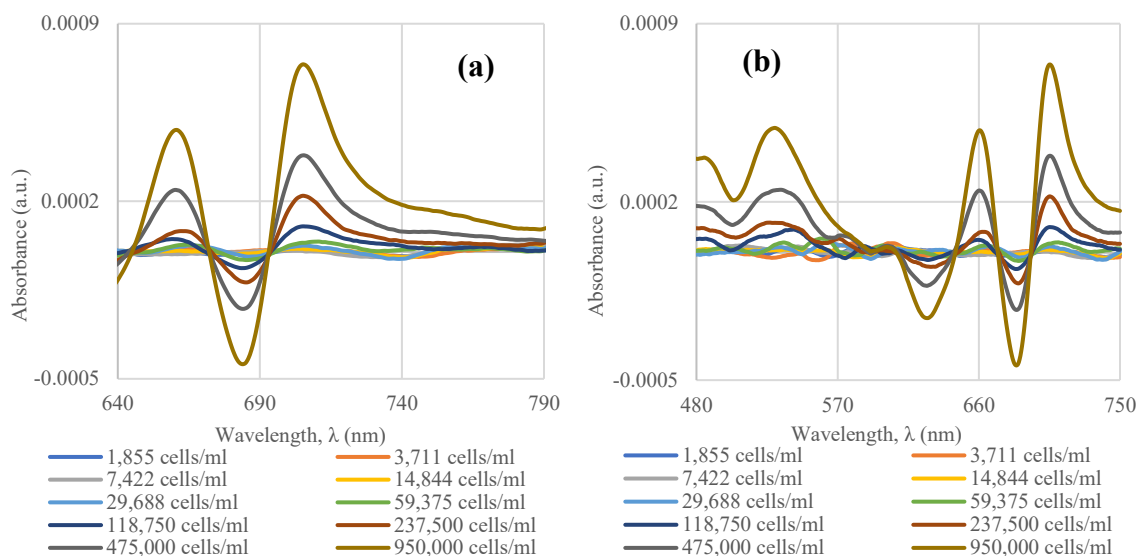


Figure 7.3: Modified Savitzky-Golay first derivative of absorbance spectra using 100 mm cuvette pathlength for 5 ppm DOC matrix water from 800 – 600 nm wavelengths (a), and 750 – 450 nm wavelengths (b).

A summary of experimental results obtained from inoculating cyanobacteria in different water quality parameters for 180 mins using 50-, and 100-mm cuvette pathlengths, are shown in Table 7.3 and Table 7.3.

Table 7.3: Critical data for *M. aeruginosa* in different water matrices for photopigment *Chl-a* over the concentration range (1,855 – 950,000 cells/mL) after 180 mins exposure.

Test	Pathlength (mm)	Parameter/Value	Slope	R ²	MDL (cells/mL)	
<i>M. aeruginosa</i> (<i>Chlorophyll</i> peak)						
Absorbance 682 nm	100	Salinity (ppt)	10	$9.2189 \times 10^{-08} \pm 1.6266 \times 10^{-09}$	0.9994	46,169
			20	$7.2840 \times 10^{-08} \pm 1.8038 \times 10^{-09}$	0.9951	59,678
			30	$6.5492 \times 10^{-08} \pm 2.4481 \times 10^{-09}$	0.9889	73,085
	50	10	$2.9644 \times 10^{-08} \pm$	0.9975	70,687	

				5.2034×10^{-10}		
			20	$2.7996 \times 10^{-08} \pm$ 5.5611×10^{-10}	0.9968	77,991
			30	$3.1151 \times 10^{-08} \pm$ 1.0580×10^{-09}	0.9908	89,650
	100	DOC (ppm)	1	$9.8205 \times 10^{-08} \pm$ 1.0939×10^{-09}	0.9990	33,113
			5	$8.0182 \times 10^{-08} \pm$ 1.1887×10^{-09}	0.9982	55,075
			10	$7.0897 \times 10^{-08} \pm$ 1.8950×10^{-09}	0.9943	70,869
	50	DOC (ppm)	1	$4.4368 \times 10^{-08} \pm$ 7.9992×10^{-10}	0.9974	59,851
			5	$3.9800 \times 10^{-08} \pm$ 1.6700×10^{-09}	0.9861	80,508
			10	$3.4847 \times 10^{-08} \pm$ 8.9360×10^{-10}	0.9947	101,250
	100	Turbidity (NTU)	10	$8.5963 \times 10^{-08} \pm$ 8.3962×10^{-09}	0.9290	56,795
			50	$6.1053 \times 10^{-08} \pm$ 1.0587×10^{-09}	0.8060	68,191
			100	$7.9866 \times 10^{-08} \pm$ 3.3407×10^{-09}	0.8031	268,626
	50	Turbidity (NTU)	10	$4.0419 \times 10^{-08} \pm$ 2.1007×10^{-09}	0.9788	115,880
			50	$4.0437 \times 10^{-08} \pm$ 9.5018×10^{-09}	0.8693	150,697
			100	$3.5728 \times 10^{-08} \pm$ 3.3402×10^{-09}	0.8108	311,348
	100	Salinity	10	$1.1389 \times 10^{-09} \pm$	0.9996	11,157

S-G first derivative of absorbance 706 nm		(ppt)		7.7970×10^{-12}			
			20	$8.5649 \times 10^{-10} \pm 9.6081 \times 10^{-12}$	0.9989	16,154	
			30	$7.7963 \times 10^{-10} \pm 1.3196 \times 10^{-11}$	0.9977	18,124	
		50	DOC (ppm)	10	$3.4845 \times 10^{-10} \pm 7.5270 \times 10^{-12}$	0.9962	20,583
				20	$3.5492 \times 10^{-10} \pm 9.3685 \times 10^{-12}$	0.9944	30,354
				30	$3.6556 \times 10^{-10} \pm 9.7717 \times 10^{-12}$	0.9943	38,200
	100	DOC (ppm)	1	$1.1611 \times 10^{-09} \pm 7.7970 \times 10^{-12}$	0.9994	11,083	
			5	$9.3710 \times 10^{-10} \pm 7.5672 \times 10^{-12}$	0.9994	13,853	
			10	$8.2547 \times 10^{-10} \pm 1.4600 \times 10^{-11}$	0.9975	15,826	
		50	Turbidity (NTU)	1	$5.3551 \times 10^{-10} \pm 8.0253 \times 10^{-12}$	0.9982	13,966
				5	$4.4298 \times 10^{-10} \pm 8.5647 \times 10^{-12}$	0.9970	25,730
				10	$4.2947 \times 10^{-10} \pm 1.2373 \times 10^{-11}$	0.9934	26,858
	100	Turbidity (NTU)	10	$1.0914 \times 10^{-09} \pm 4.9855 \times 10^{-11}$	0.9835	11,142	
			50	$7.0836 \times 10^{-10} \pm 5.3408 \times 10^{-11}$	0.9565	13,833	
			100	$8.0379 \times 10^{-10} \pm 8.1501 \times 10^{-11}$	0.9240	46,834	
			50	10	$4.8068 \times 10^{-10} \pm$	0.9646	31,587

				3.2552×10^{-11}		
			50	$4.2938 \times 10^{-10} \pm$ 5.2199×10^{-11}	0.8724	60,953
			100	$4.4151 \times 10^{-10} \pm$ 6.5436×10^{-11}	0.8505	76,775

Table 7.4: Critical data for *M. aeruginosa* in different water matrices for photopigment phycocyanin over the concentration range (1,855 – 950,000 cells/mL) after 180 mins exposure.

Test	Pathlength (mm)	Parameter/Value	Slope	R ²	MDL (cells/mL)		
<i>M. aeruginosa</i> (Phycocyanin peak)							
Absorbance 632 nm	100	Salinity (ppt)	10	$9.9764 \times 10^{-08} \pm$ 1.9241×10^{-09}	0.9970	54,544	
			20	$7.3441 \times 10^{-08} \pm$ 2.0372×10^{-09}	0.9938	71,861	
			30	$6.5761 \times 10^{-08} \pm$ 2.3667×10^{-09}	0.9897	72,677	
	50		10	$2.9758 \times 10^{-08} \pm$ 4.8143×10^{-10}	0.9979	72,933	
			20	$2.8390 \times 10^{-08} \pm$ 5.2284×10^{-10}	0.9972	87,761	
			30	$3.1340 \times 10^{-08} \pm$ 9.5068×10^{-10}	0.9920	95,133	
	100		DOC (ppm)	1	$1.0067 \times 10^{-07} \pm$ 1.1522×10^{-09}	0.9989	36,127
				5	$8.4159 \times 10^{-08} \pm$ 9.8225×10^{-10}	0.9989	56,638
				10	$7.3908 \times 10^{-08} \pm$	0.9946	74,363

	50			1.9090×10^{-09}				
			1	$4.4661 \times 10^{-08} \pm$ 7.5658×10^{-10}	0.9977	61,906		
			5	$4.1715 \times 10^{-08} \pm$ 1.6094×10^{-09}	0.9882	86,011		
	100	50		10	$3.6892 \times 10^{-08} \pm$ 7.4595×10^{-10}	0.9967	105,068	
				Turbidity (NTU)	10	$8.3824 \times 10^{-08} \pm$ 8.3620×10^{-10}	0.9262	65,288
					50	$6.2677 \times 10^{-08} \pm$ 9.5660×10^{-09}	0.8429	77,840
		100	$6.2755 \times 10^{-08} \pm$ 7.1381×10^{-09}		0.8844	308,530		
		50		10	$4.1448 \times 10^{-08} \pm$ 2.2858×10^{-09}	0.9762	119,984	
				50	$3.6378 \times 10^{-08} \pm$ 8.5264×10^{-09}	0.8694	165,791	
				100	$3.1331 \times 10^{-08} \pm$ 9.3947×10^{-09}	0.8476	389,335	
		S-G first derivative of absorbance 660 nm	100		10	$6.2861 \times 10^{-10} \pm$ 3.4459×10^{-12}	0.9970	13,902
					Salinity (ppt)	20	$5.5483 \times 10^{-10} \pm$ 1.4330×10^{-11}	0.9946
30	$5.2107 \times 10^{-10} \pm$ 6.2349×10^{-12}					0.9988	21,036	
50			10	$2.3968 \times 10^{-10} \pm$ 8.0827×10^{-12}		0.9909	30,386	
			20	$2.1565 \times 10^{-10} \pm$ 8.2556×10^{-12}	0.9984	37,685		
			30	$2.3962 \times 10^{-10} \pm$	0.9845	42,852		

				1.0609×10^{-11}		
	100	DOC (ppm)	1	$8.0965 \times 10^{-10} \pm$ 6.2739×10^{-12}	0.9995	12,632
			5	$7.1655 \times 10^{-10} \pm$ 7.6877×10^{-12}	0.9990	14,922
			10	$6.1079 \times 10^{-10} \pm$ 9.3379×10^{-12}	0.9981	19,174
	50		1	$3.4961 \times 10^{-10} \pm$ 4.9587×10^{-12}	0.9983	15,064
			5	$3.4717 \times 10^{-10} \pm$ 1.0991×10^{-11}	0.9920	28,589
			10	$3.3557 \times 10^{-10} \pm$ 2.5761×10^{-11}	0.9915	33,055
	100	Turbidity (NTU)	10	$6.7324 \times 10^{-10} \pm$ 5.7467×10^{-11}	0.9449	13,922
			50	$4.5767 \times 10^{-10} \pm$ 6.3860×10^{-11}	0.8652	19,126
			100	$5.4611 \times 10^{-10} \pm$ 6.65744×10^{-11}	0.8937	67,577
	50		10	$3.4664 \times 10^{-10} \pm$ 3.8020×10^{-11}	0.9122	36,379
			50	$3.4704 \times 10^{-10} \pm$ 2.7844×10^{-11}	0.8436	87,583
			100	$3.4063 \times 10^{-10} \pm$ 7.6480×10^{-11}	0.9084	115,343

7.3.4 Comparison of *M. aeruginosa* spectra in D.I. water and different water matrices.

The next phase of this study investigated the differences in the absorbance spectra of *M. aeruginosa* in D.I. water and under different WQPs, and their impact on detection limits. Almost identical cell concentrations of *M. aeruginosa* were tested using 100 mm pathlength, and the resultant absorbance and derivative absorbance spectra are shown in Figure 7.4. Upon comparing the D.I. water absorbance spectra (Figure 7.4 a) to that obtained by different WQPs (Figure 7.1), it was observed that the three primary peaks of interest remained consistent at 632- and 682-nm wavelengths. However, for the D.I. water results, clear peaks for photopigments *Chl-a* and PC could be observed at a concentration close to 30,000 cells/mL as they were free from interference factors that are observed for the WQP tests. The MDL for zero-order absorbance in D.I. water at 682 nm was found to be 22,038 cells/mL, whilst the lowest MDL among the WQP tests was found to be 33,113 cells/mL for 1 ppm DOC (Table 7.3). Similarly, for S-G derivative of absorbance graphs (Figure 7.4 b and Figure 7.2), the peaks were displayed at 660- and 706-nm wavelengths for both D.I. water and WQP tests. This consistency indicates the good applicability of the method for in-field applications. The MDL using S-G technique at 706 nm for D.I. water was calculated to be 4,916 cells/mL and the lowest MDL for the WQP tests was found for 1 ppm DOC to be at 11,083 cells/mL (Table 7.3).

The final part of this phase involved analyzing calibration slope differences. The results indicate that at lower WQP levels (such as 10 ppt, 1 ppm, and 10 NTU), a good correlation between the slopes of D.I. water and WQP could be observed. However, at higher WQP levels, a deviation in slope is observed, which is likely due to the presence of a higher

amount of interference particles generated by the WQP mixture. For example, at 682 nm using 100 mm pathlength, the D.I. water had a slope of $9.1427 \times 10^{-08} \pm 1.4469 \times 10^{-09}$, and salinity at 10 ppt displayed a slope of $9.2189 \times 10^{-08} \pm 1.6266 \times 10^{-09}$; while 100 NTU turbidity slope was found to be $7.9866 \times 10^{-08} \pm 3.3407 \times 10^{-09}$ (Table 7.3).

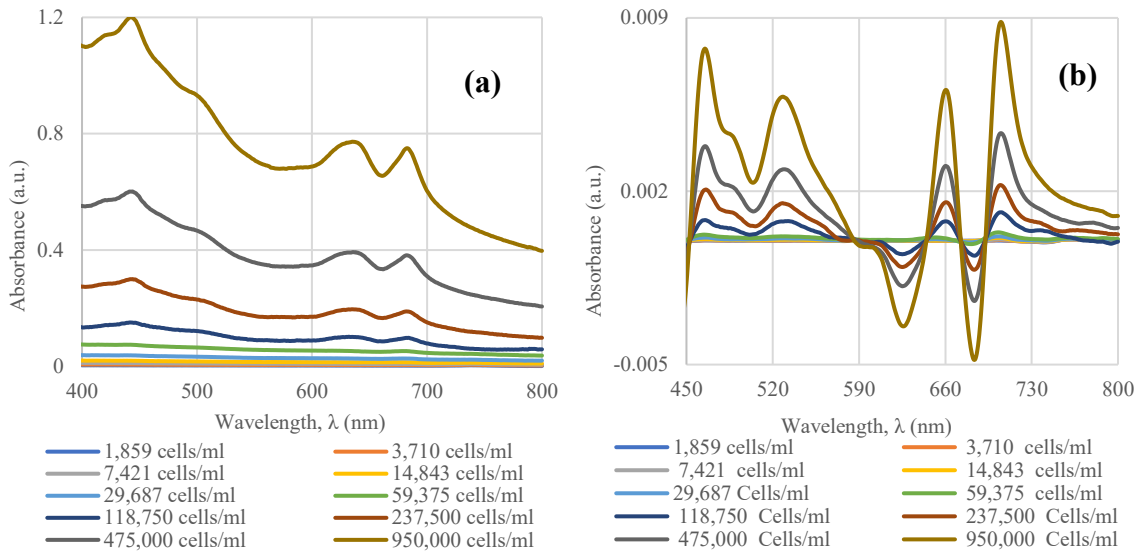


Figure 7.4: Absorbance (a) and Savitzky-Golay first derivative of absorbance (b) spectra of *M. aeruginosa* in D.I. water using 100 mm cuvette pathlength, respectively.

7.4 Discussion

The cyanobacterial data under different water quality parameters reveal that spectrophotometry, when applied in combination with S-G derivative technique, can be potentially used to detect and monitor cyanobacteria in a wide variety of water conditions. Typically, natural salt in oceans and brackish sources is present below 35 ppt (or 53.065 mS/cm) (Agriculture Victoria, 2018; Rosen et al., 2018). The common range of DOC in lakes and surface water is between 0.7 – 15 mg/L (Adams et al., 2018; Hiriart-Baer, 2013), while turbidity is ordinarily below 30 NTU but can go over 100 NTU during a weather event (Huey & Meyer, 2010; Whiting, 2017). Conventionally, the river water will have

higher WQP values because of high flows and erosion, but lakes will contain significantly lower WQP values. For example, the five great lakes have average turbidity below 15 NTU year-round (Son & Wang, 2019), which would result in a lower impact on spectrophotometric detection of cyanobacteria. It should be noted that the DOC and turbidity for all the algal experiments add to the natural DOC and turbidity produced by algae (Adams et al., 2018). Different WQPs testing allowed for assessing method accuracy and sensitivity considering typical surface water conditions prone to cyanobacterial blooms.

Analysing two peaks (*Chl-a* and PC) simultaneously allows for the identification of cyanobacterial algae from common green algae (McQuaid et al., 2011). With increasing WQP levels, the photopigment PC showed a decreasing overall absorbance for spectrophotometric measurements while *Chl-a* continued to be consistently detected (Figure 7.1Figure 6.1). More research is needed to understand the molecular impact of higher level WQPs on cyanobacterial absorbance. Regulations and management practices for cyanobacteria around the world vary, at the same time, several water authorities follow recommendations set by the WHO (Chorus, 2012; WHO, 2017). According to WHO, a cyanobacterial biomass concentration of < 20,000 cells/mL is considered as low risk with minimal health effects on exposure in recreational waters (WHO, 2003, 2017). The aim of this study was to detect cyanobacteria at the lowest possible biomass so that the method could be useful as an early warning system with varying WQPs. The lowest detection limits were obtained after the application of S-G derivative method and using 100 mm cuvette pathlength. Apart from the 100 NTU turbidity and 30 ppt salinity tests, the MDL using the S-G method were all found to be below the WHO guideline of 20,000 cells/mL as shown

in Table 7.3 and Table 7.4, making the method described a promising application for real-time monitoring and early detection of cyanobacteria.

Calibration curves based on absorbance and concentration data are principally used to estimate unknown concentrations of cyanobacteria in source water (Burgess & Thomas, 2017; Millie et al., 2002). As this cyanobacterial study was conducted using multiple WQPs and with two major exposure times as well as pathlengths (i.e., 90 and 180 mins, and 50- and 100-mm, respectively), analyzing and comparing slopes (at both wavelengths of interest) becomes fundamental to understand potential changes/deviations for field monitoring application. Broadly, the two exposure times resulted in slopes of regression being approximate to each other at similar WQP levels and concentration ranges, suggesting that higher exposure would not impact the slope any further (see Table 7.3, Table 7.4 and Table F.5). For discussion purposes, higher exposure results are discussed hereon for reference. 50 mm pathlength slopes indicate higher slope stability with increasing WQP levels but lower sensitivity considering the overall detection limit. For example, consider turbidity 50 and 100 NTU using S-G derivative at *Chl-a* peak, their respective slopes were found to be $4.2938 \times 10^{-10} \pm 5.2199 \times 10^{-11}$ and $4.4151 \times 10^{-10} \pm 6.5436 \times 10^{-11}$, while the MDLs were calculated to be 31,587 and 76,775 cells/mL, respectively. Whereas for 100 mm pathlength, at the same peak and WQP levels, the slopes of regression were found to be $7.0836 \times 10^{-10} \pm 5.3408 \times 10^{-11}$ and $8.0379 \times 10^{-10} \pm 8.1501 \times 10^{-11}$; and the MDL was determined to be much lower at 13,833 and 46,834 cells/mL, respectively. With increasing WQP tests, a noticeable change in slope was observed using the 100 mm pathlength, which is expected as with longer pathlength, a higher quantity of incident light is absorbed by the sample (Burgess & Thomas, 2017). Additionally, at lower

WQP levels, comparable slopes are observed between different WQP; however, with an increasing amount of interferences (organic and/or inorganic) in a source sample, the calibration slopes deviated slightly as is expected and was also demonstrated in previous studies (AlMomani & Örmeci, 2018; Mukhopadhyay & Mason, 2013). For descriptive purposes, focusing on the highest level of WQPs namely 30 ppt salinity, 10 ppm DOC, and 100 NTU turbidity at PC peak using 100 mm pathlength; the slopes were observed to be at $5.2107 \times 10^{-10} \pm 6.2349 \times 10^{-12}$, $6.1079 \times 10^{-10} \pm 9.3379 \times 10^{-12}$, and $5.4611 \times 10^{-10} \pm 6.65744 \times 10^{-11}$, respectively, indicating a slight deviation from each other.

Cyanobacteria can be detected using several methods based on chromatography, screening assays, and/or molecular techniques such as qPCR (Al-Tebrineh et al., 2011; Azevedo et al., 2011). These techniques are very sensitive in terms of detection but require highly skilled personnel for operation, require sample preparation and/or toxin/pigment extraction, and cannot be implemented with ease for field monitoring of cyanobacteria (Liu et al., 2020; Zamyadi et al., 2016). The main advantage of the spectrophotometric method is that it can measure multiple water parameters (such as BOD, UV254, TSS, UVT, and Nitrogen-compounds) and microalgal photopigments concurrently (Burgess & Thomas, 2017; Mukhopadhyay & Mason, 2013). Furthermore, this method can be employed by on-line spectrophotometers to provide real-time quantification of algal concentration, which can greatly assist water authorities in making early decisions for source water management (AlMomani & Örmeci, 2018). Derivative spectrophotometry can be implemented using a code in spectrophotometric instruments for real-time results. This method does not require sample preparation/extraction, making it straightforward and easy to use. Additionally, the sample scan time can be reduced by narrowing the scan range based on monitoring need

(for example, 400 – 800 nm scan range in this study) and cyanobacterial concentrations as high as 3,800,000 cells/mL can be confidently detected using 100 mm pathlength. However, spectrophotometry is susceptible to slope changes with changing water parameters as discussed earlier and previous study conducted by Agberien & Örmeci (2019) reported that it was not possible to differentiate between non-toxigenic and toxigenic cyanobacteria using spectrophotometry (Burgess & Thomas, 2017). Despite applying derivative spectrophotometric method, the sensitivity is still lower than traditional methods, but the capability of one instrument to measure multiple components is a potentially affordable alternative for field monitoring and detection of cyanobacteria (Altenburger et al., 2015).

Fluorometry is a technique that gained popularity for field use for cyanobacterial monitoring due to its specificity, sensitivity and that it does not rely on a cuvette for analysis (Zamyadi et al., 2016). The detection limit of fluorometers has been reported to be as low as 2,000 cells/mL, but there has not been enough research verifying the consistency of the MDLs (Bowling et al., 2016; Garrido et al., 2019). However, fluorometry is incapable of multi-parameter and multi-pigment monitoring using a single instrument and has a lower working range (< 200,000 cells/mL) in comparison to spectrophotometry (Bowling et al., 2017). In addition, fluorometers measure biomass in terms of relative fluorescence units and have to be calibrated for a known/expected pigment before use (Bertone et al., 2018). Despite being more sensitive, fluorometry, as well as spectrophotometry, are impacted by similar sources of interferences. They include but are not limited to interferences such as varying cell pigment content, cell size, agglomeration, presence of the other phycobilin/*Chl-a* containing phytoplankton, viable but nonculturable

(VBNC) cells, water turbidity, temperature, light scattering and bias due to calibration algorithms (Liu et al., 2020; Zamyadi et al., 2016). For public safety, both monitoring methods while measuring photopigments assume that the cyanobacteria measured is potentially toxic and this information can be used as an early warning system to determine the correction steps required and whether detailed sample analysis is necessary.

7.5 Conclusion

The impact of critical water quality parameters (such as salinity, DOC, and turbidity) on spectrophotometric determination of cyanobacteria were investigated. Considering potential field application for real-time monitoring of cyanobacteria, studying these WQPs impact indicated that spectrophotometry when applied in tandem with higher cell pathlengths (100 mm) and derivative spectrophotometry, can be used for early detection and monitoring of cyanobacteria. Compared to traditional spectrophotometry, using Savitzky-Golay derivative method, the detection sensitivity was increased by a minimum of 2-fold and a maximum of 5-fold for different WQPs. The lowest MDL for *M. aeruginosa* using derivative spectrophotometry (100 mm pathlength) was found to be 11,083 cells/mL and 12,632 cells/mL for 1 ppm DOC at wavelengths 706-, and 660-nm, which correspond to the photopigments *Chl-a* and PC, respectively. Except for results from 100 NTU turbidity and 30 ppt salinity tests, all the other detection limits calculated using derivative spectrophotometry were found to be below the WHO guideline of 20,000 cells/mL, meaning low potential hazard of harmful health effects (WHO, 2017). Overall, with increasing WQP levels, the number of interfering particles increased, which in turn resulted in slight variations in slopes of calibration. Although less sensitive, 50 mm pathlength results showed higher stability in slope with changing WQPs when compared to 100 mm

results. The capability of spectrophotometry to measure multiple parameters and pigments simultaneously using a single instrument makes it a utilitarian tool for potential real-time monitoring purposes. This can result in reducing gross cost and space requirements associated with employing multiple instruments. Lastly, spectrophotometry is non-destructive and non-intrusive technique requiring no pigment extraction/reagent, simple, rapid, and can be implemented in the field for real-time monitoring purposes, which can consecutively assist water authorities to take prompt management decisions for source waters.

Acknowledgment

This research was funded by the Natural Sciences Engineering Research Council of Canada (NSERC) and CREATE grant (TEDGIEER) program. The authors would also like to thank Real Tech Inc. (Whitby, Ontario).

Conflicts of interest: The authors declare no conflict of interest.

7.6 References

- Adams, J. L., Tipping, E., Feuchtmayr, H., Carter, H. T., & Keenan, P. (2018). The contribution of algae to freshwater dissolved organic matter: Implications for UV spectroscopic analysis. *Inland Waters*, 8(1), 10–21. <https://doi.org/10.1080/20442041.2017.1415032>
- Agberien, A. V., & Örmeci, B. (2019). Monitoring of Cyanobacteria in Water Using Spectrophotometry and First Derivative of Absorbance. *Water*, 12(1), 124. <https://doi.org/10.3390/w12010124>
- Agriculture Victoria. (2018). *Measuring the salinity of water*. Agriculture Victoria.
- AlMomani, F. A., & Örmeci, B. (2018). Monitoring and measurement of microalgae using the first derivative of absorbance and comparison with chlorophyll extraction method. *Environmental Monitoring and Assessment*, 190(2), 90. <https://doi.org/10.1007/s10661-018-6468-y>
- Al-Tebrineh, J., Gehringer, M. M., Akcaalan, R., & Neilan, B. A. (2011). A new quantitative PCR assay for the detection of hepatotoxigenic cyanobacteria. *Toxicon*, 57(4), 546–554. <https://doi.org/10.1016/j.toxicon.2010.12.018>
- Altenburger, R., Ait-Aissa, S., Antczak, P., Backhaus, T., Barceló, D., Seiler, T.-B., Brion, F., Busch, W., Chipman, K., de Alda, M. L., de Aragão Umbuzeiro, G., Escher, B. I., Falciani, F., Faust, M., Focks, A., Hilscherova, K., Hollender, J., Hollert, H., Jäger, F., ... Brack, W. (2015). Future water quality monitoring—Adapting tools to deal with mixtures of pollutants in water resource management. *Science of The Total Environment*, 512–513, 540–551. <https://doi.org/10.1016/j.scitotenv.2014.12.057>
- Álvarez, S. D., Kruk, C., Martínez de la Escalera, G., Montes, M. A., Segura, A. M., & Piccini, C. (2020). Morphology captures toxicity in *Microcystis aeruginosa* complex: Evidence from a wide environmental gradient☆. *Harmful Algae*, 97, 101854. <https://doi.org/10.1016/j.hal.2020.101854>
- American Water Works Association (Ed.). (2011). *Algae: Source to Treatment* (1st ed.). American Water Works Association. (ISBN 1-58321-787-8)

- Azevedo, J., Osswald, J., Guilhermino, L., & Vasconcelos, V. (2011). Development and Validation of an SPE-HPLC-FL Method for the Determination of Anatoxin-a in Water and Trout (*Oncorhincus mykiss*). *Analytical Letters*, 44(8), 1431–1441. <https://doi.org/10.1080/00032719.2010.512682>
- Baxa, D. V., Kurobe, T., Ger, K. A., Lehman, P. W., & Teh, S. J. (2010). Estimating the abundance of toxic Microcystis in the San Francisco Estuary using quantitative real-time PCR. *Harmful Algae*, 9(3), 342–349. <https://doi.org/10.1016/j.hal.2010.01.001>
- Berry, J. P., Lee, E., Walton, K., Wilson, A. E., & Bernal-Brooks, F. (2011). Bioaccumulation of microcystins by fish associated with a persistent cyanobacterial bloom in Lago de Patzcuaro (Michoacan, Mexico). *Environmental Toxicology and Chemistry*, 30(7), 1621–1628. <https://doi.org/10.1002/etc.548>
- Bertone, E., Burford, M. A., & Hamilton, D. P. (2018). Fluorescence probes for real-time remote cyanobacteria monitoring: A review of challenges and opportunities. *Water Research*, 141, 152–162. <https://doi.org/10.1016/j.watres.2018.05.001>
- Bowling, L. C., Shaikh, M., Brayan, J., & Malthus, T. (2017). An evaluation of a handheld spectroradiometer for the near real-time measurement of cyanobacteria for bloom management purposes. *Environmental Monitoring and Assessment*, 189(10), 495. <https://doi.org/10.1007/s10661-017-6205-y>
- Bowling, L. C., Zamyadi, A., & Henderson, R. K. (2016). Assessment of in situ fluorometry to measure cyanobacterial presence in water bodies with diverse cyanobacterial populations. *Water Research*, 105, 22–33. <https://doi.org/10.1016/j.watres.2016.08.051>
- Burgess, C., & Thomas, O. (2017). UV-Visible Spectrophotometry of Water and Wastewater. In *UV-Visible Spectrophotometry of Water and Wastewater* (pp. 1–524). Elsevier. (ISBN 978-0-444-63897-7) <https://doi.org/10.1016/B978-0-444-63897-7.00001-9>

Canadian Psychological Culture Centre. (2013, September 16). *Canadian Psychological Culture Centre*. Canadian Psychological Culture Centre. <https://uwaterloo.ca/canadian-psychological-culture-centre/home>

Chorus, I. (2012). Current approaches to Cyanotoxin risk assessment, risk management and regulations in different countries. *Federal Environment Agency*, 2, 151.

Craig, I. W., & Carr, N. G. (1968). C-phycoerythrin and allophycoerythrin in two species of blue-green algae. *Biochemical Journal*, 106(2), 361–366. <https://doi.org/10.1042/bj1060361>

Dzialowski, A. R., Smith, V. H., Wang, S.-H., Martin, M. C., & Jr., F. deNoyelles. (2011). Effects of non-algal turbidity on cyanobacterial biomass in seven turbid Kansas reservoirs. *Lake and Reservoir Management*, 27(1), 6–14. <https://doi.org/10.1080/07438141.2011.551027>

EPA, U. (2015). *Recommendations for Public Water Systems to Manage Cyanotoxins in Drinking Water*. <https://www.epa.gov/sites/production/files/2017-06/documents/cyanotoxin-management-drinking-water.pdf>

Falconer, I. R. (1999). An Overview of problems caused by toxic blue–green algae (cyanobacteria) in drinking and recreational water. *Environmental Toxicology*, 14(1), 5–12. [https://doi.org/10.1002/\(SICI\)1522-7278\(199902\)14:1<5::AID-TOX3>3.0.CO;2-0](https://doi.org/10.1002/(SICI)1522-7278(199902)14:1<5::AID-TOX3>3.0.CO;2-0)

Furevik, B. R., Durand, D., & Pettersson, L. (2004). Multi-Sensor Synergy for Monitoring of Algal Blooms in the North Sea. *Proceedings of the 2004 Envisat & ERS Symposium (ESA SP-572)*, 7.

Garrido, M., Cecchi, P., Malet, N., Bec, B., Torre, F., & Pasqualini, V. (2019). Evaluation of FluoroProbe® performance for the phytoplankton-based assessment of the ecological status of Mediterranean coastal lagoons. *Environmental Monitoring and Assessment*, 191(4), 204. <https://doi.org/10.1007/s10661-019-7349-8>

Graham, J. L., Loftin, K. A., Meyer, M. T., & Ziegler, A. C. (2010). Cyanotoxin Mixtures and Taste-and-Odor Compounds in Cyanobacterial Blooms from the Midwestern United

States. *Environmental Science & Technology*, 44(19), 7361–7368.
<https://doi.org/10.1021/es1008938>

Health Canada. (2016). Cyanobacterial Toxins in Drinking Water—Document for Public Consultation. *Federal-Provincial-Territorial Committee on Drinking Water*, 1–171. (ISBN 0273-1223)

Hiriart-Baer, V. (2013). Dissolved organic matter quantity and quality in Lake Simcoe compared to two other large lakes in southern Ontario. *Inland Waters*, 3(2), 139–152.
<https://doi.org/10.5268/IW-3.2.535>

Hudnell, H. K. (Ed.). (2008). *Cyanobacterial Harmful Algal Blooms: State of the Science and Research Needs*. Springer. (ISBN 978-0-387-75864-0)

Huey, G. M., & Meyer, M. L. (2010). Turbidity as an Indicator of Water Quality in Diverse Watersheds of the Upper Pecos River Basin. *Water*, 2(2), 273–284.
<https://doi.org/10.3390/w2020273>

IHSS. (2020). *Elemental Compositions and Stable Isotopic Ratios of IHSS Samples* [Natural Organic Matter Research]. International Humic Substances Society. <http://humic-substances.org/elemental-compositions-and-stable-isotopic-ratios-of-ihss-samples/>

Johengen, T. (2016). *Protocols for the Performance Verification of In Situ Nutrient Analyzers Submitted to the Nutrient Sensor Challenge*. Alliance for Coastal Technologies; 08/08/2020. http://www.act-us.info/nutrients-challenge/Download/Nutrient_Challenge_Test%20Protocols_PV16_01.pdf

Kus, S., Marczenko, Z., & Obarski, N. (1996). Derivative UV-VIS Spectrophotometry in Analytical Chemistry. *Chern. Anal. (Warsaw)*, Department of Analytical Chemistry, Technical University of Warsaw, 00-664 Warszawa, Poland, 31.

Lane, C. E., Gutierrez-Wing, M. T., Rusch, K. A., & Benton, M. G. (2012). Homogeneous detection of cyanobacterial DNA via polymerase chain reaction: Uniform cyanobacteria PCR detection. *Letters in Applied Microbiology*, 55(5), 376–383.
<https://doi.org/10.1111/j.1472-765X.2012.03304.x>

- Li, Z., Zhao, Y., Xu, X., Han, R., Wang, M., & Wang, G. (2018). Migration and transformation of dissolved carbon during accumulated cyanobacteria decomposition in shallow eutrophic lakes: A simulated microcosm study. *PeerJ*, 6, e5922. <https://doi.org/10.7717/peerj.5922>
- Liu, J.-Y., Zeng, L.-H., & Ren, Z.-H. (2020). Recent application of spectroscopy for the detection of microalgae life information: A review. *Applied Spectroscopy Reviews*, 55(1), 26–59. <https://doi.org/10.1080/05704928.2018.1509345>
- Malhotra, A., & Örmeci, B. (2021). Monitoring of Cyanobacteria using Derivative Spectrophotometry and improvement of the method detection limit by changing pathlength. *Manuscript Submitted for Publication, Department of Civil and Environmental Engineering, Carleton University*, 1–46.
- McQuaid, N., Zamyadi, A., Prévost, M., Bird, D. F., & Dorner, S. (2011). Use of in vivo phycoerythrin fluorescence to monitor potential microcystin-producing cyanobacterial biovolume in a drinkingwater source. *J. Environ. Monit.*, 13(2), 455–463. <https://doi.org/10.1039/C0EM00163E>
- Millie, D. F., Schofield, O. M. E., Kirkpatrick, G. J., Johnsen, G., & Evens, T. J. (2002). Using absorbance and fluorescence spectra to discriminate microalgae. *European Journal of Phycology*, 37(3), 313–322. <https://doi.org/10.1017/S0967026202003700>
- Moreira, C., Ramos, V., Azevedo, J., & Vasconcelos, V. (2014). Methods to detect cyanobacteria and their toxins in the environment. *Applied Microbiology and Biotechnology*, 98(19), 8073–8082. <https://doi.org/10.1007/s00253-014-5951-9>
- Mukhopadhyay, S. C., & Mason, A. (Eds.). (2013). *Smart Sensors for Real-Time Water Quality Monitoring* (Vol. 4). Springer Berlin Heidelberg. (ISBN 978-3-642-37005-2) <https://doi.org/10.1007/978-3-642-37006-9>
- Oren, A. (2014). *Cyanobacteria: An Economic Perspective* (N. K. Sharma, A. K. Rai, & L. J. Stal, Eds.). John Wiley & Sons, Ltd. (ISBN 978-1-118-40223-8) <https://doi.org/10.1002/9781118402238.ch1>

- Owen, T. (1998). *Fundamentals of Modern UV-Visible Spectroscopy*. Hewlett-Packard Company. <https://trove.nla.gov.au/work/32688247>
- Pelaez, M., Antoniou, M. G., He, X., Dionysiou, D. D., de la Cruz, A. A., Tsimeli, K., Triantis, T., Hiskia, A., Kaloudis, T., Williams, C., Aubel, M., Chapman, A., Foss, A., Khan, U., O'Shea, K. E., & Westrick, J. (2010). Sources and Occurrence of Cyanotoxins Worldwide. In D. Fatta-Kassinos, K. Bester, & K. Kümmerer (Eds.), *Xenobiotics in the Urban Water Cycle* (Vol. 16, pp. 101–127). Springer Netherlands. (ISBN 978-90-481-3508-0) https://doi.org/10.1007/978-90-481-3509-7_6
- Rosen, B. H., Loftin, K. A., Graham, J. L., Stahlhut, K. N., Riley, J. M., Johnston, B. D., & Senegal, S. (2018). *Understanding the Effect of Salinity Tolerance on Cyanobacteria Associated with a Harmful Algal Bloom in Lake Okeechobee, Florida* (Scientific Investigations Report 2018–5092 No. 5092; p. 32). U.S. Geological Survey, U.S. Department of the Interior.
- Ruffin, C., King, R. L., & Younan, N. H. (2008). A Combined Derivative Spectroscopy and Savitzky-Golay Filtering Method for the Analysis of Hyperspectral Data. *GIScience & Remote Sensing*, 45(1), 1–15. <https://doi.org/10.2747/1548-1603.45.1.1>
- Saini, D. K., Pabbi, S., & Shukla, P. (2018). Cyanobacterial pigments: Perspectives and biotechnological approaches. *Food and Chemical Toxicology*, 120, 616–624. <https://doi.org/10.1016/j.fct.2018.08.002>
- Savitzky, Abraham., & Golay, M. J. E. (1964). Smoothing and Differentiation of Data by Simplified Least Squares Procedures. *Analytical Chemistry*, 36(8), 1627–1639. <https://doi.org/10.1021/ac60214a047>
- Sobiechowska-Sasim, M., Stoń-Egiert, J., & Kosakowska, A. (2014). Quantitative analysis of extracted phycobilin pigments in cyanobacteria—An assessment of spectrophotometric and spectrofluorometric methods. *Journal of Applied Phycology*, 26(5), 2065–2074. <https://doi.org/10.1007/s10811-014-0244-3>
- Son, S., & Wang, M. (2019). VIIRS-Derived Water Turbidity in the Great Lakes. *Remote Sensing*, 11(12), 1448. <https://doi.org/10.3390/rs11121448>

- Srivastava, A., Singh, S., Ahn, C.-Y., Oh, H.-M., & Asthana, R. K. (2013). Monitoring Approaches for a Toxic Cyanobacterial Bloom. *Environmental Science & Technology*, 47(16), 8999–9013. <https://doi.org/10.1021/es401245k>
- Stefanelli, M., Vichi, S., Stipa, G., Funari, E., Testai, E., Scardala, S., & Manganelli, M. (2014). Survival, growth and toxicity of *Microcystis aeruginosa* PCC 7806 in experimental conditions mimicking some features of the human gastro-intestinal environment. *Chémico-Biological Interactions*, 215, 54–61. <https://doi.org/10.1016/j.cbi.2014.03.006>
- Vincent, W. F. (2009). Cyanobacteria. In G. E. Likens (Ed.), *Encyclopedia of Inland Waters* (pp. 226–232). Academic Press. (ISBN 978-0-12-370626-3) <https://doi.org/10.1016/B978-012370626-3.00127-7>
- Voigtman, E. (2017). The Hubaux and Vos Method. In *Limits of Detection in Chemical Analysis* (pp. 325–329). John Wiley & Sons, Inc. (ISBN 978-1-119-18900-8) <https://doi.org/10.1002/9781119189008.app5>
- WDNR. (1996). *Analytical Detection Limit Guidance & Laboratory Guide for Determining Method Detection Limits* (Analytical Guide PUBL-TS-056-96). Wisconsin Department of Natural Resources Laboratory Certification Program. <https://dnr.wi.gov/regulations/labcert/documents/guidance/-LODguide.pdf>
- Whiting, M. (2017). *A Turbidity Study for the Union River and a Discussion of Water Level Fluctuations in Graham Lake*. 17.
- WHO. (2003). *Guidelines for Safe Recreational Water Environments: Coastal and fresh waters*. World Health Organization. (ISBN 978-92-4-154580-8)
- WHO. (2017). *Guidelines for drinking-water quality*. (ISBN 978-92-4-154995-0)
- Winter, J. G., DeSellas, A. M., Fletcher, R., Heintsch, L., Morley, A., Nakamoto, L., & Utsumi, K. (2011). Algal blooms in Ontario, Canada: Increases in reports since 1994. *Lake and Reservoir Management*, 27(2), 107–114. <https://doi.org/10.1080/07438141.2011.557765>

Ye, L., Shi, X., Wu, X., Zhang, M., Yu, Y., Li, D., & Kong, F. (2011). Dynamics of dissolved organic carbon after a cyanobacterial bloom in hypereutrophic Lake Taihu (China). *Limnologia*, *41*(4), 382–388. <https://doi.org/10.1016/j.limno.2011.06.001>

Zamyadi, A., Choo, F., Newcombe, G., Stuetz, R., & Henderson, R. K. (2016). A review of monitoring technologies for real-time management of cyanobacteria: Recent advances and future direction. *TrAC Trends in Analytical Chemistry*, *85*, 83–96. <https://doi.org/10.1016/j.trac.2016.06.023>

Zamyadi, A., McQuaid, N., Prévost, M., & Dorner, S. (2012). Monitoring of potentially toxic cyanobacteria using an online multi-probe in drinking water sources. *J. Environ. Monit.*, *14*(2), 579–588. <https://doi.org/10.1039/C1EM10819K>

Zhao, M., Qu, D., Shen, W., & Li, M. (2019). Effects of dissolved organic matter from different sources on *Microcystis aeruginosa* growth and physiological characteristics. *Ecotoxicology and Environmental Safety*, *176*, 125–131. <https://doi.org/10.1016/j.ecoenv.2019.03.085>

Appendix F

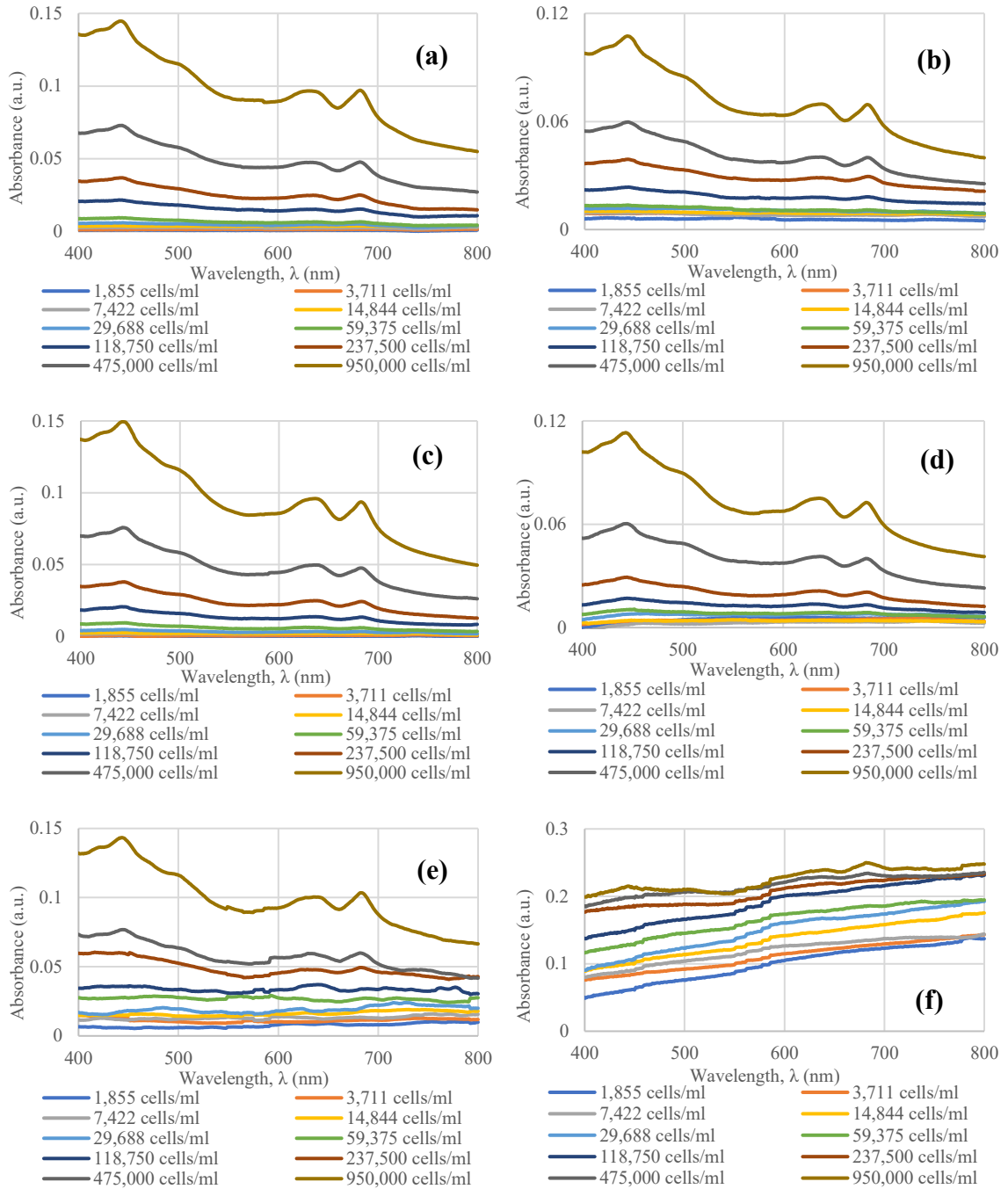


Figure F.5: Absorbance spectra of *M. aeruginosa* (180 mins exposure) using 100 mm cuvette pathlength for 10 and 30 ppt salinity (a, b), 1 and 10 ppm DOC (c, d), and 10 and 100 NTU turbidity (e, f).

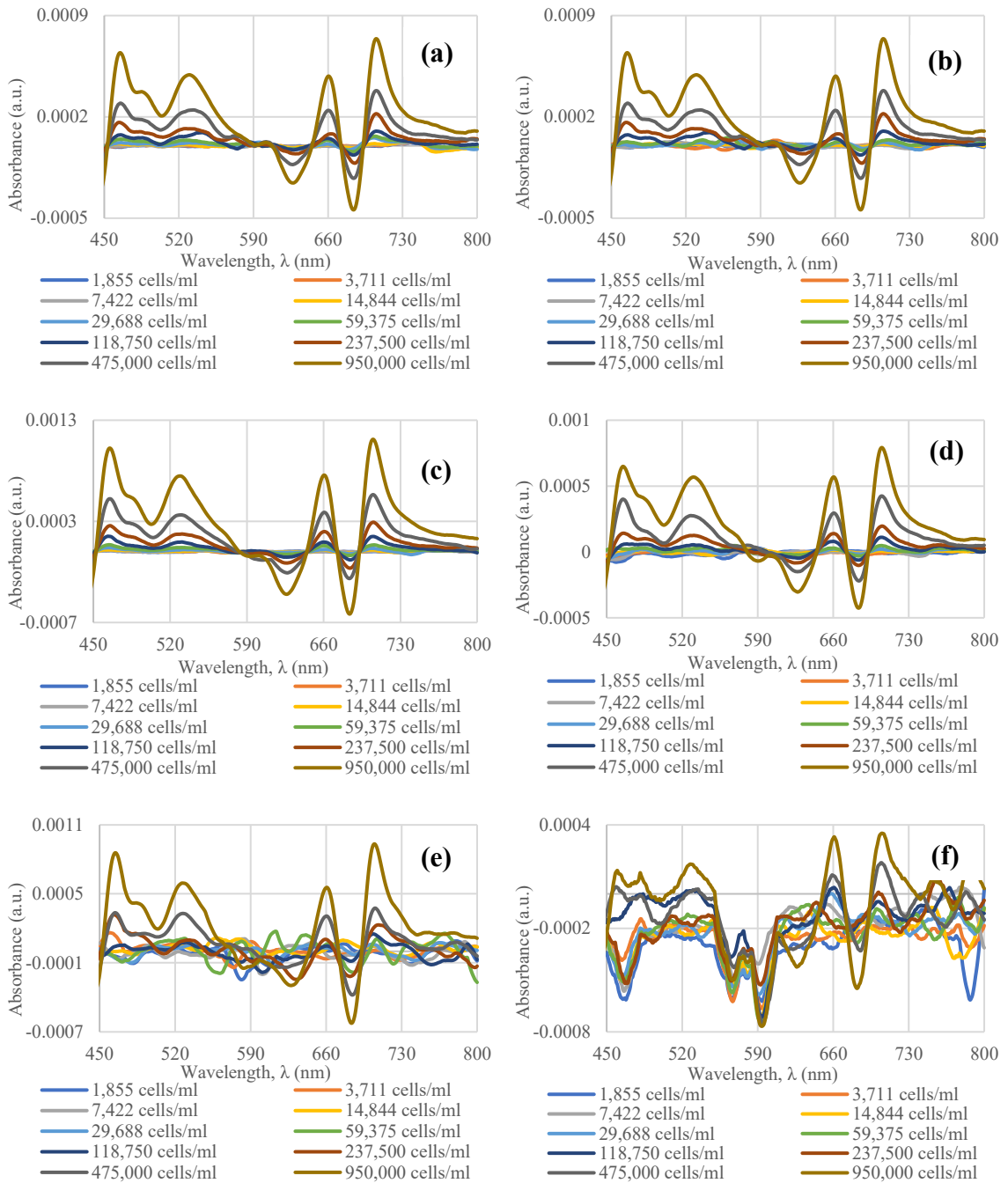


Figure F.6: Savitzky-Golay first derivative of absorbance spectra of *M. aeruginosa* (180 mins exposure) using 100 mm cuvette pathlength for 10 and 30 ppt salinity (a, b), 1 and 10 ppm DOC (c, d), and 10 and 100 NTU turbidity (e, f).

Table F.5: Critical data for *M. aeruginosa* in different water quality matrices for photopigments *Chl-a* and *Phycocyanin* over the concentration range (1,855 – 950,000 cells/mL) after 90 mins exposure.

Test	Pathlength (mm)	Parameter/Value	Slope	R ²	MDL (cells/mL)	
<i>M. aeruginosa</i> (Chlorophyll peak)						
Absorbance 682 nm	100	Salinity (ppt)	10	$9.6178 \times 10^{-08} \pm 4.7922 \times 10^{-10}$	0.9997	46,020
			20	$7.3056 \times 10^{-08} \pm 1.8412 \times 10^{-09}$	0.9949	59,676
			30	$6.5583 \times 10^{-08} \pm 2.4958 \times 10^{-09}$	0.9885	73,127
			10	$2.9015 \times 10^{-08} \pm 1.5971 \times 10^{-10}$	0.9996	70,658
			20	$2.8293 \times 10^{-08} \pm 4.4694 \times 10^{-10}$	0.9980	77,989
			30	$3.1363 \times 10^{-08} \pm 1.0266 \times 10^{-09}$	0.9915	89,661
	50	DOC (ppm)	1	$9.7963 \times 10^{-08} \pm 1.0718 \times 10^{-09}$	0.9990	33,110
			5	$7.9529 \times 10^{-08} \pm 1.3117 \times 10^{-09}$	0.9978	55,062
			10	$7.2000 \times 10^{-08} \pm 1.7370 \times 10^{-09}$	0.9953	70,881
			1	$4.4041 \times 10^{-08} \pm 9.1706 \times 10^{-10}$	0.9965	59,845
			5	$3.9425 \times 10^{-08} \pm 1.5883 \times 10^{-09}$	0.9871	80,513
			10	$3.4423 \times 10^{-08} \pm 8.7479 \times 10^{-10}$	0.9948	101,238

	100	Turbidity (NTU)	10	$7.5808 \times 10^{-08} \pm$ 7.4163×10^{-09}	0.9288	56,782	
			50	$6.0039 \times 10^{-08} \pm$ 2.9998×10^{-09}	0.8108	68,742	
			100	$7.5301 \times 10^{-08} \pm$ 3.4027×10^{-09}	0.8047	268,587	
	50		10	$3.7322 \times 10^{-08} \pm$ 1.7747×10^{-09}	0.9822	115,862	
			50	$3.9741 \times 10^{-08} \pm$ 9.5018×10^{-09}	0.8748	150,578	
			100	$3.2790 \times 10^{-08} \pm$ 9.9137×10^{-09}	0.8256	308,767	
S-G first derivative of absorbance 706 nm	100	Salinity (ppt)	10	$1.0979 \times 10^{-09} \pm$ 5.2883×10^{-12}	0.9997	11,118	
			20	$8.5991 \times 10^{-10} \pm$ 9.5617×10^{-12}	0.9990	16,162	
			30	$7.7587 \times 10^{-10} \pm$ 1.2843×10^{-11}	0.9978	18,146	
	50		10	$3.3655 \times 10^{-10} \pm$ 3.8035×10^{-12}	0.9987	20,567	
			20	$3.4799 \times 10^{-10} \pm$ 7.7677×10^{-12}	0.9960	30,362	
			30	$3.8132 \times 10^{-10} \pm$ 1.4661×10^{-11}	0.9883	38,198	
	100		DOC (ppm)	1	$1.1644 \times 10^{-09} \pm$ 7.5720×10^{-12}	0.9996	11,082
				5	$9.1014 \times 10^{-10} \pm$ 1.4380×10^{-11}	0.9980	13,862
				10	$7.9916 \times 10^{-10} \pm$ 2.2211×10^{-11}	0.9938	15,834

	50		1	$5.2546 \times 10^{-10} \pm$ 9.1701×10^{-12}	0.9975	13,985
			5	$4.4030 \times 10^{-10} \pm$ 8.5219×10^{-12}	0.9970	25,734
			10	$4.0603 \times 10^{-10} \pm$ 1.1985×10^{-11}	0.9930	26,871
	100	Turbidity (NTU)	10	$1.0462 \times 10^{-09} \pm$ 7.3007×10^{-11}	0.9625	11,143
			50	$7.1021 \times 10^{-10} \pm$ 8.6733×10^{-11}	0.8934	13,912
			100	$7.8583 \times 10^{-10} \pm$ 6.4435×10^{-11}	0.8936	46,902
	50	Turbidity (NTU)	10	$4.2677 \times 10^{-10} \pm$ 2.4983×10^{-11}	0.9733	31,577
			50	$3.9276 \times 10^{-10} \pm$ 2.2046×10^{-11}	0.8816	60,940
			100	$3.9132 \times 10^{-10} \pm$ 9.2677×10^{-11}	0.8431	76,841
	<i>M. aeruginosa</i> (Phycocyanin peak)					
Absorbance 632 nm	100	Salinity (ppt)	10	$9.5900 \times 10^{-08} \pm$ 4.7654×10^{-10}	0.9997	54,502
			20	$7.3391 \times 10^{-08} \pm$ 1.8927×10^{-09}	0.9947	71,877
			30	$6.6062 \times 10^{-08} \pm$ 2.4794×10^{-09}	0.9888	72,652
	50	Salinity (ppt)	10	$2.8886 \times 10^{-08} \pm$ 1.7241×10^{-10}	0.9996	87,906
			20	$2.8844 \times 10^{-08} \pm$ 6.1429×10^{-10}	0.9963	87,754
			30	$3.0969 \times 10^{-08} \pm$ 9.2677×10^{-11}	0.9925	95,120

				9.9397×10^{-10}		
	100	DOC (ppm)	1	$1.0018 \times 10^{-07} \pm$ 1.0386×10^{-09}	0.9991	36,124
			5	$8.2711 \times 10^{-08} \pm$ 1.2579×10^{-09}	0.9981	56,647
			10	$7.4514 \times 10^{-08} \pm$ 1.5957×10^{-09}	0.9963	74,368
	50		1	$4.5230 \times 10^{-08} \pm$ 7.5011×10^{-10}	0.9978	61,911
			5	$4.1303 \times 10^{-08} \pm$ 1.6412×10^{-09}	0.9875	86,022
			10	$3.5863 \times 10^{-08} \pm$ 7.4227×10^{-10}	0.9965	105,069
	100	Turbidity (NTU)	10	$7.6581 \times 10^{-08} \pm$ 6.9750×10^{-10}	0.9377	65,276
			50	$5.9768 \times 10^{-08} \pm$ 8.4560×10^{-09}	0.8524	77,823
			100	$8.4293 \times 10^{-08} \pm$ 8.1823×10^{-09}	0.8577	308,279
	50		10	$3.8976 \times 10^{-08} \pm$ 1.0590×10^{-09}	0.9941	119,971
			50	$3.4297 \times 10^{-08} \pm$ 5.7867×10^{-09}	0.8821	165,664
			100	$3.5921 \times 10^{-08} \pm$ 9.4246×10^{-09}	0.8237	390,031
S-G first derivative of absorbance 660 nm	100	Salinity (ppt)	10	$5.9785 \times 10^{-10} \pm$ 4.6530×10^{-12}	0.9993	18,886
			20	$5.4267 \times 10^{-10} \pm$ 6.7974×10^{-12}	0.9987	19,622
			30	$5.1151 \times 10^{-10} \pm$	0.9965	21,014

				1.0605×10^{-11}		
	50		10	$2.1574 \times 10^{-10} \pm$ 2.8619×10^{-12}	0.9982	30,382
			20	$2.1986 \times 10^{-10} \pm$ 8.9933×10^{-12}	0.9931	37,686
			30	$2.4748 \times 10^{-10} \pm$ 1.0365×10^{-11}	0.9861	42,874
	100	DOC (ppm)	1	$7.9694 \times 10^{-10} \pm$ 4.3725×10^{-12}	0.9997	12,638
			5	$7.2790 \times 10^{-10} \pm$ 9.9051×10^{-12}	0.9990	14,924
			10	$6.2112 \times 10^{-10} \pm$ 1.8072×10^{-11}	0.9932	19,171
	50		1	$3.5978 \times 10^{-10} \pm$ 3.7145×10^{-12}	0.9991	15,059
			5	$3.3437 \times 10^{-10} \pm$ 1.2386×10^{-11}	0.9891	28,576
			10	$3.2537 \times 10^{-10} \pm$ 9.3494×10^{-12}	0.9902	33,103
	100	Turbidity (NTU)	10	$6.2888 \times 10^{-10} \pm$ 4.5007×10^{-11}	0.9606	13,913
			50	$4.6187 \times 10^{-10} \pm$ 6.1711×10^{-11}	0.8765	19,147
			100	$5.2929 \times 10^{-10} \pm$ 7.2148×10^{-11}	0.8434	67,498
	50		10	$3.2374 \times 10^{-10} \pm$ 3.7757×10^{-11}	0.9018	36,362
			50	$3.3169 \times 10^{-10} \pm$ 2.1006×10^{-11}	0.8474	87,576
			100	$3.3437 \times 10^{-10} \pm$	0.8642	116,253

				6.5129×10^{-11}		
--	--	--	--	--------------------------	--	--

8. Sensitive Determination of Chromium (VI) using Derivative Spectrophotometry and Monitoring Implications in Different Water Matrices using Longer Pathlengths

Amitesh Malhotra and Banu Örmeci

Department of Civil and Environmental Engineering, Carleton University

1125 Colonel By Drive, Ottawa ON K1S 5B6, Canada

Abstract

In the present work, a simple method was proposed for the determination of Cr (VI) using spectrophotometry and longer cuvette pathlengths (50- and 100-mm), followed by application of Savitzky-Golay first-order derivative of absorbance to improve method detection limit (MDL). Effect of different water matrices (i.e., deionized (D.I.), surface, and tap water) and water quality parameters (i.e., pH, dissolved organic carbon (DOC)) were investigated at Cr (VI) concentrations ranging from 1 – 100 µg/L. The results obtained showed derivative spectrophotometry with 100 mm pathlength to be the most sensitive for Cr (VI) detection. Furthermore, the peaks of interest shifted in the absorbance spectra with changing pH and displayed higher stability and response with increasing pH under alkaline conditions, indicating the importance of pH for spectrophotometric monitoring of Cr (VI). DOC is another important parameter as presence of organics can reduce Cr (VI) to Cr (III), potentially impacting spectrophotometric measurements. A decrease in pH was observed with increasing DOC concentration; nonetheless, the peaks of interest stayed consistent despite increasing DOC. There was a strong linear relationship between chromium concentration and absorbance for all water matrix tests ($R^2 > 0.96$). Comparing the MDLs

of zero-order absorbance with derivative absorbance, the derivative method was more sensitive at least by 20%. Excellent MDLs were obtained with Cr (VI) detection limits as low as 2-, and 5- $\mu\text{g/L}$ for tap water and surface water, respectively. Overall, the results indicate that the derivative spectrophotometry can be used for in-lab measurement or real-time monitoring of Cr (VI) and the method proved to be sensitive even in environmental samples.

Keywords: chromium; water; monitoring; early detection; derivative spectrophotometry.

8.1 Introduction

Heavy metals such as hexavalent chromium can accumulate in the environment and pose a health risk to humans and animals alike. Cr (VI) is a pollutant that can be found naturally in plants, rocks, soils, river waters, groundwaters, and anthropogenically due to industrial processes such as electroplating or ore processing (Canter, 1985; EPA, 2010). In water, chromium exists in two oxidation states; trivalent Cr (III) and hexavalent Cr (VI) forms. Cr (VI) is the oxidized and most toxic form of chromium, whereas Cr (III) is the most stable and less oxidized form. Cr (III) predominates in soil as Cr (VI) is readily reduced to Cr (III) by organic matter. Cr (VI) is 100-fold more toxic than Cr (III) and is highly soluble in water, making it mobile (Saha et al., 2011). Cr (III) is an essential trace element required by the human body for maintaining normal physiological functions, while Cr (VI) is a known carcinogen and has potential mutagenic capabilities (McNeill et al., 2012; Moffat et al., 2018; Rockett et al., 2015). Jarczewska et al. (2015) conducted a study on absorption of Cr (VI) in the form of potassium dichromate ($\text{K}_2\text{Cr}_2\text{O}_7$), which resulted in a direct correlation between increasing dose and induced DNA damage in an immobilized system. The immobilized system was prepared by modifying gold disk electrodes with a monolayer

of double-stranded DNA (Jarczewska et al., 2015). Chronic exposure to Cr (VI) results in higher concentrations of chromium in red blood cells, plasma, liver, and kidney when ingested over a lifetime period (Moffat et al., 2018; Saha et al., 2011; WHO, 2017). Upon acute Cr (VI) ingestion, humans exhibit severe liver and kidney damage, cardiovascular collapse, and several gastrointestinal disorders. Several deaths have been reported due to acute exposure of chromium in children and adults (Agency for Toxic Substances and Disease Registry, 2012; Sutton, 2010). Hexavalent chromium is not effectively removed by traditional alum and ferric coagulants and hence, can pass through the drinking water treatment system with ease (Saha et al., 2011). Cr (VI) must be reduced to Cr (III) during the treatment process to meet safety standards for drinking water consumption (WHO, 2019). Instances of chromium contamination have been reported all over the world, including UK, Europe, the Americas (North & South), and Asia, increasing the need for early and sensitive detection of Cr (VI) in water sources (American Water Works Association, 2013; EPA, 1998, 2010; Health Canada, 2018; McLean et al., 2012; WHO, 2019).

With increasing industrial applications and growing wastewater generation, the need for monitoring will increase every year. The concentration of Cr (VI) in drinking water is regulated to low parts per billion (ppb) levels by water authorities worldwide. Regulations vary based on local government directives, and the countries without chromium regulations follow guidance values recommended by the World Health Organization (WHO), which is 50 µg/L of total chromium (WHO, 2019), and it is assumed that the amount measured contains potentially toxic Cr (VI) in totality (EPA, 2010; WHO, 2017). Table 8.1 shows a few examples of chromium guidance values in drinking water around the world. In

addition, the European Commission currently follows the WHO guideline for 50 µg/L as the maximum contaminant level for total chromium but plans to reduce the value by 50% by forcing the directive to 25 µg/L across Europe starting 2027 (European Commission, 2017). With the world trend moving towards a stricter guideline value for Cr (VI), quick and simple detection and monitoring techniques are imperative for Cr (VI) detection.

Table 8.1: Guidance values (GV) examples for total/hexavalent chromium in drinking water around the world.

Country/ Source	Contaminant	GV	Reference
Canada	Total chromium	50 µg/L	(Health Canada, 2018)
WHO	Total chromium	50 µg/L	(WHO, 2017)
EPA	Total chromium	100 µg/L	(EPA, 2010)
UK	Cr (VI)	50 µg/L	(Rockett et al., 2015)
Australia	Cr (VI)	50 µg/L	(NRMMC, 2017)
European Union	Total chromium	50 µg/L	(European Commission, 2017)

Given the low concentration detection requirement for Cr (VI), highly sensitive analytical methods are required for measurement. Current chromium detection methods rely on fluorometry, spectrophotometry, colorimetry, chemiluminescence, inductive coupled plasma-mass spectrometry, atomic absorption/emission spectrometry, chromatography based methods, and electrochemical methods (Elavarasi et al., 2014; Guertin et al., 2005; Harris & Lucy, 2015; Jena & Raj, 2008; Lace et al., 2019; Neubauer et al., 2003; Perkin Elmer, 2018; Sanchez-Hachair & Hofmann, 2018; Sanz-Medel et al., 2009; Vaz et al., 2017; Yarbro, 1976). Some of these techniques are highly sensitive and selective for

measuring Cr (VI). For example, a method using ion-chromatography in tandem with UV spectrophotometry reported the detection limit to be 0.015 $\mu\text{g/L}$ in drinking and tap water, but required sample preparation using solid-phase extraction (SPE) and formation of Cr (VI)-diphenylcarbazide (DPC) complex, before analysis (EPA, 2011). Techniques based on atomic absorption/emission spectrometry reported varying Cr (VI) method detection limits (MDL) based on the water matrix and ranged from 0.01 $\mu\text{g/L}$ in seawater to 145 $\mu\text{g/L}$ in groundwater (de Jong & Brinkman, 1978; Krishna et al., 2005). This high variability reduces reliability for early and rapid detection of Cr (VI). Most of the methods listed above require sample preparation commonly via SPE, acidification, liquid microextraction, solubilization, and/or using combination with ethylenediaminetetraacetic acid/DPC before sample analysis. This adds to method complexity, increases the time required to run a sample, and requires skilled personnel to operate and interpret results for quantification (Burgess & Thomas, 2017).

Spectrophotometry, on the other hand, is a well-established method that requires no pretreatment or sample preparation prior to analysis (Burgess & Thomas, 2017). Quantification of Cr (VI) using spectrophotometry is based on the absorption spectra of chromate and dichromate ions. Previous studies using spectrophotometry were conducted using 10 mm and 50 mm pathlength, which do not rely on any reagent or pretreatment showing viability for direct measurements (Sanchez-Hachair & Hofmann, 2018; Thomas et al., 1990). The study by Thomas et al. (1990) showed a detection limit of 10 $\mu\text{g/L}$ using the 50 mm pathlength for direct UV measurements of chromium and reported the method to be applicable for the 5 – 1000 $\mu\text{g/L}$ concentration range. A higher optical pathlength is thus necessary for the detection of Cr (VI) because of stringent effluent and drinking water

regulation constraints. Additionally, real-time spectrophotometers are available in the market which are capable of multi-component measurements such as dissolved organic matter (DOM), total organic carbon (TOC), biological and chemical oxygen demand (BOD & COD), UV-transmittance (UVT), and microalgae/cyanobacteria, among others (AlMamani & Örmeci, 2018; Burgess & Thomas, 2017; Malhotra & Örmeci, 2021). This makes them a low-cost, single equipment alternative to conventional water monitoring techniques. However, spectrophotometry has been known to be vulnerable to high spectral noise in the presence of absorbing organic/inorganic contaminants and is prone to baseline shifts with changing seasonal water properties (Owen, 1998). Nevertheless, studies have shown that the impact on resultant spectra due to baseline shifts can be reduced by applying derivative spectrophotometry techniques, indicating applicability (Agberien & Örmeci, 2019; Malhotra & Örmeci, 2021).

The aim of this research was to utilize longer pathlengths for the detection of Cr (VI) using spectrophotometry and investigate the application of derivative spectrophotometry to improve MDL. The focus was to develop a method that is non-intrusive and non-destructive and has the potential to be applied as an early monitoring system. Initial experiments using cuvettes of 10-, 50-, and 100-mm pathlengths were performed to analyze the improvement in Cr (VI) detection with increasing pathlength. Due to lack of testing in different water matrices, further experimentation was conducted using 100 mm pathlength to examine pH, surface water, tap water, and dissolved organic carbon (DOC) response on Cr (VI) detection in different water matrices. Finally, MDLs for all the tests were obtained, slopes were established, and sensitivity analyses were performed by comparing the zero-order absorbance data with the Savitzky-Golay first-order derivative of absorbance.

8.2 Materials and Methods

8.2.1 Sample preparation and characterization for analysis

Cr (VI) was prepared using analytical-reagent grade potassium dichromate (Sigma-Aldrich, $\geq 99.0\%$ purity, ACS reagent grade). To prepare 50 mg/L of stock Cr (VI) solution, 141.4 mg of dried potassium dichromate ($K_2Cr_2O_7$) crystals were dissolved in deionized (D.I.) water and diluted to 1000 mL (EPA, 1992). The fresh stock solution was prepared right before experimentation to avoid potential contamination and interferences in the spectral scans. Cr (VI) experiments used the following water matrices for testing: D.I. water, varying pH waters, surface water, tap water, and DOC water. Dilutions using stock Cr (VI) solution were performed by inoculating Cr (VI) in respective water matrices and performing dilutions to get 7 concentration levels ranging from 100 $\mu\text{g/L}$ to 1 $\mu\text{g/L}$. For each individual water matrix test, equivalent concentration levels were made, and the same concentration range was tested to aid in analysis. The prepared water matrices were verified on the day of the tests, and equipments used for verification were calibrated using their respective manufacturers' standards for accuracy purposes. All verification measurements were carried out in three technical replicates ($n = 3$) from each water matrix to ensure consistency.

8.2.1.1 D.I. water

Fresh D.I. water from Direct-Q UV Water Purification System (Millipore Sigma, USA) was used to prepare Cr (VI) sample dilutions on the day of the experiment. Stored water was not used for testing purposes as that could result in potential contamination and change to D.I. water properties.

8.2.1.2 pH water preparation

To prepare stock solutions at selected pH values, analytical grade sodium hydroxide (NaOH) and hydrochloric acid (HCL) were added to 1L of D.I. water in a clean, autoclaved glass container, and kept under constant stirring. Cr (VI) was tested at pH 5, 6, 7, 9 and 10. Most drinking water samples can be pH adjusted by adding 1 mL or less of adjustment buffer per 100 mL of sample, which introduces an acceptable 1% dilution error (Basumallick & Rohrer, 2016). The pH of the prepared water matrix was verified using a pH meter (Orion 5-star, Thermo Scientific, Canada) while under constant stirring. The pH of the final water matrix was measured as three technical replicates ($n = 3$), which had a standard deviation of ± 0.01 between individual readings.

8.2.1.3 Surface and tap water

A clean container was used to collect surface water from Rideau River (Ottawa, Ontario) on the day of the experiments, and the water was acclimatized to room temperature before use. Surface water was used without any filtration to better represent realistic environmental conditions during detection. Surface water was kept under continuous mixing at 200 rpm using a magnetic stirrer to avoid particulate settling during sample preparation. Tap water was collected on the day of the experiment using a clean and sterile glass bottle at Carleton University (Ottawa, Ontario) and was used as is for experimental purposes. Both surface and tap waters were analyzed for chemical oxygen demand (COD), hexavalent chromium, turbidity, total organic carbon (TOC), and pH using USEPA Reactor Digestion Method 8000, USEPA 1,5 diphenylcarbohydrazide method 8023, HACH 2100AN Turbidimeter (Hach, USA), Shimadzu TOC-V_{CPH/CPN} analyzer (Shimadzu Scientific Instruments, USA), and pH meter (Orion 5-star, Thermo Scientific, Canada). In

addition to these tests, tap water was analyzed for free and total chlorine using USEPA DPD (N,N-diethyl-p-phenylenediamine) method 8021 and 8167, respectively (EPA, 2010; Rice et al., 2017).

8.2.1.4 DOC water preparation

DOC water was prepared using EPA-recommended Upper Mississippi River Natural Organic Matter standard (cat # 1R110N), obtained from the International Humic Substance Society (IHSS, 2020; Johengen, 2016). DOC response was tested in the presence of 1-, 5-, and 10 mg/L C. To prepare 1 mg/L of DOC water, for example, 2 mg of the natural organic matter was mixed per 1000 mL of D.I. water. The DOC solution was stirred at a constant speed of 350 rpm using a magnetic stirrer to maintain a homogenous mixture during sample preparation. DOC preparation was established on the basis of the elemental composition of the standard material provided by the IHSS, where approximately 50% of the total composition consists of carbon (IHSS, 2020) as shown in Table 8.2.

Table 8.2: Elemental composition of Upper Mississippi River Natural Organic Matter standard (IHSS, 2020).

Cat. #	H ₂ O	Ash	C	H	O	N	S	P
1R110N	8.55	8.05	49.98	4.61	41.4	2.36	2.62	–

Where, H₂O content is the %(w/w) of H₂O in the air-equilibrated sample; Ash is the %(w/w) of inorganic residue in a dry sample; and C, H, O, N, S, and P are the elemental composition in %(w/w) of a dry, ash-free sample.

8.2.1.5 Hexavalent chromium verification

Initial analytical verification of prepared sample concentrations in the 10 – 100 µg/L range was performed using HACH method 8023 based on the USEPA 1,5 diphenyl carbohydrazid method to ensure that the concentrations used for testing were accurate. The

test samples for verification were prepared by inoculating Cr (VI) stock solution in D.I. water and subsequently analyzing them using a DR 2800 Spectrophotometer (HACH, CO, USA). As the method sensitivity is limited to 10 $\mu\text{g/L}$, the Cr (VI) concentration levels below 10 $\mu\text{g/L}$ were not verified.

8.2.2 UV-Vis Spectrophotometry

A Jenway 6850 Double Beam Spectrophotometer (Cole-Parmer, UK) was used for sample analysis. The spectrophotometer's light path was cleaned with lint-free foam swabs and warmed up for at least 30 mins before use to attain light source stability. The equipment was zeroed to D.I. water and calibrated prior to running any test. Initial D.I. water tests were conducted using 10-, 50-, and 100-mm pathlength quartz cuvettes, while all the other tests were conducted using only 100 mm pathlength. In order to maintain consistency, the same sample volume was maintained between all tests for the 10-, 50-, and 100-mm pathlengths at 3-, 17.5-, and 35-mL, respectively. The spectral absorbance scan was set over the range of 190 nm to 800 nm, with a constant step interval of 1 nm. The final absorbance values were obtained by subtracting the scanned blanks of the individual water matrix from the scanned absorbance values of Cr (VI) spiked samples . All samples were analyzed as three technical replicates ($n=3$). The same cuvettes, in the same orientation, were used for all the experiments to obtain representative results. The samples were analyzed starting from the lowest concentration towards higher concentration and the cuvettes were rinsed thoroughly using D.I. water between each experiment. All the tests were performed at standard room temperature and Cr (VI) was exposed to the individual water parameter that was tested for 60 mins before analysis.

8.2.3 Savitzky-Golay first-order derivative of absorbance

The use of first or higher derivatives by measuring the rate of change in absorbance with respect to the wavelength is known as derivative spectrophotometry (Burgess & Thomas, 2017). Derivative spectrophotometry does not increase the amount of information obtained from zero-order/normal spectrum; rather, it allows for data to be analyzed in a robust manner by amplifying the signal observed (Owen, 1995). Savitzky-Golay (S-G) first-order derivative of absorbance is a method that can be applied to obtain the simultaneous first-order derivative of absorbance and smoothen the observed data (Savitzky & Golay, 1964). The method performs a local polynomial regression for each data point by taking a set number of adjacent data points and applying the simplified least squares method to determine the final smoothed value (Chen et al., 2014). S-G method results in reduced noise features observed by traditional first-order derivative and strengthens the observed signal by increasing the number of distinct peaks observed (Ruffin et al., 2008). S-G first derivative of absorbance is calculated using:

$$a_j = \frac{\sum_{i=-\frac{m-1}{2}}^{\frac{m-1}{2}} C_i F_{j+i}}{N} \frac{m+1}{2} \leq j \leq n - \frac{m-1}{2}$$

Where, a_j = Savitzky-Golay first derivative of absorbance; m = number of data points used; F = absorbance value measured at a specific wavelength; C_i = Savitzky-Golay filter coefficient; j = smoothened data point; N = standardization factor.

Each absorbance data point was smoothened using twenty three distinct points so that $i = -11, -10, \dots, 10, 11$; $C_i = -11, -10, \dots, 10, 11$; $m = 23$; $N = 1012$; following a linear convolution and applying Savtizky-Golay recommended filter coefficients (Ruffin et al.,

2008; Savitzky & Golay, 1964). Further, S-G method is useful in removing slow-changing baselines and revealing spectral features, which are difficult to observe using traditional spectrophotometry and/or the first derivative of absorbance.

8.2.4 Establishing detection limits

The minimum detection limit for each individual test of Cr (VI) was calculated according to Hubaux and Vos (H-V) statistical method, which requires a minimum of 3 data points (with a maximum of 12) for the calculation of method detection limit (MDL) (Berthouex & Brown, 2002; Hubaux & Vos, 1970). A Microsoft Excel based calculator developed by Chemiasoft was used to determine MDL and the wavelength with the best sensitivity (highest peak) was selected. The H-V MDL is calculated based on the assumption that the measured absorbance and the standard concentration are linearly correlated (Voigtman, 2017). For high accuracy, 3 technical replicates ($n = 3$) at 7 concentration levels were used for the calculation of the MDL. All MDLs in this study were calculated at a minimum confidence level of 95%.

8.2.5 Statistical analysis

Microsoft Office Excel was used for statistical analysis of the measured Cr (VI) data. Zero-order absorbance and S-G first derivative of absorbance graphs were plotted over the entire test concentration range (100 $\mu\text{g/L}$ to 1 $\mu\text{g/L}$). Standard calibration curves were plotted at the wavelengths of interest to verify whether the data was in accordance with the Beer–Bouguer–Lambert Law. The mean values of the measured triplicates were used to plot the final curves, and linearity was verified by calculating the coefficient of determination (R^2) and slopes (\pm standard deviation) based on the wavelengths of peaks observed.

8.3 Results and Discussions

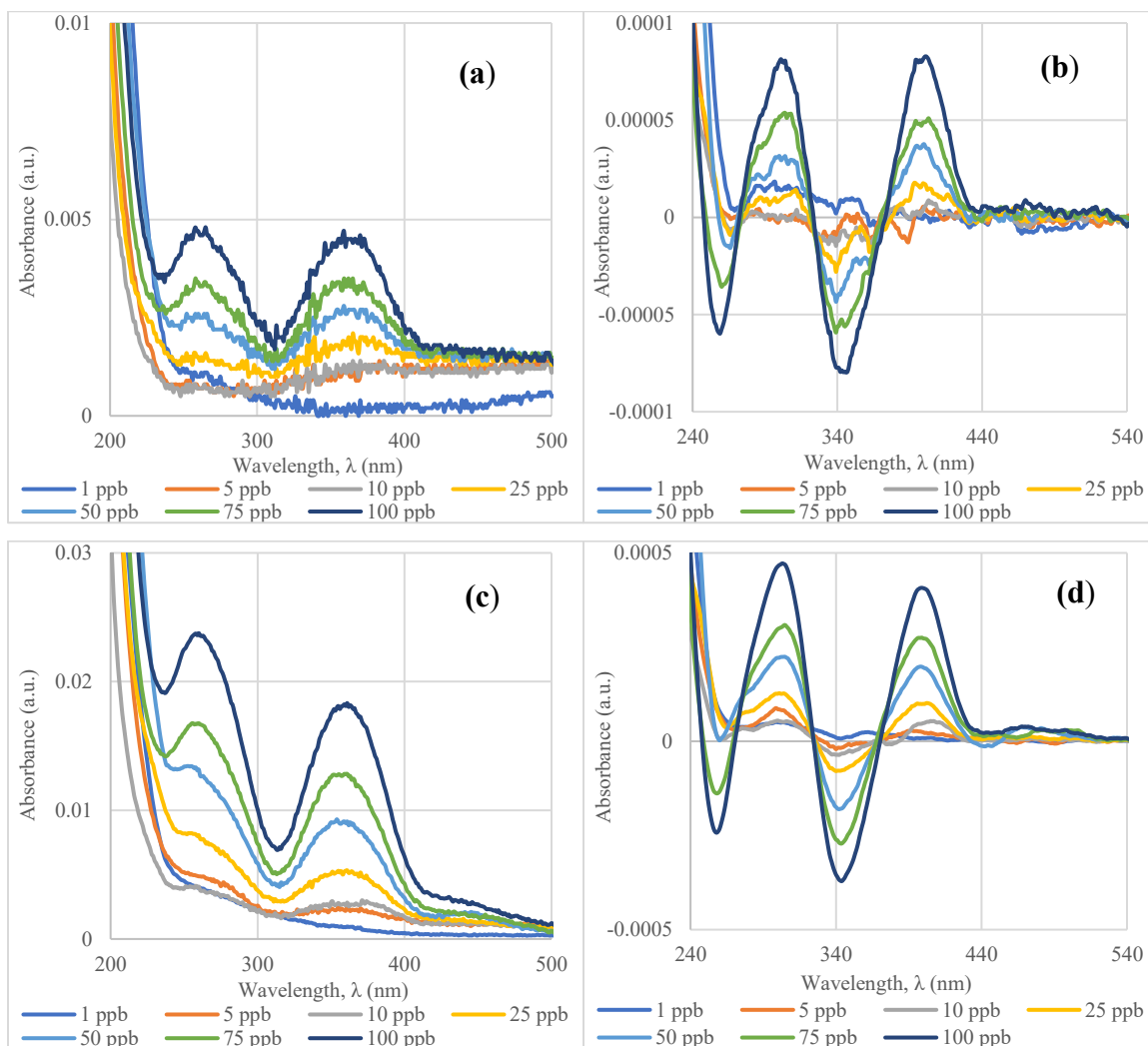
8.3.1 Spectrophotometric measurements of Cr (VI) in D.I. water

Initial spectrophotometric experiments for Cr (VI) determination were carried out using D.I. water to establish interference-free spectra and verify the applicability of spectrophotometry for detection by scanning between 190 and 800 nm wavelengths. 10-, 50-, and 100-mm cuvette pathlengths were employed to examine the improvement in detection with increasing pathlength. Cr (VI) can be found in 7 forms, namely: dichromate ($\text{Cr}_2\text{O}_7^{2-}$), chromate (CrO_4^{2-}), dihydrogen chromate (H_2CrO_4), hydrogen chromate (HCrO_4^-), hydrogen dichromate (HCr_2O_7^-), trichromate ($\text{Cr}_3\text{O}_{10}^{2-}$), and tetrachromate ($\text{Cr}_4\text{O}_{13}^{2-}$). Their distribution is based on the pH of the aqueous solution and of these, the last three ions do not exist in solutions where pH is greater than 0 (Rakhunde et al., 2012). The absorbance spectra of Cr (VI) solution in D.I. water resulted in two peaks (maximum absorbance wavelengths) of interest at 260 and 360 nm (Figure 8.1 a, c, e). The peaks were found to be consistent with changing cuvette pathlength. It was observed that the Cr (VI) compounds absorb light in the ultraviolet (UV) regions of the spectrum, with the first peak observed in the UV-C (100 – 280 nm) region, while the second peak observed in the UV-A (320 – 400 nm) region, which coincides with previously reported studies (Fournier-Salaün & Salaün, 2007; Sanchez-Hachair & Hofmann, 2018). When pH is greater than 6.4, CrO_4^{2-} predominates the solution. Both peaks represent Cr (VI) absorption with the UV-A peak representing direct CrO_4^{2-} absorption and the UV-C peak corresponding to the absorption due to charge transfer between O and Cr (VI) ion (Bensalem et al., 1997; Sanchez-Hachair & Hofmann, 2018).

In addition to zero-order absorbance, S-G first derivative of absorbance was applied to investigate the potential improvement in the detection of Cr (VI). S-G method resulted in sharper and more distinct peaks than the absorbance spectra. They were located at 304 and 400 nm, corresponding to the UV-C and UV-A peaks, respectively, observed in the zero-order absorbance spectra (Figure 8.1 b, d, f). A shift in peak was observed, which is expected and is a characteristic property of derivative spectrophotometry, as it was determined by plotting the rate of change in absorbance with respect to wavelength (Agberien & Örmeci, 2019; Kus et al., 1996). This study focused on the peak observed in the UV-A region, as most organic/inorganic compounds absorb light in the UV-C region, which can result in improper signals due to interfering particles (Buck et al., 1954; Burgess & Thomas, 2017). Further, as the peak of interest was in the UV region, the analysis focused on the wavelengths range from 200 – 500 nm.

For both traditional and derivative spectra (Figure 8.1), increasing cuvette pathlength resulted in higher overall absorbance and linearly increasing absorbance values with increasing Cr (VI) concentration, validating the Beer–Bouguer–Lambert Law (Burgess & Thomas, 2017). The coefficient of determination for all three pathlengths exhibited strong linear relationships between the measured absorbance and Cr (VI) concentration ($R^2 > 0.99$) at the representative UV-A peak. The MDLs calculated showed an improvement in detection with the application of the S-G derivative method and with increasing cuvette pathlength. For example, zero-order absorbance using 10 and 100 mm pathlength had the MDL values of 55 and 5 $\mu\text{g/L}$ Cr (VI), while the S-G derivative resulted in the MDL of 44 and 3 $\mu\text{g/L}$ Cr (VI), respectively (Table 8.4). By increasing pathlength from 10 to 100 mm, there was an approximately 11-fold improvement in detection for zero-order absorbance,

during which S-G derivative method resulted in an approximately 15-fold improvement with increasing pathlength. The results indicate that 100 mm pathlength was the most sensitive for detecting Cr (VI) and thus was be the primary pathlength for the remaining tests.



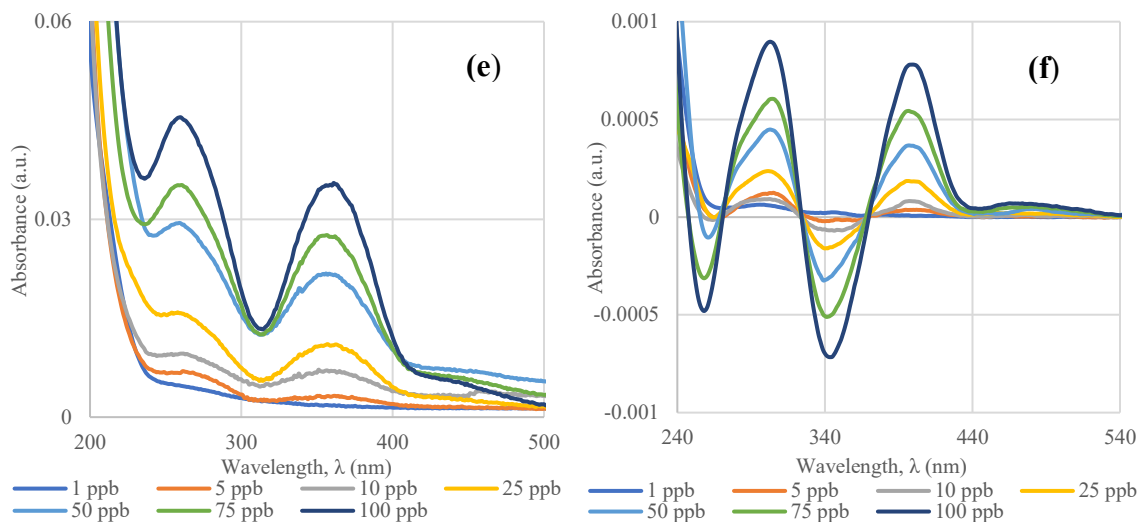


Figure 8.1: Absorbance and Savitzky-Golay first derivative of absorbance spectra of *Cr* (VI) in D.I. water using 10- (a, b), 50- (c, d), and 100 mm (e, f) cuvette pathlengths, respectively.

8.3.2 pH response

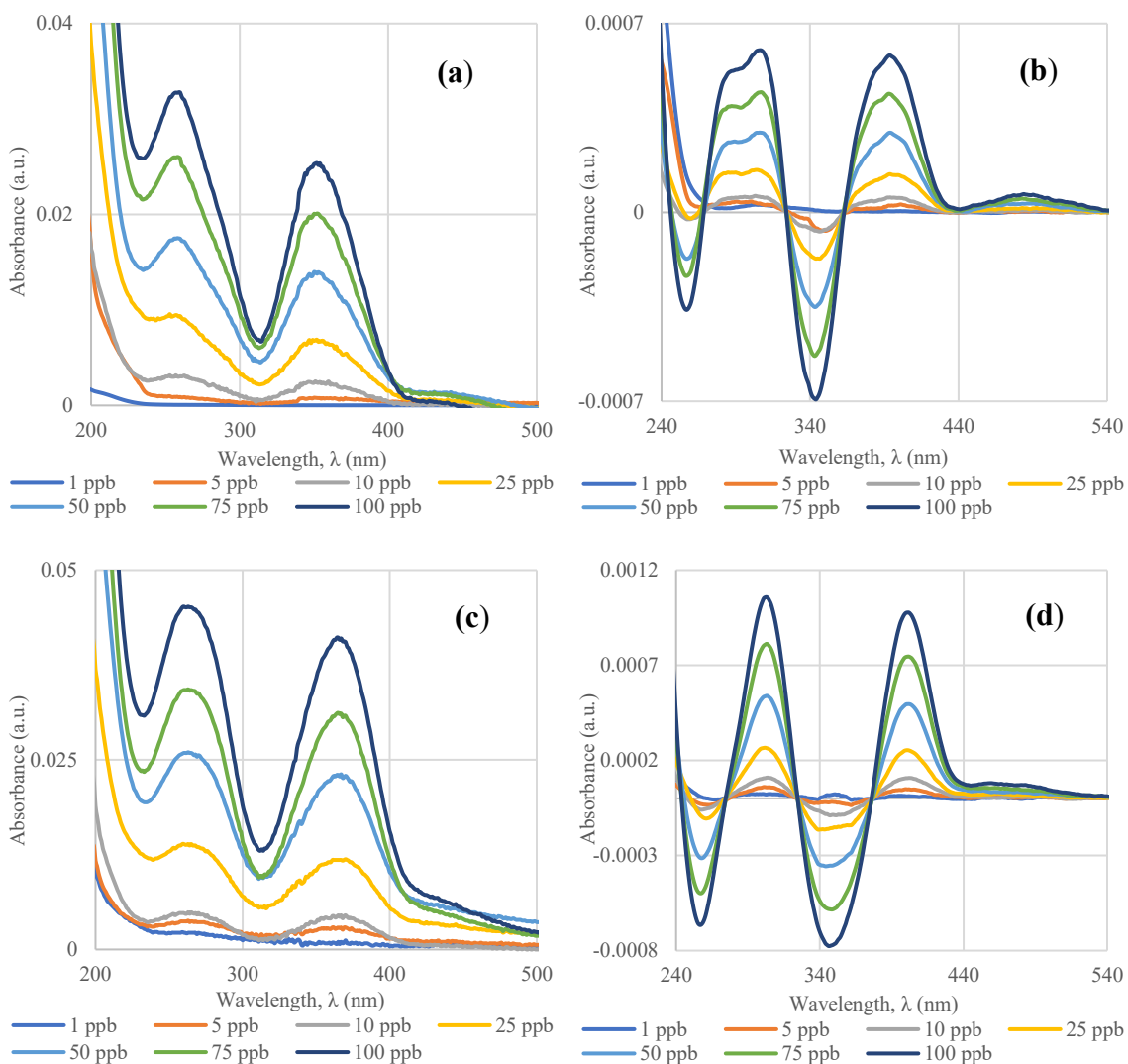
Studies have shown that the pH of the aqueous solution impacts *Cr* (VI) peaks observed via UV-Vis spectrophotometry (Buerge & Hug, 1997; Hagendorfer & Goessler, 2008; Rakhunde et al., 2012). The shift in peak with pH change of the solution makes studying pH a vital factor in detecting *Cr* (VI). Studies by Tandon et al. (1984) and Fournier-Salaün & Salaün (2007) reported the following: if the pH is between 4.2 – 6, the primary species that exist in the solution are CrO_4^{2-} (0.5% to 23%), HCrO_4^- (95% to 25%) and $\text{Cr}_2\text{O}_7^{2-}$ (5% to 1%); pH between 9 – 13.3 only consists of CrO_4^{2-} ; and at pH around 7, the species distribution in the solution comprises of CrO_4^{2-} (75%) and HCrO_4^- (25%). Further, they reported that the O–H bonding was the sole reason for shifts in absorption band, as long as no interference particles/reducing agents were present in the sample.

Cr (VI) in the presence of varying pH (from 5 – 10) was studied using 100 mm cuvette pathlength and absorbance spectra were obtained over the concentration range from 1 to

100 µg/L as illustrated in Figure 8.2 a, c, e, g, i. Analogous with the zero-order absorbance, two peaks of interest were observed, but the maximum absorbance wavelengths differed with changing pH. Increasing pH values resulted in shift of the UV-A peak gravitating towards visible region (as is expected and reported in previous studies) (Levitskaia et al., 2008). The UV-A peak at pH 5 was observed at 352 nm (Figure 8.2 a), while pH 6 and 7 displayed the peak at 364 and 370 nm (Figure 8.2 c, e), respectively. The peak for pH 9 and 10 was found to be at 372 nm, which is the maximum absorbance wavelength of Cr (VI) (Figure 8.2 g, i). With increasing pH from 7 to 10, a mild shift in peak was observed as chromate predominates in the solution and Cr (VI) as chromate exhibits a higher overall absorbance in comparison to hydrogen- and dihydrogen-chromate. Thus, resulting in a stronger UV-A peak response under alkaline conditions.

Similar to the D.I. water results, the S-G derivative graphs exhibited strong absorbance response and showed a shift in peak wavelength compared to the zero-order absorbance graph. The new peaks for pH 5, 6, 7, 9, and 10 were located at 394, 400, 402, 404, and 404 nm, respectively (Figure 8.2 b, d, f, h, j). Unlike zero-order absorbance, the peaks for S-G derivative were closer to each other. This can be attributed to the fact that S-G method relies on applying polynomial function over 23 data points to obtain the final derivative absorbance value. Both zero-order absorbance and S-G derivative of absorbance Cr (VI) tests for different pH water matrices displayed a strong linear relationship ($R^2 > 0.99$) between absorbance and Cr (VI) concentration, validating that the analysis followed Beer–Bouguer–Lambert Law. The slopes for absorbance graphs at lower pH values showed higher variation but with increasing pH, the slope values stabilized. Consider absorbance slopes for pH 5 and 7, they were found to be $2.6242 \times 10^{-04} \pm 6.4635 \times 10^{-06}$ and $4.0580 \times$

$10^{-04} \pm 1.0191 \times 10^{-05}$, respectively; whilst slopes were established at $9.9307 \times 10^{-04} \pm 1.4790 \times 10^{-05}$ and $9.2541 \times 10^{-04} \pm 1.3327 \times 10^{-05}$ for pH 9 and 10, respectively (Table 8.4). Likewise for S-G derivative, the slopes at higher pH exhibited lower variations as well. The MDLs calculated were found to improve in sensitivity with increasing pH (due to stronger absorbance response) and was estimated to be as low as 2 $\mu\text{g/L}$ at a pH of 10 using S-G derivative data. The MDLs obtained for S-G derivative were found to be slightly lower than zero-order absorbance and resulted in the overall improvement (greater than 20%).



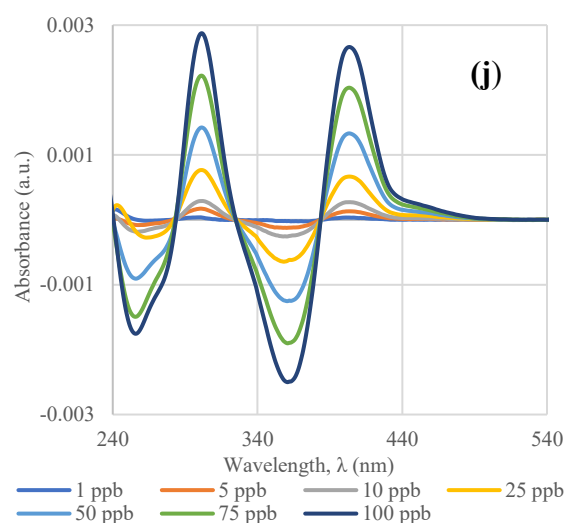
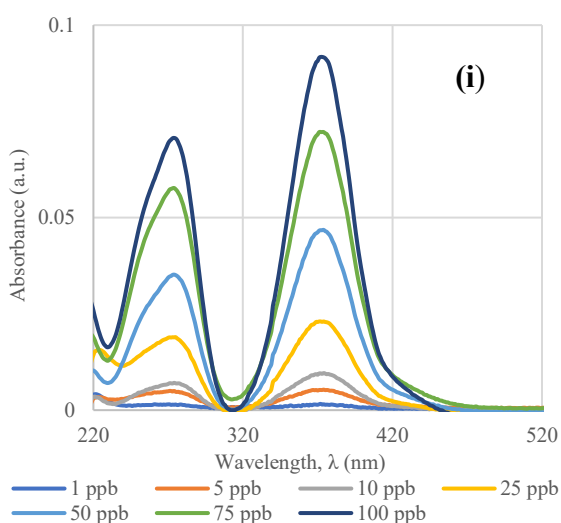
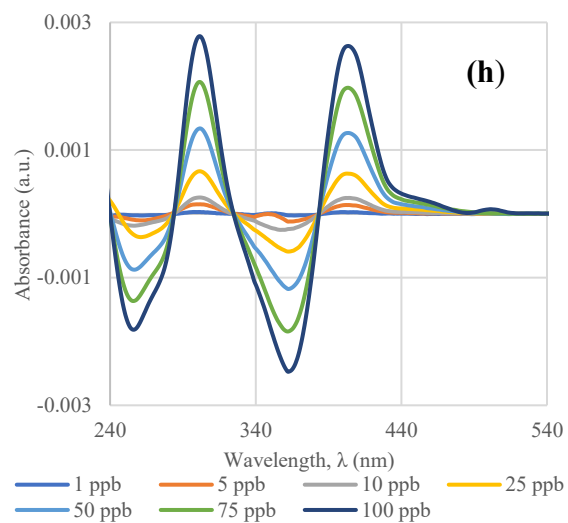
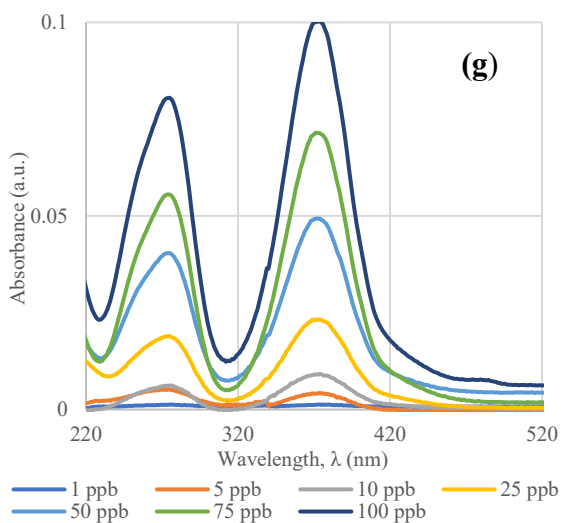
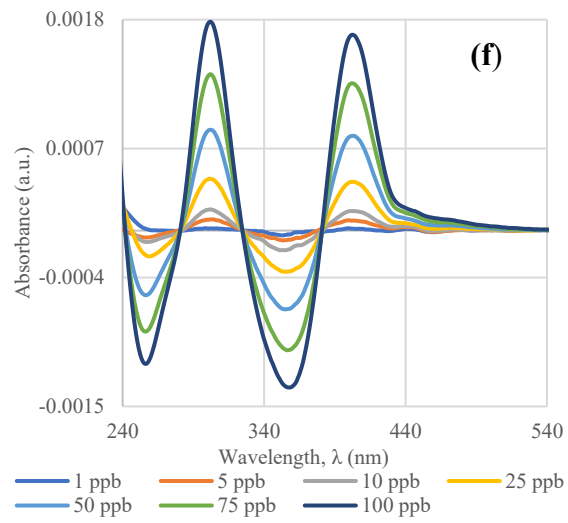
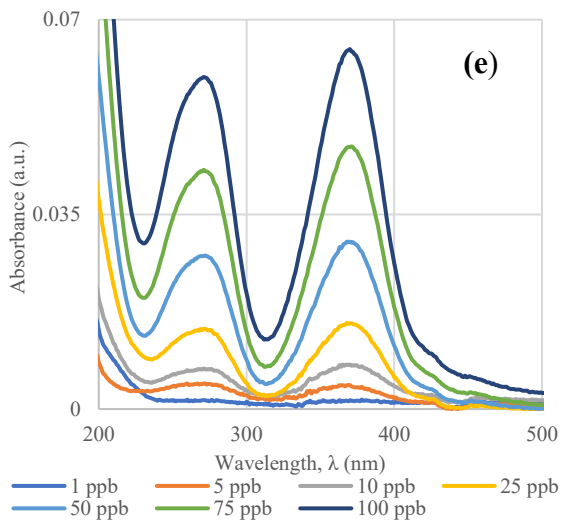


Figure 8.2: Absorbance and Savitzky-Golay first derivative of absorbance spectra of *Cr* (VI) using 100 mm cuvette pathlength at pH 5 (**a, b**), 6 (**c, d**), 7 (**e, f**), 9 (**g, h**), and 10 (**i, j**), respectively.

8.3.3 Surface and tap water response

To determine the applicability of the spectrophotometric method for Cr (VI) determination in uncontrolled environmental samples, tests were carried out using surface water and tap water source (without subjecting them to particulate filtration). The water source(s) were characterized for their pH, COD, TOC, turbidity, free- and total-chlorine as technical triplicates and their respective results in terms of mean values with standard deviation (SD) are shown in Table 8.3. Characterization assists in understanding the potential source of interferences observed during experimentation. The pH of both source waters was measured to be in the proximity of each other; whilst COD, TOC, and turbidity were found to be much higher for surface water than tap water as is expected in presence of natural contaminants. Primarily, surface water pH varies within 6.8 – 8.6; COD, DOC, and TOC are found between 2 – 30 mg/L, 0.7 – 15 mg/L, and 2 – 20 mg/L, respectively; whilst turbidity is generally below 20 NTU but in the presence of weather events, high turbidity (> 40 NTU) have been reported (Health Canada, 2019, 2020b; Jain & Singh, 2003; OEHHA, 2011; Potter & Wimsatt, 2005; Puig et al., 2016; Zamyadi et al., 2012). On the other hand, considering Canadian tap water quality data, pH ranges between 7 – 10.5; COD, DOC, TOC, and turbidity are present below 5 mg/L, 4 mg/L, 2 mg/L, and 1 NTU respectively; meanwhile guideline limits dictate free chlorine should be in the range of 0.04 – 2 mg/L and total chlorine should be below 4 mg/L (Health Canada, 2019, 2020a, 2020b; Moore et al., 1999). The results from surface and tap water characterization indicate that

they conform within conventionally observed values and thus, can act as a good representation of realistic conditions during monitoring.

Spectrophotometric measurements of Cr (VI) were carried out in surface and tap water over the concentration range from 1 – 100 µg/L (Figure 8.3). Similar to the results obtained from previous tests, the absorbance spectra of surface and tap water (Figure 8.3 a, c, respectively) resulted in two peaks observed at 274 and 372 nm, with the UV-A peak (at 372 nm) being the most prominent (to be used for Cr (VI) detection). For surface water (Figure 8.3 a), the peak in the UV-C region diminishes rapidly below 75 µg/L Cr (VI) concentration and overlapping spectral lines can be observed. This can be rationalized by the fact that natural samples contain interfering organic/inorganic contaminants (of varying degree), which can impact the peak observed in the absorbance spectra (Burgess & Thomas, 2017). The objective of testing using different source waters was not to characterize the impact of different water parameters on detection, rather to check the effectiveness of spectrophotometry using 100 mm cuvette pathlength for Cr (VI) detection.

Table 8.3: Results from surface water and tap water characterization (mean value ± SD).

Parameter	Surface Water	Tap Water
pH	8.02 ± 0.04	8.42 ± 0.05
COD (mg/L)	21 ± 1	5 ± 0.4
TOC (mg/L)	14.21 ± 1.19	2.04 ± 0.37
Turbidity (NTU)	12 ± 0.8	0.20 ± 0.02
Free Chlorine (mg-Cl ₂ /L)	–	0.10 ± 0.01
Total Chlorine (mg-Cl ₂ /L)	–	1.35 ± 0.02

The S-G first order derivative spectra for surface and tap water resulted in peaks to be observed at 302 and 404 nm wavelengths, corresponding to the UV-C and UV-A peaks observed in zero-order absorbance spectra. Comparing the surface water zero-order absorbance spectra with S-G derivative spectra (Figure 8.3 a, b), S-G spectra resulted in clearer spectral lines that do not overlap in the UV-C region over the concentration range of 25 – 100 µg/L. Nonetheless, both tests exhibited strong linear relationship ($R^2 > 0.98$) between absorbance and Cr (VI) concentration for zero-order and derivative spectra, supporting Beer–Bouguer–Lambert Law. The slopes for surface and tap water tests were found to be close to each other, indicating applicability of using spectrophotometry for sensitive Cr (VI) detection. For example, consider the absorbance spectra, the slopes for surface and tap water were found to be $8.4938 \times 10^{-04} \pm 4.1017 \times 10^{-05}$ and $8.6012 \times 10^{-04} \pm 2.0092 \times 10^{-05}$, respectively (Table 8.4). Additionally, pH of both source waters was measured in the alkaline range, which might explain the adjacency of observed slope. Further, the MDLs obtained using S-G derivative data was found to be more sensitive (> 20%) than their traditional counterparts. The lowest MDLs for Cr (VI) under surface and tap water were found to be 5 and 2 µg/L, respectively (Table 8.4). Upon comparing the D.I. water test with surface and tap water, the MDLs obtained were in close proximity to each other, indicating applicability.

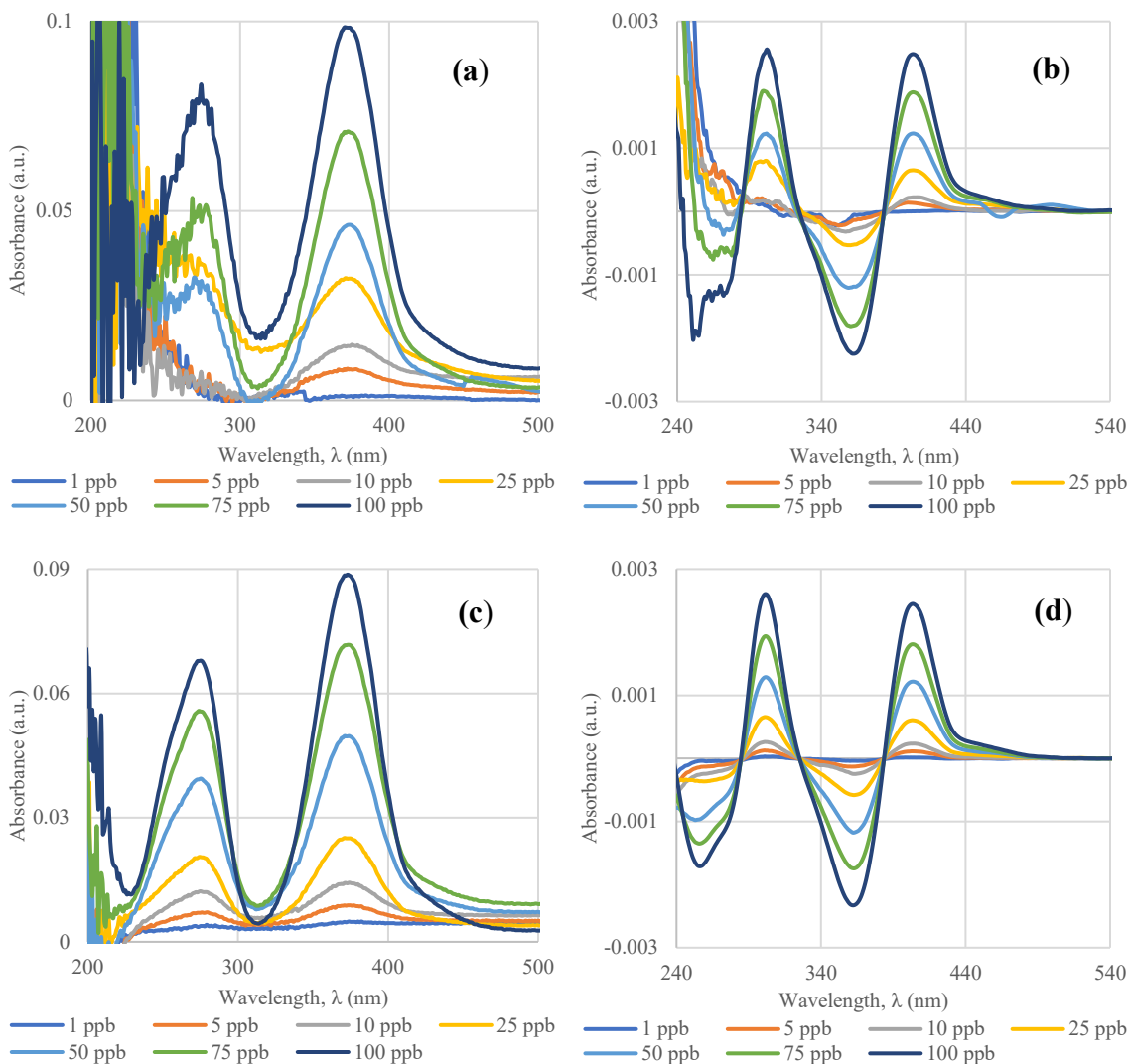


Figure 8.3: Absorbance and Savitzky-Golay first derivative of absorbance spectra of *Cr* (VI) in surface water (a, b) and tap water (c, d) using 100 mm cuvette pathlength.

8.3.4 DOC response

Spectrophotometric measurements of *Cr* (VI) were determined in the presence DOC at three concentration levels (aka 1, 5 and 10 mg/L), over the concentration range of 1 – 100 $\mu\text{g/L}$ *Cr* (VI). The test was conducted using a 100 mm pathlength to check the effect of DOC on *Cr* (VI) detection. The absorbance spectra of *Cr* (VI) resulted in two clear peaks at 258 and 352 nm wavelengths (corresponding to UV-C and UV-A regions) to be observed

at 1 mg/L of DOC (Figure 8.4 a); while at 5 mg/L of DOC exposure, the UV-C peak rapidly diminishes with reducing Cr (VI) concentration and is not visible below 50 $\mu\text{g/L}$ (Figure 8.4 c). On the other hand, with increasing DOC concentration to 10 mg/L, the UV-C peak completely disappears (Figure 8.4 e). This is likely because most organic compounds tend to absorb light in the UV-C region, resulting in increasing interference in observed absorbance, with higher DOC content (Mostofa et al., 2013). It should also be noted that, at 10 mg/L of DOC, the solution exhibits yellow color since it contains high levels of Humic substances. For DOC tests above 1 mg/L, it becomes difficult to readily distinguish between signal and noise observed at the UV-A peak below Cr (VI) concentration of 25 $\mu\text{g/L}$ (Figure 8.4 b, c). Nonetheless, the UV-A peak is more prominent and less prone to overall interferences in the presence of contaminants.

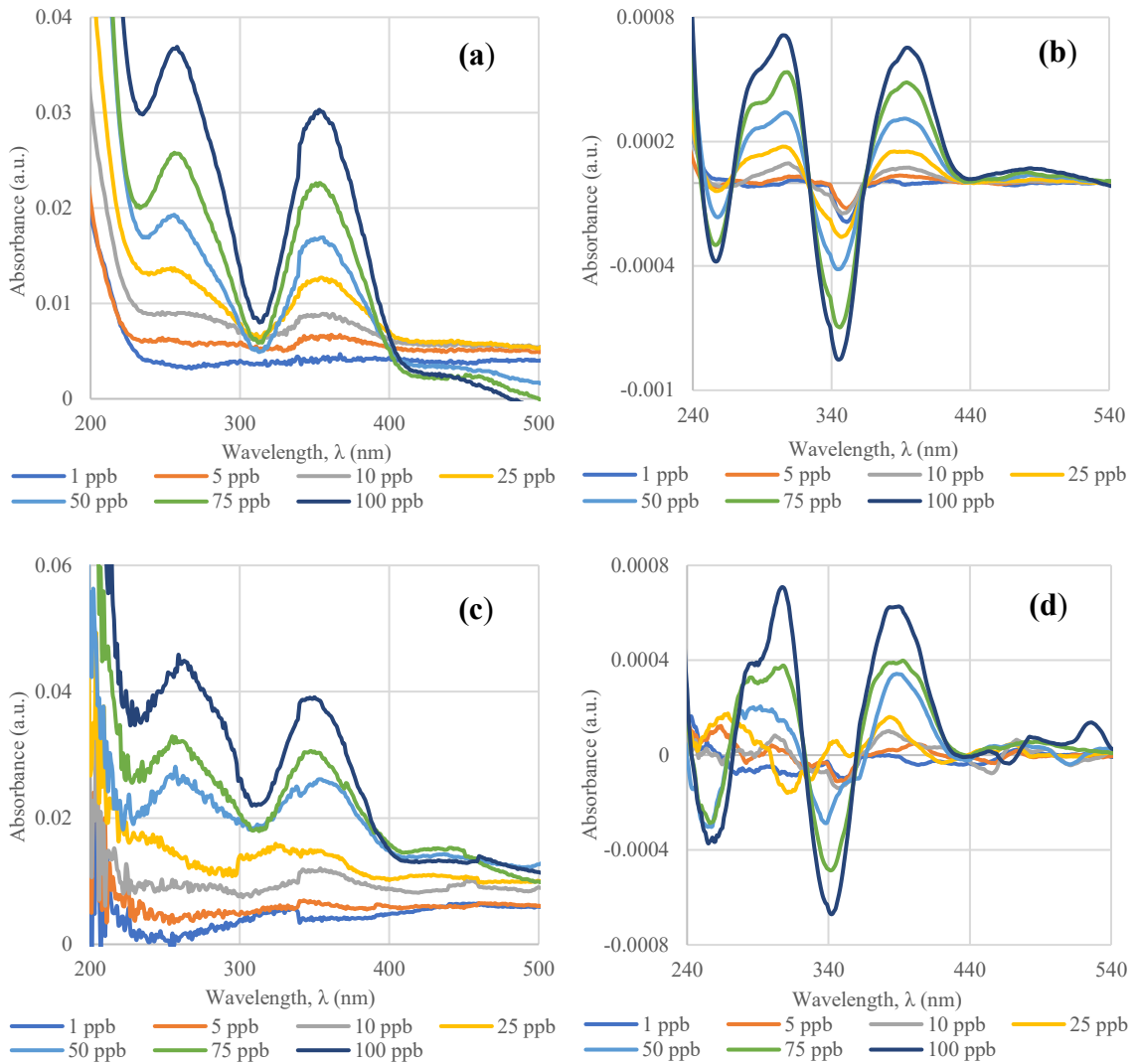
Research has shown that in the presence of organic matter, where a source of electrons is present and with decreasing pH, Cr (VI) reduces to Cr (III) (Chang et al., 2012; Stollenwerk & Grove, 1985). Further, some forms of dissolved sulfides and inorganic metals, such as Fe (II), can also reduce Cr (VI) (Buerge & Hug, 1998). These factors can potentially impact the overall Cr (VI) observed during spectrophotometric measurements, resulting in lower detection. Moreover, as it is known that pH plays an important role in Cr (VI) detection, the prepared DOC standards were tested for pH. For 1-, 5-, and 10-mg/L of DOC, the pH was measured at 5.60 ± 0.04 , 4.72 ± 0.06 , and 4.34 ± 0.03 , respectively. The measured pH indicates that increasing DOC content resulted in reducing pH, which can in turn lead to higher detection limits for Cr (VI).

To amplify the observed signal and improve detection of Cr (VI), the S-G derivative method was applied. In character with previous tests, the S-G derivative resulted in more

distinct peaks, aiding in analysis. The peaks of interest were observed at 307 and 387 nm wavelengths for the derivative spectra (Figure 8.4 b, d,f). In comparison to the zero-order absorbance, the derivative spectra for 5 and 10 mg/L DOC resulted in peaks observed at 25 $\mu\text{g/L}$ and 10 $\mu\text{g/L}$ (Figure 8.4 c, d, e, f). With increasing Cr (VI) concentrations, an incremental increase in measured absorbance was observed ($R^2 > 0.96$), following Beer–Bouguer–Lambert Law. In general, with increasing DOC concentration tests, the linearity decreased, which is expected as higher amount of compounds act as interfering particles for absorbance signal. For example, the coefficient of determination was found to be $R^2 = 0.9980$ and $R^2 = 0.9617$ using S-G derivative data at 1 and 10 mg/L of DOC (Table 8.4). However, the slopes at higher DOC concentrations were found to be approximately the same, while a mild variation was observed at low concentrations. The slopes obtained from absorbance data of 1-, 5-, and 10-mg/L DOC were found to be $2.4226 \times 10^{-04} \pm 1.2075 \times 10^{-05}$, $3.3775 \times 10^{-04} \pm 2.1215 \times 10^{-05}$, and $3.3813 \times 10^{-04} \pm 2.1461 \times 10^{-05}$, respectively.

Lastly, MDLs were calculated, and the lowest MDL was observed at 3 $\mu\text{g/L}$ for the 1 mg/L DOC test, using S-G derivative method. A 20% improvement in Cr (VI) detection was observed between the zero-order absorbance MDL and S-G derivative MDL at 1 mg/L DOC; however, with 5 and 10 mg/L DOC response tests, over 2-fold of improvement in detection was seen. For example, at 5 mg/L DOC, the zero-order absorbance and S-G derivative MDLs were calculated to be 33 $\mu\text{g/L}$ and 12 $\mu\text{g/L}$, respectively (Table 8.4). Comparing surface water tests to DOC response tests, surface water tests showed more favorable results in terms of detection (5 $\mu\text{g/L}$), despite having comparable organic matter. The measured pH of surface water was found to be in the alkaline range, which might have contributed to the sensitive detection of Cr (VI). Additionally, comparing DOC response

to D.I. water test using 100 mm pathlength, the slopes at higher DOC (5 and 10 mg/L) were found to be closer to the D.I. water test, but at lower DOC (1 mg/L), the slope displayed a deviation (Table 8.4). Further research is needed to understand the complex interactions of Cr (VI) with DOC to understand the impact on absorbance and overall detection.



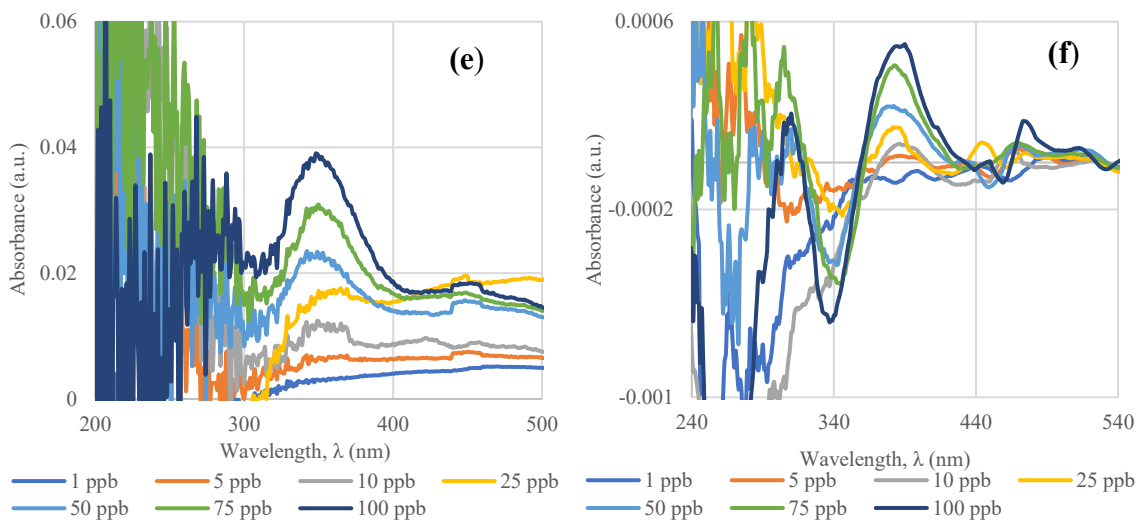


Figure 8.4: Absorbance and Savitzky-Golay first derivative of absorbance spectra of *Cr* (VI) using 100 mm cuvette pathlength at DOC 1- (a, b), 5- (c, d), and 10 mg/L (e, f), respectively.

Table 8.4: Summary of critical data for Cr (VI) in different water matrices over the concentration range (1 – 100 $\mu\text{g/L}$).

Parameter	Pathlength (mm) or value	Wavelength	Slope \pm standard deviation	R^2	MDL ($\mu\text{g/L}$)
Absorbance					
D.I	10	360 nm	$3.3565 \times 10^{-05} \pm$ 1.3169×10^{-06}	0.9923	55
	50		$1.6270 \times 10^{-04} \pm$ 4.9477×10^{-06}	0.9953	18
	100		$3.1853 \times 10^{-04} \pm$ 1.3583×10^{-05}	0.9909	5

pH	5	352 nm	$2.6242 \times 10^{-04} \pm$ 6.4635×10^{-06}	0.9969	10
	6	364 nm	$4.0580 \times 10^{-04} \pm$ 1.0191×10^{-05}	0.9968	6
	7	370 nm	$6.2614 \times 10^{-04} \pm$ 1.3631×10^{-05}	0.9976	4
	9	372 nm	$9.9307 \times 10^{-04} \pm$ 1.4790×10^{-05}	0.9988	4
	10	372 nm	$9.2541 \times 10^{-04} \pm$ 1.3327×10^{-05}	0.9989	3
DOC (mg/L)	1	352 nm	$2.4226 \times 10^{-04} \pm$ 1.2075×10^{-05}	0.9877	4
	5		$3.3775 \times 10^{-04} \pm$ 2.1215×10^{-05}	0.9806	33
	10		$3.3813 \times 10^{-04} \pm$ 2.1461×10^{-05}	0.9802	39
Surface water		372 nm	$8.4938 \times 10^{-04} \pm$ 4.1017×10^{-05}	0.9884	6
Tap water			$8.6012 \times 10^{-04} \pm$ 2.0092×10^{-05}	0.9972	4
S-G first derivative of absorbance					
D.I	10	400 nm	$7.2828 \times 10^{-07} \pm$	0.9907	44

			3.1472×10^{-08}		
	50		$3.8299 \times 10^{-06} \pm$ 1.3418×10^{-07}	0.9939	12
	100		$7.5255 \times 10^{-06} \pm$ 2.0455×10^{-07}	0.9963	3
pH	5	394 nm	$5.8691 \times 10^{-06} \pm$ 3.0013×10^{-08}	0.9998	8
	6	401 nm	$9.7787 \times 10^{-06} \pm$ 6.1195×10^{-08}	0.9998	4
	7	402 nm	$1.6681 \times 10^{-05} \pm$ 1.2494×10^{-07}	0.9997	3
	9	404 nm	$2.6298 \times 10^{-05} \pm$ 2.3282×10^{-07}	0.9996	3
	10	404 nm	$2.6608 \times 10^{-05} \pm$ 1.4583×10^{-07}	0.9998	2
DOC (mg/L)	1	387 nm	$6.5436 \times 10^{-06} \pm$ 1.2944×10^{-07}	0.9980	3
	5		$5.3795 \times 10^{-06} \pm$ 2.5904×10^{-07}	0.9885	12
	10		$5.4393 \times 10^{-06} \pm$ 4.8501×10^{-07}	0.9617	16
Surface water		404 nm	$2.4992 \times 10^{-05} \pm$	0.9995	5

		2.3311×10^{-07}		
Tap water		$2.4476 \times 10^{-05} \pm$ 1.0001×10^{-07}	0.9999	2

8.3.5 Cr (VI) verification results

The test was conducted using three technical replicates (n = 3). The USEPA 1,5 diphenyl carbohydrazide resulted in verifying individual concentration levels from 10 – 100 µg/L of Cr (VI) in D.I. water, with a maximum observed standard deviation value of 0.4. Concentrations below 10 µg/L were assumed to be linear with data verified between the concentration range of 10 – 100 µg/L.

Several analytical methods exist for quantification of Cr (VI), which rely on the individual or combined use of spectrophotometry, spectroscopy (mass, flame or atomic type), chromatography (such as ion-, or liquid- chromatography), inductive coupled plasma (ICP) and electrochemical methods (using nanoparticles or capillary electrophoresis) (Ernstberger & Neubauer, 2015; Guertin et al., 2005; Harris & Lucy, 2015; McSheehy et al., 2010; Perkin Elmer, 2018; Weldy et al., 2013). Some of these techniques are highly selective and sensitive for the detection of Cr (VI) and can detect Cr (VI) to as low as 0.01 µg/L using IC-MS (Basumallick & Rohrer, 2016). Currently, the Canadian Drinking Water Quality Guidelines rely on the EPA recommended method for Cr (VI) determination in drinking water (Method 218.7), which uses IC with post-column derivatization and UV-Vis spectroscopy, and has an MDL of 0.012 µg/L (Health Canada, 2016). Further, Weldy et al. (2013) reported an MDL of 2 µg/L for tap and river water samples using electrospray

ionization-mass spectrometry, but required DPC reagent and derivatization to attain the final sample for analysis. Most of these commonly used techniques are complex, require SPE/sample preparation and skilled personnel for operation, which lead to longer times for sample analysis (Fayad et al., 2015). Rapid determination is critical and of utmost importance to water managers, as it aids in applying timely corrective measures, which consecutively protects source waters and human health (Altenburger et al., 2015).

The proposed spectrophotometric method using 100 mm pathlength for determination of Cr (VI) in a variety of water matrices was found to be sensitive to detect concentrations below 20 µg/L. This is well below the WHO and Health Canada guidelines of 50 µg/L of total chromium (Health Canada, 2015, 2018; WHO, 2017). The results indicate feasibility in realistic conditions (such as surface and tap water) and show that with worsening water quality (increasing DOC), the Savitzky-Golay derivative method can be successfully applied to improve the sensitivity for Cr (VI) detection. Monitoring at source is important as hexavalent chromium is not effectively removed by traditional alum and ferric coagulants and hence, can pass through the drinking water treatment system with ease (Saha et al., 2011). Additionally, spectrophotometry has a broader working range of detection when compared to other techniques, and higher concentrations of Cr (VI) like in the case of industrial wastewaters can be easily monitored by using shorter cuvette pathlengths that do not rely on sample dilution (Guertin et al., 2005; Kowsalya et al., 2019). From a water monitoring and management perspective, spectrophotometry would be extremely beneficial as it can be used to simultaneously measure important water quality parameters such as UV254, UVT, BOD, COD, DOM, total suspended solids (TSS),

nitrogen compounds, and microalgae, among others, in tandem with Cr (VI) at source (AlMomani & Örmeci, 2018; Malhotra & Örmeci, 2021).

However, the detection is highly reliant on the pH of the sample, which in turn dictates the slope that can be applied for Cr (VI) quantification. For example, considering zero-order absorbance slopes in D.I. water and at a pH of 7, they were found to be $3.1853 \times 10^{-04} \pm 1.3583 \times 10^{-05}$ and $6.2614 \times 10^{-04} \pm 1.3631 \times 10^{-05}$, respectively, indicating deviation. However, at higher pH considering S-G derivative slopes for pH 9 and surface water (pH = 8), they were obtained at $2.6298 \times 10^{-05} \pm 2.3282 \times 10^{-07}$ and $2.4992 \times 10^{-05} \pm 2.3311 \times 10^{-07}$, respectively, demonstrating stability with increasing pH. A pH meter would be needed to accompany the spectrophotometer for Cr (VI) determination. Moreover, some metallic compounds like Cu (II), Fe (III), Pb (II), and Hg (II) can potentially result in interference for Cr (VI) measurement. However, Fe (III) is an exception as the error is lower than 5% if the iron concentration is between 0.5 – 1 mg/L, while the error in measurement due to other ions is lower than 15% for spectrophotometry (Buerge & Hug, 1998). Under acidic conditions, iron (III) absorbs at around 300 nm, which can result in interference when Fe^{3+} is dissolved in water. But, with increasing pH (up to a value of 9), the hydroxide form of iron precipitates and reduces interference for measurement (Burgess & Thomas, 2017). Typically, drinking water contains less than 1 mg/L of total iron, reducing probable interference (American Water Works Association, 2013). In addition, spectrophotometry is not able to readily differentiate between different forms of Cr (VI), but despite that Fournier-Salaün & Salaün (2007) showed a method which can be used to quantitatively determine total Cr (VI) concentration, by using molar absorptivity based on the pH of the sample. Nonetheless, this method can be applied at source for on-line

monitoring using existing real-time spectrophotometers without relying on sample preparation or reagents.

8.4 Conclusion

In this study, spectrophotometry was utilized for rapid detection of Cr (VI) and Savitzky-Golay first-order derivative of absorbance technique has been applied to improve the detection limit. The effect of changing cuvette pathlengths (10-, 50-, and 100-mm) was tested, and 100 mm cuvette pathlength was found to provide the most sensitive results. The proposed method using longer pathlengths is simple, requires no extraction, reagent, or sample preparation, and results have shown reliability for sensitive determination of Cr (VI) in realistic conditions. Further, variability in peaks was observed with altering pH and higher method stability (slopes) was observed with increasing (alkaline) pH values. DOC results indicated that with increasing concentration, pH reduced making it harder to determine Cr (VI). Despite that, the UV-C peak remained consistent aiding in analysis. The lowest MDLs were observed using the derivative method and were found to be as low as 2-, 3-, and 5- $\mu\text{g/L}$ in tap water, D.I. water and surface water, respectively. The MDLs obtained in this study were significantly lower than the recommended guideline value of 50 $\mu\text{g/L}$ by Health Canada, European Union and WHO (European Commission, 2017; Health Canada, 2018; WHO, 2017). Lastly, this method can be applied with ease in existing real-time spectrophotometers, that could be used for routine field monitoring and early detection of Cr (VI) without relying on expensive reagents/solvents that generate waste, are time-consuming, or alternative techniques that are intricate in nature.

Acknowledgment

This research was funded by the Natural Sciences Engineering Research Council of Canada (NSERC) and CREATE grant (TEDGIEER) program. The authors would also like to thank Real Tech Inc. (Whitby, Ontario).

Conflicts of interest: The authors declare no conflict of interest.

8.5 References

Agberien, A. V., & Örmeci, B. (2019). Monitoring of Cyanobacteria in Water Using Spectrophotometry and First Derivative of Absorbance. *Water*, 12(1), 124. <https://doi.org/10.3390/w12010124>

Agency for Toxic Substances and Disease Registry. (2012). *Toxicological Profile for Chromium* (p. 592). Agency for Toxic Substances and Disease Registry. <https://www.atsdr.cdc.gov/toxprofiles/tp7.pdf>

AlMomani, F. A., & Örmeci, B. (2018). Monitoring and measurement of microalgae using the first derivative of absorbance and comparison with chlorophyll extraction method. *Environmental Monitoring and Assessment*, 190(2), 90. <https://doi.org/10.1007/s10661-018-6468-y>

Altenburger, R., Ait-Aissa, S., Antczak, P., Backhaus, T., Barceló, D., Seiler, T.-B., Brion, F., Busch, W., Chipman, K., de Alda, M. L., de Aragão Umbuzeiro, G., Escher, B. I., Falciani, F., Faust, M., Focks, A., Hilscherova, K., Hollender, J., Hollert, H., Jäger, F., ... Brack, W. (2015). Future water quality monitoring—Adapting tools to deal with mixtures of pollutants in water resource management. *Science of The Total Environment*, 512–513, 540–551. <https://doi.org/10.1016/j.scitotenv.2014.12.057>

American Water Works Association. (2013). Chromium in Drinking Water: A Technical Information Primer. *American Water Works Association*, 11.

Basumallick, L., & Rohrer, J. (2016). Sensitive Determination of Hexavalent Chromium in Drinking Water. *Thermo Scientific, Application Update 179*, 6.

Bensalem, A., Weckhuysen, B. M., & Schoonheydt, R. A. (1997). In Situ Diffuse Reflectance Spectroscopy of Supported Chromium Oxide Catalysts: Kinetics of the Reduction Process with Carbon Monoxide. *The Journal of Physical Chemistry B*, 101(15), 2824–2829. <https://doi.org/10.1021/jp962488p>

Berthouex, P. M., & Brown, L. C. (2002). *Statistics for Environmental Engineers*. 463.

- Buck, R. P., Singhadeja, Samang., & Rogers, L. B. (1954). Ultraviolet Absorption Spectra of Some Inorganic Ions in Aqueous Solutions. *Analytical Chemistry*, 26(7), 1240–1242. <https://doi.org/10.1021/ac60091a051>
- Buerge, I. J., & Hug, S. J. (1997). Kinetics and pH Dependence of Chromium(VI) Reduction by Iron(II). *Environmental Science & Technology*, 31(5), 1426–1432. <https://doi.org/10.1021/es960672i>
- Buerge, I. J., & Hug, S. J. (1998). Influence of Organic Ligands on Chromium(VI) Reduction by Iron(II). *Environmental Science & Technology*, 32(14), 2092–2099. <https://doi.org/10.1021/es970932b>
- Burgess, C., & Thomas, O. (2017). UV-Visible Spectrophotometry of Water and Wastewater. In *UV-Visible Spectrophotometry of Water and Wastewater* (pp. 1–524). Elsevier. (ISBN 978-0-444-63897-7) <https://doi.org/10.1016/B978-0-444-63897-7.00001-9>
- Canter, L. W. (1985). *River water quality monitoring*. Lewis Publishers. (ISBN 978-0-87371-011-4)
- Chang, H., Singer, J. H., & Seaman, J. C. (2012). In Situ Chromium(VI) Reduction Using Iron(II) Solutions: Modeling Dynamic Geochemical Gradients. *Vadose Zone Journal*, 11(2). <https://doi.org/10.2136/vzj2011.0172>
- Chen, K., Zhang, H., Wei, H., & Li, Y. (2014). Improved Savitzky–Golay-method-based fluorescence subtraction algorithm for rapid recovery of Raman spectra. *Applied Optics*, 53(24), 5559. <https://doi.org/10.1364/AO.53.005559>
- de Jong, G. J., & Brinkman, U. A. Th. (1978). Determination of chromium(III) and chromium(VI) in sea water by atomic absorption spectrometry. *Analytica Chimica Acta*, 98(2), 243–250. [https://doi.org/10.1016/S0003-2670\(01\)84052-6](https://doi.org/10.1016/S0003-2670(01)84052-6)
- Elavarasi, M., Alex, S. A., Chandrasekaran, N., & Mukherjee, A. (2014). Simple fluorescence-based detection of Cr(III) and Cr(VI) using unmodified gold nanoparticles. *Anal. Methods*, 6(24), 9554–9560. <https://doi.org/10.1039/C4AY01978D>

- EPA. (1992). *SW-846 Test Method 7196A: Chromium, Hexavalent (Colorimetric)*. EPA. <https://www.epa.gov/sites/production/files/2015-12/documents/7196a.pdf>
- EPA. (1998). *Toxicological Review of Hexavalent Chromium*. EPA. https://cfpub.epa.gov/ncea/iris/iris_documents/documents/toxreviews/0144tr.pdf
- EPA. (2010). *Chromium-6 in Drinking Water*. EPA. <https://www.bendoregon.gov/home/showdocument?id=2737>
- EPA. (2011). Method 218.7: Determination of Hexavalent Chromium in Drinking Water by Ion Chromatography with Post-Column Derivatization and UV-Visible Spectroscopic Detection. *U. S. ENVIRONMENTAL PROTECTION AGENCY*, 31.
- Ernstberger, H., & Neubauer, K. (2015). Chromium Speciation in Drinking Water by LC-ICP-MS. *PerkinElmer, Application Note*, 6.
- European Commission. (2017). *Directive of the European parliament and of the council on the quality of water intended for human consumption (recast) (753 final)*. https://eur-lex.europa.eu/resource.html?uri=cellar:8c5065b2-074f-11e8-b8f5-01aa75ed71a1.0016.02/DOC_1&format=PDF
- Fayad, P. B., Roy-Lachapelle, A., Duy, S. V., Prévost, M., & Sauvé, S. (2015). On-line solid-phase extraction coupled to liquid chromatography tandem mass spectrometry for the analysis of cyanotoxins in algal blooms. *Toxicon*, 108, 167–175. <https://doi.org/10.1016/j.toxicon.2015.10.010>
- Fournier-Salaün, M.-C., & Salaün, P. (2007). Quantitative determination of hexavalent chromium in aqueous solutions by UV-Vis spectrophotometer. *Open Chemistry*, 5(4), 1084–1093. <https://doi.org/10.2478/s11532-007-0038-4>
- Guertin, J., Jacobs, J. A., Avakian, C. P., & Independent Environmental Technical Evaluation Group (Eds.). (2005). *Chromium (VI) handbook*. CRC Press. (ISBN 978-1-56670-608-7)

Hagendorfer, H., & Goessler, W. (2008). Separation of chromium(III) and chromium(VI) by ion chromatography and an inductively coupled plasma mass spectrometer as element-selective detector. *Talanta*, 76(3), 656–661. <https://doi.org/10.1016/j.talanta.2008.04.010>

Harris, D. C., & Lucy, C. A. (2015). *Quantitative Chemical Analysis* (9th ed.). Kate Parker. (ISBN 978-1-4641-3538-5)

Health Canada. (2015). *Chromium in Drinking Water*. Federal-Provincial-Territorial Committee on Drinking Water. <https://www.canada.ca/content/dam/canada/health-canada/migration/healthy-canadians/health-system-systeme-sante/consultations/chromium-chrome/alt/chromium-chrome-eng.pdf>

Health Canada. (2016). *Guidelines for Canadian drinking water quality: Guideline technical document - pH of drinking water*. (ISBN 978-0-660-04436-1) <http://oaresource.library.carleton.ca/wcl/2016/20160519/H144-28-2016-eng.pdf>

Health Canada. (2018). *Guidelines for Canadian drinking water quality: Guideline technical document - chromium*. Federal-Provincial-Territorial Committee on Drinking Water (Canada). (ISBN 978-0-660-06563-2) http://epe.lac-bac.gc.ca/100/201/301/weekly_acquisitions_list-ef/2018/18-07/publications.gc.ca/collections/collection_2018/sc-hc/H144-36-2017-eng.pdf

Health Canada. (2019). *Guidance on Natural Organic Matter in Drinking Water*. Health Canada. <https://www.canada.ca/content/dam/hc-sc/documents/programs/consultation-organic-matter-drinking-water/NOM20190129-eng.pdf>

Health Canada. (2020a). *Guidance on natural organic matter in drinking water*. Health Canada. (ISBN 978-0-660-33628-2) https://epe.lac-bac.gc.ca/100/201/301/weekly_acquisitions_list-ef/2020/20-31/publications.gc.ca/collections/collection_2020/sc-hc/H144-67-2020-eng.pdf

Health Canada. (2020b). *Guidelines for Canadian Drinking Water Quality Summary Table*. Federal-Provincial-Territorial Committee on Drinking Water of the Federal-Provincial-Territorial Committee on Health and the Environment. <https://www.canada.ca/content/dam/hc-sc/migration/hc-sc/ewh->

sem/alt_formats/pdf/pubs/water-eau/sum_guide-res_recom/summary-table-EN-2020-02-11.pdf

Hubaux, Andre., & Vos, Gilbert. (1970). Decision and detection limits for calibration curves. *Analytical Chemistry*, 42(8), 849–855. <https://doi.org/10.1021/ac60290a013>

IHSS. (2020). *Elemental Compositions and Stable Isotopic Ratios of IHSS Samples* [Natural Organic Matter Research]. International Humic Substances Society. <http://humic-substances.org/elemental-compositions-and-stable-isotopic-ratios-of-ihss-samples/>

Jain, S. K., & Singh, V. P. (2003). Chapter 13—Water Quality Modeling. In S. K. Jain & V. P. Singh (Eds.), *Developments in Water Science* (Vol. 51, pp. 743–786). Elsevier. [https://doi.org/10.1016/S0167-5648\(03\)80067-9](https://doi.org/10.1016/S0167-5648(03)80067-9)

Jarczewska, M., Ziółkowski, R., Górski, Ł., & Malinowska, E. (2015). Electrochemical Detection of Chromium(VI): Induced DNA Damage. *Journal of The Electrochemical Society*, 162(12), B326–B331. <https://doi.org/10.1149/2.0401512jes>

Jena, B. K., & Raj, C. R. (2008). Highly sensitive and selective electrochemical detection of sub-ppb level chromium(VI) using nano-sized gold particle. *Talanta*, 76(1), 161–165. <https://doi.org/10.1016/j.talanta.2008.02.027>

Johengen, T. (2016). *Protocols for the Performance Verification of In Situ Nutrient Analyzers Submitted to the Nutrient Sensor Challenge*. Alliance for Coastal Technologies; 08/08/2020. http://www.act-us.info/nutrients-challenge/Download/Nutrient_Challenge_Test%20Protocols_PV16_01.pdf

Kowsalya, B., Anusha Thampi, V. V., Sivakumar, V., & Subramanian, B. (2019). Electrochemical detection of Chromium(VI) using NiO nanoparticles. *Journal of Materials Science: Materials in Electronics*, 30(15), 14755–14761. <https://doi.org/10.1007/s10854-019-01847-3>

Krishna, M., Chandrasekaran, K., Rao, S. V., Karunasagar, D., & Arunachalam, J. (2005). Speciation of Cr(III) and Cr(VI) in waters using immobilized moss and determination by ICP-MS and FAAS. *Talanta*, 65(1), 135–143. <https://doi.org/10.1016/j.talanta.2004.05.051>

- Kus, S., Marczenko, Z., & Obarski, N. (1996). Derivative UV-VIS Spectrophotometry in Analytical Chemistry. *Chern. Anal. (Warsaw), Department of Analytical Chemistry, Technical University of Warsaw, 00-664 Warszawa, Poland*, 31.
- Lace, A., Ryan, D., Bowkett, M., & Cleary, J. (2019). Chromium Monitoring in Water by Colorimetry Using Optimised 1,5-Diphenylcarbazide Method. *International Journal of Environmental Research and Public Health*, 16(10). <https://doi.org/10.3390/ijerph16101803>
- Levitskaia, T. G., O'Hara, M. J., Sinkov, S. I., & Egorov, O. B. (2008). Direct Spectrophotometric Analysis of Cr(VI) Using a Liquid Waveguide Capillary Cell. *Applied Spectroscopy*, 62(1), 107–115. <https://doi.org/10.1366/000370208783412690>
- Malhotra, A., & Örmeci, B. (2021). Monitoring of Cyanobacteria using Derivative Spectrophotometry and improvement of the method detection limit by changing pathlength. *Manuscript Submitted for Publication, Department of Civil and Environmental Engineering, Carleton University*, 1–46.
- McLean, J. E., McNeill, L. S., Edwards, M. A., & Parks, J. L. (2012). Hexavalent chromium review, part 1: Health effects, regulations, and analysis. *Journal - American Water Works Association*, 104(6), E348–E357. <https://doi.org/10.5942/jawwa.2012.104.0091>
- McNeill, L., McLean, J., Edwards, M., & Parks, J. (2012). State of the Science of Hexavalent Chromium in Drinking Water. *Water Research Foundation*, 36.
- McSheehy, S., Séby, F., & Nash, M. (2010). *The Determination of Trivalent and Hexavalent Chromium in Mineral and Spring Water using HPLC-ICP-MS*. Thermo Scientific. <https://static.thermoscientific.com/images/D02228~.pdf>
- Moffat, I., Martinova, N., Seidel, C., & Thompson, C. M. (2018). Hexavalent Chromium in Drinking Water: JOURNAL AWWA. *Journal - American Water Works Association*, 110(5), E22–E35. <https://doi.org/10.1002/awwa.1044>

- Moore, D. R. J., British Columbia, & Environment and Resource Management Department. (1999). *Ambient water quality guidelines for organic carbon in British Columbia*. Environment and Resource Management Dept. (ISBN 978-0-7726-3980-6)
- Mostofa, K. M. G., Yoshioka, T., Mottaleb, A., & Vione, D. (Eds.). (2013). *Photobiogeochemistry of Organic Matter*. Springer Berlin Heidelberg. (ISBN 978-3-642-32222-8) <https://doi.org/10.1007/978-3-642-32223-5>
- Neubauer, K., Reuter, W., & Perrone, P. (2003). Chromium Speciation in Water by HPLC/ICP-MS. *PerkinElmer, Application Note*, 8.
- NHMRC, & NRMCC. (2017). *Australian Drinking Water Guidelines Paper 6 National Water Quality Management Strategy* (Version 3.4). National Health and Medical Research Council, National Resource Management Ministerial Council. (ISBN 1-86496-511-8) <https://www.nhmrc.gov.au/sites/default/files/documents/reports/aust-drinking-water-guidelines.pdf>
- Owen, A. J. (1995). *Uses of Derivative Spectroscopy*. Agilent Technologies. https://www.who.edu/cms/files/derivative_spectroscopy_59633940_175744.pdf
- Owen, T. (1998). *Fundamentals of Modern UV-Visible Spectroscopy*. Hewlett-Packard Company. <https://trove.nla.gov.au/work/32688247>
- Perkin Elmer. (2018). Atomic Spectroscopy, A Guide to Selecting the Appropriate Technique and System. *Atomic Spectroscopy*, 16.
- Potter, B. B., & Wimsatt, J. C. (2005). *Determination of Total Organic Carbon and Specific UV Absorbance at 254 nm in Source Water and Drinking Water*. https://cfpub.epa.gov/si/si_public_record_report.cfm?Lab=NERL&dirEntryId=103917
- Puig, A., Olgúin Salinas, H. F., & Borús, J. A. (2016). Relevance of the Paraná River hydrology on the fluvial water quality of the Delta Biosphere Reserve. *Environmental Science and Pollution Research*, 23(12), 11430–11447. <https://doi.org/10.1007/s11356-015-5744-4>

- Rakhunde, R., Deshpande, L., & Juneja, H. D. (2012). Chemical Speciation of Chromium in Water: A Review. *Critical Reviews in Environmental Science and Technology*, 42(7), 776–810. <https://doi.org/10.1080/10643389.2010.534029>
- Rice, E. W., Baird, R. B., & Eaton, A. D. (2017). *Standard Methods for the Examination of Water and Wastewater* (23rd ed.). American Public Health Association, American Water Works Association, Water Environment Federation. (ISBN 978-0-87553-287-5)
- Rockett, L., Benson, V., Clementson, A. J., Doyle, T., Hall, T., Harman, M., Jonsson, J., Rumsby, P., Young, W., Wilkinson, D. J., & Warwick, P. (2015). *Understanding the Significance of Chromium in Drinking Water* (p. 187). WRc plc. <http://www.dwi.gov.uk/research/completed-research/reports/DWI70-2-275.pdf>
- Ruffin, C., King, R. L., & Younan, N. H. (2008). A Combined Derivative Spectroscopy and Savitzky-Golay Filtering Method for the Analysis of Hyperspectral Data. *GIScience & Remote Sensing*, 45(1), 1–15. <https://doi.org/10.2747/1548-1603.45.1.1>
- Saha, R., Nandi, R., & Saha, B. (2011). Sources and toxicity of hexavalent chromium. *Journal of Coordination Chemistry*, 64(10), 1782–1806. <https://doi.org/10.1080/00958972.2011.583646>
- Sanchez-Hachair, A., & Hofmann, A. (2018). Hexavalent chromium quantification in solution: Comparing direct UV–visible spectrometry with 1,5-diphenylcarbazide colorimetry. *Comptes Rendus Chimie*, 21(9), 890–896. <https://doi.org/10.1016/j.crci.2018.05.002>
- Sanz-Medel, A., Pereiro, R., & Costa-Fernández, J. M. (2009). Chapter 1. A General Overview of Atomic Spectrometric Techniques. In J. M. Andrade-Garda (Ed.), *Basic Chemometric Techniques in Atomic Spectroscopy* (pp. 1–50). Royal Society of Chemistry. (ISBN 978-0-85404-159-6) <https://doi.org/10.1039/9781847559661-00001>
- Savitzky, Abraham., & Golay, M. J. E. (1964). Smoothing and Differentiation of Data by Simplified Least Squares Procedures. *Analytical Chemistry*, 36(8), 1627–1639. <https://doi.org/10.1021/ac60214a047>

- Sedman, R., Beaumont, J., Budroe, J., & Vidair, C. (2011). *California Public Health Goals for Chemicals in Drinking Water—Hexavalent Chromium Cr (VI)*. Office of Environmental Health Hazard Assessment California Environmental Protection Agency. <https://oehha.ca.gov/media/downloads/water/chemicals/phg/cr6phg072911.pdf>
- Stollenwerk, K. G., & Grove, D. B. (1985). Reduction of Hexavalent Chromium in Water Samples Acidified for Preservation. *Journal of Environmental Quality*, 14(3), 396–399. <https://doi.org/10.2134/jeq1985.00472425001400030017x>
- Sutton, R. (2010). Chromium-6 in U.S. Tap Water. *Environmental Working Group*, 24.
- Tandon, R. K., Crisp, P. T., Ellis, J., & Baker, R. S. (1984). Effect of pH on chromium(VI) species in solution. *Talanta*, 31(3), 227–228. [https://doi.org/10.1016/0039-9140\(84\)80059-4](https://doi.org/10.1016/0039-9140(84)80059-4)
- Thomas, O., Gallot, S., & Naffrechoux, E. (1990). Ultraviolet multiwavelength absorptiometry (UVMA) for the examination of natural waters and wastewaters. *Fresenius Journal of Analytical Chemistry*, 3(338), 241–244. <https://doi.org/10.1007/bf00323016>
- Vaz, R., Bettini, J., Júnior, J. G. F., Lima, E. D. S., Botero, W. G., Santos, J. C. C., & Schiavon, M. A. (2017). High luminescent carbon dots as an eco-friendly fluorescence sensor for Cr(VI) determination in water and soil samples. *Journal of Photochemistry and Photobiology A: Chemistry*, 346, 502–511. <https://doi.org/10.1016/j.jphotochem.2017.06.047>
- Voigtman, E. (2017). The Hubaux and Vos Method. In *Limits of Detection in Chemical Analysis* (pp. 325–329). John Wiley & Sons, Inc. (ISBN 978-1-119-18900-8) <https://doi.org/10.1002/9781119189008.app5>
- Weldy, E., Wolff, C., Miao, Z., & Chen, H. (2013). Selective and sensitive detection of chromium(VI) in waters using electrospray ionization mass spectrometry. *Science & Justice*, 53(3), 293–300. <https://doi.org/10.1016/j.scijus.2012.12.003>
- WHO. (2017). *Guidelines for drinking water quality*. World Health Organization. (ISBN 978-92-4-154995-0)

WHO. (2019). *Chromium in Drinking-water* (p. 34) [Peer review draft]. World Health Organization. https://www.who.int/water_sanitation_health/water-quality/guidelines/chemicals/draft-chromium-190924.pdf

Yarbro, S. K. (1976). *Two photometric methods for the determination of chromium in biological materials* [Georgia Institute of Technology]. <https://smartech.gatech.edu/handle/1853/25982>

Zamyadi, A., MacLeod, S. L., Fan, Y., McQuaid, N., Dorner, S., Sauvé, S., & Prévost, M. (2012). Toxic cyanobacterial breakthrough and accumulation in a drinking water plant: A monitoring and treatment challenge. *Water Research*, 46(5), 1511–1523. <https://doi.org/10.1016/j.watres.2011.11.012>

9. Conclusions and Future Work

9.1 Conclusions

The major findings from this study and potential areas for future research are presented below.

Chapter 4 and 5

- By increasing cuvette pathlength from conventional 10-mm to 50- and 100-mm and applying S-G derivative spectrophotometry, a substantial improvement in sensitivity was observed for early detection and monitoring of cyanobacteria.
- Compared to the 10 mm pathlength conventionally used for absorbance measurements in the field, adoption of 100 mm pathlength and application of S-G derivative spectra improved the detection limit from 337,398 cells /mL to 4,916 cells/mL for *M. aeruginosa* and from 650,414 cells /mL to 11,661 cells /mL. for *C. vulgaris*.
- Spectrophotometry was also able to differentiate *M. aeruginosa* from *C. vulgaris* based on the variations in their pigment absorbance peaks, which could provide a useful tool in identifying blooms of interest.
- In a mixed-culture setting, the *Chl-a* peak of *M. aeruginosa* from *C. vulgaris* overlapped, while PC peak could be distinctly observed, indicating the presence of cyanobacteria in the microalgal mixture.

Chapter 6 and 7

- The results for *M. aeruginosa* and *C. vulgaris* showed viability for early detection using S-G derivative method in river water (unfiltered), with clear peaks visible at low concentrations.

- The lowest MDL for *M. aeruginosa* for the photopigments PC and *Chl-a* was estimated to be 12,798 cells/mL and 8,546 cells/mL, respectively; whilst *C. vulgaris* resulted in a detection limit of and 13,695 cells/mL for photopigment *Chl-a* in surface water. In support of previous results, 100 mm pathlength was found to be the most sensitive.
- Further testing using derivative spectrophotometry under different controlled water quality parameters (such as salinity, DOC, and turbidity) showed that detection limits were still below the WHO guidelines (except for 100 NTU) even under challenging water quality conditions.
- The lowest MDL for *M. aeruginosa* using derivative spectrophotometry and 100 mm pathlength was found to be 11,083 cells/mL and 12,632 cells/mL for 1 mg/L DOC for photopigments *Chl-a* and PC, respectively.
- Spectrophotometry can be used to measure multiple water quality parameters and pigments simultaneously reducing cost and space requirements. It is a simple, rapid, non-destructive, non-intrusive technique requiring no pigment extraction/reagent and can be implemented in-line for real-time monitoring purposes.

Chapter 8

- Variability in peaks was observed with altering pH and higher slope stability was observed in alkaline pH waters for Cr (VI).
- A minimum of 20% improvement in detection was observed with the S-G derivative method in comparison to zero-order absorbance. However, with worsening water quality (i.e., 10 mg/L DOC), over 2-fold of improvement in detection was observed, indicating significance of derivative spectrophotometry with changing water quality.

- The MDLs obtained in this study were significantly lower than the widely accepted guidance value of 50 $\mu\text{g/L}$ of total chromium with lowest MDL observed at 2 $\mu\text{g/L}$ in tap water.
- Proposed method is simple, does not rely on expensive reagents/solvents that generate waste, or sample preparation, and results have shown reliability for sensitive determination of Cr (VI) in realistic conditions.

Overall conclusion and research implications

Using existing affordable spectrophotometry technology and implementing the use of longer cuvette pathlengths allows for sensitive and early-detection of cyanobacteria and Cr (VI). In addition, this research can be applied to existing on-line water monitoring spectrum systems for real-time detection and monitoring purposes. However, real-time systems do come with their own set of potential issues that have to be taken into consideration. For example, equipments can get fouled and clogged over the course of regular operation and might require manual cleaning for continuous operation. If clogging is an issue, t-type strainers should be used to prevent damage of the flow cell, but would result in more frequent manual clearing of the strainer, increasing labor costs.

Cr (VI) results show that its detection is highly dependent on the pH of the solution. Despite this condition, it can be implemented in a real-time system which concurrently monitors pH of the source water using a probe. Algorithm conditions can be set to implement different regression slopes for estimation of Cr (VI) in source waters based either solely on the pH or other water quality parameters. A similar technique can be implemented for early-detection and monitoring of cyanobacteria/microalgae as well. Nevertheless, the

strongest leverage that the method described in this research has is that it has shown good applicability for both biological and chemical applications.

9.2 Future work

Future work for the investigation of microalgae monitoring includes testing different genus of microalgae using spectrophotometry and potentially checking their individual spectral fingerprints. Further, tests using longer pathlengths (up to 250 mm) should be investigated to potentially improve detection limits at higher water quality parameter levels (such as turbidity and DOC). Research should also be conducted on effect of mixing different WQPs and different cyanobacteria/microalgae together and checking its impact on detection. Furthermore, experiments using mixed micoralgal cultures with varying photopigment content should be studied and its response to varying pH levels. Although, with longer pathlengths, the overall working range might decrease but sensitive detection might be possible by compensating for absorbance observed due to turbidity. In addition, interactions of cyanobacteria and microalgae with different water quality parameters and nutrients should be researched to better understand the intricacies and their resultant impact on absorbance.

Recommendations for further areas of study for Cr (VI) include: testing a wider range of concentrations, inoculating Cr (VI) in different source waters (such as groundwater, surface water and brackish water) to check response, and investigating the potential impact of heavy metals and different chlorine/chloramine concentrations in Cr (VI) water. Further research using this method should also explore the presence of different water contaminants that might absorb at or close to the same wavelengths of interest as Cr (VI) and its impact on detection. Other future research could involve applying the methodology

described in this work for the potential detection of different biological and chemical water contaminants (such as permanganate, disinfection byproducts, among others) using spectrophotometry.